A complex NLR signalling network mediates immunity to diverse plant pathogens

Chih-Hang Wu

Thesis submitted to the University of East Anglia for the Degree of Doctor of Philosophy

September 2016

Abstract

Both plants and animals rely on nucleotide-binding domain leucine-rich repeat-containing (NLR) proteins to respond to invading pathogens and activate immune responses. An emerging concept in NLR biology is that “sensor” NLR proteins are often paired with “helper” NLR proteins to mediate immune signalling. However, the degree to which NLRs form signalling networks beyond sensor and helper pairs is poorly understood. In this thesis, I discovered that a large NLR immune signalling network with a complex architecture mediates immunity to oomycetes, bacteria, viruses, nematodes, and insects. Helper NLRs in the NRC (NLR-required for cell death) family are functionally redundant but display distinct specificities towards diverse sensor NLRs. Several sensor NLRs, including Rx, Bs2 and Sw5b, signal via interchangeable NRC2, NRC3 or NRC4, whereas some other sensor NLRs have a more limited downstream spectrum. For example, Prf signals via interchangeable NRC2 or NRC3 but not NRC4, and Rpi-blb2 signals via only NRC4. These helper/sensor NLRs form a unique phylogenetic superclade, with the NRC clade sister to the sensor NLR clades. The network has emerged over 100 million years ago from an NLR pair that diversified into up to one half of the NLRs of asterids. I propose that this NLR network increases evolvability and robustness of immune signalling to counteract rapidly evolving plant pathogens.

Table of Contents

List of Tables

List of Figures

Abbreviations

ADR1	ACTIVATED DISEASE RESISTANCE 1
ARC	Adaptor shared by APAF-1, R proteins, and CED-4
ATR1	*Arabidopsis thaliana* recognised 1
AVR	Avirulence protein
CC	Coiled-coil
CC_R	RPW8-like coiled-coil
CNL	CC-NB-LRR
dpi	Days post infiltration/infection
EDS1	ENHANCED DISEASE SUSCEPTIBILITY 1
HMA	Heavy metal-associated domain
HR	Hypersensitive response
HSP90	Heat shock protein 90
LRR	Leucine-rich repeats
MHD	Methionine-histidine-aspartate
myr	Million years
NAIP	NLR Family, Apoptosis Inhibitory Protein)
NB	Nucleotide binding
NDR1	NON-RACE SPECIFIC DISEASE RESISTANCE 1
NLR	NOD-like receptor or nucleotide-binding domain leucine-rich repeat-containing
NLRC4	NLR family CARD domain-containing protein 4
NRC	NLR required for cell death
NRG1	N REQUIRED GENE 1
NSm	Non-structural movement protein
PRRs	Pattern recognition receptors
PVX	*Potato virus X*
R	Resistance
RAR1	REQUIRED FOR MLA12 RESISTANCE 1
RLK	Receptor-like kinase
RLP	Receptor-like protein
RNL	CC_R-NB-LRR
Rpi-	Resistance to *Phytophthora infestans*
RPP	RECOGNITION OF PERONOSPORA PARASITICA
RPS	RESISTANCE TO PSEUDOMONAS SYRINGAE
RPW8	RESISTANCE TO POWDERY MILDEW 8
RRS1	RESISTANCE TO RALSTONIA SOLANACEARUM 1
SERK3	SOMATIC EMBRYOGENESIS RELATED KINASE 3
SGN	Sol Genomics Network
SGT1	Suppressor of G2 allele of skp1
SNC1	SUPPRESSOR OF NPR1-1, CONSTITUTIVE 1
SPL6	SQUAMOSA PROMOTER BINDING PROTEIN-LIKE 6
TIR	Toll/interleukin 1 receptor
TMV	*Tobacco mosaic virus*

TNL	TIR-NB-LRR
ToMV	*Tomato mosaic virus*
TSWV	*Tomato spotted wilt virus*
VIGS	Virus-induced gene silencing
wpi	Weeks post infection
Pi	*Phytophthora infestans*

Acknowledgements

First and foremost, I would like to thank Sophien Kamoun for his supervision and being an inspiring role model for my career. Thanks for all the generous support and guidance during these four years. I am glad that I had this great experience working with such an excellent and open-minded scientist.

Furthermore, I would like to thank my secondary supervisors Silke Robatzek and Hanna Kuhn for their encouragements and useful suggestions about my work.

Special thanks to my collaborators Ahmed Abd-El-Haliem and Jack H. Vossen, Wageningen University, for exchanging ideas and experimental materials. We would not have these exciting new discoveries without your efforts.

I would like to also thank my mentors, Tolga O. Bozkurt and Khaoula Belhaj for sharing their knowledge and helping me on establishing all the assays for this research.

I would like to show my big appreciation to people who have helped me on thesis writing, particularly Ben Petre, Lida Derevnina, Erin Zess, and Ola Białas, who carefully read my thesis and gave many helpful feedbacks.

Big thanks to everyone in the Kamounity. No words can express my appreciation to Joe Win, who is always being very patient and very helpful on everything. Also big thanks to Suomeng Dong, Yasin F. Dagdas, Angela Chaparro-Garcia, Ronny Kellner, Marina Pais, Vladimir Nekrasov and Artemis Giannakopoulou for being very good friends and colleagues, and also for having lots of fruitful discussion during lab meetings, and lots of fun outside of the lab. I really enjoyed working with all of you.

Thank you to TSL Tissue Culture and Transformation team and JIC Horticulture Service, particularly Timothy Wells who is being very professional and prepared all the N. benthamiana plants for me.

Thank you to Pingtao Ding, Shushu Jiang, Yan Ma, Julie Ku and Liping Xing for being very good friends and being very supportive.

I would like to also acknowledge all the present and past TSL students who made the student experience at TSL memorable.

Of course, I cannot forget my dear housemates, Zane Duxbury, Leonie Luginbuehl, Jelle Postma, and Jan Bettgenhauser, who made my life very enjoyable with lots of international experiences.

Last but not least, my family who support my decision for pursing PhD abroad and David Male for sharing lots of enjoyable moments with me.

Chapter 1: General Introduction

1.1 Plant innate immune system

Plants use a sophisticated innate immune system to protect themselves against invading pathogens. Studies in the past two decades have found that the recognition of invading pathogens is mediated by cell surface immune receptors and cytoplasmic immune receptors (Dodds and Rathjen, 2010; Jones and Dangl, 2006; Win et al., 2012). Cell surface immune receptors, also known as pattern-recognition receptors (PRRs), are transmembrane proteins that provide the first layer of surveillance to the surrounding environment. These proteins are typically receptor-like kinases (RLKs) or receptor-like proteins (RLPs) that recognise pathogen-associated molecular patterns (PAMPs). In addition to general surveillance, some PRRs recognise apoplastic effector proteins secreted from the pathogen. The defence response mediated by PRRs is known as PRR-triggered immunity (Dodds and Rathjen, 2010; Win et al., 2012). In contrast, cytoplasmic immune receptors operate inside plant cells and have no direct contact with molecules outside of the cell. Typically, they are nucleotide-binding domain leucine-rich repeat-containing proteins (NLR, also known as NB-LRR in the literature) that sense pathogen effectors that are delivered into the plant cell. Generally, the immune response triggered by NLRs is associated with a rapid and localised host cell death, known as the hypersensitive response (HR), and is referred to as effector- or NLR-triggered immunity (Dodds and Rathjen, 2010; Win et al., 2012).

1.2 Architecture and functions of NLR domains

Plant NLR proteins generally share a conserved tripartite domain architecture (Takken et al., 2006; Takken and Goverse, 2012). The N-terminal domain is usually a TIR (Toll/interleukin 1 receptor), CC (coiled-coil), or CC_R (RPW8-like coiled-coil) domain, which is involved in protein-protein

interaction as well as immune signalling activation (Shao et al., 2016; Takken et al., 2006; Takken and Goverse, 2012). The N-terminal domain is followed by the NB-ARC domain (Nucleotide-Binding adaptor shared with APAF-1, plant resistance proteins, and CED-4 domain). The NB-ARC domain is the central part of the protein and is the most conserved region across distantly related NLRs (Takken et al., 2006; van der Biezen and Jones, 1998). It has ATP binding and hydrolysis activity, which is essential for the function of many NLR proteins (McHale et al., 2006; Takken et al., 2006). The C-terminal domain, usually a LRR (Leucine-rich repeat) domain, is mostly involved in protein-protein interactions, particularly ligand binding and inter-domain interactions (McHale et al., 2006; Padmanabhan et al., 2009).

One widely-known model of NLR signalling activation is the “molecular switch” hypothesis (Takken et al., 2006; Takken and Goverse, 2012). According to this hypothesis, in the absence of pathogen stimuli, NLR proteins fold into a ADP-bound “OFF” state; in the presence of pathogen stimuli, the protein turns into the ATP-bound “ON” state, where it undergoes conformational changes that lead to signalling activation (Takken et al., 2006; Takken and Goverse, 2012). Thus, NLR proteins function like molecular switches that sense the presence of pathogens and activate immune response (Takken et al., 2006; Takken and Goverse, 2012).

1.2.1 The NB-ARC domain

The NB-ARC domain can be further divided into NB, ARC1, and ARC2 subdomains, which together form a nucleotide-binding pocket (Takken and Goverse, 2012). The NB subdomain contains the p-loop motif that is essential for ATP binding and hydrolysis (Tameling et al., 2002). Mutations in the p-loop motif reduce ATP binding and/or the hydrolysis activity of several NLRs, including I2, Mi, N, and M (Tameling et al., 2002; Ueda et al., 2006; Williams et al., 2011). NLRs with mutations in the p-loop motif generally display loss-of-function phenotype in immune signalling activation, indicating that ATP binding and hydrolysis play a critical role in NLR immune signalling activation

(Tameling et al., 2002). However, some NLRs display p-loop independent activity. For example, the p-loop mutation in RRS1 does not affect the immune responses triggered by AvrRps4 or Pop2, and mutation in the p-loop of RGA5 does not affect the response to Avr-Pia (Cesari et al., 2014b; Williams et al., 2014). Interestingly, the activity of ADR1, a helper NLR that is required for the immunity of several other NLRs, is independent of p-loop in NLR-triggered immunity but is dependent on intact p-loop for autoactivation (Bonardi et al., 2011; Roberts et al., 2013).

In addition to the NB subdomain, ARC1 and ARC2 also contribute to NLR signalling regulation and activation. The ARC1 subdomain includes the conserved GxP (GLPL) motif, which was shown to be essential for the activity of Rx and RPM1 (Bendahmane et al., 2002; Tornero et al., 2002). The ARC2 subdomain contains the MHD motif that is important for controlling the NLR 'switch' (van Ooijen et al., 2008). Substituting aspartic acid for valine in the MHD motif generally leads to autoactivation of NLR proteins (van Ooijen et al., 2008). The ARC2 subdomain is also important for coordinating with NB-ARC1 and LRR to control autoinhibition and to facilitate signal activation for several NLRs (Rairdan and Moffett, 2006; Slootweg et al., 2013; Steinbrenner et al., 2015; van Ooijen et al., 2008). Furthermore, random mutagenesis of the NB-ARC domain of NRC1 revealed several point mutations that induce autoactivation (Sueldo et al., 2015). Most of these residues are predicted to be centred around the bound nucleotide in the NLR structure, suggesting that regulation of nucleotide binding and hydrolysis plays a critical role in signalling activation (Sueldo et al., 2015).

1.2.2 The N-terminal domain: TIR, CC, or CC_R

There are three different types of N-terminal domains in plant NLRs: TIR (Toll/interleukin 1 receptor), CC (coiled-coil), or CC_R (RPW8-like coiled-coil). These three types of domains distinguish plant NLRs into TNL, CNL, or RNL groups, respectively (Collier et al., 2011; Shao et al., 2016). Several studies suggest that these N-terminal domains are the minimal functional unit

to activate defence signalling. For example, expression of the TIR domain of RPP1, RPS4, or L6 induces effector-independent cell death (Bernoux et al., 2016; Krasileva et al., 2010; Michael Weaver et al., 2006; Swiderski et al., 2009; Williams et al., 2014). In addition, the expression of the CC domain of MLA10 or the CC_R domains of NRG1 and ADR1 also induces effector-independent cell death (Collier et al., 2011; Maekawa et al., 2011).

TIR or CC domains can also mediate the formation of higher order NLR complexes, and the formation of these complexes appears to be important for signalling activation. A study of the co-crystal structure of TIR-TIR from the *Arabidopsis thaliana* NLR pair, RPS4 and RRS1, suggested that these two proteins form a heterodimer through their TIR domains. In addition, the interface between the two TIR domains play a critical role in coordinating the two NLRs for responding to their corresponding effectors (Williams et al., 2014). Structure-function analysis of the TIR domain of the flax rust NLR L6 revealed that mutations that abolish the self-association property also abolish the signalling activation (Bernoux et al., 2011). Furthermore, the crystal structure of CC domain from MLA10, a Barley NLR that confers resistance to powdery mildew, revealed that the CC domain forms a homodimer, and that this self-association is important for immune signalling activation (Maekawa et al., 2011).

For several NLR proteins, the CC or TIR domain may also participate in association with non-NLR partners to mediate effector recognition. For instance, the CC domain of Rx associates with RanGAP2, which is essential for nucleocytoplasmic partitioning of Rx as well as responding to the coat protein of PVX (Hao et al., 2013; Sacco et al., 2007; Tameling and Baulcombe, 2007; Tameling et al., 2010). Furthermore, the NLR RPS5 of *A. thaliana* associates with the guardee PBS1 through the CC domain, although it may not directly recognise the cleavage product of PBS1 induced by AvrPphB (Ade et al., 2007; Qi et al., 2014). The resistance protein N of tobacco associates with the chloroplast protein NRIP1 through its TIR domain. NRIP1 also associates with the helicase p50 from TMV (*Tobacco mosaic virus*), and is required for p50 recognition by N (Caplan et al., 2008). Overall,

these results indicate that both the TIR and CC domains play multiple roles, including mediating downstream signalling, participating in formation of NLR homodimers or heterodimers, and bridging the interactions with other proteins to mediate pathogen recognition.

1.2.3 The LRR domain

The C-terminal domain of NLRs is usually a LRR domain. This domain is shared by many other categories of proteins, and usually plays roles in protein-protein interaction and ligand binding (Kobe and Kajava, 2001; McHale et al., 2006; Padmanabhan et al., 2009; van der Biezen and Jones, 1998). The major feature of the LRR domain is the repeating hydrophobic LRR units that contain the conserved LxxLxxLxL motif. Based on the 3D structures of LRR containing proteins, the repeating LRR units generate an array of β-sheets that form the concave face of the domain, whereas the residues in-between the LRR units form the convex and exposed face (Enkhbayar et al., 2004; McHale et al., 2006). The possible roles of the LRR domain in plant NLRs include binding to the corresponding effector and determining the recognition specificity (Krasileva et al., 2010; Ravensdale et al., 2012). For instance, the LRR domain of RPP1, a NLR protein of *A. thaliana* that provides resistance to *Hyaloperonospora arabidopsidis*, associates with the corresponding effector ATR1 (Krasileva et al., 2010; Steinbrenner et al., 2015). By testing chimeric proteins of L5 and L6, two flax rust resistance proteins, the recognition specificity to variants of the effector AvrL567 was mapped to the N- and C-terminal regions of the LRR domain (Ravensdale et al., 2012). In addition to ligand binding and recognition specificity, the LRR domain may also play a role in inter-domain interactions and regulation of NLR complexes (Moffett et al., 2002; Slootweg et al., 2013). For example, the LRR domain of Rx interacts with the NB-ARC domain when expressed *in trans*, and this interaction is disrupted by the coat protein of *PVX* (Moffett et al., 2002; Slootweg et al., 2013).

1.2.4 Integrated domains

Several plant NLR proteins have evolved to accommodate integrated domains, which were shown to mediate effector recognition in some cases (Kroj et al., 2016; Sarris et al., 2016). Genome annotation of 31 plant species with computational approaches predicted that around 3.5% of NLR proteins have integrated domains (Kroj et al., 2016). At least 61 different types of integrated domains have been identified thus far, and these integrated domains may link to various molecular functions, including transcription, hormone signalling, redox reaction, and protein phosphorylation (Sarris et al., 2016). Integration of these domains can occur at the N-terminal or C-terminal of the canonical NLR domains, or in between the CC-NB or NB-LRR domains (Kroj et al., 2016; Sarris et al., 2016). These domains may have evolved from effector virulence targets or decoy proteins that were somehow fused with the coding region of NLR proteins during evolution. However, although some of the integrated domains have been shown to mediate effector recognition, the degree to which they are implicated in other biological processes is not clear (Cesari et al., 2014a; Krasileva et al., 2010; Kroj et al., 2016; Sarris et al., 2016; Wu et al., 2015).

Some of the integrated domains associate with pathogen effectors via direct binding and contribute to effector recognition (Cesari et al., 2014a; Sarris and Jones, 2015). For instance, the WRKY domain of RRS1 associates with the effector Pop2 from *Ralstonia solanacearum*. Pop2 can acetylate the WRKY domain of RRS1 and thus block the DNA binding activity of the RRS1 WRKY domain (Le Roux et al., 2015; Sarris et al., 2015). As Pop2 can also acetylate other WRKY domain-containing proteins, it appears that, during evolution, RRS1 acquired an integrated WRKY domain to detect pathogen perturbation of WRKY transcription factors (Cesari et al., 2014a; Le Roux et al., 2015; Sarris et al., 2015; Sarris and Jones, 2015). Another example is the integration of HMA domains into the rice NLRs, Pik-1 and RGA5. Both Pik-1 and RGA5 associate with their corresponding effectors AVR-PikD and AVR-Pia, respectively, through the HMA domain (Cesari et al., 2014b; Cesari et al., 2013; Kanzaki et al., 2012; Maqbool et al., 2015). One model is that the rice

blast pathogen targets HMA containing proteins to promote infection and rice NLRs acquired integrated HMA domains to detect the pathogen (Cesari et al., 2014a; Cesari et al., 2013; Fukuoka et al., 2009; Maqbool et al., 2015).

1.3 Some NLR proteins function together

1.3.1 NLR pairs

Recently, an increasing number of studies indicated that some NLR proteins work in pairs to respond to effectors and mediate disease resistance (Cesari et al., 2013; Lee et al., 2009; Loutre et al., 2009; Narusaka et al., 2009; Sinapidou et al., 2004; Zhai et al., 2011). These NLR pairs are usually encoded by two tightly linked NLR genes on the same chromosome. The first identified NLR pair in *A. thaliana* was RPP2A and RPP2B, which are encoded by two head-to-tail linked TNL genes, that provide disease resistance to *H. arabidopsidis* (Sinapidou et al., 2004). RPP2A is an unusual NLR with two incomplete TIR-NB domains, whereas RPP2B is a typical TNL protein. Both RPP2A and RPP2B are required for resistance to *H. arabidopsidis*, yet the mechanism by which this NLR pair recognises the pathogen is unknown (Sinapidou et al., 2004). One of the best-studied NLR pairs reported thus far is the RPS4/RRS1 pair, which is encoded by two head-to-head linked TNL genes. This NLR pair recognises AvrRps4 from *P. syringae*, Pop2 from *R. solanacearum*, and an unknown effector from *Colletotrichum higginsianum* (Narusaka et al., 2009).

As mentioned previously, RPS4 and RRS1 physically interact through their TIR domains and RRS1 contains an integrated WRKY domain that may have originated from an effector target (Le Roux et al., 2015; Sarris et al., 2015; Williams et al., 2014). Studies of the recognition of AvrRps4 in the *rrs1/rps4* mutant background led to the identification of the RPS4B/RRS1B pair, a NLR pair paralogous to RPS4/RRS1. RPS4B/RRS1B recognises AvrRps4, but not Pop2. Genome annotation along with phylogenetic analysis revealed that several NLR pairs similar to the RPS4/RRS1 pair that occurs in different Brassicaceae species (Saucet et al., 2015).

NLR pairs also commonly exist in important crops such as rice and wheat. Several NLR pairs in rice confer resistance to the rice blast fungus. For example, the NLR pair RGA4/RGA5 is encoded by two head-to-head NLR genes, and recognises the effectors AVR-Pia and AVR1-CO39 through the integrated HMA domain at the C-terminal of RGA5 (Cesari et al., 2014b; Cesari et al., 2013). The Pik-1/Pik-2 pair, also encoded by two head-to-head NLR genes, recognises the effector AVR-Pik through direct biding to the integrated HMA domain in Pik-1 (Maqbool et al., 2015; Zhai et al., 2011). *Pi5-1* and *Pi5-2*, two linked NLRs in rice, are both required to confer resistance to the rice blast fungus (Lee et al., 2009). Interestingly, *Pi5-2* is a constitutively expressed gene, whereas *Pi5*-1 is expressed only after pathogen challenge (Lee et al., 2009). These studies suggest that NLR pairs have emerged independently in many different plant species.

1.3.2 Helper NLRs

Some NLR proteins are classified as “helper NLR”; these NLRs mediate signalling following the activation of their partner “sensor NLRs” that recognise pathogen effectors directly or indirectly (Bonardi et al., 2011). In contrast to the previously discussed linked NLR pairs, these helper NLRs are not necessarily linked with their sensor NLR partners.

One of the better-known examples of helper NLRs is the ADR1 family. This family encodes several NLR proteins with the RPW8-like coiled-coil domain (CC_R) and are thus referred to as RNL proteins (Collier et al., 2011; Shao et al., 2016). The ADR1 family consists of at least three homologs (ADR1, ADR1-like1, and ADR1-like2), and are functionally redundant in immunity mediated by the sensor NLRs RPS2 (CNL), RPP2 (TNL) and RPP4 (TNL) (Bonardi et al., 2011). In addition, the ADR1 family is also required for the autoimmunity of *snc1* and *chs2-1* (gain-of-function RPP4 mutant) mutants, indicating that the ADR1 family is involved in defence signalling triggered by several different NLRs (Bonardi et al., 2011; Dong et al., 2016). Another helper NLR is *N. benthamiana* NRG1, which is also a RNL protein (Collier et

al., 2011; Peart et al., 2005). *NRG1* is required for the function of the NLR N to mediate resistance to TMV, but whether NRG1 is also required for the function of other NLR proteins of solanaceous plants remains unknown (Peart et al., 2005). In addition to ADR1 and NRG1, tomato NRC1 also functions as a helper NLR. NRC1 is a typical CNL in a lineage that is distantly related to the RNL clade (Andolfo et al., 2014; Gabriels et al., 2006; Gabriels et al., 2007b). NRC1 is required for the cell death mediated by several NLR proteins including Rx, Prf and Mi-1.2, as well as responses mediated by cell surface receptors including Cf-4, Ve1, and LeEix (Fradin et al., 2009; Gabriels et al., 2006; Gabriels et al., 2007b).

In summary, helper NLR proteins are now thought to play critical roles in immune signalling, as they are required for immunity mediated by many different immune receptors. Nonetheless, it is still unclear how the biochemical activities of helper NLRs are distinct from those of sensor NLRs which determine pathogen recognition.

1.4 Mechanisms that regulate NLR immune signalling

Despite identification of components involved in effector recognition, many studies focused on mechanisms that participate in the downstream signalling or play regulatory roles in NLR-triggered immunity. Although it is not clear the extent to which a general mechanism governs the immune responses mediated by distantly related NLRs, some of these mechanisms have broad implications on regulation of NLR immune signalling.

1.4.1 HSP90/SGT1/RAR1 chaperone complex

The HSP90/SGT1/RAR1 chaperone complex is one of the best-understood regulatory components in NLR-triggered immunity. These three proteins form a ternary complex that associates and regulates the stability of NLR proteins, and, therefore, are essential for immunity mediated by many

TNLs and CNLs (Botër et al., 2007; Kadota and Shirasu, 2012; Zhang et al., 2010).

HSP90 is a highly conserved molecular chaperone in eukaryotes and is involved in many essential processes in plants such as immunity, chloroplast development, and shoot and meristem development (Cao et al., 2003; Ishiguro et al., 2002; Kadota and Shirasu, 2012; Pearl and Prodromou, 2006). Similar to HSP90, SGT1, a co-chaperone of HSP90, is also required for the function of many plant NLRs. In eukaryotes, SGT1 participates in several biological processes including kinetochore assembly, ubiquitination, activation of the cyclic AMP pathway, and immunity in plants (Dubacq et al., 2002; Kitagawa et al., 1999; Peart et al., 2002). RAR1 is a zinc-binding protein that is involved in development in nematodes and immunity in plants (Shirasu et al., 1999). Silencing or knockout of components of the HSP90-RAR1-SGT1 complex revealed that this complex is essential for immunity mediated by several NLR proteins, including N, Rx, Prf, Tm-2^2 MLA6, RPM1, RPS2 and RPS5, most of which accumulate to lower levels when the HSP90 chaperone complex is disrupted (Azevedo et al., 2006; Bieri et al., 2004; Du et al., 2013; Hubert et al., 2003; Peart et al., 2002; Takahashi et al., 2003). More recently, MIP1, a co-chaperone protein that associates with SGT1 in *N. benthamiana*, was found to be required for resistance mediated by Tm-2^2 and cell death mediated by Pto/Prf complex (Du et al., 2013). However, the degree to which other NLR proteins also require MIP1 is unknown. Interestingly, not all of the tested NLRs require all three components in the HSP90-RAR1-SGT1 complex. For example, both Mi-1 and Rpi-blb2 require HSP90 and SGT1 but not RAR1, indicating that the mechanisms by which protein chaperone complexes regulate NLR mediated immunity varies depending on the NLR (Bhattarai et al., 2007; Oh et al., 2014a; Oh et al., 2014b).

1.4.2 Transcription factors

Several other studies showed that some transcription factors associate with NLR proteins and regulate defence-related gene expression prior to and

post effector recognition (Chang et al., 2013; Inoue et al., 2013; Padmanabhan et al., 2013; Xu et al., 2014). For example, barley MLA immune receptor interacts with MYB6 and WRKY1, two antagonistically acting transcription factors that induce transcriptional reprogramming upon effector recognition by MLA (Chang et al., 2013). The rice blast resistance protein Pb1 associates with the WRKY45 transcription factor. This association is important for the localization of Pb1 to the nucleus, as well as for immunity to the rice blast fungus (Inoue et al., 2013). Similarly, the TNL immune receptor N in *N. benthamiana* associates with SPL6 transcription factor in a distinct nuclear compartment. This association requires an intact p-loop of N and exists only in the presence of the helicase p50 from TMV. In addition to mediating N-dependent immunity to TMV, the homolog of SPL6 in *A. thaliana* is also required for the function of the NLR RPS4, indicating that the SPL6 transcription factor may participate in a general mechanism shared by different NLR proteins (Padmanabhan et al., 2013). Members of the bHLH84 transcription factor family associate with RPS4 as well as SNC1 in *A. thaliana* (Xu et al., 2014). A triple knockout of the bHLH84 homologs compromised RPS4 mediated immunity and *snc1* autoimmunity, indicating that these transcription factors play redundant roles and contribute to the robustness of the immune responses mediated by different NLRs (Xu et al., 2014). Altogether, these studies suggested that some NLR proteins may associate with transcription factors for nuclear partitioning as well as to stimulate transcriptional reprograming immediately after effector perception.

1.4.3 EDS1 complex

EDS1 encodes a nucleocytoplasmic lipase-like protein that participates in both NLR-triggered immunity and basal defence. It is required for the responses mediated by many TNL proteins, including RPP2, RPP4, RPP5, RPS4, N, and Bs4, and thus is considered a downstream component shared by TNL immune receptors (Aarts et al., 1998; Liu et al., 2002b; Schornack et al., 2004). EDS1 forms an exclusive complex with SAG1 or PAD4 (Feys et al., 2005; Wagner et al., 2013). Interestingly, the EDS1-SAG101 complex was

observed only in the nucleus, whereas the EDS1-PAD4 complex was observed in both the nucleus and cytoplasm, suggesting that the dynamic interactions of EDS1 in different cell compartments may contribute to the regulation of defence signal activation (Feys et al., 2005). In addition, EDS1 also associates with TNL proteins (Bhattacharjee et al., 2011). Perception of effectors AvrRps4 and HopA1 disrupt the interaction between EDS1-RPS4 and EDS1-RPS6, respectively, suggesting that the perturbation of EDS1-NLR association may trigger EDS1-dependent immune signalling (Bhattacharjee et al., 2011). In summary, these results suggest that the dynamics of EDS1, including association with partners and subcellular partitioning, play an important role in NLR-triggered immunity.

1.4.4 DNA binding

Two recent studies suggest a striking hypothesis for NLR immune signalling activation: NLR proteins may directly bind DNA and perturb DNA conformation upon pathogen perception (Fenyk et al., 2016; Fenyk et al., 2015). Based on structure modelling, the NB domain of Rx shows homology to Cdc6/Orc1, a protein that is involved in origin recognition and DNA replication in Archaea and eukaryotes (Fenyk et al., 2015). Further *in vitro* analyses showed that the NB domain of Rx is able to bend and melt DNA. This activity is ATP-dependent and requires an intact p-loop. Additionally, the corresponding effector, the coat protein from PVX, specifically activates the DNA binding activity of Rx *in vivo* (Fenyk et al., 2015). The NB domain of I-2, similarly, also displays ATP-dependent DNA binding activity (Fenyk et al., 2016). These results suggest that DNA binding may be a general feature for a subset of NLR proteins (Fenyk et al., 2016; Fenyk et al., 2015).

1.5 Evolution of plant NLRs

Over the past few years, advances in genome sequencing and annotation in different plant species, including model systems and important crop species, have allowed scientists to comprehensively study the genetic

landscape and evolution of NLR genes. To date, genome-wide analyses of NLR genes have been performed with several different plant genomes, including plants belonging to the rosid and asterid lineages of dicots, and Poaceae of monocots (Andolfo et al., 2014; Arya et al., 2014; Baumgarten et al., 2003; Christopoulou et al., 2015; Guo et al., 2011; Jupe et al., 2012; Lozano et al., 2012; Meyers et al., 2003; Stam et al., 2016; Tarr and Alexander, 2009; Zhou et al., 2004). These include studies that compared the NLR genetic landscape at plant family scale and the angiosperm scale (McHale et al., 2006; Shao et al., 2016; Shao et al., 2014; Zhang et al., 2014; Zhang et al., 2016). These studies provide insights into how NLR lineages expanded and contracted during evolution, as well as the differential evolutionary history of NLRs in distantly related plant lineages.

1.5.1 The number of NLR genes varies among plant genomes

One of the most interesting observations from comparative studies is that species often have very different numbers of NLR genes in their genomes (Sarris et al., 2016). For example, one of the plant species with highest number of NLR genes identified thus far is *Medicago truncatula*, with around 571 NLR genes. In contrast, its Legume family relative *Cajanus cajan* has around 289 NLR genes (Shao et al., 2016). *A. thaliana* has around 165 NLR genes, similar to its close relative *Arabidopsis lyrata*, which has 198 NLR genes. Interestingly, *Carica papaya*, which is in the same plant order (Brassicales) as *A. thaliana*, has only 34 NLR genes, and is the seed plant with lowest number of NLR genes reported thus far (Porter et al., 2009; Sarris et al., 2016).

1.5.2 Most NLRs occur in clusters with uneven chromosomal distribution

Across plant species, NLR loci are found as either isolated genes (singletons) or as an array of NLR genes (gene clusters) (Holub, 2001; Leister, 2004). Most NLR clusters possess homologous genes, and are referred to as homogenous clusters (Holub, 2001; Leister, 2004). In contrast,

some gene clusters contain distantly related NLR genes, and are referred to as heterogeneous clusters (Holub, 2001; Leister, 2004). Interestingly, the majority of NLR genes exist as clusters with uneven distribution across different chromosome. For example, 85% of *A. thaliana* NLRs exist in clusters, with the largest cluster on chromosome 5 containing 12 NLR genes (Zhang et al., 2016). In tomato, 66% of the NLR genes exist in clusters, with the largest cluster containing 14 NLR genes on the short arm of chromosome 4 (Andolfo et al., 2014). This uneven distribution pattern and NLR clustering are general features also observed in several other species (Andolfo et al., 2014; Arya et al., 2014; Baumgarten et al., 2003; Christopoulou et al., 2015; Guo et al., 2011; Jupe et al., 2012; Lozano et al., 2012; Meyers et al., 2003; Stam et al., 2016; Tarr and Alexander, 2009; Zhou et al., 2004).

1.5.3 Three types of duplication events contribute to NLR evolution

There are three different types of duplication events (tandem, segmental, and ectopic) which contribute to the clustering, expansion, and uneven distribution of NLRs observed in plant genomes (Leister, 2004). Tandem duplication involves local duplication of genes, resulting in homogenous cluster with an array of NLR copies that are highly similar to each other. Segmental duplication involves duplication and translocation of a large chromosomal fragment to another linked or unlinked locus, resulting in two chromosomal regions that show synteny with one another. Ectopic duplication is where only a small set of NLR genes or an individual NLR gene is transferred to another chromosome (Leister, 2004). Some NLR genes that exists as singletons could be the result of this type of duplication (Leister, 2004). Studies of synteny among closely related species indicate that these three types of duplication may differentially contribute to expansion and distribution of NLRs (Andolfo et al., 2014; Arya et al., 2014; Shao et al., 2014).

1.5.4 Different NLR classes display distinct expansion patterns

The three different NLR classes (TNL/CNL/RNL) show distinct gain and loss patterns during angiosperm evolution (Shao et al., 2016). CNL genes adopted “gradual expansion” in the early stage (prior to 100 million years ago) of angiosperm evolution, and showed massive expansion after the “Cretaceous-Paleogene (K-P) boundary”, particularly in the Solanaceae and Poaceae families (Shao et al., 2016). In contrast, no expansion of TNL occurred before the K-P boundary, but clear expansions of TNL were observed after the K-P boundary in the Fabaceae and Brassicaceae family (Shao et al., 2016). RNL (CC_R-NB-LRR) genes, on the other hand, are relatively stable in the evolution of different angiosperm species (Shao et al., 2016). The results of evolutionary analysis inferred that an ancient whole genome duplication in angiosperm resulted in two RNL lineages, the ADR1-like lineage and the NRG1-like lineage (Shao et al., 2016).

Not all the plant species contain all three NLR classes. For example, several studies indicated that monocot plants such as rice (*Oryza sativa*), wheat (*Triticum aestivum*), and banana (*Musa acuminata*) do not have TNL-type NLR genes, suggesting a gene loss event occurred in the common ancestor of monocot plants (Sarris et al., 2016; Shao et al., 2016; Tarr and Alexander, 2009). Furthermore, sesame (*Sesamum indicum*) and monkey flower (*Mimulus guttatus*), both of which are in the order Lamiales of asterids, also do not have TNL genes (Sarris et al., 2016; Shao et al., 2016), suggesting a recent gene loss of TNLs during the evolution of lineages of asterids.

1.5.5 “*Birth-and-death”* evolution of NLRs

The best model to elucidate the high turnover evolution of NLR is the “birth-and-death process” (Michelmore and Meyers, 1998). That is, following the diversification by recombination or mutations, the continuous selection pressures favor the NLRs that have increased efficiency. Sequences with advantages in disease resistance will increase in the population, while some

rare unequal crossing-over events cause duplication or deletion of single gene or blocks of genes. Recently duplicated sequences are relatively unstable due to having high frequency of unequal crossing-over, which leads to further duplication, deletion, or altered specificity (Michelmore and Meyers, 1998). Repeating the “birth-and-death” process in evolution may eventually lead to expansion and functional diversification of NLR gene families (McHale et al., 2006; Michelmore and Meyers, 1998). Consequently, some NLR gene families exist in lineage-specific manner, while others are shared by distantly related plant lineages (McHale et al., 2006). Several recent genome-wide studies on NLR genes also support the hypothesis of “birth-and-death process” in NLR evolution, in which the presence/absence polymorphism of NLR phylogenetic clades are frequently observed when comparing distantly related species as well as closely related species (Shao et al., 2016; Shao et al., 2014; Zhang et al., 2016).

1.6 Resistance genes of solanaceous plants

Solanaceae is a plant family of great economic importance. This family includes several major crops and ornamental plants, such as potato (*Solanum tubersum*), tomato (*Solanum lycopersicum*), eggplant (*Solanum melongena*), pepper (*Capsicum* spp.), tobacco (*Nicotiana* spp.), and *Petunia* spp. Many of the solanaceous plants have been domesticated a long time ago, bred for higher yield, better disease resistance, and/or other traits that are advantageous for cultivation. For example, potato, one of the largest food crops in the world, has been domesticated more than 8000 years ago and bred into thousands of different verities (National Research Council (U.S.). Advisory Committee on Technology Innovation., 1989). Apart from plants with agriculture and horticulture importance, *Nicotiana benthamiana* is also of interest worldwide because it is the most widely used experimental plant in the laboratory (Goodin et al., 2008).

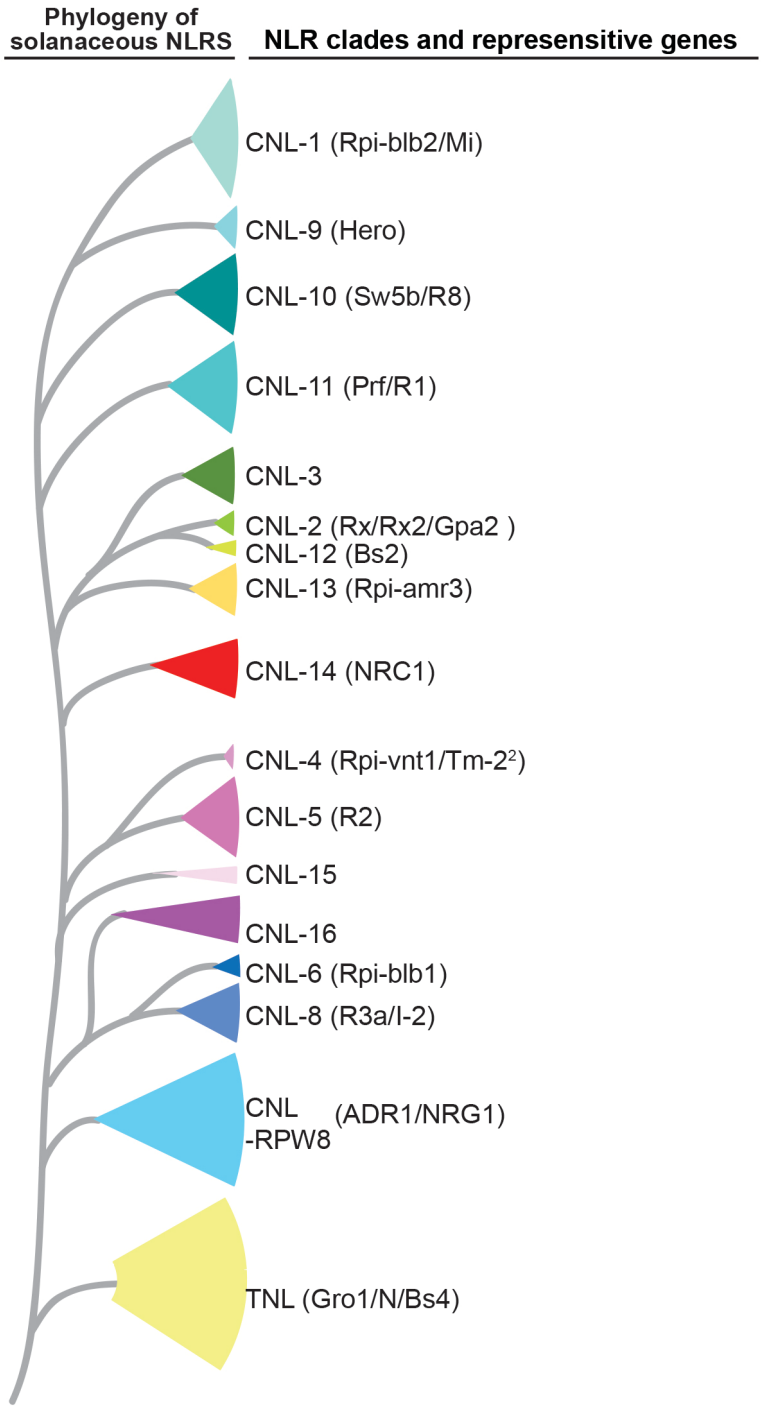

Figure 1. 1 Phylogenetic tree of solanaceous NLR proteins

The phylogenetic tree of solanaceous NLR proteins was modified from Andolfo et al. (2014). The naming of the CNL clades in Andolfo et al. (2014) and the representative families are indicated. Addition information of some of the NLRs are summarised in Table A2.1.

Solanaceous crops are infected by many different pathogens that often cause important yield losses (Strange and Scott, 2005). To circumvent these problems, breeders and scientists have been using the wild relatives of solanaceous crops as a source of disease resistance breeding and disease resistance gene cloning. Particularly, wild *Solanum* species, such as *S. demissum* and *S. pimpinellifolium,* have been used for breeding and identifying resistance genes for potato and tomato (Blanca et al., 2015; Vleeshouwers et al., 2011). To date, more than 20 NLR-type resistance genes that provide resistance to different pathogens of solanaceous plants have been identified, many of which confer resistance to devastating plant pathogens such as *Phytophthora infestans*, an oomycete that triggered the Irish potato famine in the 19th century (Fry, 2008; Vleeshouwers et al., 2011). Nonetheless, little is known about the mechanisms by which these NLR proteins sense the pathogen effectors and the downstream signalling mediated by these NLRs. Here, I introduce these solanaceous NLR-type resistance genes according to their phylogenetic clades and families (Fig. 1.1), and summarise our current understanding of these genes.

1.6.1 *Rpi-blb2/Mi-1.2* family and *Hero* family

One of the most interesting NLR families of solanaceous plants is the *Rpi-blb2/Mi-1.2* family. *Rpi-blb2* originates from *Solanum bulbocastanum* and encodes a CNL protein that confers broad-spectrum resistance to *P. infestans* in potato (van der Vossen et al., 2005). It is located in an NLR cluster together with closely related homologs on the short arm of chromosome 6, and is functional when transformed into tomato (van der Vossen et al., 2005). Rpi-blb2 gives responses to AVRblb2, a haustoria-localized RXLR effector that interferes with host vesicle secretion during infection (Bozkurt et al., 2011; Oh et al., 2009).

Mi-1.2 originates from *Solanum peruvianum* and shares 82% protein sequence identity with *Rpi-blb2* (Milligan et al., 1998; van der Vossen et al., 2005). *Mi-1.2* confers resistance to root-knot nematodes (*Meloidogyne* spp.),

potato aphid (*Macrosiphum euphorbiae*), and sweet potato whitefly (*Bemisia tabaci*) in tomato (Milligan et al., 1998; Nombela et al., 2003; Rossi et al., 1998). In eggplant, however, *Mi-1.2* provides resistance to root-knot nematode but not potato aphid, suggesting that *Mi-1.2*-mediated resistance has different requirements for different pathogens (Goggin et al., 2006). Although the nematode or aphid proteins sensed by Mi-1.2 are unknown, treatment with aphid saliva induces conformational changes of SERK1-Mi-1.2 complex. This suggests that Mi1-.2 senses a molecular pattern or effector protein that exists in the aphid saliva (Peng et al., 2016). *CaMi,* identified from hot pepper, is another resistance gene belonging to the *Rpi-blb2/Mi-1.2* family*. CaMi* shares 99% sequence identity with Mi-1.2 and confers resistance to root-knot nematode (Chen et al., 2007).

The *Hero* gene family shares the same origin with the *Rpi-blb2/Mi1.2* family, yet phylogenetically belongs to a different clade (Fig. 1.1) (Andolfo et al., 2014; Ernst et al., 2002). *Hero* is located in an NLR gene cluster on the short arm of chromosome 4, and was introgressed into tomato from *S. pimpinellifolium* (Ernst et al., 2002). *Hero* confers resistance to the potato cyst nematode *Globodera rostochiensis,* and partial resistance to *Globodera pallida*. The nematode protein sensed by *Hero* is currently unknown (Ernst et al., 2002).

1.6.2 *Sw5b/R8* family

The *Sw5b/R8* family also shares the same origin with the *Rpi-blb2/Mi-1.2* and *Hero* families, but forms a distinct clade in the phylogenetic tree (Fig. 1.1). (Andolfo et al., 2014). *Sw5b* and *R8* share 89% protein sequence identity, but provide resistance to different pathogens (Brommonschenkel et al., 2000; Vossen et al., 2016). *Sw5b*, originated from *S. peruvianum,* confers resistance to *Tomato spotted wilt virus* (TSWV) by sensing the cell-to-cell movement protein NSm (Hallwass et al., 2014; Peiro et al., 2014). Although the LRR domain of Sw5b is able to give response to NSm on its own, resistance to TSWV still requires the full-length Sw5b protein (Chen et al.,

2016). *R8* from *S. demissum* was mapped to the same region as *Rpi-smira2* in potato cultivar Sarpo Mira (Jo, 2013; Jo et al., 2011), and encodes a CNL protein with high homology to Sw5b. R8 recognises RXLR effector AVR8 (AvrSmira2) and confers resistance to *P. infestans* (Rietman et al., 2012; Vossen et al., 2016).

1.6.3 *R1* family *and Prf* family

R1 and *Prf* are classified in the same phylogenetic clade, yet detailed topology showed that these two genes are in different subclades (Fig. 1.1). (Andolfo et al., 2014; Jupe et al., 2012; Witek et al., 2016). Both *R1* and *Prf* are located on the short arm of chromosome 5 (Andolfo et al., 2014). *R1* originates from *S. demissum* and has been introgressed into many potato cultivars (Ballvora et al., 2002; Trognitz and Trognitz, 2007). *R1* gives response to *P. infestans* RXLR effector AVR1. However, R1-mediated resistance has been overcome by the majority of *P. infestans* isolates, and thus the agricultural value of *R1* is limited (Du et al., 2015b; Trognitz and Trognitz, 2007). *Prf* confers resistance to *Pseudomonas syringae* by recoginsing Type III effector proteins AvrPto and AvrPtoB (Abramovitch et al., 2003; Ronald et al., 1992). Prf associates with Pto kinase through the N-terminal extension, and guards the interaction or perturbation of Pto caused by AvrPto and AvrPtoB (Mathieu et al., 2014; Mucyn et al., 2006; Ntoukakis et al., 2013; van der Hoorn and Kamoun, 2008; Xiang et al., 2008; Xing et al., 2007).

1.6.4 *Rx/Rx2/Gpa2* family and *Bs2* family

Both *Rx* (also referred to as *Rx1*) and *Gpa2* have been introgressed into potato from *Solanum andigena* and are homologs of NLR genes from the same cluster on chromosome 12 (van der Vossen et al., 2000). They share 88% protein sequence identity but provide disease resistance to two different pathogens: *Rx* confers resistance to potato virus X (PVX) and *Gpa2* confers resistance to potato cyst nematode (G. *pallida*) (van der Vossen et al., 2000).

In contrast, Rx2, which shares 95% protein sequence identity with Rx, has been introgressed into potato from *Solanum acaule* and is located on chromosome 5 (Bendahmane et al., 2000; van der Vossen et al., 2000). *Rx* and *Rx2* sense the coat protein from PVX, whereas *Gpa2* gives response to the nematode effector RBP-1 (Bendahmane et al., 1995; Bendahmane et al., 2000; Sacco et al., 2009). Ran GTPase-activating protein 2 (RanGAP2) associates with both the CC domain of Rx and Gpa2, and is essential for the responses mediated by both these NLR proteins. This suggests that RanGAP2 is involved in the recognition of Rx and Gpa2 to pathogen proteins (Sacco et al., 2009; Sacco et al., 2007; Tameling and Baulcombe, 2007; Tameling et al., 2010).

Bs2 was identified from pepper (*Capsicum annuum*) and provides resistance in tomato to bacterial spot disease caused by *Xanthomonas campestris* pv. *vesicatoria* (Tai et al., 1999). It recognises type III effector AvrBs2 from *X. campestris*. (Andolfo et al., 2014; Tai et al., 1999). Despite having only few copies in the tomato and potato genomes, the Bs2 family is massively expanded in the pepper genome (Fig. 1.1) (Andolfo et al., 2014; Seo et al., 2016).

1.6.5 *Rpi-amr3* family

Rpi-amr3 was recently cloned from *Solanum americanum, a* diploid non-tuber-bearing wild potato, using resistance gene sequence capture (RenSeq) with single-molecule real-time (SMRT) sequencing (SMRT RenSeq) (Witek et al., 2016). *Rpi-amr3* was mapped to a locus on chromosome 4 with 14 homologous NLR genes in four clusters. One of the homologs*, Rpi-amr3i*, confers resistance to *P. infestans* when introduced into *N. benthamiana* and potato by transient expression or stable transformation (Witek et al., 2016). The effector protein recognised by *Rpi-amr3* is currently unknown.

1.6.6 *Rpi-vnt1*/*Tm-2*^{2} family

Several *Rpi-vnt1* allelic variants (*Rpi-vnt1.1, Rpi-vnt1.2, Rpi-vnt1.3*) were identified from different accessions of *Solanum venturii* (Foster et al., 2009; Pel et al., 2009). These *Rpi-vnt1* variants are located on the long arm of chromosome 9, and confer resistance to *P. infestans* in potato, tomato, and *N. benthamiana* (Foster et al., 2009; Pel et al., 2009). The effector protein recognised by Rpi-vnt1 is Avrvnt1 (Vleeshouwers et al., 2011). *Rpi-mcq1* from *Solanum mochiquense* was also found to be a homolog of *Rpi-vnt1*, but showed a different recognition spectrum (Smilde et al., 2005; Vleeshouwers et al., 2011).

Tm-2^2, which shares 75% protein sequence identity with Rpi-vnt1, provides resistance to *Tomato mosaic virus* (ToMV) and *Tobacco mosaic virus* (TMV) in tomato and *N. benthamiana* (Du et al., 2013; Lanfermeijer et al., 2003; Zhang et al., 2013b). Recently, rubisco small subunit was found to be involved in resistance mediated by Tm-2^2 to TMV (Zhao et al., 2013). However, it is still not clear whether rubisco small subunit is specifically required for Tm-2^2-TMV interaction or has a general implication in plant defence. Additionally, two recently identified late blight resistance genes, *Ph-3* from *S. pimpinellifolium* and *R9a* from *S. demissum,* also belong to the *Rpi-vnt1/Tm-2*^{2} family (Jo et al., 2015; Zhang et al., 2013a).

1.6.7 *R2* family

The *R2* resistance gene family incudes multiple late blight resistance genes originating from several different plant species. These include, but are not limited to *R2* from *S. demissum*, *Rpi-blb3* from *S. bulbocastanum*, and *Rpi-mcd1* from *Solanum microdontum* (Vleeshouwers et al., 2011). *R2* is located on chromosome 4 in proximity to the *Rpi-amr3* locus (Witek et al., 2016). According to sequence comparison and phylogenetic analysis, *R2* is a homolog of *A. thaliana*, *RPP13*, which confers resistance to *H. arabidopsidis* (Andolfo et al., 2014; Vleeshouwers et al., 2011). Several R2 homologs recognise proteins in the Avr2 RXLR effector family, but some may show

different recognition spectrums. For example, *Rpi-mcd1* does not give response to any of the Avr2 family members (Vleeshouwers et al., 2011).

1.6.8 *Rpi-blb1* family

The *Rpi-blb1* resistance gene family is located on chromosome 8 and includes several late blight resistance genes originating from different *Solanum* species, including *Rpi-blb1* and *Rpi-bt1* from *S. bulbocastanum,* and *Rpi-sto1 and Rpi-pta1* from *Solanum stoloniferum* (Oosumi et al., 2009; van der Vossen et al., 2003; Vleeshouwers et al., 2008)

6.9 *R3a/I2* family

R3a originated from *S. demissum* and provides resistance to *P. infestans* (Huang et al., 2005). It is located on the short arm of chromosome 11 together with closely related homologs and gives response to RXLR effector Avr3a (Armstrong et al., 2005; Huang et al., 2005). There are two different AVR3a alleles in the *P. infestans* population, $Avr3a^{KI}$ and $Avr3a^{EM}$. R3a gives responses to $Avr3a^{KI}$, but only weakly to $Avr3a^{EM}$ (Armstrong et al., 2005). R3b shares 73% protein sequence identity with R3a, but gives response to a different RXLR effector AVR3b (Huang et al., 2004; Li et al., 2011).

I-2 was introgressed from *S. pimpinellifolium* into tomato and provides resistance to race 2 of *Fusarium oxysporum f. sp. lycopersici* (Ori et al., 1997; Simons et al., 1998). It is located at the same locus as *R3a* and shares 83% protein sequence identity to R3a (Huang et al., 2005). *I-2* recognises *F. oxysporum* Avr2, which is an effector that is translocated into the plant cell during infection (Ma et al., 2013). In addition to responding to Avr2 of *F. oxysporum*, I-2 also gives weak response to Avr3a from *P. infestans* and can be engineered to confer partial resistance to *P. infestans* (Giannakopoulou et al., 2015).

1.6.10 TNL family: *Gro1.4*, *N*, and *Bs4*,

According to sequence homology and phylogeny, the TNL family in solanaceous plants can be grouped into four subclades (Fig. 1.1) (Andolfo et al., 2014). The resistance gene *Gro1.4* is in subclade B, whereas *N* and *Bs4* are in subclade D (Andolfo et al., 2014). *Gro1.4* originated from *Solanum spegazzinii* and is located on chromosome 12. It provides resistance to pathotype Ro1 of potato cyst nematode *G. rostochiensis* (Barone et al., 1990; Paal et al., 2004). The effector sensed by Gro1.4 is currently not known. *N* gene, which confers resistance to TMV, was identified from tobacco (Whitham et al., 1994). N recognises p50 of TMV, which is a helicase that is essential for virus replication (Erickson et al., 1999). *Bs4* encodes a TNL gene that confers resistance to *X. campestris* pv. *vesicatoria* in tomato (Schornack et al., 2004). It gives responses to the Type III effectors AvrBs3, AvrBs4 from *X. campestris* pv. *vesicatoria* as well as Hax3 and Hax4 from *X. campestris* pv. *armoraciae*, all of which are TAL effectors in the AvrBs3 family (Kay et al., 2005; Schornack et al., 2004).

1.7 Aims of the thesis

The primary aim of this thesis is to understand the function of helper NLR proteins in the NRC family. To investigate the roles of NRC family members in plant immunity, I revisited a previous study about NRC1 (Gabriels et al., 2007) using a combination of genome annotation, phylogenetics, and genetics approaches. The results revealed that *N. benthamiana* lacks a close homolog of *NRC1*, and the genes responsible for Pto/Prf-mediated immunity are *NRC2* and *NRC3* (**Chapter 3**). Together with my collaborator (Dr. Jack H. Vossen, Wageningen University), we found that NRC4, a member of the NRC family, is required for immunity mediated by both Rpi-blb2 and R1. Interestingly, NRC2, NRC3, and NRC4, play redundant roles in immunity mediated by Rx, Bs2, Sw5b and R8. These results suggest that members in the NRC family act as “helper NLRs” that form an essential signalling network for the immunity mediated by a large number of “sensor NLRs”. Based on

results of evolutionary analyses, I propose that this NRC signalling network has emerged over 100 million years ago from an NLR pair that diversified into up to one half of the NLRs of asterids (**Chapter 4**). To further understand the basis of helper-sensor partner specificity in the NRC-signalling network, I generated and tested the activities of chimeric proteins between NRC3 and NRC4. I found that the LRR region, particularly the amino acids between two typical LRR units, determines the sensor specificity of NRC3 and NRC4 (**Chapter 5**). Altogether, these results provide new insights into molecular mechanisms and evolution of a NLR signalling network that confers resistance to multiple pathogens.

Chapter 2: Materials and Methods

2.1 Plant Materials

2.1.1 Wild type and transgenic *Nicotiana benthamiana* lines

Wild type and transgenic *N. benthamiana* lines were grown in a controlled growth chamber with temperature 22-25°C, humidity 45-65% and 16/8-h light/dark cycle. Details of transgenic *N. benthamiana* lines expressing different NLR genes are listed in Table 2.1.

2.1.2 Tomato plants

Tomato (*Solanum lycopersicum*) bacterial speck resistant line (Rio Grande 76R [*Pto*/*Pto Prf*/*Prf*]) and near-isogenic susceptible line (Rio Grande 76S [*pto*/*pto Prf*/*Prf*]) were described previously in the literature (Salmeron et al., 1994). Plants were grown in a controlled growth chamber with temperature 22-25°C, humidity 45-65% and16/8-h light/dark cycle.

Table 2. 1 List of transgenic *N. benthamiana* lines used in this study

NLR expressed	Pathogen recognised	Effector/avirulence factor	Reference
***Prf* (with *Pto*)**	*Pseudomonas syringae* pv. *tomato DC3000*	AvrPto, AvrPtoB	R411B (Balmuth and Rathjen, 2007)
Rpi-blb2	*Phytophthora infestans*	AVRblb2	(Bozkurt et al., 2011)
Rx	*Potato virus X*	Coat protein	(Lu et al., 2003)
R3a	*Phytophthora infestans*	AVR3a	(Schornack et al., 2010)
Rpi-blb1	*Phytophthora infestans*	AVRblb1	(Oh et al., 2009)

2.2 Cloning of NRC homologs and other NLR genes

2.2.1 Identification of *NRC2* and *NRC3*

Tomato NRC1 (Solyc01g090430) was used to identify homologs in the predicted protein databases (*N. benthamiana* Genome v0.4.4 predicted protein, Tomato proteins ITAG release 2.40, and Potato ITAG release 1 predicted proteins) on Solanaceae Genomics Network (SGN). Top hits of BLASTP search results were collected for further analyses. NRC2 homologs in potato were missing in Potato ITAG release 1 predicted proteins database. Therefore, two NRC2 sequences of potato identified in Potato PGSC DM v3.4 protein sequences were included in the analyses. The phylogenetic tree of NRC homologs was built using MEGA6-Beta2 (Fig. 3.1) (Tamura et al., 2013) with Neighbour-joining and Maximum-likelihood methods and with bootstrap values based on 1000 iterations. Assignments of NRC homologs to chromosomes were based on information of tomato and potato genomes.

2.2.2 Cloning of *NRC1*, *NRC2* and *NRC3*

Cloning of tomato *NRC* homologs was performed with Gateway cloning kit (Invitrogen) following the manufacturer's instruction. cDNA fragments of tomato *NRC* homologs were amplified with corresponding primer pairs listed in Table 2.2. The amplified fragments were cloned into pENTR/D-TOPO (Invitrogen) and then introduced into the pK7WG2 destination vector (Karimi et al., 2002) using Gateway LR recombination enzymes (Invitrogen). *N. benthamiana NRC2a, NRC2b and NRC3* were amplified with the corresponding primer pairs listed in Table 2.2 from cDNA and cloned into pCR8/GW/TOPO (Invitrogen) by TA cloning. The fragments were then used for further amplification and subcloning into pICH86988 using the Golden Gate cloning method (Weber et al., 2011). The synthetic fragments of *NbNRC2a/b* and *NbNRC3* were designed manually to introduce synonymous substitution in every codon possible, and the syntheses of these fragments were performed by GENEWIZ (South Plainfield, NJ, USA). The synthetic fragments were then subcloned into pICH86988 together with the remaining

NbNRC2a, NbNRC2b or *NbNRC3* fragment to generate full-length *NbNRC* variants.

Table 2. 2 List of primers used for *NRC1*, *NRC2* and *NRC3* cloning

Primer name	Sequence (5'-3')	Usage in this study	Reference
***Sl*NRC1-F**	*CACCATGGTTGATGTAGGGGTTGAATTTC*	Gateway cloning of tomato NRC1	This study
***Sl*NRC1-R**	*CTAAGAAGCTGTCTGTACATCAGAATC*	Gateway cloning of tomato NRC1	This study
***Sl*NRC2-F**	*CACCATGGCGAACGTAGCAGTGGAATTTC*	Gateway cloning of tomato NRC2	This study
***Sl*NRC2-R**	*TCAGAGATCAGGAGGGAATATGGAAAG*	Gateway cloning of tomato NRC2	This study
***Sl*NRC3-F**	*CACCATGGCGGATGTAGCAGTAAAGTTCTTA*	Gateway cloning of tomato NRC3	This study
***Sl*NRC3-R**	*TTACAATCCAAGATCATGAGGGAAT*	Gateway cloning of tomato NRC3	This study
***Nb*NRC2a-F**	*CACCATGGCGAACGTTGCGGTGGAGTTTCT GG*	Gateway cloning of tomato NRC2a	This study
***Nb*NRC2a-R**	*TCAGAGATCGGGAGGGAATATAGAGAGCTT*	Gateway cloning of tomato NRC2a	This study
***Nb*NRC2b-F**	*ATGGCGAACGTTGCGGTGGA*	Gateway TA cloning of tomato NRC2b	This study
***Nb*NRC2b-R**	*AATTGGTCTCTAAGCTTAGAGATCGGGAGGG AATATAGAG*	Gateway TA cloning of tomato NRC2b	This study
***Nb*NRC3-F**	*AATTGGTCTCTAATGGCAGATGCAGTAGTGA ATTTTCTGGTG*	Gateway TA cloning of tomato NRC3	This study
***Nb*NRC3-R**	*ATTGGTCTCGAAGCTTACTGTGTGGCCTTGG ATCCAGCTTC*	Gateway TA cloning of tomato NRC3	This study

2.2.3 Cloning of *NRC4*

Sequences of primers used in cloning of NRC4 variants are listed in Table 2.3. *NRC4* was amplified from *N. benthamiana* cDNA and cloned into pENTR/D-TOPO (Invitrogen). This plasmid was then used for further subcloning of NRC4 into pCR8/GW/D-TOPO (Invitrogen) as a level 0 module for follow-up Golden Gate cloning (Weber et al., 2011). GFP:NRC4 was generated by Golden Gate assembly with pICSL12008 (35S promoter, TSL SynBio), pICSL30006 (GFP, TSL SynBio), pCR8-NRC4, pICH41432 (OCS

terminator) into binary vector pICH86966 (Engler et al., 2014; Weber et al., 2011). To make a level 0 module for NRC4 c-terminal tagging, the stop codon was removed in pCR8-NRC4 to generate pCR8-NRC4-ns. NRC4:myc was generated by assembling pCR8-NRC4-ns with pICSL50010(4xmyc, TSL SynBio) in pICH86988**.** The synthetic fragment (1-272bp) of *NRC4* was designed manually to introduce synonymous substitution in every codon possible. The fragment was synthesized by GENEWIZ (South Plainfield, NJ, USA) and then subcloned into binary vector pICH86988 together with the remaining part of NRC4 (273-2646bp) by Golden Gate cloning to generate a full-length NRC4 variant. To confirm the accumulation of proteins in control or *NRC4*-silenced background, 4xmyc tag was fused to the C-terminal of NRC4 and cloned into pICH86988. Three days after agroinfiltration in control or *NRC4*-silenced leaves, total plant proteins were extracted and analysed by western blot analyses. Anti-myc (A-14, Santa Cruz Biotechnology) and anti-rabbit antibody conjugated to horseradish peroxidase (Sigma-Aldrich) were used as primary and secondary antibodies.

2.2.4 Site-directed mutagenesis of Rpi-blb2 and NRC4

To determine whether an intact p-loop is essential for the function of Rpi-blb2 and NRC4, a lysine (K) to arginine (R) mutation was introduced into the p-loop of both proteins independently. Primers listed in Table 2.2 were used for introducing the mutations by inverse PCR with Phusion High-Fidelity DNA Polymerase (Thermo). The mutated variants were verified by sequencing, and then subcloned into pK7WGF2 (for GFP:Rpi-blb2) or pICH86966 (for NRC4:myc). To confirm the accumulation of these proteins, wild type and mutated GFP:Rpi-blb2 or NRC4:myc were transiently expressed independently in *N. benthamiana* leaves. Samples were collected 3 days after infiltration for immunoblot analysis with anti-GFP or anti-myc antibodies.

2.2.5 DNA sequences and accession numbers of NRC homologs

Sequences of *NRC* homologs in this study can be found in the Solanaceae Genomics Network (SGN) or GenBank/EMBL databases under the following accession numbers: *Sl*NRC1 (Solyc01g090430, NP_001234202), *Sl*NRC2 (Solyc10g047320), *Sl*NRC3 (XP_004238948.1), *Nb*NRC2a (NbS00018282), *Nb*NRC2b (NbS00026706), *Nb*NRC2c (NbS00031134), *Nb*NRC3 (NbS00011087), *St*NRC3 (Sotub05g007690), NbNRC4 (NbS00002971, NbS00016103). Sequences of *SlNRC1*, *SlNRC2*, *SlNRC3* and *NbNRC3* were confirmed by cDNA sequencing, and are identical to the sequences in the database with accession numbers listed above. Sequences of *NbNRC2a and NbNRC2b* were re-annotated with sequences obtained from cDNA clones and submitted to NCBI under accession number KT936525, KT936526, respectively.

2.3 Virus induced gene silencing and PCR of *NRC* homologs

2.3.1 Virus-induced gene silencing (VIGS)

VIGS was performed in *N. benthamiana* as described by Liu *et al.* (2002). Suspension of *Agrobacterium tumefaciens* strain GV3101 harbouring TRV RNA1 (pYL155) and TRV RNA2 (pYL279) (Liu et al., 2002a), with corresponding fragments from indicated genes, were mixed in a 2:1 ratio in infiltration buffer (10 mM MES, 10 mM $MgCl_2$, and 150 μM acetosyringone, pH5.6) to a final OD_{600} of 0.3. Two-week-old *N. benthamiana* plants were infiltrated with *A. tumefaciens* for VIGS assays, upper leaves were used two to three weeks later for further agroinfiltration. For silencing of *NRC2/3* homologs in *N. benthamiana*, 5' coding region of each gene (*NbNRC2a/b*, 1-429b; *NbNRC2c*, 1-426bp; *NbNRC3*, 1-444bp) were cloned into TRV RNA2 vector. For co-silencing of *NbNRC2a/b* and *NbNRC3*, the fragments were fused by overlap PCR and cloned into TRV RNA2 vector.
For silencing of *NRC4*, a 395bp fragment from 3'UTR (-123) to 5' coding region (+272) were cloned into pYL279. For triple silencing of *NRC2/3/4*, fragments of *NRC4* (1-272), *NRC3* (1-295) and *NRC2a* (1-285) were

synthesized as one fragment by GENEWIZ and then subcloned into pYL279. The following primers were designed for generating the TRV2-*SlNRC1* construct based on the *SlNRC1* fragment that was used for silencing by Gabriels et al. (2007): 5'-CACCTTAAAGTCATTCCGAAACATGTTGG-3' and 5'-TCGAGAGAACATACTCAGTGCAGC-3'. The silencing constructs for *SGT1* and *SERK3* were described previously (Heese et al., 2007; Peart et al., 2002).

Table 2. 3 List of primers used for *NRC4* and *Rpi-blb2* cloning

Primer name	Sequence (5'-3')	Usage in this study	Reference
NRC4_CACC_F	*CACCATGGCAGATGCAGTAGTGAATTTTCT*	Gateway cloning of NRC4	This study
NRC4_R	*TCAGAAAACATGAGTAGCACCATATCCATG*	Gateway cloning of NRC4 (3'UTR)	This study
GG_NRC4_F	*AATTGGTCTCTAATGGCAGATGCAGTAGTGAATT TTCTGGTG*	NRC4 cloning GG	This study
GG_NRC4 _R	*ATTGGTCTCGAAGCTTACTGTGTGGCCTTGGAT CCAGCTTC*	NRC4 cloning GG	This study
GG_NRC4_ns_R	*ATTGGTCTCTCGAATACTGTGTGGCCTTGGATCC AGCTTCA*	NRC4 cloning GG C-tag	This study
Rpiblb2_K566R_R	*/5-PHOS/ TCGACCTAAACCCGGCATACCAATGATCGA*	Rpi-blb2 p-loop mutant	This study
Rpiblb2_K566R_F	*/5-Phos/ ACTACTTTGGCGTACAAAGTATACAATGAT*	Rpi-blb2 p-loop mutant	This study
NRC4_K190R_R	*/5-Phos/ TCTTCCAAGTCCCGGCATACCCACCACCGG*	NRC4 p-loop mutant	This study
NRC4_K190R_F	*/5-Phos/ ACCACACTAGCAAGAAAAATCTACAAGGAT*	NRC4 p-loop mutant	This study

2.3.2 PCR and RT-PCR of the NRC family members

DNeasy Plant Mini Kit (Qiagen) was used for extracting genomic DNA from *N. benthamiana* leaves according to manufacturer's instruction. For testing PCR primer pairs for amplification of NRC family members, 5ng of genomic DNA was used in 20μL reaction. Plant total RNA was extracted using RNeasy Mini Kit (Qiagen). DNA contamination in the RNA sample was removed by on-column digestion with RNase-Free DNase Set (Qiagen).

Subsequently, 2μg of each RNA sample was subject to first strand cDNA synthesis using Ominiscript RT Kit (Qiagen). PCR and semi-quantitative RT-PCR was performed using DreamTaq (Thermo Scientific) with 25 to 35 amplification cycles followed by electrophoresis with 2% agarose gel stained with ethidium bromide. The primers used in the RT-PCR and PCR are listed in Table 2.4.

2.4 Disease resistance assays

2.4.1 Rpi-blb2-mediated resistance

Assays of disease resistance to *P. infestans* were performed by applying droplets of zoospore suspension on detached leaves as described before (Song et al., 2009). *NRC* homologs were silenced by VIGS in *Rpi-blb2* transgenic *N. benthamiana* as described above. Three weeks after TRV inoculation, mature leaves were detached and used for disease resistance assay. Zoospore suspension from *P. infestans* 88069 was prepared as described previously and adjusted to 100 zoospores/μL (Song et al., 2009). To inoculate the pathogen, 10μL drops of zoospore were applied to the abaxial side of the leaves. The leaves were then kept in moist chamber at room temperature (21-24°C) for 4 days, and imaged under UV light for visualization of the lesions. For each biological replicate, 4 leaves from 2 independent silencing plants were used and 6 spots on each leaf were inoculated with the pathogen. Experiments were repeated 3 times. For the complementation assay, suspensions of *A. tumefaciens* containing empty vector or expression construct of synthetic *NRC4* were adjusted to OD_{600} of 0.6 and infiltrated into the leaves one day before pathogen inoculation. The processes and responses of agroinfiltration delayed the progress of *P. infestans* infection. Hence, the leaves were imaged at 5 days after inoculation. To check the accumulation of Rpi-blb2 in *NRC4*-silenced plants, RFP:Rpi-blb2 was transiently expressed in control and *NRC4*-silenced leaves by agroinfiltration. Leaf samples were collected at three days after infiltration for immunoblot with anti-GFP antibody.

Table 2. 4 List of primers used for PCR and RT-PCR of *Nb*NRC homologs

Primer name	Sequence (5'-3')	Usage in this study	Reference
NRC4_RT_F	*AAACAAATCTGCGGGTTGAC*	PCR/RT-PCR of NRC4	This study
NRC4_RT_R	*GGATGGCATTGAAGTCACCT*	PCR/RT-PCR of NRC4	This study
NRC4L-4611_F	*AGCTGCTGATGAGGGTCTTT*	PCR/RT-PCR of NRC4-like_4611	This study
NRC4L-4611_R	*AGGCTACGTACATCAGCCAA*	PCR/RT-PCR of NRC4-like_4611	This study
NRC4L-20047_F	*AAAATGCAGCGGATTACCAC*	PCR/RT-PCR of NRC4-like_20047	This study
NRC4L-20047_R	*GGCGAAGCAATACAAGAAGC*	PCR/RT-PCR of NRC4-like_20047	This study
NRC4L-11331_F	*GTGATCGAGCGTCTTGTTGA*	PCR/RT-PCR of NRC4-like_11331	This study
NRC4L-11331_R	*CTCTTCAATGCGTTTCGTGA*	PCR/RT-PCR of NRC4-like_11331	This study
NRC4L-04466_F	*CACCATGGATCGAGCGGTGGCTATG*	PCR/RT-PCR of NRC4-like_04466	This study
NRC4L-04466_R	*TGGCGAATTTCTCGCAATTCTTTG*	PCR/RT-PCR of NRC4-like_04466	This study
NRC3_RT_F	*CCTCGAAAAGCTGAAGTTGG*	PCR/RT-PCR of NRC3	This study
NRC3_RT_R	*TGTCCCCTAAACGCATTTTC*	PCR/RT-PCR of NRC3	This study
NRC2a/b_RT_F	*AGTGGATGAGAGTGTGGGTG*	PCR/RT-PCR of NRC2a/b	This study
NRC2a/b_RT_R	*AAGCAGGGATCTCAAAGCCT*	PCR/RT-PCR of NRC2a/b	This study
NRC2c_RT_F	*TCAAAACATGCCGTGTTCAT*	PCR/RT-PCR of NRC2c	This study
NRC2c_RT_R	*CCTGCGGGTTTTGTACTGAT*	PCR/RT-PCR of NRC2c	This study
NRCL-30243_F	*CCAAGTGCATCAATCTGTGG*	PCR/RT-PCR of NRC-like_30243	This study
NRCL-30243_R	*ATGGCCTTTGTTCTGGAATG*	PCR/RT-PCR of NRC-like_30243	This study
NbEF1α_F	*AAGGTCCAGTATGCCTGGGTGCTTGAC*	PCR/RT-PCR of EF1α	(Segonzac et al., 2011)
NbEF1α_R	*AAGAATTCACAGGGACAGTTCCAATACCAC*	PCR/RT-PCR of EF1α	(Segonzac et al., 2011)

2.4.2 R1-mediated resistance

For analysis of R1-mediated resistance, suspensions of *A. tumefaciens* containing empty vector or R1 expression construct were adjusted to OD_{600} of 0.5 and then infiltrated into *NRC4*-silenced or control *N. benthamiana*. For the comparison of disease resistance on the same leaf, half of each leaf was infiltrated with *A. tumefaciens* containing empty vector plasmid whereas the other half of the leaf was infiltrated with *A. tumefaciens* containing R1 expression vector. Experiments were repeated four times with 21 inoculation sites per condition in each biological replicate. *P. infestans* T30-4 was used for R1-mediated resistance assay. The zoospore suspension was prepared as described above and adjusted to 200 zoospores/μL. For the complementation assay, R1 was co-expressed with empty vector or synthetic *NRC4* in *NRC4*-silenced or control *N. benthamiana* on day before pathogen inoculation.

2.4.3 Rpi-blb1 and R3a-mediated resistance

NRC homologs were silenced by using VIGS as described above in *Rpi-blb1* and *R3a* transgenic *N. benthamiana*. *Rpi-blb2* transgenic plants were used in parallel as controls for silencing and successful pathogen inoculation. *SGT1*-silencing was used as an additional control for this experiment as it was demonstrated to be essential for the responses mediated by R3a and Rpi-blb1 in the cell death assay. Three weeks after TRV inoculation, mature leaves of the plants were used for disease resistance assay according the description above. For the inoculation on *Rpi-blb2* and *Rpi-blb1* transgenic plants, *P. infestans* 88069 was used. However, this isolate contains homozygous $AVR3a^{EM}$ allele and has overcome *R3a*-mediated resistance. Therefore, for the inoculation on *R3a* transgenic *N. benthamiana, P. infestans* NL00228, which contains homozygous $AVR3a^{KI}$ allele and is not virulent on R3a plants, was used (Giannakopoulou et al., 2015; Zhu et al., 2012). The experiments were repeated three times with 24 inoculation sites per condition in each biological replicate. Pictures were taken at 4 days after pathogen inoculation

for the analysis with *P. infestans* 88069 and 5 days after inoculation for the analysis with *P. infestans* NL00228.

2.4.4 Rx-mediated resistance

NRC homologs or *SGT1* were silenced by VIGS as described above in *Rx* transgenic *N. benthamiana*. Three weeks after TRV infection, *Potato virus X* (PVX, pGR106) was inoculated on the leaves through agroinfection as described previously (Tameling and Baulcombe, 2007). To generate PVX-GFP, a DNA fragment of GFP was amplified from pK7WGF2 with the primers listed in Table 2.5 and cloned in to pGR106. Suspension of *A. tumefaciens* carrying the PVX vector pGR106 or pGR106-GFP was adjusted to OD_{600} of 0.005 and then infiltrated into the mature leaves of Rx *N. benthamiana*. This concentration of *A. tumefaciens* only causes infection of few cells in the infiltrated area and thus no visible necrotic lesion could be observed when the resistance response is strong and rapid, i.e. extreme resistance. The infiltrated area was then circled with a marker pen. The trailing necrotic lesions were observed at inoculated leaves of the *NRC2/3/4*-silenced *Rx* plants starting from 10 days after inoculation, and the necrotic lesion spread gradually to the upper leaves and apical buds. Photos were taken at 15 days after inoculation under daylight or UV light. Samples from the upper leaves were collected at 15 days after inoculation and analysed by immunoblot analysis to detect GFP accumulation. To check the accumulation of Rx in *NRC2/3/4* or *SGT1* silenced *N. benthamiana*, leaf samples were collected at three weeks after TRV inoculation and anti-HA antibody (3F10, Roche) was used as primary antibody for immunoblot analysis. For complementation assay with synthetic NRC variants, we took advantage of the toothpick inoculation method (Du et al., 2014) that allowed us to examine the spreading of trailing necrotic lesions from the inoculated spots. One day before PVX toothpick inoculation, synthetic NRC variants were expressed by agroinfiltration on leaves of *Rx* plants silenced with *NRC2/3/4*. Toothpicks were dipped into the culture of *A. tumefaciens* harbouring PVX-GFP vector and then used to pierce small holes on the leaves of *N. benthamiana*. Photos

were taken at 10 days after PVX inoculation, and the size of the lesions were measured in ImageJ. Scatterplot of the lesion size was generated with R, using ggplot2 package and script published previously (Petre et al., 2016). A cork borer (0.9 cm^2) was used to collect leaf discs from the inoculation sites for immunoblot analysis.

Table 2. 5 List of primers used for generating PVX-GFP

Primer name	Sequence (5'-3')	Usage in this study	Reference
ClaI_GFP_F	*AATTATCGATATGAGCAAGGGCGAGGAGCTGTTC*	Cloning of GFP into pGR106	This study
GFP_SalI_R	*AATTGTCGACCTTGTACAGCTCGTCCATGCCGAG*	Cloning of GFP into pGR106	This study

2.4.5 Prf/Pto-mediated resistance

VIGS was used to silence *NRC2a/b, NRC3* and *NRC4* in both wild type and *Pto/Prf* transgenic (R411B) *N. benthamiana* plants (Balmuth and Rathjen, 2007). Bacteria growth assay were performed as previously described with minor modifications (Balmuth and Rathjen, 2007). The *Pseudomonas syringae* pv. *tomato* DC3000 *ΔhopQ1-1* culture (Wei et al., 2007) was adjusted to OD_{600} of 0.2 and then diluted 10,000-fold with 10 mM $MgCl_2$. Five-week-old *N. benthamiana* with VIGS control or *NRC2a/b/3*-silencing were inoculated with the bacterial culture using needleless syringe. Four replicate plants were sampled using 0.33cm^2 cork borer at each time points, and then the sample were homogenized in 10 mM $MgCl_2$ for serial dilution and plating. Experiments were repeated three times with similar results. Polyclonal anti-myc antibody A-14 (Santa Cruz Biotechnology) was used for detecting accumulation of Prf:5myc.

For testing *Pto/Prf*-mediate resistance to *P. syringae* pv. *tomato* DC3000 in tomato, the resistant and susceptible lines (cv. Rio Grande 76R and 76S) were used (Salmeron et al., 1994). Cotyledons of two-week-old tomato seedlings were inoculated with VIGS constructs targeting *Sl*NRC1, *Sl*NRC2 and/or *Sl*NRC3. Inoculation of *P. syringae* DC3000 was performed 2-3 weeks after VIGS inoculation according to previous description with minor

modifications (Balmuth and Rathjen, 2007). Briefly, *P. syringae* pv. *tomato* DC3000 culture was adjusted to OD_{600} of 0.2 and then diluted 10,000-fold with 10 mM $MgCl_2$ with 0.02% Silwet L-77. The bacteria suspension was then vacuum-infiltrated into leaves of tomato plants described above. Two replicate plants were sampled using 0.33cm^2 cork borer at each time point, and then the samples were homogenized in 10 mM $MgCl_2$ for serial dilution and plating. Experiments were repeated three times with similar results.

2.5 Cell death assays

2.5.1 Expression constructs used in cell death assay

NLR immune receptor *R1* was amplified from genomic DNA of *Solanum demissum* with primers listed in Table 2.6, and then cloned into pK7WG2 by using Gateway cloning kit (Invitrogen). *AVR1* was amplified from genomic DNA of *P. infestans* T30-4 with primers listed in Table 2.6 and then cloned into pK7WGF2 by using Gateway cloning kit (Invitrogen). Sw5b (NCBI_AAG31014.1) (Brommonschenkel et al., 2000; Spassova et al., 2001) and NSm (NCBI_S58512.1) of TSWV (*Tomato spotted wilt virus*) (Hallwass et al., 2014; Peiro et al., 2014) were synthesized by GENEWIZ as Golden Gate level 0 modules and then subcloned into binary vector pICSL86977 (TSL SynBio). Tomato NLR *CNL-11990* was amplified from tomato (cv. Moneymaker) cDNA with the primers listed in Table 2.6 and then cloned into pICH86988 by Golden Gate cloning (Weber et al., 2011). Information on other constructs used in the cell death assay are summarised in Table 2.7.

2.5.2 Cell death assay in *NRC*-silenced *N. benthamiana*

Transient expression of NLR immune receptors and corresponding effectors (or other proteins that induce cell death) were performed according to methods described previously (Bos et al., 2006). Briefly, four to five-week-old *N. benthamiana* plants (i.e. two to three weeks after virus inoculation) were infiltrated with *A. tumefaciens* stains carrying the expression vector of different

proteins indicated. *A. tumefaciens* suspensions were adjusted in infiltration buffer (10 mM MES, 10 mM $MgCl_2$, and 150 μM acetosyringone, pH5.6) to the density as indicated in Table 2.7. The hypersensitive response (HR) cell death phenotype was scored at 7 dpi, according to a previously described scale, which was modified from 0 (no HR observed) to 7 (confluent necrosis) (Segretin et al., 2014).

Table 2. 6 List of primers used for NLR and AVR cloning

Primer name	Sequence (5'-3')	Usage in this study	Reference
R1_F_CACC	*CACCATGAATTTCAACAATGAATTGTCTGATC TG*	Cloning of R1	This study
R1_dHMA_R2	*CTATCTTATTTCTGCAAGAATATTTTTTAC*	Cloning of R1	This study
Avr1_Pentry_F	*CACCGTGTCGAAATTGCCGTCG*	Cloning of AVR1	This study
Avr1_Pentry_R	*TTAAAATGGTACCACAACATGTCCACC*	Cloning of AVR1	This study
CNL11990_GG_F	*AATTGGTCTCTAATGGCAGCTTATAGTGCTGT AATTTC*	Cloning of CNL11990	This study
CNL11990_GG_R	*AATTGGTCTCTAAGCTTAGTTCCTGTAATTAT AGATGTCGAC*	Cloning of CNL11990	This study
CNL11990_D474V_G G_R	*AATTGGTCTCTAACATGTATTCCACATGCTTT TATCTC*	Mutagenesis of CNL11990	This study
CNL11990_D474V_G G_F	*AATTGGTCTCATGTTATACTGCGCGAGTTCTG TTTGATT*	Mutagenesis of CNL11990	This study

2.5.3 Complementation assay of cell death

For the complementation assay of cell death in the *NRC*-silenced background, suspensions of *A. tumefaciens* containing empty vector or expression construct of synthetic *NRC2, NRC3, or NRC4* were adjusted to OD_{600} of 0.6 and co-infiltrated with the *A. tumefaciens* strains carrying the expression constructs indicated. The hypersensitive response (HR) was scored at 7 days after infiltration from 0 (no cell death observed) to 7 (confluent necrosis). To examine the protein accumulation of synthetic NRC variants, tomato and *N. benthamiana* NRCs were subcloned into pK7WGF2 or pICH86966 with N-terminal GFP fusion, or into pICH86988 with C-terminal myc fusion (Karimi et al., 2002; Weber et al., 2011). Three days after agroinfiltration in control or

NRC-silenced leaves, total plant proteins were extracted and analysed by immunoblot analysis according to methods described below.

Table 2. 7 List of constructs used in the cell death assays

Protein name	Vector backbone	Concentration (OD_{600})	Reference
Rpi-blb2	pK7WGF2	0.2	(Bozkurt et al., 2011)
AVRblb2	pGWB12	0.1	(Bozkurt et al., 2011; Oh et al., 2009)
Mi-1.2^{T557S}	pCTAPi	0.8	(Lukasik-Shreepaathy et al., 2012)
Sw5b	pICSL86977	0.6	This study and Spassova et al. (2001)
NSm	pICSL86977	0.6	This study and Hallwass et al. (2014)
R8	pBINPLUS	0.1	(Vossen et al., 2016)
AVR8	pK7WG2	0.05	(Vossen et al., 2016)
R1	pK7WG2	0.2	This study and Ballvora et al. (2002)
AVR1	pK7WGF2	0.1	This study and Du et al. (2015b)
Pto	pTFS40	0.6	(de Vries et al., 2006; Rathjen et al., 1999)
AvrPto	pTFS40	0.1	(de Vries et al., 2006; Rathjen et al., 1999)
Rx	pBI	0.1	(Lu et al., 2003; Tameling and Baulcombe, 2007)
CP	pBIN61	0.05	(Tameling and Baulcombe, 2007)
Bs2	pMD1	0.2	(Tai et al., 1999)
AvrBs2	pMD1	0.1	(Tai et al., 1999)
CNL-11990^{D474V}	pICH86977	0.4	This study
Rpi-vnt1	pGRAB	0.1	(Foster et al., 2009; Pel et al., 2009)
AVRvnt1	pK7WG2	0.05	(Pel, 2010)
R2	pDEST	0.3	(Lokossou et al., 2009)
AVR2	pK7WGF2	0.2	(Saunders et al., 2012)
Rpi-blb1	pBINPLUS	0.6	(van der Vossen et al., 2003; Vleeshouwers et al., 2008)
AVRblb1	pK7WGF2	0.6	(Vleeshouwers et al., 2008)
R3a	pCB302	0.3	(Bos et al., 2006)
AVR3a^{KI}	pK7WG2	0.2	(Bos et al., 2006)
BS4	pGWB20	0.4	(Schornack et al., 2004)
AvrBs3	pK7WG2	0.4	(Schornack et al., 2004)
Cf-4	pK7WGF2	0.4	(Liebrand et al., 2012)
AVR4	pAVR4	0.4	(Van der Hoorn et al., 2000)
INF1	pCB302	0.3	(Bos et al., 2006)

2.6 Phylogenetic analysis

2.6.1 Phylogenetic analysis of the NRC family

Protein sequences of *N. benthamiana* NRC2, NRC3 and NRC4 were used to identify the homologs from predicted protein databases (*N. benthamiana* Genome v0.4.4 predicted protein, Tomato proteins ITAG release 2.40, and Potato ITAG release 1 predicted proteins) on Solanaceae Genomics Network (SGN). The BLAST search results were compared to the previously published phylogeny (Andolfo et al., 2014), which revealed that the top hits of our BLASTP search results are all in the CNL-14 in the phylogenetic tree of solanaceous NLRs. We thus referred to this clade as the NRC family and combined all the candidate sequences in this clade for generating a phylogenetic tree. The protein sequences of the NRC family members were aligned by using Clustal Omega and then manually edited in MEGA7. The gaps in the alignment were deleted and only the NB-ARC domains were used for producing the phylogenetic tree (Fig. A2.1). The maximum-likelihood phylogenetic tree of the NRC family was built using MEGA7 (Kumar et al., 2016) with Jones-Taylor-Thornton (JTT) substitution model and bootstrap values based on 1000 iterations.

2.6.2 Phylogenetic analysis of solanaceous NLR

NLR-parser was used to identify the NLR sequences from the predicted protein databases of tomato, potato, *N. benthamiana*, and pepper downloaded from SGN (Tomato ITAG release 2.40, Potato PGSC DM v3.4, *N. benthamiana* Genome v0.4.4, Pepper cv CM334 v.1.55) (Steuernagel et al., 2015). In the output format of NLR-parser, the predicted NLR sequences were classified into TNL and CNL, with complete or partial NLR features. Only CNL sequences with complete NLR features were used for further phylogenetic analysis. Sequences of characterized solanaceous NLR-type resistance proteins were included as reference for the clades described in literatures (Andolfo et al., 2014). The sequences were aligned by using MAFFT and then manually edited in MEGA7 (Katoh and Standley, 2013; Kumar et al., 2016).

The gaps in the alignment were deleted manually and only the NB-ARC domains were used for generating the phylogenetic tree. The maximum-likelihood tree of the NRC family was produced using MEGA7 with JTT model and bootstrap values based on 100 iterations (Fig. 4.2 and Fig. A2.7). The resulting tree was then visualized using FigTree v1.2.4 (http://tree.bio.ed.ac.uk/software/figtree/). To simplify the phylogenetic tree, some branches were collapsed together into the same clade according to the bootstrap supports of the nodes.

2.6.3 Phylogenetic analysis of NLR from rosids, asterids and caryophyllales

The protein databases of *Arabidopsis thaliana*, soybean (*Glycine max*), strawberry (*Fragaria vesca*), cassava (*Manihot esculenta*), grape (*Vitis vinifera*) and monkey flower (*Erythranthe guttata*, synonym: *Mimulus guttatus*) were downloaded from Phytozome v10 genomes (https://phytozome.jgi.doe.gov/pz/portal.html). The protein database of tomato was downloaded from SGN as indicated above. The databases of other species, which were not included in the Phytozome website, were downloaded from the sources indicated below: kiwifruit (http://bioinfo.bti.cornell.edu/cgi-bin/kiwi/home.cgi) (Huang et al., 2013), coffee (http://coffee-genome.org) (Denoeud et al., 2014), ash tree (http://www.ashgenome.org) (Harper et al., 2016), and sugar beet (http://bvseq.molgen.mpg.de/index.shtml, RefBeet-1.2) (Dohm et al., 2014). NLR-parser was used to identify the NLR sequences from the databases of different plant species. Only CNL sequences with complete NLR features were used for further phylogenetic analysis. The sequences were aligned by using MAFFT and manually edited in MEGA7 (Katoh and Standley, 2013; Kumar et al., 2016). The gaps were removed and only the NB-ARC domains were used for phylogenetic analysis. To further confirm that kiwifruit and sugar beet have fewer sequences in the NRC-superclade compared to other asterid species, the sequences of these two species were further examined manually with BLASTP search and phylogenetic analysis. Consequently, two more sequences from sugar beet and one sequence from

kiwifruit were added into the phylogenetic analysis with other asterids and caryophyllales species. The maximum-likelihood phylogenetic trees were generated using MEGA7 (Fig. 4.6 and Fig. A2.14-17) (Kumar et al., 2016) with JTT model and bootstrap values based on 100 iterations. The resulting tree was then visualized using FigTree v1.2.4. The phylogeny of the plant species analysed here was constructed using PhyloT (http://phylot.biobyte.de) based on NCBI taxonomy.

2.7 Chimeric protein construction and functional analysis

2.7.1 Construction of chimeric proteins of NRC3 and NRC4

Protein sequences of NRC3 and NRC4 were aligned by using Clustal OMEGA, and 5 breakpoints were selected based on positions of the domain and subdomain in the sequence alignment. These 5 breakpoints divided the proteins into CC, NBD, ARC1, ARC2, LRR1-7 and LRR8-13 domains/subdomains. Subsequently, each domain/subdomain was cloned into pCR8/GW/TOPO (Invitrogen) as individual Golden Gate level 0 modules by using primers listed in Table 2.8. The CC domains of NRC3 and NRC4 were synthesized by GENEWIZ (South Plainfield, NJ, USA) to introduce synonymous substitutions as described above. The overhangs for Golden Gate cloning were designed based on the sequence of NRC3 or NRC4. The full-length chimeric constructs were assembled into binary vector pICH86988 and transformed into *A. tumefaciens* GV3101. Primers listed in Table 2.9 were used to generate level 0 modules for constructing proteins with chimeric LRR domain.

2.7.2 Functional analysis of chimeric proteins

Functional analysis of chimeric proteins was performed in the same way as the complementation assay described above. The NRC3/NRC4 chimeric proteins were co-expressed with Pto/AvrPto in a *NRC2/3*-silenced background or with Rpi-blb2/AVRblb2 in a *NRC4*-silenced background.

Expressions without the R/AVR pairs were used as controls. The hypersensitive response (HR) was scored at 7 days after infiltration from 0 (no cell death observed) to 7 (confluent necrosis). To compare the accumulation of the chimeric proteins, the constructs were subcloned into pICH86988 with C-terminal myc fusion (Karimi et al., 2002; Weber et al., 2011). Three days after agroinfiltration, total plant proteins of the infiltrated areas were extracted and analysed by immunoblot analysis.

2.8 Molecular biology methods

2.8.1 DNA methods

2.8.1.1 Gateway cloning

Gateway cloning (Invitrogen) was performed following the manufacturer's instructions. Two different entry vectors, pENTR/D-TOPO and pCR8/GW/TOPO, were used, depending on the antibiotic selection marker in the destination binary vector or the design of the whole cloning procedure. TOPO cloning reactions were performed at least 30 minutes at room temperature and then transformed into *Escherichia coli* chemical competent cells One Shot TOP10 (Invitrogen). LR reaction was performed by mixing 0.5μL LR Clonase II (Invitrogen), 100ng entry clone, and 250ng destination vector in TE buffer (pH8.0) to a final volume of 5μL. The reaction was incubated at room temperature for at least 2 hours before chemically transformed into *E. coli* One Shot TOP10 competent cells.

2.8.1.2 Golden Gate cloning

Golden Gate assembly was performed with a protocol modified from the literature (Weber et al., 2011). The restriction-ligation reactions were set up by mixing 100ng of each level 0 modules and binary vector, 2U (unit) of *BsaI* (NEB), 4U of T4 DNA ligase (Invitorgen), 1x BSA (NEB) in Invitrogen T4 DNA ligase buffer in a final volume 20μL. The reaction was incubated in a

thermocycler for 30 seconds at 37°C, followed by 50 cycles of 5min at 37°C and 5min at 20°C, and 10min at 50°C, and then 10min at 80°C. The reaction was then chemically transformed into subcloning efficiency DH5α competent cells (Invitrogen) using heat shock method or into *A. tumefaciens* GV3101 by electroporation.

Table 2. 8 List of primers used for chimeric NRC3/4 construction I

Primer name	Sequence (5'-3')	Usage in this study	Reference
GG_NRC4-NB_F	*AATTGGTCTCAACAACTCAGCAGGGTCCTGCATTG GAG*	Chimeric protein NRC4_NB	This study
GG_NRC4C-NB_R	*AATTGGTCTCTGAGGATCTGAATTGGCATAAGTAG CCAGAAC*	Chimeric protein NRC4_NB	This study
GG_NRC4-A1_F	*AATTGGTCTCTCCTCACGATCTGAAATTTTTGACTC C*	Chimeric protein NRC4_ARC1	This study
GG_NRC4C-A1_R	*AATTGGTCTCTTTATAAGATGCTGAACCACATTTCT CTCAAC*	Chimeric protein NRC4_ARC1	This study
GG_NRC4-A1_R	*TTAAGGTCTCTTATAAAGATGCTGAACCACATTTCT CTCAAC*	Chimeric protein NRC4_ARC1	This study
GG_NRC4-A2_F	*AATTGGTCTCTTATACGAATAGCGAAGAAAGCTGCT TG*	Chimeric protein NRC4_ARC2	This study
GG_NRC4C-A2_R	*AATTGGTCTCTGCCCTAGACTGACTTCTTGAAAAAG CCATTTG*	Chimeric protein NRC4_ARC2	This study
GG_NRC4-A2_R	*TTAAGGTCTCTGTGTTAGACTGACTTCTTGAAAAAG CCATTTG*	Chimeric protein NRC4_ARC2	This study
GG_NRC4-LRR1_F	*AATTGGTCTCAACACCTGATCAAGCCATTCCTATTG AA*	Chimeric protein NRC4_LRR1-7	This study
GG_NRC4C-LRR1_R	*AATTGGTCTCCCGTCCTTGTAAGCACCAAGAAAAG CTGCCAT*	Chimeric protein NRC4_LRR1-7	This study
GG_NRC4-LRR1_R	*TTAAGGTCTCCCACCCTTGTAAGCACCAAGAAAAG CTGCCAT*	Chimeric protein NRC4_LRR1-7	This study
GG_NRC4-LRR2_F	*AATTGGTCTCGGGTGGAATCAACAATCTTGTAGAG CTT*	Chimeric protein NRC4_LRR8-13	This study
NbNRC4_R	*ATTGGTCTCTAAGCTTACTGTGTGGCCTTGGATCCA GCT*	Chimeric protein NRC3_LRR8-13	This study
GG_NbNRC3sm_F	*AATTGGTCTCGAGGAAGGTCCCTGTAGTTGAGGAA G*	Chimeric protein NRC3_NB	This study
GG_NRC3B-NB_R	*AATTGGTCTCTGAGGTTTATCGTTGCAAGACTTAGC CACATTG*	Chimeric protein NRC3_NB	This study
GG_NRC3-A1_F	*AATTGGTCTCACCTCATGATCTAAAGTTTTTGACTG AA*	Chimeric protein NRC3_ARC1	This study
GG_NRC3B-A1_R	*AATTGGTCTCGTATAGAGGTGCTCACCCACACTGT CAGCCAC*	Chimeric protein NRC3_ARC1	This study
GG_NRC3-A1_R	*AATTGGTCTCGTTATGAGGTGCTCACCCACACTGT CAGCCAC*	Chimeric protein NRC3_ARC1	This study
GG_NRC3-A2_F	*AATTGGTCTCCATAAATAGAGATCCAGAGAACTGCA AG*	Chimeric protein NRC3_ARC2	This study
GG_NRC3B-A2_R	*AATTGGTCTCGGTGTTCGTTTGATTTCTTGGAATAG ATTTTC*	Chimeric protein NRC3_ARC2	This study
GG_NRC3-A2_R	*AATTGGTCTCGGCCCTCGTTTGATTTCTTGGAATAG ATTTTC*	Chimeric protein NRC3_ARC2	This study
GG_NRC3-LRR1_F	*AATTGGTCTCAGGGCAAGAACATTCTTTTCCAGAGA AAC*	Chimeric protein NRC3_LRR1-7	This study
GG_NRC3-LRR1_R2	*AATTGGTCTCCCGTCCTTACTGGTTTCTAGAAGTGC ATCTAT*	Chimeric protein NRC3_LRR1-7	This study
GG_NRC3B-LRR1_R2	*AATTGGTCTCCCACCCTTACTGGTTTCTAGAAGTGC ATCTAT*	Chimeric protein NRC3_LRR1-7	This study
GG_NRC3-LRR2_F	*AATTGGTCTCGGACGGGTCCAGTTCTGGTTTGTTC AGC*	Chimeric protein NRC3_LRR8-13	This study
NbNRC3_R	*ATTGGTCTCTAAGCTTACAATCCGAGATCTGGAGG AAAT*	Chimeric protein NRC3_LRR8-13	This study

Table 2. 9 List of primers used for chimeric NRC3/4 construction II

Primer name	Sequence (5'-3')	Usage in this study	Reference
GG_NRC4C_LRR1.1R	*AATTGGTCTCAGTTTTTTGGAGAGGAAGTCTTTCAAATT*	Chimeric protein NRC4_LRR	This study
GG_NRC4C_LRR1.2R	*AATTGGTCTCAAGGGAAACGCTTTGTGAATGAGTTTAATG*	Chimeric protein NRC4_LRR	This study
GG_NRC4C_LRR1.3R	*AATTGGTCTCAATTTGTTAAAATCCTTTGAGAAGAGAAAT*	Chimeric protein NRC4_LRR	This study
NRC4C_LRR1.5R	*AATTGGTCTCATGTCTGCTTTTACATCAAGGGTGGACTCT*	Chimeric protein NRC4_LRR	This study
GG_NRC4C_LRR1.6R	*AATTGGTCTCTAAACTTCTTTCTCGCAACTTTCCGGTGCA*	Chimeric protein NRC4_LRR	This study
GG_NRC4C_LRR2.8R	*AATTGGTCTCTATGCTTGAGGGAGGTGAGGTGCTTTATTC*	Chimeric protein NRC4_LRR	This study
GG_NRC4C_LRR2.9R	*AATTGGTCTCAATAGTTTATCTGCCTCACTCCAAGCAAACC*	Chimeric protein NRC4_LRR	This study
GG_NRC4_LRR2.13F	*AATTGGTCTCTGAGCTGGCTAATTTATCTGACCTTTATG*	Chimeric protein NRC4_LRR	This study
GG_NRC4_LRR2.12F	*AATTGGTCTCTTCGGAGATTAACTTCCCCGTGCTTAGG*	Chimeric protein NRC4_LRR	This study
GG_NRC3_LRR1.2_F	*AATTGGTCTCAAAACCCTTTGCTGAACATGTTAGG*	Chimeric protein NRC3_LRR	This study
GG_NRC3_LRR1.3_F	*AATTGGTCTCTCCCTTGCTTAGGGTACTCGATGCT*	Chimeric protein NRC3_LRR	This study
GG_NRC3_LRR1.4_F	*AATTGGTCTCCAAATTATTCCATTTGAGGTACATT*	Chimeric protein NRC3_LRR	This study
GG_NRC3_LRR1.6_F	*AATTGGTCTCAGACATTTGGAATATGACAAGATTA*	Chimeric protein NRC3_LRR	This study
GG_NRC3_LRR1.7_F	*AATTGGTCTCAGTTTTTACTAGAACTCCTAATCTC*	Chimeric protein NRC3_LRR	This study
GG_NRC3_LRR2.9_F	*AATTGGTCTCAGCATATATTTTTCCTCAGAAGCTA*	Chimeric protein NRC3_LRR	This study
GG_NRC3_LRR2.10_F	*AATTGGTCTCTCTATTAGAGTACCTTGAAGTGCTG*	Chimeric protein NRC3_LRR	This study
GG_NRC3B_LRR2.12R	*AATTGGTCTCAGCTCAGCTGGTAGTTCCTTAAGATTATC*	Chimeric protein NRC3_LRR	This study
GG_NRC3B_LRR2.11R	*AATTGGTCTCACCGAGGCCTTCCAAGAAGATAGATCTGT*	Chimeric protein NRC3_LRR	This study
GG_NRC4_LRR1.4_R	*TTAAGGTCTCAAGGGATGGCATTGAAGTCACCTGAGATA*	Chimeric protein NRC4_LRR	This study
GG_NRC4C_LRR1.4_R	*TTAAGGTCTCAAGGAATGGCATTGAAGTCACCTGAGATA*	Chimeric protein NRC4_LRR	This study
GG_NRC4_LRR1.5_F	*AATTGGTCTCTCCCTTTGACCTTTGGTAAATTTTGG*	Chimeric protein NRC4_LRR	This study
GG_NRC4_LRR2.10_R	*TTAAGGTCTCTTGGCTTCCAAGAATCACCCGCGAATGC*	Chimeric protein NRC4_LRR	This study
GG_NRC4C_LRR2.10_R	*TTAAGGTCTCTTGGTTTCCAAGAATCACCCGCGAATGC*	Chimeric protein NRC4_LRR	This study
GG_NRC4_LRR2.11_F	*AATTGGTCTCAGCCAAAGATGGGATTTAGTGCACTC*	Chimeric protein NRC4_LRR	This study
GG_NRC3_LRR1.4_R	*AATTGGTCTCTAGGAATGGTCATAATCGAGTCAGTTGA*	Chimeric protein NRC3_LRR	This study
GG_NRC3B_LRR1.4_R	*AATTGGTCTCTAGGGATGGTCATAATCGAGTCAGTTGA*	Chimeric protein NRC3_LRR	This study

Table 2. 9 List of primers used for chimeric NRC3/4 construction II (continued)

Primer name	Sequence (5'-3')	Usage in this study	Reference
GG_NRC3_LRR 1.5_F	*AATTGGTCTCTTCCTACAAACATTGGGAATCTTT GG*	Chimeric protein NRC4_LRR	This study
GG_NRC3_LRR 2.10_R	*AATTGGTCTCCTGGTTCCCACGACTGTCCCCTA AACGC*	Chimeric protein NRC4_LRR	This study
GG_NRC3B_LR R2.10_R	*AATTGGTCTCCTGGCTCCCACGACTGTCCCCTA AACGC*	Chimeric protein NRC4_LRR	This study
GG_NRC3_LRR 2.11_F	*AATTGGTCTCAACCAGAGGATAGTGGTTTTCCT CGTC*	Chimeric protein NRC4_LRR	This study
NbNRC3_ns_R	*ATTGGTCTCTCGAATACAATCCGAGATCTGGAG GAAAT*	Chimeric protein NRC4_LRR	This study
NbNRC4_ns_R	*ATTGGTCTCTCGAATACTGTGTGGCCTTGGATC CAGCTTCA*	Chimeric protein NRC4_LRR	This study

2.8.1.3 Traditional cloning

Traditional cloning was performed with restriction enzymes from NEB (New England Biolabs) and T4 DNA ligase from Invitrogen according to the manufacturer's instructions. The digested fragments were purified using QIAquick Gel Extraction Kit (Qiagen). The ligation reaction was performed at room temperature overnight and transformed into *A. tumefaciens* GV3101 by electroporation.

2.8.1.4 Bacterial transformation

Transformations of One Shot TOP10 and subcloning efficiency and DH5α chemically competent cells were performed according to the manufacturer's instructions (Invitrogen). Ligation products were mixed with competent cells and incubated on ice for 15 minutes. Cells were then subjected to heat shock at 42°C for 45 second (TOP10) or 30 second (DH5α), and left on ice for 2 minutes. SOC medium (Invitrogen) 250μL were added to the cells and incubated at 37°C for 45 minutes. The cells were plated on LB agar plates with appropriate antibiotics (kanamycin 50μg/mL or spectinomycin 50μg/mL) and incubated at 37°C overnight. Electroporation of *A. tumefaciens* was performed using an electroporation cuvette with 1 mm width and a Biorad electroporator with the following settings: voltage = 1.8kV, capacitance = 25μF, resistance = 200Ω. Immediately after the electroporation, 1mL LB

medium was added to the electroporated cells and incubated at 28°C for an hour. The cells were plated on LB agar plates with appropriate antibiotics (kanamycin 50µg/mL with rifampicin 100µg/mL or spectinomycin 50µg/mL with rifampicin 100µg/mL) and incubate at 28°C overnight.

2.8.1.5 Colony PCR and plasmid preparation

Colony PCR was performed using DreamTaq DNA polymerase according to manufacturer's instructions (ThermoFisher Scientific). Plasmid extraction was performed using QIAprep Spin Miniprep Kit according to manufacturer's instructions (Qiagen).

2.8.2 RNA methods

2.8.2.1 RNA extraction

Plant total RNA was extracted using RNeasy Mini Kit (Qiagen) according to manufacturer's instructions. DNA contamination in the RNA sample was removed by on-column digestion with RNase-Free DNase Set (Qiagen) according to the manufacturer's instructions.

2.8.2.1 cDNA synthesis

For cDNA synthesis, 2 µg of RNA was subjected to first strand cDNA synthesis using Ominiscript RT Kit (Qiagen) with RNaseOUT™ Recombinant Ribonuclease Inhibitor (Invitrogen) according to the manufacturer's instructions.

2.8.3 Protein methods

2.8.3.1 Plant total protein extraction

Proteins were expressed in *N. benthamiana* leaves and collected as indicated above. The leaves were grounded into fine powder in liquid nitrogen

with mortars and pestles. For protein extraction, 1g of plant tissue was mixed together with 2mL GTEN protein extraction buffer (150 mM Tris-HCl, pH7.5, 150 mM NaCl, 10% (w/v) glycerol, 10 mM EDTA with freshly added 10 mM dithiothreitol, 2% (w/v) polyvinylpolypyrrolidone, 1% (v/v) protease inhibitor cocktail (Sigma), and 0.2% (v/v) Nonidet P-40). After centrifugation at13000rpm at 4°C for 10 minutes, the supernatants were mixed with protein loading dye (5X final concentration: bromophenol blue 0.2%(w/v), Tris-HCl (pH6.8) 200 mM, Glycerol 2.5% (v/v), and SDS 4% (w/v)) and incubated at 70°C for 10 minutes before electrophoresis with SDS-PAGE.

2.8.3.2 SDS-PAGE electrophoresis

Homemade 10% SDS-PAGE or commercial 4-20% SDS-PAGE (Bio-Rad) were used for protein electrophoresis in Tris-glycine buffer (25 mM Tris, 250 mM glycine pH8.3, 0.1% (w/v) SDS) for 1.5 hours at 150V. PageRuler Plus (Fermentas) was used as protein size marker.

2.8.3.3 Immunoblot analysis

Following the SDS-PAGE electrophoresis, the proteins were transferred on to a PVDF membrane using Trans-Blot Turbo Transfer System (Bio-Rad) according to the manufacturer's instructions. Immunoblot analysis was performed according to a protocol described previously (Win et al., 2011). Anti-GFP (A11122, Invitrogen), anti-RFP (5F8, Chromotek, Munich, Germany), or anti-myc (A-14, Santa Cruz Biotechnology) were used as primary antibodies, and anti-rabbit or anti-rat antibody conjugated to horseradish peroxidase (Sigma-Aldrich) were used as secondary antibodies. Pierce ECL Western Blotting Substrate (ThermoFisher Scientific) or SuperSignal West Femto Maximum Sensitivity Substrate (ThermoFisher Scientific) and X-ray film (Fuji) were used for detection of chemifluorescence. SimplyBlue SafeStain (Invitrogen) was used for coomassie blue staining.

Chapter 3: Helper NLR proteins NRC2a/b and NRC3 but not NRC1 are required for *Pto*-mediated cell death and resistance in *Nicotiana benthamiana*[1]

3.1 Introduction

Plants defend against pathogens using both cell surface and intracellular immune receptors (Dodds and Rathjen, 2010; Win et al., 2012). Plant cell surface receptors include receptor-like kinases (RLKs) and receptor-like proteins (RLPs), which respond to pathogen-derived apoplastic molecules (Boller and Felix, 2009; Thomma et al., 2011). In contrast, plant intracellular immune receptors are typically nucleotide-binding leucine-rich repeat (NB-LRR or NLR) proteins, which respond to translocated effectors from a diversity of pathogens (Bonardi et al., 2012; Eitas and Dangl, 2010). These receptors engage in microbial perception either by directly binding pathogen molecules or indirectly by sensing pathogen-induced perturbations (Win et al., 2012). However, the signalling events downstream of pathogen recognition remain poorly understood.

In addition to their role in microbial recognition, some NLR proteins contribute to signal transduction and/or amplification (Bonardi et al., 2011; Cesari et al., 2014b; Gabriels et al., 2007). An emerging model is that NLR proteins often function in pairs, with "helper" proteins required for the activity of "sensors" that mediate pathogen recognition (Bonardi et al., 2012; Bonardi et al., 2011). Among previously reported NLR helpers, NRC1 (NB-LRR protein required for HR-associated cell death 1) stands out for having been reported as a signalling hub required for the cell death mediated by both cell surface

[1] Most parts of this chapter have been published in the following literature:
Wu, C.H., K. Belhaj, T.O. Bozkurt, M.S. Birk, and S. Kamoun. 2016. Helper NLR proteins NRC2a/b and NRC3 but not NRC1 are required for *Pto*-mediated cell death and resistance in *Nicotiana benthamiana. New Phytol*. 209:1344-1352.
The permission to reuse the contents is under the licence number 3954170412971 (Copyright Clearance Center Inc., U.S.).

immune receptors, such as Cf-4, Cf-9, Ve1, and LeEix2, as well as intracellular immune receptors, namely Pto, Rx, and Mi-1.2 (Fradin et al., 2009; Gabriels et al., 2006; Gabriels et al., 2007). Although most of these studies were done in *N. benthamiana*, the genome sequence and putative homologs in this species were not take into account, and thus it remains questionable whether *NRC1* is indeed required for the reported phenotypes in *N. benthamiana*.

Functional analysis of NRC1 in *N. benthamiana* was performed using virus-induced gene silencing (VIGS), a method that is popular for genetic analyses in several plant systems (Burch-Smith et al., 2004; Gabriels et al., 2007). Although commonly used, VIGS experiments can sometimes produce unreliable results as the technique can result in off-target silencing (Senthil-Kumar and Mysore, 2011). Furthermore, heterologous gene fragments from other species (e.g. tomato) have been frequently used to silence homologs in *N. benthamiana*, particularly in studies that predate the availability of the *N. benthamiana* genome (Burton et al., 2000; Gabriels et al., 2006; Gabriels et al., 2007a; Lee et al., 2003; Liu et al., 2002b; Oh et al., 2010; Senthil-Kumar et al., 2007). This strategy has been successful in characterising the function of many genes, yet the targets, off-target effects, and corresponding phenotypes may require further careful examination. In the studies about NRC1, a fragment of a tomato gene corresponding to the LRR domain was used for silencing in *N. benthamiana* (Gabriels et al., 2006; Gabriels et al., 2007). Further functional studies of *NRC1* were performed in *N. benthamiana* based on the conclusion from previous VIGS experiments (Sueldo, 2014; Sueldo et al., 2015), even though the corresponding homolog in *N. benthamiana* was not validated. Given that a draft genome sequence of *N. benthamiana* has been generated (Bombarely et al., 2012) and silencing prediction tools have become available (Fernandez-Pozo et al., 2015), we can now design more accurate VIGS assays and thus revisit previously published studies to tease apart the validity of previously reported phenotypes.

In aiming to clarify the role of *NRC1* in *N. benthamiana*, two questions arise. First, is there a *NRC1* ortholog in *N. benthamiana*? Second, does

silencing of *NRC1* ortholog in *N. benthamiana* cause the reported phenotypes? To address these questions, I investigated *NRC1*-like genes in solanaceous plants using a combination of genome annotation, phylogenetics, and gene silencing followed by genetic complementation experiments. I discovered that a close ortholog of tomato NRC1 is missing in *N. benthamiana*. However, three paralogs of *NRC1*, termed *NRC2a, NRC2b* and *NRC3*, were identified. These three NRC homologs redundantly contribute to the hypersensitive cell death and resistance mediated by Pto/Prf. Silencing of *NRC2a/b* and *NRC3* does not compromise the cell death triggered by Rx and Mi-1.2. *NRC2a/b* and *NRC3* only weakly contribute to the hypersensitive cell death triggered by Cf-4. Our results highlight the importance of applying genetic complementation assays to accurately determine gene function and eliminate off target effects in RNA silencing experiments.

3.2 Results and Discussion

3.2.1 NRC1 and related NLR proteins form a complex family in solanaceous plants

To identify putative homologs of NRC1 in *N. benthamiana*, potato, and tomato genomes, I performed a BLASTP (Altschul et al., 1990) search against the predicted protein databases in Sol Genomics Network (SGN) using the polypeptide sequence of tomato NRC1 (Solyc01g090430) as a query. Phylogenetic analyses and sequence comparisons of the top protein hits indicated that the NRC family is composed of at least three subclades (NRC1-3) belonging to clade CNL-14 described by Andolfo *et al*. (2014). This NRC/CNL-14 clade is distinct from a previously described clade CC_R/CNL-RPW8, which includes helper NLRs ADR1 and NRG1 (Andolfo et al., 2014; Collier et al., 2011). Surprisingly, a *N. benthamiana* ortholog was missing in the NRC1 subclade and a tomato ortholog was also missing in the NRC3 subclade.

To determine whether the missing sequences are due to misannotation in the tomato and *N. benthamiana* genomes, I searched all the available

nucleotide and protein databases of *N. benthamiana* and tomato in SGN with representative NRC sequences. I could not identify sequences that show high similarity to tomato NRC1 in *N. benthamiana* databases, even after searching scaffolds and contigs sequences in both SGN and the *Nicotiana benthamiana* genome database (www.benthgenome.com) (Naim et al., 2012; Nakasugi et al., 2014). Therefore, I concluded that *NRC1* is probably missing in the *N. benthamiana* genome, although it may have been somehow omitted from the assembly. In contrast, by doing TBLASTN search, I detected a misannotated tomato gene in contig SL2.40ct02653 with high similarity to potato NRC3. Based on sequence comparisons, this gene has three exons and two introns; the first two exons were annotated as Solyc05g009630, whereas the third exon was missing in the annotation (Fig. A1.1). To validate the sequence and expression of tomato *NRC3*, I designed primers based on our predicted full-length sequence and performed PCR using tomato cDNA and genomic DNA as template. I successfully amplified a fragment from genomic DNA and cDNA (Fig. A1.1). The amplified cDNA fragment was cloned and sequenced. The protein sequence identity between this cloned fragment and potato NRC3 is 95%, consistent with our interpretation that the encoding gene is the *NRC3* ortholog in tomato (Fig. A1.1).

Phylogenetic analysis that includes the newly identified tomato NRC3 revealed that the sequences in the NRC family fall into three subclades that are supported by robust bootstrap values (Fig. 3.1). Pairwise comparisons indicated that protein sequences from the same subclade have at least 78% sequence identity (Fig. 3.1, Fig. A1.2 and Table A1.1). According to the genome information of potato and tomato, sequences in these three clades are located on three different chromosomes (Fig. 3.1), consistent with the view that genes within the same NRC subclade are orthologs.

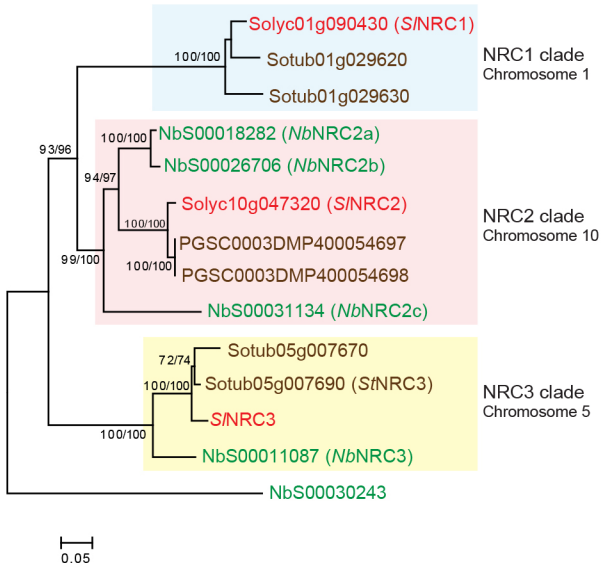

Figure 3. 1 Phylogenetic tree of NRC homologs in solanaceous plants

Top hits of BLASP search with tomato NRC1 (*Sl*NRC1) protein sequence were analysed in MEGA6 to generate Neighbour-joining (NJ) and Maximum-likelihood (ML) trees. Chromosome assignments are based on the potato and tomato genomes. Numbers at branches indicate bootstrap support values (1000 replicates) with NJ/ML methods at each node, and branch lengths indicate the evolutionary distance in amino acid substitution per site. Sequences from tomato (Solyc-), potato (Sotub-, PGSC-) and *N. benthamiana* (NbS-) are marked in red, brown and green, respectively.

3.2.2 Silencing of NRC family members suppresses cell death mediated by Pto

I exploited the *N. benthamiana* genome sequence and associated gene silencing target prediction tool (SGN VIGS tool; http:// http://vigs.solgenomics.net) to analyse the specificity of the *NRC1* VIGS fragment that was used in the *NRC1* VIGS experiments (Gabriels et al., 2007). I found that the tomato *NRC1* (*SlNRC1*) fragment, which matches the LRR domain, would most probably target the *N. benthamiana* genes *NbNRC2a/b* and *NbNRC2c*, and possibly *NbNRC3*. Based on pairwise sequence comparisons, this *SlNRC1*-LRR fragment has 70-80% sequence identity to *NbNRC2a/b/c* and *NbNRC3* (Fig. A1.3). This prompted us to test the degree to which silencing of the individual *NRC2a/b*, *NRC2c* or *NRC3* genes could

suppress the cell death mediated by different immune receptors. To design specific silencing constructs for individual *NbNRC* paralogs, I analysed the *NbNRC* sequences with the VIGS tool (Fernandez-Pozo et al., 2015). The 5' coding regions of each gene provided the highest silencing specificity and were selected to generate new gene silencing constructs. *N. benthamiana* plants were subjected to VIGS and challenged with the cell death triggered by immune receptors Pto, Rx, and Mi-1.2. Silencing of *NRC2a/b* or *NRC3* moderately but significantly reduced the cell death mediated by Pto but not Rx and Mi-1.2 (Fig. 3.2A). Semi-quantitative RT-PCR indicated that silencing with these VIGS constructs reduced the expression of the targeted gene with no detectable effects on the other paralogs (Fig. 3.2C).

Given that silencing of *NRC2a/b* and *NRC3* both partially compromised Pto-mediated cell death, I hypothesised that *NRC2a/b* and *NRC3* may be functionally redundant for Pto-mediated responses. I combined the two *NRC2a/b* and *NRC3* silencing fragments in one construct with the aim of obtaining co-silencing effect. Interestingly, the double-silencing construct that targets both *NRC2a/b* and *NRC3* dramatically suppressed Pto-mediated cell death (Fig. 3.2A, and 3.2C). Rx and Mi-1.2-mediated cell death remained unaffected by single or double *NRC*-silencing, whereas silencing *SGT1* compromised all the cell death tested in this experiment (Fig. 3.2A). These results suggest that *NRC2a/b* and *NRC3* are functionally redundant in Pto-mediated responses.

Gabriels *et al*. (2006, 2007) reported that silencing with tomato *NRC1* fragment in *N. benthamiana* reduced the cell death induced by AVR4 and INF1, which are recognised extracellularly by RLPs (Du et al., 2015a; Rivas and Thomas, 2005). I tested whether silencing of *NRC2a/b*, *NRC2c* or *NRC3* also impair cell death triggered by these proteins. However, I found that silencing of *NRC2a/b* and/or *NRC3* weakly reduced the Cf-4/AVR4 cell death but did not affect INF1-triggered cell death, whereas silencing of *SERK3* reduced both Cf-4/AVR4- and INF1- mediated cell death (Fig. 3.2B).

Our *NbNRC* silencing experiments did not fully match the results of Gabriels *et al*. (2006, 2007) given that I did not observe effects on cell death

mediated by Rx, Mi-1.2, and INF1 with any of the tested constructs (Fig. 3.2A). This prompted us to perform VIGS with the original fragment used in Gabriels *et al.* (2006, 2007) (Fig. A1.4, see also nucleotide alignment of this fragment with *NbNRCs* in Fig. A1.3). The results of our VIGS experiments revealed moderate effects on Pto and Mi-1.2 mediated cell death, but no detectable alteration of cell death mediated by Rx, Cf-4 and INF1 (Fig. A1.4). The discrepancy between our results and those of Gabriels *et al.* (2006, 2007) are striking, but could still be due to differences in experimental set up and materials used in the experiments. To summarize, I observed robust reduction of Pto-mediated cell death after silencing *NRC2a/b* and *NRC3*. I decided to focus on these genes in the follow up experiments.

3.2.3 Tomato NRC3 mediates Pto-induced cell death

To determine the tomato NRC homologs that are able to mediate Pto/Prf-activated cell death, I performed complementation experiments in *N. benthamiana* plants silenced for endogenous *NRC* genes (Fig. 3.1 and Fig. 3.2). Our motivation for this was driven by the observation that the tomato *NRC* sequences may appear divergent enough from the *N. benthamiana* orthologs to be resilient to silencing. These experiments revealed that *SlNRC3* partially rescued Pto-elicited cell death, *SlNRC2* showed weak complementation activity, and *SlNRC1* did not rescue Pto-mediated cell death (Fig. A1.5). To test whether *NbNRC* silencing affects protein accumulation of *Sl*NRC1, 2 and 3, I generated GFP-tagged *Sl*NRC1, 2 and 3 and performed immunoblot analysis. The results indicated that although the protein levels of *Sl*NRC variants were significantly reduced, the proteins were still detectable in *NRC2a/b/3*-silenced leaves (Fig. A1.5). Based on these results and the observation that the *NRC1* ortholog is missing in *N. benthamiana*, I reasoned that *NRC1* is not the gene responsible for Pto-elicited hypersensitive response.

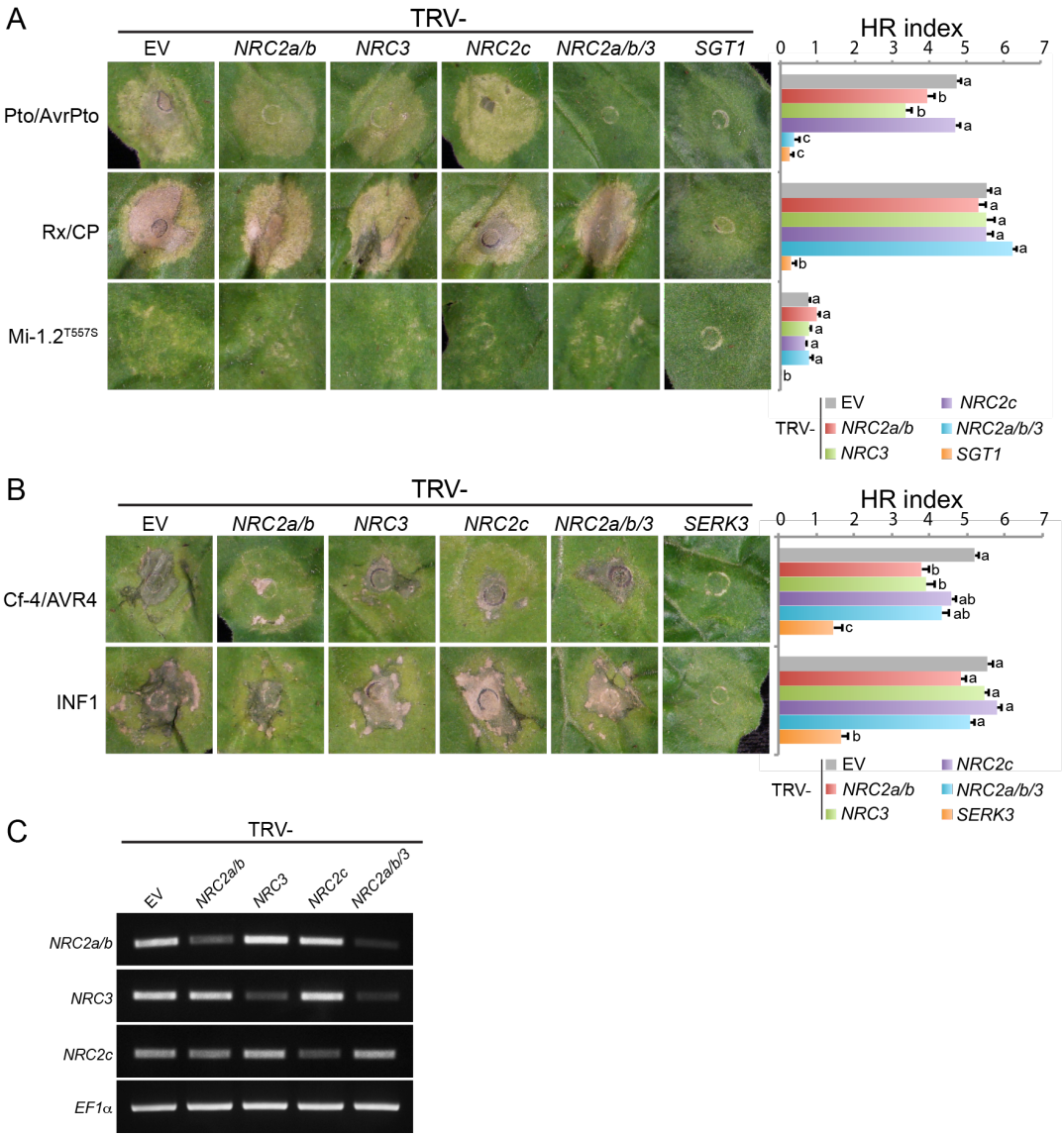

Figure 3. 2 Silencing of *N. benthamiana NRC* homologs suppress cell death mediated by Pto/AvrPto

(A and B) Immune receptors and corresponding AVR proteins, autoactive immune receptor (Mi-1.2^{T557S}), or elicitin (INF1) were transiently expressed in *N. benthamiana* leaves silenced with different *NRC* homologs. *SGT1* and *SERK3* silencing were used as control. The HR results are presented with representative images. Cell death (HR) was scored at 7 days post infiltration (dpi). Bars represent mean + SE of 24 infiltrations from one representative biological replicate. Statistical differences among the samples were analysed with ANOVA and Tukey's HSD test (p-value < 0.001). Experiments were performed at least three times with similar results. (C) Semi-quantitative RT-PCR of *NRC* silencing in *N. benthamiana*. Leaves were collected three weeks after virus inoculation. Elongation factor-1α *(EF1α*) was used as an internal control.

3.2.4 Genetic complementation with synthetic *NbNRC2a* and *NbNRC3* genes

I aimed to confirm that *N. benthamiana NRC* homologs are functionally redundant in cell death elicited by Pto. I focused on *NRC2a/b* and *NRC3*, as silencing of *NRC2c* did not yield reduction of cell death (Fig. 3.2). To achieve this, I generated synthetic variants of *NbNRC2a*, *NbNRC2b* and *NbNRC3*, termed *NbNRC2a*^{syn}, *NbNRC2b*^{syn} and *NbNRC3*^{syn}, which contain fragments with shuffled synonymous codons to render them divergent enough to evade VIGS (Fig. 3.3A, Fig, A1.6, and Fig. A1.7). Expression of *NbNRC2a*^{syn}, *NbNRC2b*^{syn} or *NbNRC3*^{syn} in *NRC2*- and *NRC3*-silenced *N. benthamiana* leaves rescued the cell death mediated by Pto, whereas the endogenous *NbNRC2a/b or NbNRC3* failed to complement the cell death phenotype (Fig. 3.3B, Fig, A1.6, and Fig. A1.7). To confirm that the synthetic variants of *NbNRC2a/b* and *NbNRC3* evade VIGS, I generated GFP-tagged *Nb*NRC2a/b and *Nb*NRC3 variants and assessed protein accumulation in *NRC2ab/3* silenced leaves. *Nb*NRC2a/b^{syn} and *Nb*NRC3^{syn} accumulated to levels similar to control treatments whereas the original *Nb*NRC2a/b and *Nb*NRC3 variants were undetectable in *NRC*-silenced leaves, indicating that the synonymous codons enabled predicted VIGS evasion (Fig. 3.3C, Fig, A1.6, and Fig. A1.7). These experiments clearly demonstrated that *NbNRC2a, NbNRC2b* and *NbNRC3* are functionally redundant and are the responsible *N. benthamiana* genes that mediate hypersensitive death following Pto perception of AvrPto.

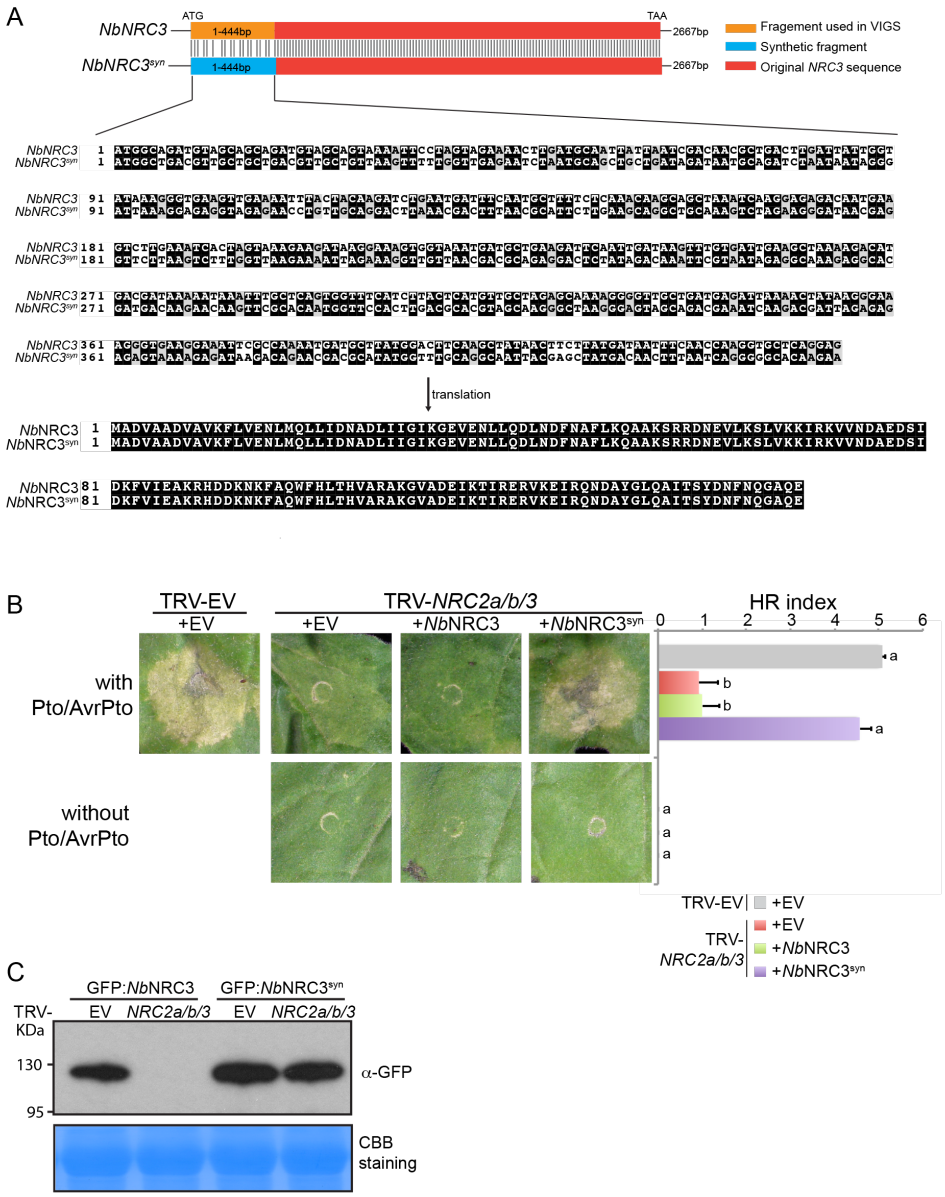

Figure 3. 3 Expression of synthetic *Nb*NRC3 rescues Pto-mediated cell death in *NRC*-silenced *N. benthamiana*

(A) Schematic representation of experimental design, DNA and protein sequences of the synthetic region. Shuffled synonymous codons were introduced into the synthetic sequence (*NbNRC3*^{syn}) without changing the identity in protein sequence. (B) Expression of *NbNRC3*^{syn} rescues the cell death of Pto/AvrPto. *NbNRC3* and *NbNRC3*^{syn} were co-expressed with Pto/AvrPto in *NRC2a/b/3*-silenced *N. benthamiana* leaves. Expression of Pto/AvrPto in VIGS control (EV), and expression of NbNRC3/NbNRC3^{syn} without Pto/AvrPto were used as controls. HR was scored at 7 days post infiltration (dpi). Bars represent mean + SE of 14 infiltrations from one biological replicate. Statistical differences among the samples were analysed with ANOVA and Tukey's HSD test (p-value < 0.001). Experiments were performed at least three times with similar results. (C) Protein accumulation of NRC3 variants in VIGS control and *NRC2a/b/3*-silenced leaves. GFP is fused to NRC3 variants at N-terminal and transiently expressed in VIGS control and *NRC2a/b/3*-silenced *N. benthamiana*. Samples were collected at 3dpi for immunoblot analysis.

3.2.5 NRC2 and NRC3 are required for *Pto/Prf*-mediated resistance in *N. benthamiana* and tomato

In the previous study, Gabriels *et al*. (2007) showed that silencing of *NRC1* does not affect Pto-mediated resistance. Since I have now identified that *NRC2a/b* and *NRC3* are the genes required for Pto-mediated cell death, I decided to test whether silencing of *NRC2a/b* and *NRC3* compromise Pto-mediated resistance. According to the literature, *Pto/Prf* transgenic *N. benthamiana* has higher resistance to *P. syringae* DC3000 compared to wild type plants (Balmuth and Rathjen, 2007). Hence, I silenced *NRC2a/b* and *NRC3* in *Pto/Prf* transgenic *N. benthamiana* (R411B), and inoculated *P. syringae* DC3000 *ΔhopQ1-1* by syringe infiltration. Quantification of bacterial growth revealed that Pto-mediated resistance is compromised in only *NRC2a/b* and *NRC3* co-silenced leaves but not in controls (Fig. 3.4A), demonstrating that *NRC2a/b* and *NRC3* are required for Pto-mediated resistance in *N. benthamiana*. The immunoblot analysis revealed that *NRC2a/b* and *NRC3* silencing does not affect the protein accumulation of Prf (Fig. 3.4B), excluding the possibility that the loss-of-resistance phenotype is due to the effect on Prf accumulation.

To further validate that *NRC2* and *NRC3* are required for *Pto/Prf*-mediated resistance in tomato, I generated VIGS constructs that target tomato *NRC2*, *NRC3* and both genes at the same time. Consistent with our observation in the *N. benthamiana* system, the population of bacteria was significantly higher when *NRC2* and *NRC3* were silenced together in tomato. Silencing of *NRC1*, *NRC2* or *NRC3* individually did not compromise Pto/Prf-mediated resistance (Fig. A1.8). Furthermore, I observed bacterial speck symptoms upon simultaneous silencing of *NRC2* and *NRC3*, but not when *NRC1*, *NRC2*, or *NRC3* were silenced individually (Fig. A1.8). These results indicate that *NRC2* and *NRC3* are functionally redundant and are required for *Pto/Prf*-mediated disease resistance in tomato.

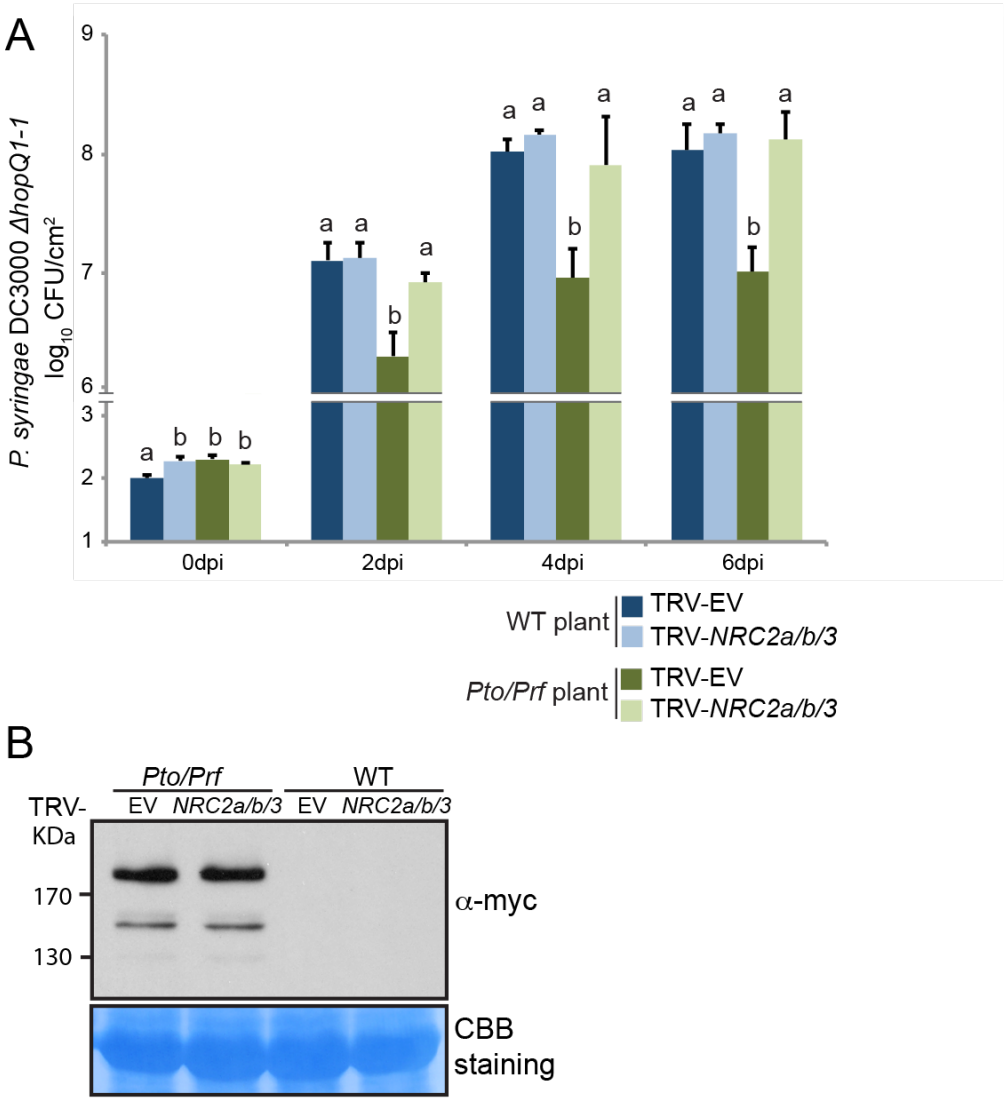

Figure 3. 4 Silencing of *NbNRC2a/b* and *NRC3* compromised *Pto/Prf*-mediated resistance

(A) Growth of *P. syringae* DC3000 *ΔhopQ1-1* in VIGS control and *NRC2a/b/3*-silenced wild type or *Pto/Prf* transgenic (R411B) *N. benthamiana.* Samples were collected at 0, 2, 4, 6 days after inoculation. Error bars indicate the standard deviation of population from four replicates in one representative biological replicate. The different letters at the top of the columns indicate statistical significant differences based on ANOVA and Tukey's HSD test (p-value < 0.05). Experiments were performed three times with similar results. (B) Protein accumulation of Prf:5myc in VIGS control *and NRC2a/b/3*-silenced leaves. Leaves of wild type or *Pto/Prf* transgenic (R411B) *N. benthamiana* were collected three weeks after virus inoculation. Accumulation of Prf:5myc was detected with α-myc antibody.

3.3 Conclusions

In summary, I revisited the role of NRC1 as a helper NLR protein and discovered that NRC2a/b and NRC3, rather than NRC1, are the essential NLR proteins required for *Pto/Prf*-mediated cell death and resistance in *N. benthamiana* and tomato. Therefore, the previously proposed model of NRC1 as a signalling hub for multiple immune receptors postulated by Gabriels *et al*. (2007) needs to be revised. In fact, the *N. benthamiana* genome appears to lack an ortholog of tomato *NRC1* (Fig. 3.1). Furthermore, although NRC2a/b and NRC3 are required for the hypersensitive cell death induced by Pto, silencing of these genes did not affect the response elicited by Rx and Mi-1.2. The previous finding of Gabriels *et al*. (2007) that silencing of *NRC1* suppresses Rx and Mi-1.2 –mediated cell death may be due to the effects on other *NRC1*-like sequences in *N. benthamiana*. I did observe that *NRC* silencing reduced the cell death induced by Cf-4 as reported earlier (Gabriels et al., 2007). However, the effect of *NRC2/NRC3* silencing is not as dramatic as in the case of Pto-mediated cell death (Fig. 3.2).

Our findings emphasize the importance of genetic complementation assays following RNA silencing experiments to minimize the risk of misinterpreting data due to off-target effects (Jonchere and Bennett, 2013; Kumar et al., 2006; Pliego et al., 2013). Genetic complementation can be performed using genes from a different species or using a silencing-resilient synthetic version of the gene with synonymous codon sequences. The complementation assay I developed should help dissecting the precise roles of complex network of NLRs and other signalling components in plant immunity. Furthermore, I recommend that genetic complementation should be applied to RNA silencing experiments whenever possible to avoid functional misidentification of gene-of-interest.

Chapter 4: A complex NLR signalling network mediates immunity to diverse plant pathogens

4.1 Introduction

Both plants and animals rely on nucleotide-binding domain leucine-rich repeat-containing proteins (NLR) to respond to invading pathogens (Duxbury et al., 2016; Ting et al., 2008). NLR proteins act as immune sensors that detect the molecular patterns or effector proteins derived from the pathogens. Upon detection of pathogens, some animal NLRs initiate downstream immune signalling through assembly of inflammasomes, a multiprotein oligomer that regulates inflammatory processes in mammal (Guo et al., 2015). The formation of inflammasomes results in activation of caspase-1 and subsequently leads to further inflammatory responses, including pyroptosis, a type of programmed cell death (Guo et al., 2015). Likewise, activation of plant NLRs typically results in a form of program cell death known as the hypersensitive response, which generally restricts pathogen invasion (Dodds and Rathjen, 2010; Jones and Dangl, 2006). However, the basic understanding of plant NLR complex formation and their mode of action remains limited.

Several recent studies demonstrated that NLRs, helper NLRs, can play essential roles in immune signalling upon pathogen detection by other NLRs, known as sensors (Bonardi et al., 2011; Cesari et al., 2014b; Kofoed and Vance, 2011; Le Roux et al., 2015; Sarris et al., 2015). Currently, there are two major models of NLR helper/sensor interactions. The first model is a “one-to-one” NLR model in which a single NLR functioning as a sensor is paired with a single helper or signal transducer NLR (Cesari et al., 2014a; Duxbury et al., 2016). For example, *A. thaliana* NLR RRS1, which senses the bacterial effectors Pop2 and AvrRps4 through an integrated WRKY domain, requires NLR RPS4 to confer hypersensitive cell death and disease resistance (Le Roux et al., 2015; Sarris et al., 2015). The rice NLR RGA5, which senses the effectors AVR-Pia and AVR1-CO39 from the rice blast fungus, requires RGA4

for mediating downstream responses (Cesari et al., 2014b). In these two cases, the helper and the sensor NLR genes are genetically linked; i.e. located next to each other on the chromosome (Narusaka et al., 2009; Okuyama et al., 2011). The second model is a “many-to-one” NLR model, in which several sensor NLRs detect different effectors from diverse pathogens but require a single helper NLR for downstream signalling. The best understood examples of this model involve the mammalian sensor NLRs NAIP2, NAIP5, and NAIP6, and the helper NLR NLRC4. NAIP2 recognises bacterial type III secretion component PrgJ, whereas both NAIP5 and NAIP6 recognise bacterial flagellin. The responses after activation of these NAIPs all require formation of NLRC4 inflammasome complexes (Kofoed and Vance, 2011; Tenthorey et al., 2014; Zhao et al., 2011). One of the most studied plant helper NLR families, and an additional example of the “many-to-one” NLR model, is the ADR1 family in *A. thaliana*. This family is composed of three functionally redundant homologs and is required for immunity mediated by multiple sensor NLRs, including RPS2, RPP4, and RPP2 (Bonardi et al., 2011). Another helper NLR in plants is NRG1, which is required for the function of the tobacco N gene, a NLR that provide resistance to TMV (Peart et al., 2005). To date, not all sensor NLRs have been linked to helper NLR partners. But the degree to which the hundreds of plant sensor NLRs that have been reported so far require helper NLRs for initiating defence responses remains unknown.

The Solanaceae family is one of the most important plant families in agriculture. This family includes several economically important crops such as potato, tomato, tobacco, and other ornamental plants. The extensive breeding efforts for improving disease resistance within this family has led to the identification of many NLR-type disease resistance genes from Solanaceae wild species (van Ooijen et al., 2007; Vleeshouwers et al., 2011). To date, more than 20 NLR-type disease resistance genes were identified from different solanaceous species, which confer resistance to infection by a diverse range of pathogens (van Ooijen et al., 2007; Vleeshouwers et al., 2011; Witek et al., 2016). In addition to their agricultural importance, the

solanaceous plants and their NLRs are a great experimental model system for understanding plant immunity. Many of the cloned solanaceous NLR genes recapitulate their disease resistance phenotypes when transformed into *N. benthamiana*, one of the most widely used model species for laboratory-based research (Goodin et al., 2008).

Genome-wide annotation and cross-species comparison of NLRs have revealed the dynamic feature of NLR genes during evolution. (Christopoulou et al., 2015; McHale et al., 2006; Meyers et al., 2003; Shao et al., 2016; Shao et al., 2014; Zhang et al., 2014). Several studies focused on the annotation and phylogenetic analysis of NLR genes from different solanaceous species suggested multiple duplication events after speciation (Andolfo et al., 2014; Andolfo et al., 2013; Jupe et al., 2012; Seo et al., 2016; Stam et al., 2016). Furthermore, recent advances in genome sequencing and associated techniques such as Ren-seq greatly accelerated the identification of NLR genes that are useful to provide disease resistance in solanaceous crops (Andolfo et al., 2014; Jupe et al., 2013; Witek et al., 2016). However, despite these advances, the degree to which phylogeny correlates with both the molecular mechanism of NLR activation and the convergence of signalling remains elusive.

In the previous chapter, I found that NRC2 and NRC3 are redundant and are required for the function of Prf/Pto complex in both *N. benthamiana* and tomato. However, whether NRC2 and NRC3 are essential for other sensor NLRs remained an open question. In this chapter, I addressed this question. I discovered another helper NLR, termed NRC4, which also belongs to the NRC family. NRC4 has a distinct function compared to NRC2/3 as it is required for immunity triggered by Rpi-blb2 and R1, but it is not required for Prf-mediated immunity. Surprisingly, NRC2, NRC3, and NRC4 are together functionally redundant and essential for many other sensor NLRs, including Rx, Bs2, Sw5b, and R8. I proposed that an NRC-dependent NLR immune signalling network with an intricate architecture mediates immunity to oomycetes, bacteria, viruses, nematodes, and insects. Furthermore, I performed an extensive phylogenetic analysis of plant NLRs to show that the

NRC network has emerged over 100 million years ago from an NLR pair that diversified to constitute up to one half of the NLRs of asterids. I reasoned that plants evolved this complex NLR network to increase evolvability and robustness of immune signalling pathways to counteract rapidly evolving plant pathogens.

4.2 Results and discussion

4.2.1 NRC4, a new member in the NRC family, is required for Rpi-blb2-mediated immunity

4.2.1a Rpi-blb2-mediated immunity is NRC4 dependent

Rpi-blb2 is a well-characterized sensor NLR that recognises members of the *P. infestans* AVRblb2 effector family and provides broad-spectrum resistance to late blight pathogen in potato, tomato as well as in *N. benthamiana* (Fig. 4.1A) (Oh et al., 2009; van der Vossen et al., 2005). Virus induced gene silencing (VIGS) assays in *N. benthamiana*, performed by collaborators Dr. Ahmed Abd-El-Haliem and Dr. Jack H. Vossen, Wageningen University, revealed that silencing of a NLR gene related to the NRC family abolishes the cell death mediated by Rpi-blb2. I defined this gene as a new member of the NRC family, termed NRC4, and followed up on these preliminary experiments using Rpi-blb2 transgenic *N. benthamiana* (Fig. A2.1). When *NRC4* was silenced in *N. benthamiana*, the resistance mediated by Rpi-blb2 was fully compromised (Fig. 4.1A). In contrast, silencing of *NRC2* and *NRC3* did not affect Rpi-blb2-mediated resistance (Fig. 4.1A; Fig. A2.2). Consistent with these results, *NRC4* silencing but not *NRC2/3* silencing abolished Rpi-blb2- mediated cell death upon recognition of the *P. infestans* effector AVRblb2 (Fig. 4.1B). To confirm that these loss-of-function phenotypes are not due to an effect on Rpi-blb2 accumulation, I performed immunoblot analysis of Rpi-blb2 in *NRC4*-silenced background. These results showed that silencing of *NRC4* does not affect Rpi-blb2 stability (Fig. A2.1d), excluding the possibility that *NRC4* VIGS fragment has off-target effects on Rpi-blb2 or somehow affects the protein accumulation indirectly. Taken

together, these results suggest that NRC4 is a new helper NLR that is required for the function of Rpi-blb2.

4.2.1b NRC4 forms a subclade distinct from NRC2 and NRC3 in the NRC family

In the previous chapter, I identified that *NRC2* and *NRC3* are required for Prf/Pto-mediated resistance in both tomato and *N. benthamiana*. To investigate how NRC4 relates to other members of the NRC family, I performed a phylogenetic analysis of NRCs from *N. benthamiana*, tomato, and potato. I found that NRC4 homologs form a well-supported subclade which is closely related to several NRC4-like (NRC4L) subclades (Fig. A2.1). In contrast, NRC4 has around only 49% identity (66% similarity) to NRC2a or NRC3, suggesting that NRC4 is relatively distant to the previously reported NRC2 and NRC3 subclades (Fig. A2.2).

To determine the expression patterns of *NRC* family members, I designed primers based on the sequence identified form *N. benthamiana* and performed PCR or RT-PCR using genomic DNA or cDNA from leaf tissues as templates. I found that most of the NRC4-like genes were not expressed apart from *NRC4L-4611* (Fig. A2.1b). The expression of *NRC4L-4611* was not affected by *NRC4* silencing (Fig. A2.3b), excluding the possibility that *NRC4L-4611* is responsible for the loss of Rpi-blb2 function phenotype described earlier. The expression of *NRC4*, *NRC2(a/b)* and *NRC3* appeared to be relatively higher than other homologs (Fig. A2.1b). Hence, I reasoned that *NRC2/3/4* are likely more important than other homologs of the NRC family in *N. benthamiana*.

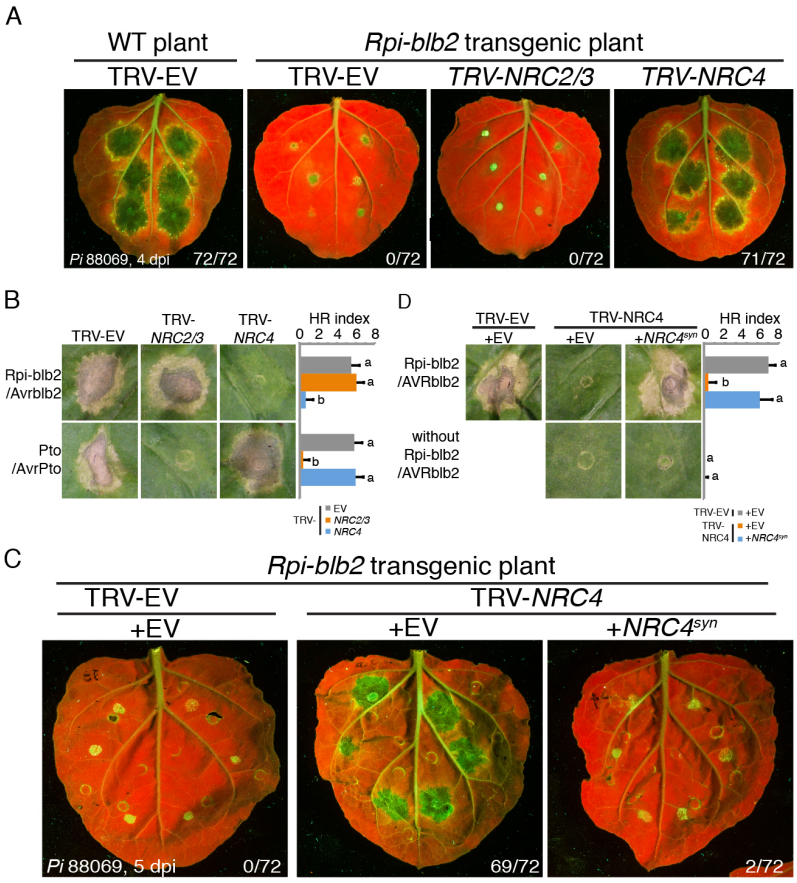

Figure 4. 1 *NRC4* is required for Rpi-blb2-mediated immunity

(A) Silencing of *NRC4* compromised Rpi-blb2-mediated resistance. *NRC2/3* or *NRC4* were silenced in *Rpi-blb2* transgenic *N. benthamiana* and then plants were inoculated with *P. infestans* 88069. Non-resistant (wild type) plants and TRV empty vector (EV) were used as controls. Experiments were repeated 3 times with 24 inoculation sites each time. The numbers on the right bottom are the sum of spreading lesion/ total inoculation sites from the three repeats. Images were taken under UV light at 4 days post inoculation (dpi). (B) Cell death assay of Rpi-blb2 and Prf (Pto/AvrPto) in *NRC2/3*-or *NRC4*-silenced plants. Rpi-blb2/AVRblb2 and Pto/AvrPto were co-expressed in *NRC2/3*- or *NRC4*-silenced plants by agroinfiltration. Hypersensitive response (HR) was scored at 7 days after agroinfiltration. Bars represent mean + SD of 24 infiltrations sites. Statistical differences among the samples were analysed with ANOVA and Tukey's HSD test (p-value < 0.001). (C) Expression of synthetic *NRC4* rescues Rpi-blb2-mediated resistance in *NRC4*-silenced plants. $NRC4^{syn}$ was expressed in *NRC4*-silenced plants through agroinfiltration one day before *P. infestans* inoculation. Experiments were repeated 3 times with 24 inoculation sites each time. The numbers on the right bottom are the sum of spreading lesion/ total inoculation sites from the three replicates. Images were taken under UV light at 5 days post inoculation (dpi). (D) Expression of synthetic *NRC4* rescues Rpi-blb2-mediated cell death in *NRC4*-silenced plants. Rpi-blb2/AVRblb2 were co-expressed with empty vector control or $NRC4^{syn}$ in *NRC4*-silenced plants through agroinfiltration. Hypersensitive response (HR) was scored at 7 days after agroinfiltration. Bars represent mean + SD of 24 infiltrations sites. Statistical differences among the samples were analysed with ANOVA and Tukey's HSD test (p-value < 0.001).

4.2.1c Expression of synthetic *NRC4* rescues Rpi-blb2-mediated immunity in *NRC4*-silenced plants

I have previously described a complementation assay with a synthetic gene that contains synonymous codons for validating gene function in silencing experiments. This also allowed me to perform further functional analysis of the gene-of-interest. I introduced synonymous substitutions into *NRC4* and tested whether this synthetic version of *NRC4*, named *NRC4^{syn}*, can rescue Rpi-blb2-mediated resistance when the chromosomal *NRC4* is silenced (Fig. A2.3a). The results of immunoblot analysis showed that *NRC4^{syn}* accumulated to similar levels with and without silencing, indicating that it is able to evade the silencing effect (Fig. A2.3c). I then tested whether transient expression of *NRC4^{syn}* in *NRC4*-silenced background can rescue Rpi-blb2-mediated resistance and cell death. The results showed that expression of *NRC4^{syn}* in the *NRC4*-silenced Rpi-blb2 plants rescued the resistance to the level similar to that in the non-silenced control plants (Fig. 3.1c). Consistent with these results, expression of *NRC4^{syn}* in the *NRC4*-silenced plant also rescued Rpi-blb2-mediated cell death (Fig. 3.1d). These results support the hypothesis that *NRC4* is essential for Rpi-blb2-mediated resistance.

4.2.1d NRC4 and Rpi-blb2 p-loops are required for the cell death mediated by Rpi-blb2

The p-loop motif in the NB-ARC domain is one of the most conserved motifs of NLRs and is essential for the function of many NLR proteins (Takken et al., 2006; Takken and Goverse, 2012). Interestingly, for RPS4/RRS1 and RGA4/RGA5 NLR pairs, only one of the p-loop in the two NLRs is essential for function (Cesari et al., 2014b; Williams et al., 2014). Furthermore, ADR1-L2 in the ADR1 helper NLR family also shows p-loop independent activity in NLR-triggered immunity (Bonardi et al., 2011). To find out whether only one of the p-loops of Rpi-blb2 or NRC4 is essential, I generated p-loop mutants of both NLRs by mutating their respective lysine (K) residues in their p-loop motifs to

arginine (R) and measured how their abilities to trigger cell death are affected. I found that the cell death-inducing activity of Rpi-blb2 was completely abolished when its p-loop is mutated, indicating that the function of Rpi-blb2 requires an intact p-loop (Fig. A2.4a and b). For the functional analysis of NRC4, I took advantage of the complementation assay with the synthetic gene I described previously. I mutated the p-loop of NRC4^{syn} and tested whether it can still rescue Rpi-blb2-mediated cell death. I found that the NRC4 variant with the p-loop mutation failed to rescue Rpi-blb2-mediated cell death in *NRC4*-silenced background (Fig. A2.4c and d), indicating that an intact p-loop is essential for the function of NRC4. These results indicated that the cell death-inducing activity of both NRC4 and Rpi-blb2 are p-loop dependent.

4.2.1e Mi-1.2, a tomato ortholog of Rpi-blb2, is also *NRC4* dependent

Mi-1.2 is an ortholog of Rpi-blb2 that provides resistance to root-knot nematode and aphids in potato. I reasoned that closely related sensor NLR immune receptors may rely on the same helper NLR to function. To test this, I expressed an autoactive form of Mi-1.2, Mi-1.2^{T557S}, in *NRC4*-silenced *N. benthamiana* and examined whether this autoactive NLR can still cause cell death. The cell death caused by Mi-1.2 ^{T557S} was completely abolished when *NRC4* was silenced, supporting the idea that close homologs of Rpi-blb2 also require NRC4 to function (Fig. A2.5).

4.2.1f. Silencing of *NRC4* does not affect Pto/Prf-mediated immunity

I have previously described that *NRC2* and *NRC3* are required for Pto/Prf-mediated resistance. To further test the hypothesis that NRC4 is representing a new member in this family and that the function is distinct from NRC2 and NRC3, I examined whether silencing of *NRC4* affects Pto/Prf-mediated cell death and resistance in *N. benthamiana*. The results showed that Pto/Prf-mediated cell death (Pto/AvrPto) was not affected by *NRC4* silencing (Fig. 3.1b); moreover, resistance to *P. syringae* also remained

unaffected when *NRC4* was silenced (Fig. A2.6). These results support the idea that NRC4 is functionally distinct from NRC2 and NRC3.

4.2.2 NRC family and NRC-dependent NLRs are in a large superclade

To gain a comprehensive overview of how the NRC family relates to other NLR families (clades) of solanaceous plants, I performed a phylogenetic analysis of Solanaceous NLRs. I first used NLR-parser to identify putative NLR sequences from four different solanaceous plants (*N. benthamiana*, potato, tomato and pepper); from this I constructed a phylogenetic tree of CNLs, together with several functional characterized solanaceous NLRs. I found that the NRC family is in a well-supported superclade (hereafter referred to as the NRC-superclade) together with several other sensor NLR clades, including clades containing Rpi-blb2, Mi-1.2 and Prf, which were demonstrated to be NRC-dependent in this study (Fig. A2.6). The NRC-superclade also contains several well-known NLRs, including Rx, Sw5b, Bs2, R8, and R1, which provide resistance to viral, bacterial, and oomycete plant pathogens (Fig. A2.7 and Fig. 2). Overall, this NRC-superclade, which includes the NRC clade and sister clades, comprises around half of the predicted CNL and more than one-third of the predicted NLR in the different species analysed here. Interestingly, half of the number of CNL-type resistance genes cloned from different solanaceous plants thus far are found within this superclade (Table A2.1).

It is very intriguing that the NRC family is in a well-supported superclade together with Rpi-blb2, Mi-1.2 and Prf, which are NRC-dependent sensor NLRs. However, it is not known whether the other sensor NLRs in this superclade also require NRC family members for their function. This prompted me to test the hypothesis that the NLRs in this superclade are also NRC dependent.

4.2.3 *NRC4* is also required for R1-mediated immunity

4.2.3a R1-mediated cell death is *NRC4*-dependent

To test whether any of the NRC2, NRC3 or NRC4 are also required for the responses mediated by other sensor NLRs, I silenced *NRC2/3* and *NRC4* independently and checked the cell death mediated by NLRs from different phylogenetic clades, including NLRs from the NRC-superclade and outside of the NRC-superclade. I did not identify any additional *NRC2/3*-dependent NLRs apart from Prf. The cell death mediated by R1, a NLR protein which provides resistance to *P. infestans*, is compromised by *NRC4* silencing (Fig. 4.2 and Fig. 4.3a). To further test the hypothesis that R1-mediated cell death is *NRC4*-dependent, I performed complementation assay with synthetic *NRC4* in the *NRC4*-silenced plants. The results showed that expression of the synthetic *NRC4* rescued R1-mediated cell death when the chromosomal *NRC4* is silenced (Fig. 4.3b)

4.2.3b R1-mediated resistance is *NRC4* dependent

To further test whether R1-mediated resistance to *P. infestans* is also *NRC4* dependent, I transiently expressed R1 in *N. benthamiana* and examined the degree to which the resistance is compromised when *NRC4* is silenced. I found that silencing of *NRC4* abolishes the resistance mediated by R1 (Fig. 4.3c), and that this phenotype can be rescued by expression of synthetic *NRC4* (Fig. 4.3d). These results demonstrate that, in addition to Rpi-blb2 and Mi-1.2, *NRC4* is also essential for R1-mediated immunity.

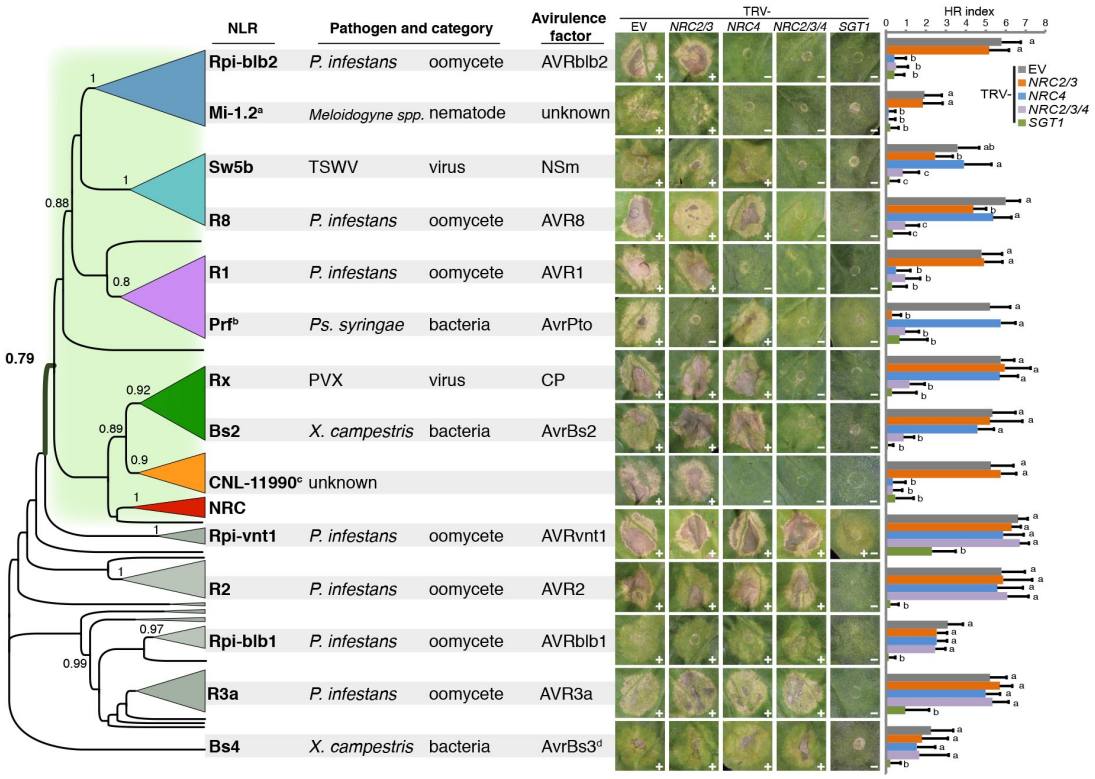

Figure 4. 2 NRCs and its sister clades form a complex signalling network

Left panel: Phylogenetic tree of NLR proteins identified from genome of solanaceous plants, simplified from Fig. A2.7. Middle panel: List of pathogen categories, name of the pathogens and avirulence factor (AVR) sensed by the corresponding NLR immune receptors. TSWV, tomato spotted wilt virus; PVX, potato virus X. Right panel: Analysis of cell death mediated by different solanaceous NLR proteins in *NRC*-silenced plants. Different NLR and AVR combinations were expressed in control, *NRC2/3*, *NRC4*, *NRC2/3/4* and *SGT1*-silenced plants by agroinfiltration. "+" indicates cell death phenotype was observed. "-" indicates cell death phenotype was compromised. Hypersensitive response (HR) was scored at 7 days after agroinfiltration. Bars represent mean + SD of 24 infiltrations sites. Statistical differences among the samples were analysed with ANOVA and Tukey's HSD test (P-value < 0.001). [a]Pathogen proteins sensed by Mi-1.2 have not been identified yet. Hence, the autoactive mutant Mi-1.2^{T557S} was used here. [b]Co-expression of Pto and AvrPto was used for testing Prf-mediated cell death. [c]CNL-11990, a CNL cloned from tomato genome, has no assigned function. The autoactive mutant CNL-11990^{D474V} was used here. [d]Bs4 sense both AvrBs3 and AvrBs4 from *X. campestris*. AvrBs3 was used here.

4.2.4 NRC-superclade members form a complex signalling network

4.2.4a Triple silencing compromises cell death mediated by NLR from the super clade

The NRC-dependent NLRs identified thus far are all in related clades within the NRC-superclade, yet not all of the NLRs in this superclade were affected by *NRC2/3* or *NRC4* silencing. I hypothesized that NRC2/3/4 could be functionally redundant for the other NLRs in this superclade, although NRC4 has only less than 50% protein sequence identity to NRC2a or NRC3 (Fig. A2.2). To test this hypothesis, I generated a VIGS construct that targets all three *NRC* homologs at the same time (Fig. A2.8). Silencing of all of the three *NRC* homologs did not cause clear developmental effects on plant growth (Fig. A2.9). I then checked the extent to which silencing of *NRC2/3/4* affected the cell death mediated by NLRs in this superclade. Silencing *NRC2/3/4* compromised cell death mediated by all the NLRs tested from the NRC-superclade, including Rx, Bs2, R8 and Sw5b (Fig. 4.2). In contrast, the activity of NLRs outside of the NRC-superclade, including Rpi-vnt1, R2, Rpi-blb1, R3a and Bs4, was not affected. Silencing of *SGT1*, which affects the cell death mediated by all the NLRs, was used as positive control (Fig. 4.2).

As one of the clades in the phylogenetic tree presented here does not contain a representative NLR-type resistance gene, I cloned a NLR from the genome of tomato, named CNL-11990, and tested whether silencing of the *NRC* homologs affected the cell death mediated by this NLR. Since there is no assigned function of CNL-11990, I generated an autoactive form of this NLR. Previously studies indicated that introducing a D to V mutation in the MHD motif in the NB-ARC domain of NLR generally leads to ligand-independent cell death. Thus I introduced this mutation into CNL-11990, resulting in CNL-11990^{D474V} that induces ligand-independent cell death (Fig. 4.2). The results indicated that silencing of *NRC4* is sufficient to abolish the cell death mediated by CNL-11990^{D474V} (Fig. 4.2), supporting the hypothesis that all of the non-NRC NLRs in the NRC-superclade are likely to be NRC-dependent.

4.2.4b. NRC2/3/4 show specificity and redundancy to different sensor NLRs in the NRC-superclade

To confirm that NRC2/3/4 display specificity to Rpi-blb2/Prf but are functionally redundant in Rx/Bs2/R8/Sw5b-mediated cell death, I performed a complementation assay in the *NRC2/3/4* triple silencing background with combination of different NRC homologs and different R/AVR pairs. I found that expression of *NRC2* and *NRC3* rescued Prf-mediated cell death but not Rpi-blb2-mediated cell death; in contrast, expression of *NRC4* rescued Rpi-blb2-mediated cell death but not Prf-mediated cell death (Fig. A2.10). Furthermore, expression of either one of the *NRC2/3/4* rescued Rx, Bs2, R8, and Sw5b-mediated cell death (Fig. A2.10), supporting the hypothesis that *NRC2/3/4* are functionally redundant for some sensor NLRs but display specificity to other sensor NLRs from the NRC-superclade.

4.2.4c Tripe silencing of *NRC2/3/4* compromised Rx-mediated resistance

To further validate that *NRC2/3/4* are essential but redundantly contribute to the immunity mediated by the NLR proteins tested here, I examined the resistance mediated by Rx to *Potato virus X* (PVX) in *N. benthamiana*. Rx is one of the most studied NLR proteins among the NLRs included in this study, and the PVX-*N. benthamiana* pathosystem is well- characterized. In line with what has been previously reported, when PVX was inoculated at very low levels on Rx plants through agroinfiltration, no symptoms could be observed due to the extreme resistance (Tameling and Baulcombe, 2007). I silenced *NRC2/3/4* individually, or in combination, in *Rx* transgenic plants and inoculated the plants with PVX (pGR106) via agroinfiltration. I found that the virus caused systemic infection with typical mosaic and leaf curling symptoms on the new leaves (Fig. 4.4a) of control wild type plants. In contrast, I observed no local or systemic symptoms in *Rx* transgenic plant when *NRC4* or *NRC2/3* were silenced individually. Interestingly, when *NRC2/3/4* were all silenced, PVX was able to induced trailing necrosis (Fig. 4.4a). This trailing necrosis is likely due to the weak remaining Rx activity that can still sense the

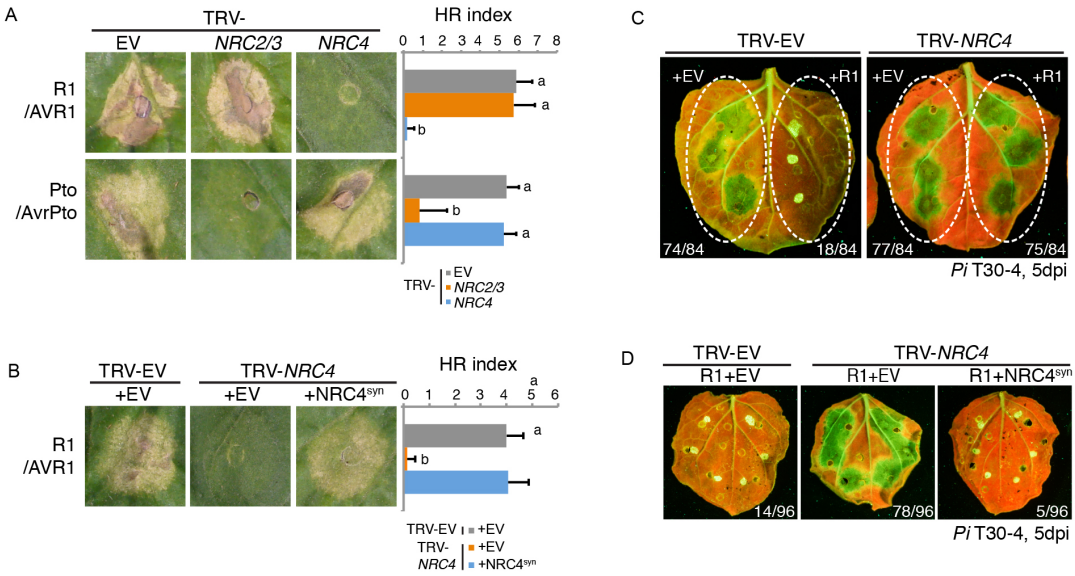

Figure 4. 3 Silencing of *NRC4* abolished R1-mediated immunity

(A) Silencing of *NRC4* abolished R1-mediated cell death. R1/AVR1 or Pto/AvrPto were expressed in *NRC2/3* or *NRC4*-silenced plants. Hypersensitive response (HR) was scored at 7 days after agroinfiltration. Bars represent mean + SD from 24 infiltrations sites. Statistical differences among the samples were analysed with ANOVA and Tukey's HSD test (p-value < 0.001). (B) Expression of synthetic *NRC4* rescued R1-mediated cell death in *NRC4*-silenced plants. R1/AVR1 were co-expressed with synthetic NRC4 or empty vector control in *NRC4*-silenced or control plants through agroinfiltration. Hypersensitive response (HR) was scored at 7 days after agroinfiltration. Bars represent mean + SD of 24 infiltrations sites. Statistical differences among the samples were analysed with ANOVA and Tukey's HSD test (p-value < 0.001). (C) Silencing of *NRC4* abolished R1-mediated resistance. R1 or empty vector control was transiently expressed in *NRC4*-silenced or control *N. benthamiana* one day before pathogen inoculation. The leaves were inoculated with 10μL zoospore suspension (200 zoospore/μL) from *P. infestans* T30-4. Experiments were repeated 4 times with 21 inoculation sites each time. The numbers on the right bottom are the sum of spreading lesion/total inoculation sites from the four replicates. Images were taken under UV light at 5 days post inoculation (dpi). (D) Expression of synthetic NRC4 rescued R1-mediated resistance in *NRC4*-silenced plants. Synthetic NRC4 or empty vector were co-infiltrated with R1 into *NRC4*-silenced or control plants one day before *P. infestans* inoculation. Experiments were repeated 4 times with 24 inoculation sites each time. The numbers on the right bottom are the sum of spreading lesion/total inoculation sites from the four biological replicates. Images were taken under UV light at 5 days post inoculation (dpi).

presence of viral coat protein (CP), but is not robust enough to restrict the spread of the virus (Tameling and Baulcombe, 2007). Consistent with previous report that *SGT1* is required for Rx-mediated resistance (Azevedo et al., 2006), I observed trailing necrosis caused by PVX on the inoculated leaves and upper leaves in *SGT1*-silenced *Rx* plants (Fig. 4.4a); this trailing necrotic symptom eventually spread throughout the whole plants after 5 weeks of inoculation (Fig. A2.11).

As an alternative way to examine the spread of PVX in the *NRC2/3/4*-silenced Rx plants, I performed the same experiment as mentioned above but inoculated the plants with PVX-GFP (pGR106-GFP). Consistent with previous observations, trailing necrotic lesions were observed only when *NRC2/3/4* were all silenced or when *SGT1* was silenced (Fig. 4.4b). The upper leaves of the wild type, *NRC2/3/4*-silenced, and *SGT1*-silenced *Rx* plant showed green fluorescence under UV light. I detected GFP accumulation in wild type plants and *Rx* plants silenced with *NRC2/3/4* or *SGT1*, whereas no GFP accumulation was detected in the empty vector control or the single or double *NRC2/3/4* silencing treatment (Fig. 4.4c). It has been shown that silencing of *SGT1* affects the accumulation of Rx and compromises the resistance (Azevedo et al., 2006). To check whether NRC homologs are similarly involved in steady-state accumulation Rx, I performed immunoblot analysis to examine the accumulation of Rx in the *NRC*-silenced or *SGT1*-silenced conditions. The results indicated that, unlike *SGT1*, silencing of the *NRC* homologs does not affect Rx accumulation (Fig. 4.4d).

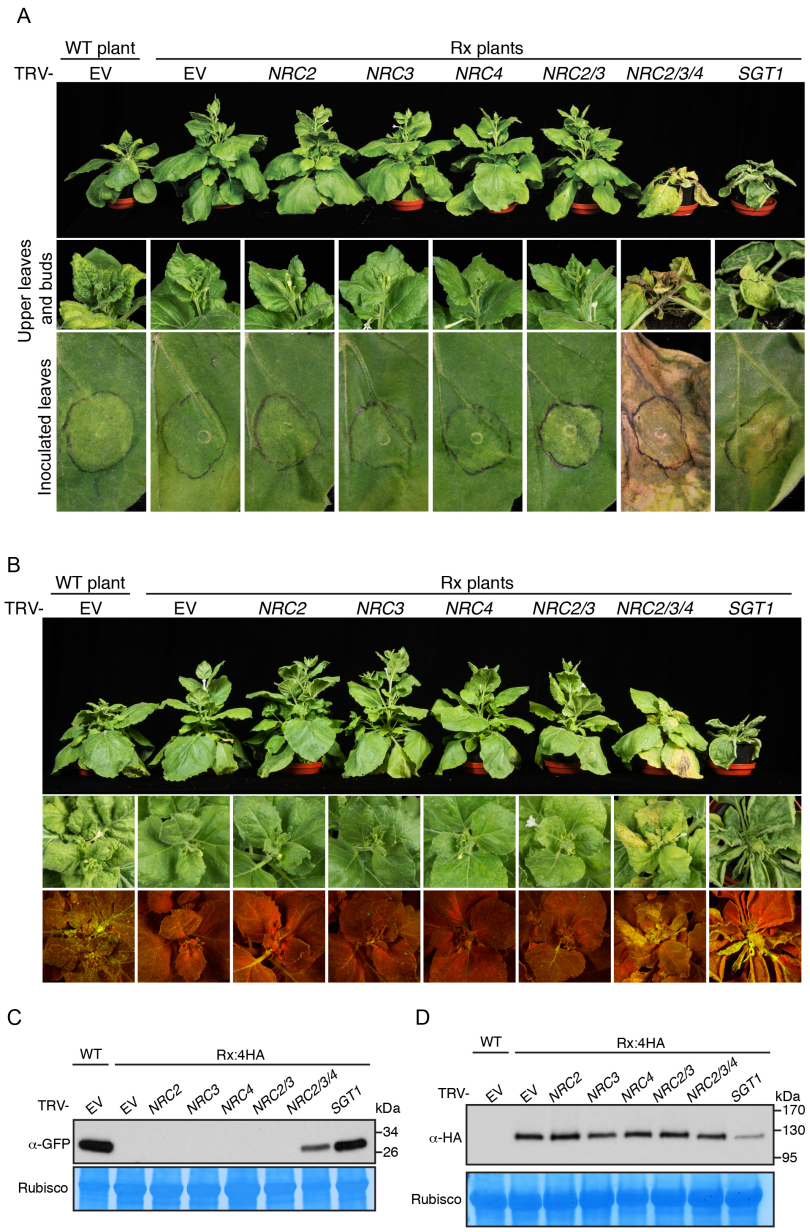

Figure 4. 4 *NRC2/3/4* triple silencing compromised Rx-mediated extreme resistance to PVX

(A) Triple silencing of *NRC2/3/4* compromised Rx-mediated resistance to PVX. *NRC2, NRC3,* or *NRC4* were silenced individually or in combination in *Rx* transgenic plants by TRV. *SGT1* silencing was used as a control for compromised Rx-mediated resistance. The circles on the inoculated leaves indicate the area of PVX inoculation through agroinfection. Pictures were taken 2 weeks after PVX inoculation. (B) Triple silencing of *NRC2/3/4* compromised Rx-mediated resistance to PVX-GFP. Experiments were performed in the same way as (A), but inoculated with PVX-GFP (pGR106-GFP). The pictures were taken under daylight and UV light at 2 weeks after PVX inoculation. (C) Immunoblot analysis of GFP accumulation with upper leaves collected from (B). (D) Silencing of *NRC2/3/4* did not affect accumulation of Rx. *NRC2, NRC3* or *NRC4* were silenced individually or in combination in Rx transgenic plants (Rx:4HA). *SGT1* silencing was used as a control. Leaf samples were collected three weeks after TRV inoculation for immunoblot analysis.

4.2.4d Expression of *NRC2/3/4* rescued Rx-mediated resistance in *NRC*-triple silencing plants

To further confirm that *NRC2/3/4* are functionally redundant in Rx-mediated resistance, I performed complementation assays by using the synthetic gene strategy previously described. I took advantage of the toothpick inoculation method that allowed me to apply the virus on a very small spot and subsequently chart the spreading of the necrotic lesions due to the partial resistance mediated by Rx. I transiently expressed synthetic *NRC2, NRC3*, or *NRC4* individually in *NRC2/3/4*-silenced Rx plants before inoculating the virus (PVX-GFP) by toothpick. I found that expression of *NRC2*, *NRC3*, or *NRC4* significantly reduced the size of the trailing necrotic lesions compared to the complementation control. In contrast, no clear trailing lesions were observed in the non-resistant (wild type) control or extreme resistant (Rx) control (Fig. A2.12a). I further validated these results by checking the accumulation of GFP by immunoblot analysis. I detected GFP accumulation in the non-resistant control and *NRC2/3/4* triple silencing conditions, whereas immunoblot signal of GFP in the complemented condition were very weak or not detectable (Fig. A2.12b). These results showed that *NRC2/3/4* are functionally redundant in Rx-mediated immunity.

4.2.4e NRC homologs are not required for resistance mediated by R3a and Rpi-blb1

To further examine whether the resistance mediated by NLR proteins outside of the NRC-superclade are affected by silencing of the *NRC* homologs, I performed disease resistance assay with *R3a* and *Rpi-blb1* transgenic *N. benthamiana*. Consistent with the previous observations, none of the *NRC* silencing conditions compromised R3a- or Rpi-blb1-mediated resistance, whereas *NRC4*- and *NRC2/3/4*-triple silencing compromised Rpi-blb2-mediated resistance. As expected, *SGT1* silencing compromised the resistance mediated by all the three NLRs tested here (Fig. A2.13).

4.2.5 A NRC-dependent NLR immune signalling network provides resistance to diverse pathogens

Based on the genetic evidence above, I proposed a NLR signalling network that mediates disease resistance to diverse plant pathogens (Fig. 4.5). This network comprises at least one-third of the NLRs in the genome of solanaceous plants. Many of them are sensor NLRs that provide disease resistance to different pathogens and pests in solanaceous crops. Interestingly, these sensor NLRs showed differential dependency on NRC homologs. Three major NRC homologs were identified, NRC2, NRC3 and NRC4, which showed both redundancy and specificity to different sensor NLRs. NRC2/3/4 might be a convergence point for mediating the conserved, yet unidentified, downstream responses. Understanding this network and identifying the downstream components will help us to understand how NLR proteins signal after pathogen recognition.

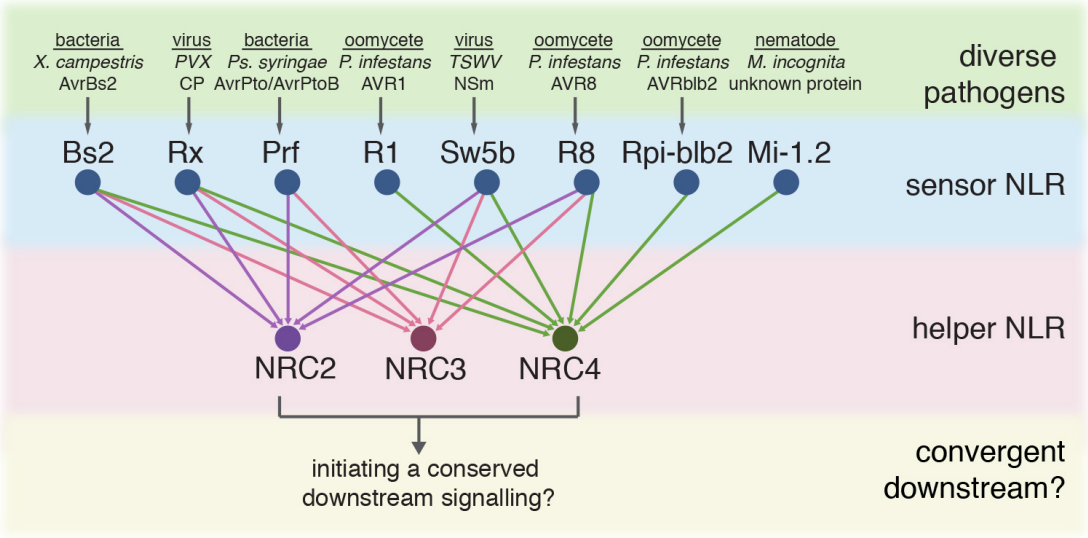

Figure 4. 5 A NRC-dependent NLR immune signalling network provides resistance to diverse pathogens

Summary of the NRC-dependent NLR immune signalling network. Several solanaceous NLR-type resistance proteins (sensor NLR) were demonstrated to be NRC (helper NLR)-dependent in this study. These NLR proteins can provide disease resistance to several different pathogens, including virus, bacteria, oomycete, nematodes and insects. The three major NRC homologs are functionally redundant but also display specificity to different sensor NLR. The NRC homologs may be the converge point of the signalling from different sensor NLR, and mediate a conserved, yet unidentified, downstream signalling.

4.2.6 Evolutionary history of the NRC-superclade

4.2.6a The NRC-superclade emerged in asterids after divergence from rosids

I was intrigued by the finding that functionally linked NLRs (NRCs and NRC-dependent NLRs) form a well-supported superclade in the phylogenetic tree of solanaceous NLRs. However, the extent to which the NRC-superclade occurs in non-solanaceous plant species is unclear. To address this question, I compared the NLRs identified from major taxonomic groups of eudicot (rosids, asterids, and Caryophyllales). The first comparison included NLRs identified from five different rosids species (grape, Arabidopsis, cassava, soybean and strawberry) and one asterids species (tomato). I used NLR-parser to annotate the CNLs (CC-NB-LRR) from the genomic databases of these rosids species, and then generated a phylogenetic tree together with the NLRs identified from tomato. I found that the CNLs from these six species fall into two well-supported major groups and one minor group that are all relatively distant from each other (Fig. 4.6A left panel). The two major groups have a lot of sequences identified from each of the species, with many of the clades clearly expanded in certain species. This suggests that most of the eudicot CNLs may have emerged from two major ancestral CNL lineages. The NRC-superclade is in one of the major CNL groups along with the solanaceous NLR R2 and Rpi-vnt1, and other NLRs from rosids plants (Fig. 4.6A left panel; Fig. A2.14). In addition, given the high complexity of NLR sequence and to challenge my conclusions, I generated another phylogenetic tree with only sequences from the major group that contains the NRC-superclade. The results showed that the NRC-superclade is well supported, containing no sequences identified from any of the rosids plants analysed here (Fig. 4.6A right panel; Fig. A2.15). These analyses suggest that the NRC-superclade is missing in the rosids and may have emerged after the diversification of rosids and asterids.

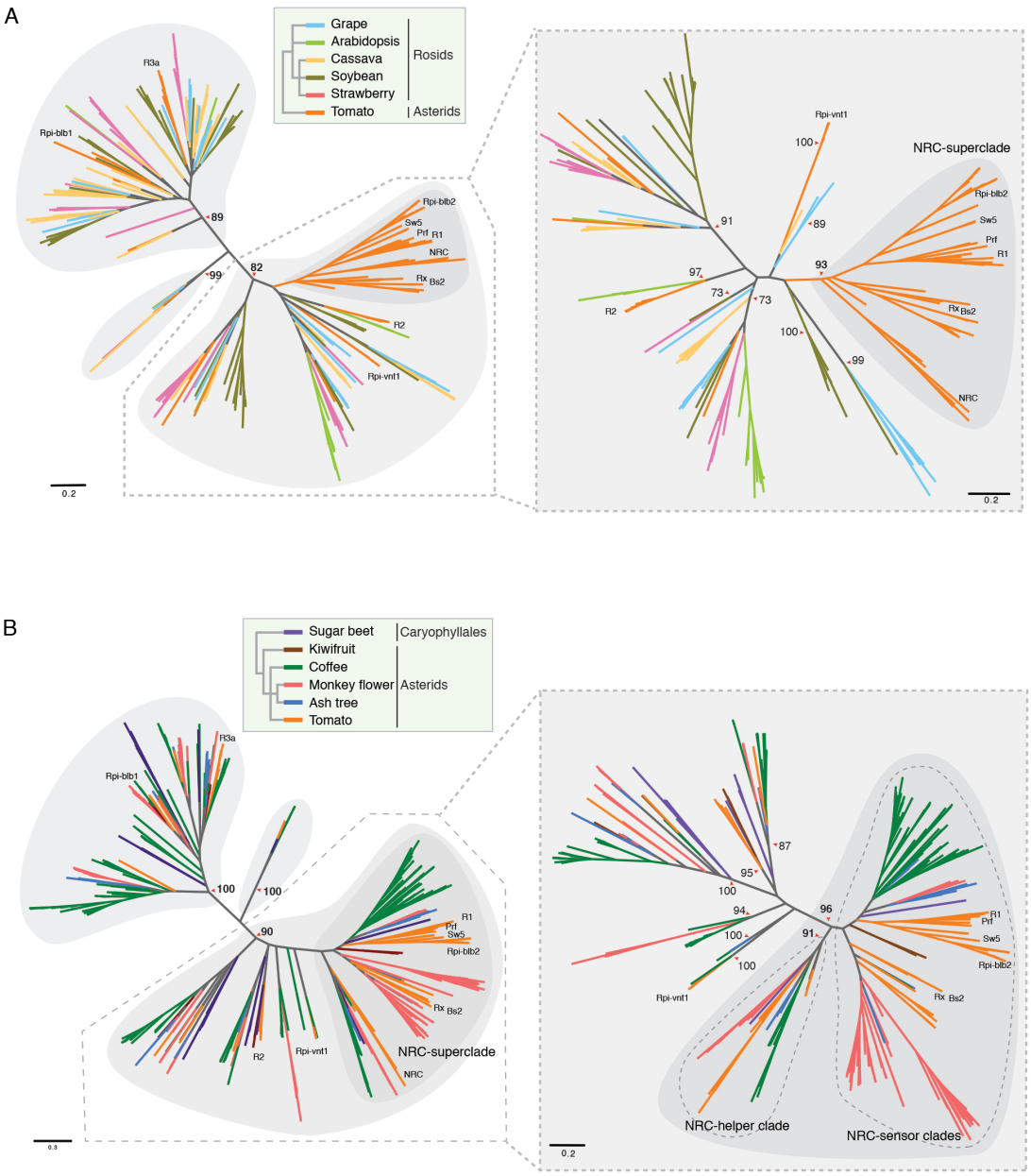

Figure 4. 6 The NRC-superclade emerged after the divergence of rosids and asterids

(A) Phylogeny of CNLs identified from rosids (grape, Arabidopsis, cassava, soybean, and strawberry) and asterids (tomato). (B) Phylogeny of CNLs identified from asterids (kiwifruit, coffee, monkey flower, ash tree and tomato) and caryophyllales (sugar beet). CNLs identified from indicated species were aligned by using MAFFT and analysed in MEGA7 to generate maximum-likelihood phylogenetic tree. Only the NB-ARC domains of the sequences were used in the analysis. Sequences identified from different species were presented with different colour as indicated. The bootstrap supports of the major nodes are indicated. The phylogenetic tree at the right panel contains only the sequences in the indicated box at the left panel. The positions of the reference solanaceous NLR sequences in the phylogenetic tree are indicated. The details of the full phylogenetic tree can be found in Fig. A2.14-17.

4.2.6b The NRC-superclade is expanded in most asterids

Next, I explored whether the NRC-superclade occurs in other species of asterids and caryophyllales. I constructed a phylogenetic tree comparing CNLs from 5 different asterid species (tomato, coffee, kiwifruit, monkey flower, and ash tree) and one caryophyllales species (sugar beet). Consistent with what I found previously, these NLR sequences fall into two well-supported major groups and one minor group (Fig. 4.6B left panel; Fig. A2.16). I further generated a phylogenetic tree with only the sequences from the CNL group that contains the NRC-superclade. The result showed that the NRC-superclade contains sequences from different asterids and caryophyllales species. Within the NRC-superclade, homologs of NRC from different species form a well-supported clade, named the NRC-helper clade, which is sister to the NRC-sensor clades (Fig. 4.6B right panel; Fig. A2.17). This NRC-helper clade contains several subclades, with each subclade containing mostly paralogs from the same species; this indicated that the expansion of each NRC-helper subclade occurred independently in the different species after diversification of asterids. The sensor NLRs in the NRC superclade fall into several clades, with each clade comprised of sequences mostly from the same species. However, the overall evolutionary history of the different NRC-sensor clades remains unclear given the weak support for the basal branches in the sensor NLR lineages. This feature may be the result of the rapid evolution and functional diversification of these sensor NLRs.

4.2.6c The NRC network emerged over 100 million years ago

To gain further insight into the evolutionary history of the NRC-superclade, I compared the phylogeny of plant species included in this study with the number of NRC-helper/sensor sequences, as determined by the phylogenetic tree generated above (Figure 4.7). I found that kiwifruit, which emerged in an early branch in the evolutionary history of asterids, has only one sequence in the NRC-helper clade and four sequences in the NRC-sensor clades. These four kiwifruit NRC-sensor paralogs are more likely a

result of recent duplication events because they are highly similar to each other (Fig. A2.18). In contrast, other asterid plants, which diverged later in the evolutionary history, have many more NRC-helper and sensor sequences (Fig. 4.7A). This implies that the initial expansion of the NRC-superclade happened after divergence of Ericales (kiwifruit) but prior to the divergence of Gentianales (coffee), which was dated between 110-100 myr (million years) ago, in the evolutionary history of asterids. The expansion of NRC-helper and sensor clades might have happened continuously and independently in different ancestral asterids lineages, resulting in differential expansion pattern in different asterids plants (Fig. 4.5B and Fig. A2.17). According to the phylogenetic tree of solanaceous NLRs generated earlier (Fig. A2.6), orthologs from different solanaceous species can be found in the same NRC helper/sensor clades, indicating that the current landscape of the NRC-superclade in Solanaceae may have been established in the ancestral solanaceous species at least 24 myr ago, the estimated time that *Nicotiana* diverged from the other Solanaceae species (Sarkinen et al., 2013). Most interestingly, sugar beet, which is in the caryophyllales, contains only one NLR sequence in the NRC-helper clade and two NLR sequences in the NRC-sensor clade. This is the most distant non-asterids species that contains NRC-helper/sensor homologs identified thus far (Fig. 4.7A).

4.2.6d The NRC-superclade may have evolved from a linked NLR pair

I further checked the location of NRC helper/sensor homologs of sugar beet with the genome browser, and found that these three sequences are located in proximity to each other on the chromosome. The NRC-helper homolog (Bv5_105990) is located at 40Kb downstream of one of the sensor homologs (Bv_105980), with no other predicted genes in between (Figure 4.7B). The two sensor paralogs are with 95% sequence identity, which might be the result of a recent duplication. Taken together, these results suggest that prior to the divergence of caryophyllales and asterids, the ancestral species may have had a NLR pair, which then expanded into the NRC-superclade in asterid lineages.

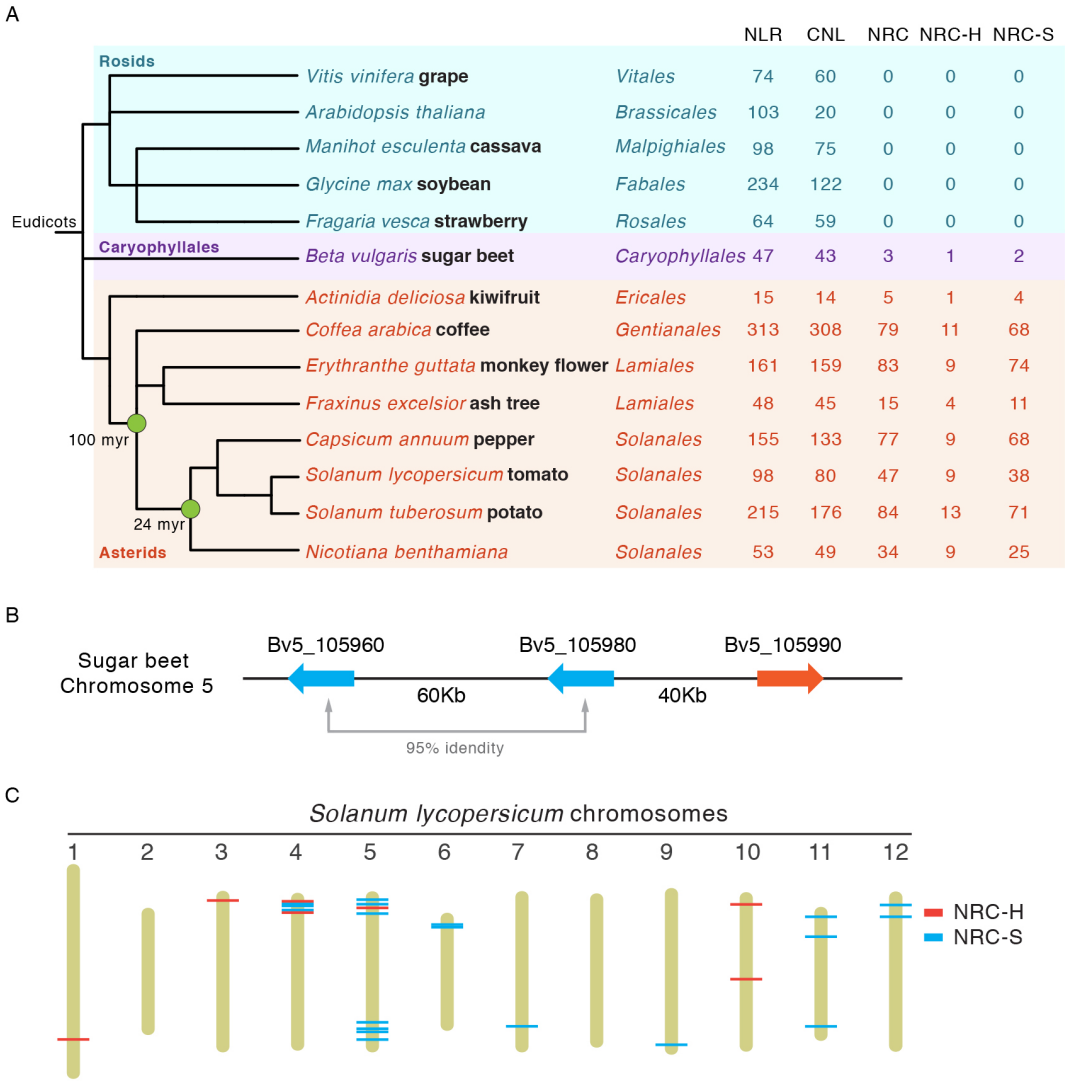

Figure 4. 7 The NRC-superclade emerged from a NLR pair over 100 million years ago

(A) Summary of phylogeny and number of NLR identified from different plant species included in this study. Phylogenetic tree was generated by using phyloT on NCBI with corresponding taxon identification number. Amount of NLRs identified in each category are based on the results of NLR-parser and the phylogenetic tree in Fig. 4.6. CNL, CC-NB-LRR; NRC, NRC-superclade; NRC-H, NRC-helper NLR; NRC-S, NRC-dependent sensor NLR. (B) Schematic representation of the NRC helper/sensor cluster on sugar beet chromosome 5 based genome browser. The two NRC-sensor paralogs are marked in blue, and the NRC-helper homolog is marked in orange. (C) Physical map of NRC helper/sensor homologs on tomato chromosomes. The NRC-sensor paralogs are marked in blue, and the NRC-helper paralogs are marked in red. Detailed information of the physical map can be found in Fig. A2.19

4.2.6e NRC helper-senor homologs are largely unlinked in the tomato genome

To examine the extent to which the members of the NRC-superclade are linked with each other, I marked the location of all the NRC helper/sensor homologs on the chromosomal map of tomato NLR (Andolfo et al., 2014). I found that the NRC-sensor sequences are on 7 different chromosomes, with some that cluster with their recently duplicated paralogs (Fig. 4.7C and Fig. A2.18). The NRC-helper sequences are on 5 different chromosomes, mostly as single copy genes, apart from a cluster on chromosome 4 that contains three NRC4 and one NRC4-like paralogs. Most of the NRC-sensor sequences are not linked with the NRC-helper sequences as they are mostly on different chromosomes. Interestingly, some of the NRC-sensor sequences are on the short arm of chromosome 4 or the short arm of chromosome 5, which contains NRC4 and NRC3, respectively. However, these helper/sensor NLRs are not tightly linked. Thus the NRC gene expansion in tomato has resulted in gene translocations across the genome.

4.2.6f A model of the evolutionary history of the NRC-superclade

Taken together, I propose a hypothesis about the evolution of the NLR signalling network of NRC-superclade (Fig. 4.8). This network may originate from a NLR pair in the ancestral asterids. At certain time before 100 million years ago, the linked sensor/helper NLR pair duplicated to different chromosomes and became unlinked sensor/helper NLRs. This enabled further duplication and expansion of both the sensor and helper NLR clades. From the number of NRC-helpers and NRC-sensors identified, I propose that the helper NLR clade is under limited expansion due to constraints on mediating downstream responses; however, the redundancy generated by these duplications increases the capacity for adaptive evolution of the immune system. Given the flexibility created by redundant NRC helpers, the sensor NLRs can undergo fast adaptive evolution with functional diversification to counteract rapid evolving pathogens.

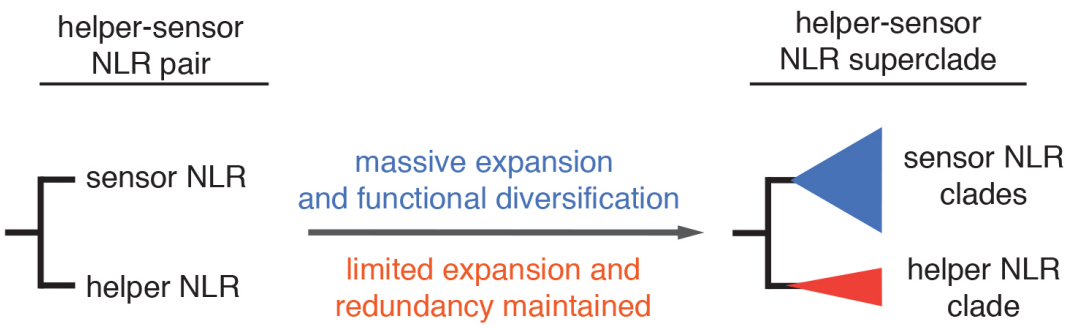

Figure 4. 8 A model of the evolutionary history of the NRC-superclade

Based on the results of functional analysis and phylogenetic analysis in this study, I proposed that the NRC-superclade and the signalling network originated from a linked NLR pair. The NLR pair expanded and adapted to accommodate rapid evolution. The NRC-helper clade has expanded to create redundancy and thus flexibility for the sensor to evolve rapidly. However, the expansion of the helper clade is limited, as it has to cope with mediating a conserved downstream signalling. In contrast, the NRC-sensor homologs have evolved into several diversified clades to sense the proteins from assortment of pathogens. This network system with redundant helper NLRs may provide a framework for rapid evolution of plant NLR-triggered immunity, in order to counteract the fast evolving pathogens.

4.3 Conclusions

In conclusion, I discovered a NLR immune signalling network that provides resistance to diverse plant pathogens. This signalling network is composed of a helper NLR NRC family along with several sensor NLR families that require members in the NRC family for mediating immunity. This signalling network is highly relevant to agriculture as many of the known NLRs that provide resistance to important plant pathogens are within this network. I would expect that more NRC-dependent NLR-type resistance genes will be identified in the future given the fact that the NRC-superclade includes one-third of the NLRs in the solanaceous genome. Altogether, the NRC family and NRC-dependent sensor NLR family form a unique superclade that is shared by asterids and caryophyllales. I propose that the whole NRC superclade might have evolved from a NLR pair in the ancestral species, and that the redundancy of helper NLR created the potential for rapid evolution of this plant immune system. These exciting new findings shed light on the molecular mechanisms of NLR immune signalling from a more comprehensive evolutionary perspective.

Chapter 5: Leucine-rich repeats determine NLR helper-sensor specificity in the NRC immune signalling network

5.1 Introduction

Plant NLR proteins generally share a conserved tripartite domain architecture with an N-terminal domain followed by the NB-ARC and LRR domains (Takken et al., 2006; Takken and Goverse, 2012). These three domains are thought to interact with each other to activate immune signalling. One of the popular hypothesis about activation of NLR signalling is that in the absence of pathogen stimuli, the proteins fold into a ADP-bound “OFF” state, whereas in the presence of pathogen stimuli, the proteins turn into the “ON” state and undergo conformational changes that lead to signalling activation (Takken et al., 2006; Takken and Goverse, 2012). Hence, these proteins function like molecular switches that sense the existence of pathogen and activate immune response at the right place and right time (Takken et al., 2006; Takken and Goverse, 2012).

The three NLR domains are thought to participate in different stages of pathogen recognition and signalling activation. The NB-ARC domain is the central part of the protein and is also the most conserved region across distantly related NLRs (Takken et al., 2006). This domain consists of NB, ARC1, and ARC2 subdomains, and these three subdomains together form a nucleotide-binding pocket in the resting state (Takken and Goverse, 2012). The NB subdomain contains the p-loop motif which is critical for ATP binding and hydrolysis (Tameling et al., 2002). Mutations in this motif lead to inactivation of the signalling activity, although the activity of some NLRs are p-loop independent (Bonardi et al., 2011; Cesari et al., 2014b; Sohn et al., 2014; Tameling et al., 2002). The ARC2 subdomain contains the MHD motif, which is important for controlling NLR activity ‘switch’ (van Ooijen et al., 2008). A substitution of aspartic acid to valine in the MHD motif generally leads to

autoactivation of the protein (van Ooijen et al., 2008). The ARC2 subdomain is important for coordinating with NB-ARC1 and LRR to control autoinhibition and facilitate signal activation (Rairdan and Moffett, 2006; Slootweg et al., 2013; Steinbrenner et al., 2015; van Ooijen et al., 2008). Interestingly, the ligand specificity determinants of NAIP2 and NAIP5, two sensor NLR in mammals, map to a region closely associated with the NB domain, indicating that the NB-ARC domain may also participate in ligand recognition in addition to signalling activation (Tenthorey et al., 2014).

The N-terminal domain of plant NLRs is usually a TIR (Toll/interleukin 1 receptor), CC (coiled-coil), or CC_R (RPW8-like coiled-coil) domain, and these distinguish plant NLRs into TNLs, CNLs, or RNLs, respectively (Shao et al., 2016). Several studies have shown that expression of NLR N-terminal domains in plants induces cell death, suggesting that this domain is sufficient to activate defence signalling (Bernoux et al., 2016; Collier et al., 2011; Krasileva et al., 2010; Maekawa et al., 2011; Michael Weaver et al., 2006; Swiderski et al., 2009). In addition, structure-function studies indicated that the homo- or hetero-dimerization of the N-terminal domain might play important roles in signalling activation (Maekawa et al., 2011; Williams et al., 2014). For instance, the CC domain mutant of MLA10, which failed to form a homodimer, also failed to induce cell death (Maekawa et al., 2011); moreover, the interface for RPS4/RRS1 TIR-TIR heterodimerization is important for activation of the NLR complex (Williams et al., 2014).

The C-terminal domain of a plant NLR is usually a LRR domain. This common protein domain functions in protein-protein interaction and ligand binding (Kobe and Kajava, 2001). The LRR domain is composed of repeating LRR units that contain a conserved LxxLxxLxL motif, which generates a β-sheet structure on the concave face, and non-leucine residues on the convex exposed surface (Enkhbayar et al., 2004; McHale et al., 2006). The predominant role of the LRR domain in plant NLRs is thought to be the recognition of pathogen ligands. The LRR domain of RPP1, a NLR protein that confers resistance to *H. arabidopsidis* in *A. thaliana*, was proposed to directly bind to the corresponding effector ATR1 (Krasileva et al., 2010; Steinbrenner

et al., 2015). Recognition specificity of the two flax rust resistance proteins L5 and L6 to the corresponding AvrL567 ligands is dependent on polymorphisms in the LRR domain (Ravensdale et al., 2012). In addition to recognition specificity, the LRR domain may also play a role in inter-domain regulation of the NLR complex. For example, the LRR domain of Rx interacts with the NB-ARC domain when expressed *in trans*, and this interaction is disrupted by the corresponding ligand, the coat protein of *Potato virus X* (Moffett et al., 2002; Slootweg et al., 2013). Interestingly, the interaction between LRR domain of RPP1 is not affected by the corresponding ligand ATR1 (Schreiber et al., 2016), suggesting that the regulation of inter-domain interaction could be distinct for different NLRs upon activation.

Chimeras between homologous NLRs have been used to understand the molecular details of NLR signalling activation and effector recognition (Rairdan and Moffett, 2006; Ravensdale et al., 2012; Saucet et al., 2015; Slootweg et al., 2013; Steinbrenner et al., 2015; Tenthorey et al., 2014). Experiments with chimeric proteins of L5 and L6, the aforementioned flax rust NLRs, revealed that both the N- and C-terminal LRRs determine recognition specificity against variants of Avr567; additionally, these experiments indicated that compatibility between the NB-ARC and LRR domain affect the strength of the recognition (Ravensdale et al., 2012). Similar results were observed with RPP1-NdA/WsB chimera with the LRR domains conferring allele specific recognition and the ARC2 subdomain critical for full activation of immunity (Steinbrenner et al., 2015). Studies on Rx and Gpa2 chimeras also showed that the interface between the ARC2 and LRR domains is important for defence signalling regulation (Rairdan and Moffett, 2006; Slootweg et al., 2013). NLR chimeras were also used to study helper/sensor specificity of the RPS4A/RRS1A and RPS4B/RRS1B pairs, and the results showed that the specific pairing between the TIR domains is not essential for determining partner specificity in the NLR pairs (Saucet et al., 2015).

In the previous two chapters, I described a signalling network that mediates disease resistance to several different pathogens. Three helper NLRs, NRC2/3/4, form a network in which they show redundancy in immunity

mediated by some sensor NLRs but also show specificity in the immunity mediated by other sensor NLRs. For example, despite being functionally redundant in responses induced by Rx, NRC3 mediates the immune responses induced by Prf but not Rpi-blb2, whereas NRC4 mediates the responses induced by Rpi-blb2 but not Prf. In this chapter, I investigated the molecular determinants of specificity in the network by performing iterative activity assays of chimeric proteins between NRC3 and NRC4. I found that the LRR domain confers sensor specificity of both NRC3 and NRC4. Furthermore, I delimited the residues between the 8th and 9th LRR units as the minimum region to confer expansion of NRC3 sensor activity. Although additional experiments are required to further validate these observations, these results shed light on the contribution of the LRR domain as a determinant of helper/sensor partner specificity in a NLR immune signalling network.

5.2 Results and discussion

5.1.1 NRC3 and NRC4 have different NLR sensor specificities

To gain insight into the molecular details of NRC helper-sensor network, I first sought to confirm differences in specificity between NRC3 and NRC4 using the previously established complementation assay. Expression of synthetic NRC3 rescued Prf-mediated cell death, but not Rpi-blb2-mediated cell death (Chapter 4, Fig. A2.10). In contrast, expression of synthetic NRC4 rescued Rpi-blb2-mediated cell death, but not Prf-mediated cell death. I hypothesise that swapping domains between NRC3 and NRC4 would alter specificity and help to delimit the NRC sequences that determine sensor specificity.

To select chimeric protein breakpoints, I first compared sequences of NRC3 and NRC4 and defined domains and subdomains from the protein sequence alignment. Based on the sequence alignment and our current understanding of NLR protein structure, I selected 5 breakpoints, which divide the sequences into six fragments; I refer to as CC, NBD, ARC1, ARC2, LRR1-7 and LRR8-13. The sequence comparisons indicated that the identity of the

domains between NRC3 and NRC4 ranged from 46% to 60%, with the CC domain and LRR8-13 the most divergent, and the ARC1/ARC2 the most similar (Fig. 5.1A).

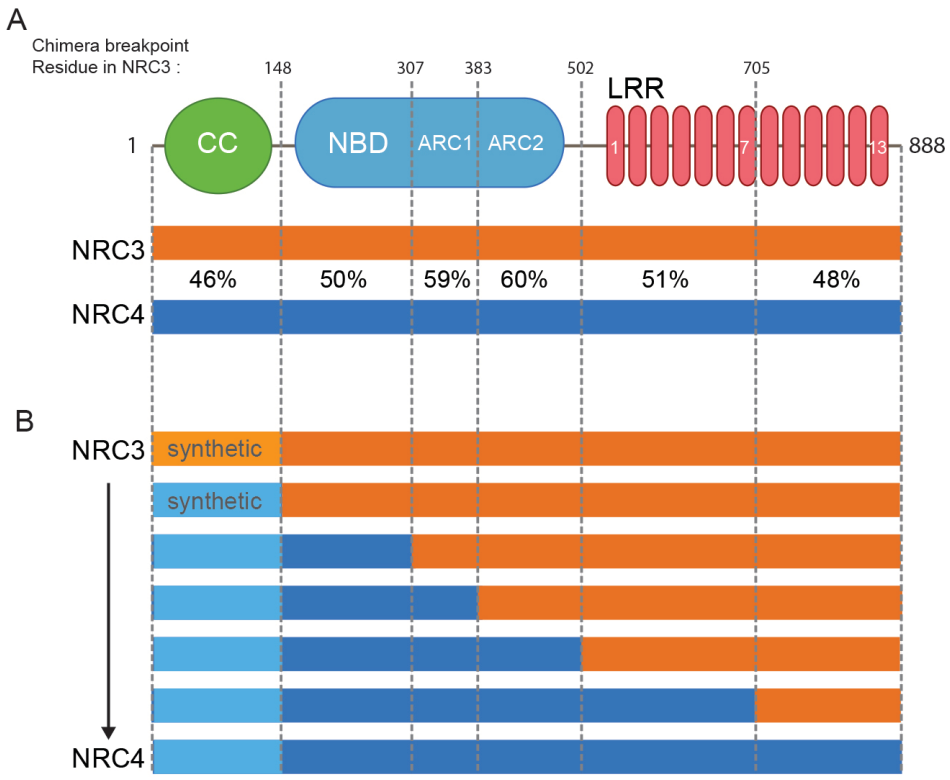

Figure 5. 1 Design of NRC3 and NRC4 chimeric proteins

(A) Schematic of predicted NRC3/NRC4 domains. The sequence identities between each domains and subdomains are indicated. (B) Schematic for design of NRC3/NRC4 chimeric proteins. To avoid VIGS silencing effect, the nucleotide sequences of the CC domain were replaced with the synthetic version that contains synonymous substitutions. The domains of the NRC3/NRC4 were swapped one-by-one, resulting a set of chimeric proteins that have sequences changed gradually from NRC3 to NRC4 or NRC4 to NRC3 (Fig. A3.1).

5.1.2 LRR determines sensor specificity of NRC3 and NRC4

I then generated chimeric proteins by changing the domains one-by-one, resulting in a series of chimeric proteins with domains swapped gradually from NRC3 to NRC4, and NRC4 to NRC3 resulting in 10 chimeras (Fig. 5.1B, Fig. A3.1). I tested whether these chimeric proteins could still rescue Prf- or Rpi-blb2-mediated cell death in *NRC2/3* or *NRC4*-silenced *N. benthamiana* leaves. Among those 10 chimeras, 6 of them did not show any activity to rescue either Prf- or Rpi-blb2-mediated cell death (Fig. A3.1). I considered the

results from these chimeric proteins as “inconclusive” and excluded them from further analysis. Chimera NRC3-4$^{NB\text{-}LRR}$, which contains the CC domain from NRC3 and the rest of the protein from NRC4, partially rescued Rpi-blb2 cell death, indicating that the CC domain is not critical in determining the specificity of NRC homologs (Fig. A3.1). Interestingly, two of the chimeric proteins (NRC4-3$^{ARC2\text{-}LRR}$ and NRC4-3^{LRR}), with the ARC2-LRR or LRR from NRC3 in an NRC4 background, were able to rescue Prf-mediated cell death but not Rpi-blb2-mediated cell death (Fig. 5.2, Fig. A3.1), suggesting that the determinants of specificity are likely in the LRR region. Surprisingly, chimera NRC4-3$^{LRR8\text{-}13}$, which contains the LRR1-7 from NRC4 with the LRR8-13 from NRC3, rescued both Prf- and Rpi-blb2-mediated cell death, indicating that the first half part of the LRR region contains features that are critical for NRC4 activity and the second half of the LRR region contains features that are critical for NRC3 activity (Fig. 5.2; Fig. A3.1).

To further identify the residues within the LRR region of NRC3 that define sensor specificity, I generated another set of chimeric proteins, with the LRRs swapped one-by-one from NRC3 to NRC4, and then tested the extent to which they could still rescue Prf- or Rpi-blb2-mediated cell death. Among these 13 newly generated chimeric proteins, 3 of them are autoactive, and 5 of them are not functional. These 8 chimeric proteins were then excluded from further comparisons (Fig. A3.2). Similar to chimera NRC4-3$^{LRR8\text{-}13}$, chimera NRC4-3$^{LRR7\text{-}13}$, which contains LRR1-6 from NRC4 and LRR7-13 from NRC3, also rescued both Prf- and Rpi-blb2-mediated cell death (Fig. 5.2; Fig. A3.2). Interestingly, chimeras NRC4-3$^{LRR9\text{-}13}$ and NRC4-3$^{LRR11\text{-}13}$, which contain LRR1-8 and LRR1-10 from NRC4, respectively, lost the activity to rescue Prf-mediated cell death but could still rescue Rpi-blb2 mediated cell death (Fig. 5.2; Fig. A3.2). Given that the major difference between chimera NRC4-3$^{LRR8\text{-}13}$ and NRC4-3$^{LRR9\text{-}13}$ is the region including the 8th LRR unit and adjacent residues (referred to as Loop$^{LRR7/8}$ and Loop$^{LRR8/9}$ hereafter; Fig. 5.3) and that these two proteins showed clear difference in their ability to rescue Prf-mediated cell death, I reasoned that residues within or in proximity to the 8th LRR unit are likely to play a critical role in determining NRC sensor specificity.

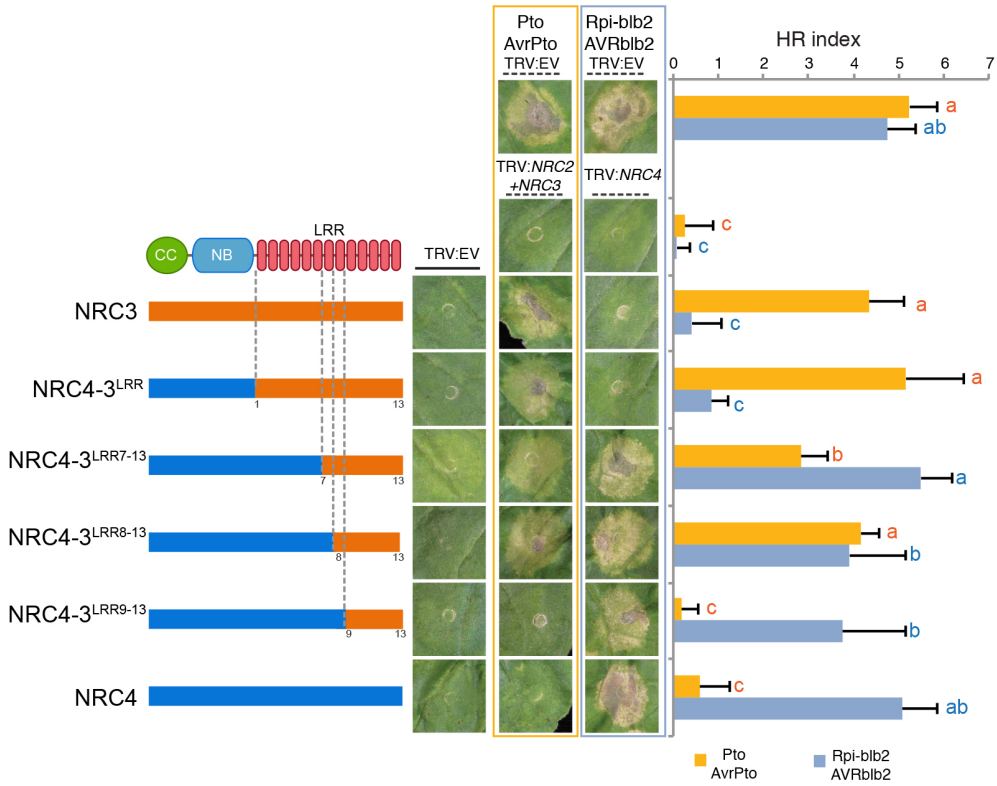

Figure 5. 2 Leucine-rich repeats determine the specificity of NRCs

The chimeric proteins generated were tested for their activity to rescue Pto- and Rpi-blb2-mediated cell death in *NRC2/3*- or *NRC4*-silenced background. The LRR breakpoints were indicated in the schematics of corresponding constructs. These chimeric proteins are not autoactive when expressing along. The chimeric proteins were co-expressed with Pto/AvrPto or Rpi-blb2/AVRblb2 in *NRC2/3*- or *NRC4*-silenced background. Hypersensitive responses (HR) were scored at 7 days post infiltration (dpi). Bars represent mean + SD of 12 infiltrations from one biological replicate. Statistical differences among the samples were analysed with ANOVA and Tukey's HSD test (p-value < 0.001). The results of preliminary test of these proteins were presented in Fig. A3.1 and Fig. A3.2.

5.1.3 The Loop$^{LRR8/9}$ plays a critical role in determining sensor specificity of NRC3

In order to pinpoint the residues that confer the observed specificity changes, I compared the sequences of chimera NRC4-3$^{LRR8-13}$ and NRC4-3$^{LRR9-13}$ in more detail. The differences between chimera NRC4-3$^{LRR8-13}$ and NRC4-3$^{LRR9-13}$ include part of the Loop$^{LRR7/8}$ (residues between 7th LRR and 8th LRR), the conserved leucine rich region (LxxLxxLxxLxL) of the 8th LRR unit, and part of the Loop$^{LRR8/9}$ (residues between 8th LRR and 9th LRR). Based on

the sequence alignment, the loop regions of the two sequences are very different whereas the leucine-rich regions are relatively similar (Fig. 5.3). I then generated chimeric proteins that encompassed the variations between these two sequences, and then tested their ability to rescue Rpi-blb2 and Prf-mediated cell death. Both chimeras NRC4-3$^{LRR8.5}$ and NRC4-3$^{LRR8.2}$ still rescued Prf- and Rpi-blb2- mediated cell death, indicating that the Loop$^{LRR7/8}$ is not decisive in driving the specificity of NRCs (Fig. 5.3). Intriguingly, chimera NRC4-3$^{LRR8.2}$ differs from chimera NRC4-3$^{LRR9-13}$ in only 8 amino acids but showed ability to rescue Prf-mediated cell death, indicating that residues in the Loop$^{LRR8/9}$ play an important role in defining the specificity of NRCs (Fig. 5.3).

To further test the hypothesis that the first half of Loop$^{LRR8/9}$ is important in determining specificity of NRC3 and NRC4, I extended the region of comparison to the whole Loop$^{LRR8/9}$. I generated more chimeric protein variants that differed from each other only in this region, with either residues from NRC3 or NRC4. In addition, to check whether these chimeric proteins variants are different in steady-state protein accumulation, I generated myc-tagged variants and checked the protein accumulation by immunoblot analysis. I found that chimeric NRC4-3$^{LRR9-13}$ has relatively low abundance comparing to most of other proteins analysed here (Fig. A3.3), which suggests that the loss of NRC3 activity phenotype could be due to changes in protein accumulation. However, chimera NRC4-3$^{LRR9.2}$, which is more abundant than chimera NRC4-3$^{LRR9-13}$, has NRC4 activity and weak NRC3 activity (Fig. A3.3), suggesting that the phenotype I observed above can still be due to the changes in specificity, rather than just protein accumulation. Chimeras NRC4-3$^{LRR9.4}$ and NRC4-3$^{LRR9.5}$, both of which contain the first half of Loop$^{LRR8/9}$ from NRC4, showed NRC4 activity and weak NRC3 activity (Fig. A3.3). In contrast, chimeras NRC4-3$^{LRR9.6}$ and NRC4-3$^{LRR9.7}$, both of which contain the first half of Loop$^{LRR8/9}$ from NRC3, showed very clear NRC3 and NRC4 activity (Fig. A3.3). These results confirm that the residues in the first half of Loop$^{LRR8/9}$ in NRC3 confer gain-of-NRC3-function in the NRC3/4 chimeric proteins. Overall,

these results suggest that loop regions between LRR units determine the sensor specificity of helper NLRs.

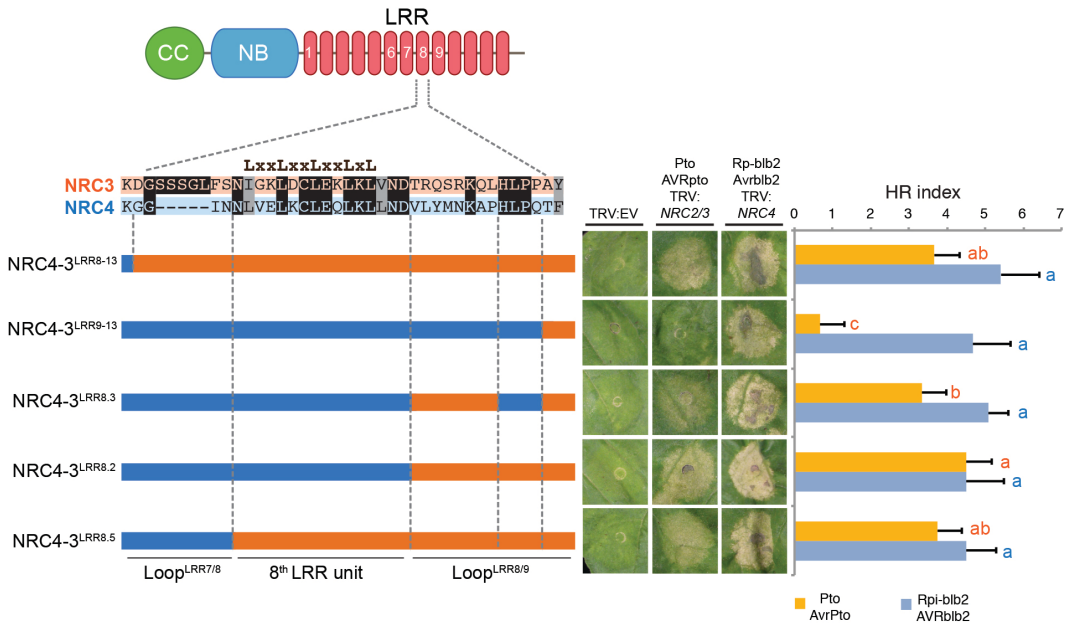

Figure 5. 3 The loop region between LRR repeats are critical in determining specificity of NRCs

The chimeric proteins generated were tested for their activity to rescue Pto- and Rpi-blb2-mediated cell death in *NRC2/3*- or *NRC4*-silenced background. The conserved Lecuine-rich motif (LxxLxxLxxLxL) of the 8th LRR and the adjacent regions were indicated. The breakpoints were indicated in the sequence alignment. These chimeric proteins are not autoactive when expressing along. The chimeric proteins were co-expressed with Pto/AvrPto or Rpi-blb2/AVRblb2 in *NRC2/3* or *NRC4* silenced background. Hypersensitive responses (HR) were scored at 7 days post infiltration (dpi). Bars represent mean + SD of 12 infiltrations from one biological replicate. Statistical differences among the samples were analysed with ANOVA and Tukey's HSD test (p-value < 0.001).

To summarise, I used an iterative series of assays with chimeric NRC proteins to determine that NLR sensor specificity in the helper NLRs, NRC3 and NRC4, lies in the LRR domain, particularly the sequences between the 8th and 9th LRR units. This finding was unexpected based on the current dogma that LRR domain of a given NLR is involved in effector recognition intra-molecular interactions. Although the specificity determinants in the NRC signalling network have not been studied from the sensor NLR perspective, it is possible that the interaction between the LRR domains of the sensor/helper NLRs play critical roles in driving partner specificity.

I narrowed down the region responsible for NRC3 sensor specificity to the residues right after the 8th LRR unit; this led us to hypothesise that the residues for conferring NRC4 sensor specificity is also in one of the regions between LRR units in the first half LRR domain. However, the chimeric proteins tested with breakpoints between the 1st and 6th LRR units are either autoactive or not functional. Thus far, I have not obtained any chimeric proteins that provide further information about the determinants that confer sensor specificity of NRC4. I am still testing additional chimeric proteins with breakpoints between the 1st and 6th LRR units to narrow down the specificity determinants for NRC4 function.

I mapped sensor specificity in NRC3 and NRC4 to distinct, non-overlapping regions of the LRRs. When I combined the two determinants in one chimera, the protein gained both NRC3 and NRC4 function. This opens up possibilities for engineering NRC helper proteins with expanded spectrum of sensor NLR partners. Such an approach may be beneficial in improving plant disease resistance in crop plants.

5.3 Conclusions

In conclusion, I used a genetic approach to discover that the LRR region of the NRC helper NLR determines their specificity towards sensor NLRs. This assigns a novel activity to NLR LRR domains, which were previously thought to function in effector recognition and intra-molecular interactions. However, unanswered questions remain regarding helper/sensor specificity in the NRC signalling network. For example, do protein-protein interactions between LRR domains of helper and sensor NLRs determine specificity? What are the determinants of helper specificity in sensor NLRs? How does the Loop$^{LRR8/9}$ region of NRC3/4 contribute to sensor specificity? Further studies should combine genetic and biochemical analyses to further dissect the molecular determinants of helper/sensor specificity in the NRC signalling network.

Chapter 6: Discussion

How NLR immune receptors mediate downstream signalling is one of the most interesting unanswered questions in plant immunity. Considering the large repertoires of NLR genes in plant species, it is reasonable to hypothesise that some common mechanisms for mediating downstream responses may apply to subsets of NLRs. Although a comprehensive understanding of the signalling events that occur after NLR activation is currently lacking, different hypotheses have been proposed to explain the mechanisms by which NLR proteins mediate downstream responses. The NRC signalling network presented in this thesis encompasses one-third to half the number of NLRs in solanaceous plants, many of which are important resistance genes that confer resistance to crop pathogens. Three major NRC homologs – NRC2, NRC3, and NRC4 – were described in this thesis. Chapter 3, which was motivated by revisiting the NRC1 study published by Gabriels *et al.* (2007) with new genomics information, described the identification of NRC2 and NRC3 that play essential roles in Pto/Prf-mediated immunity. Chapter 4 started with characterising NRC4, which is required for R1 and Rpi-blb2 mediated immunity, and then revealed that NRC2, NRC3, and NRC4 together play essential roles in immunity mediated by several other NLRs. Interestingly, together the NRC family and NRC-dependent NLR clades are part of a unique phylogenetic superclade that perhaps originated from a NLR pair in an ancestral species. Chapter 5 focuses on the specificity observed in the signalling network, and showed that some amino acid residues within the LRR domain of NRCs determine their specificity toward sensor NLRs.

6.1 Redundancy of helper NLRs contribute to robustness of the immune system

One of the major features of biological systems is robustness, which can be achieved by providing alternative pathways to the same function, *i.e.* redundancy (Kitano, 2007; Stelling et al., 2004). A common example of

redundancy is genetic redundancy through gene duplication, which allows a biological system to tolerate mutations, termed mutational robustness, a feature that is also critical to enable phenotypic plasticity in evolution (Fares, 2015; Wagner, 2014). Robustness also increases tolerance to environmental disturbance, a feature known as environmental robustness (Stelling et al., 2004). The immune system should benefit by enhanced robustness given that it deals with rapidly evolving pathogens. Network architecture of the plant immune system is thought to promote strong and stable defence signalling (Kitano and Oda, 2006; Tsuda et al., 2009). Thus, I propose that redundancy in the NRC-signalling network, as well as the dramatic evolutionary expansion of the NRC-superclade, reflect an evolutionary trend towards increased robustness in this plant immune system.

In line with the hypothesis above, redundancy of helper NLRs may provide mutational robustness for both helper NLRs and sensor NLRs. Possibly, NRCs could tolerate increased mutation load thanks to the functionally redundant genes in the genome. This may result in higher levels of polymorphisms in helper NLRs, thereby increasing flexibility and evolutionary potential of their sensor NLR. Thus sensor NLRs could diversify and acquire beneficial mutations with less constraint for NRC-dependent immune signalling. Our phylogenetic analyses are consistent with a model in which the sensor NLRs have diversified more extensively than the NRC possibly reflecting rapid coevolution with plant pathogens. Indeed, most of the solanaceous sensor NLR groups have expanded after speciation of pepper, tomato, and potato, whereas NRC family is one of a few NLR groups with no sign of recent expansion in the Solanaceae (Seo et al., 2016).

Redundancy of the NRC helpers may provide environmental robustness to this immune system. Several plant pathogens evolved effector proteins to suppress immune responses, indicating that pathogens can cause major disturbances to immune systems (Ali et al., 2015; Bos et al., 2006; Lozano-Duran et al., 2014; Postma et al., 2012). Helper NLRs, such as NRCs, would make attractive targets for pathogen effectors as this would impair the activities of multiple sensor NLRs. Thus redundancy among NRC paralogs

may have evolved to overcome suppression by pathogen effectors. Currently, with my colleagues in the Kamoun Lab, we are screening for pathogen effectors that suppress NRC activities. This would provide insights into the extent to which redundancy of NRCs have emerged to counteract pathogen effectors.

6.2 The NRC signalling network may have originated from a unique NLR pair

The genome-wide comparison of NLRs revealed one NRC-helper and two NRC-sensors from sugar beet. These sugar beet NRC helper/sensor homologs are closely linked on the chromosome, similar to many NLR pairs identified from other plant species. I hypothesised that the common ancestor of caryophyllales and asterids may have carried a single NLR pair, which expanded into a superclade in asterids plants during evolution. Due to a lack of genomic information, it is not clear whether the orthologs of NRC-helper/sensor in other caryophyllales species also show a pattern of NRC expansion. Further comparison with additional genome sequences from taxonomically diverse plants will provide additional information on how these NLRs evolved in different plant lineages.

As most NLRs are encoded by fast evolving genes that follow the “birth-and-death” process, some of the “intermediates” may have been lost during evolution. Thus, reconstructing the evolutionary history of a particular NLR group is generally difficult. Interestingly, some of the tomato NRC and NRC superclade sensor genes are genetically linked. For example, tomato *NLR-11990* (*Solyc04g011990*), a *NRC4*-dependent NLR, is clustered together with several tandemly duplicated paralogs on chromosome 4. This NLR is not tightly linked to the *NRC4* cluster (*Solyc04g00730-7070*); however, a truncated NLR (*Solyc04g00780*), with 50% protein sequence identity to *NLR-11990*, is tightly linked with the *NRC4* cluster. Thus, it is possible that the *NLR-11900* cluster originated from ectopic duplication followed by tandem duplication of a NLR gene that was closely linked with *NRC4*. Furthermore, in

tomato, a *NRC-like* sequence (DC0002NLR0020) is located within a NLR gene (*Solyc04g08120-8200*) cluster syntenic to the *Hero* gene cluster in potato (Andolfo et al., 2014; Jupe et al., 2012), indicating that some of these sensor NLRs in the NRC superclade may still be tightly linked with helper NLRs.

6.3 Downstream mechanisms of NLRs correlate with the phylogeny

Different types of NLR, i.e. TNL and CNL, proteins have different downstream signalling pathways (Aarts et al., 1998). For example, EDS1 is required for the activity of several TNL proteins, such as RPP2, RPP4, RPP5, RPP21, and RPS4, and these proteins are independent of – or weakly dependent on – NDR1. Conversely, NDR1 is required for the activity of several CNL proteins, including RPS2, RPM1, and RPS5, which are all independent of EDS1 (Aarts et al., 1998). Moreover, the ADR1 helper NLR family is required for the function of most TNL proteins tested thus far, but only a few CNL proteins (Bonardi et al., 2011; Dong et al., 2016). These results imply that the downstream pathways of sensor NLR proteins may somewhat correlate with their phylogeny and identity of N-terminus domain.

To explore whether phylogeny correlates with activity in the NRC system, I assayed NLRs form different phylogenetic clades for NRC-dependency. This approach was aided by the fact that multiple NLR-type resistance genes have been identified from different species of solanaceous plants, and phylogenetic relationship among these NLR genes have recently become clear. Interestingly, all of the NRC-dependent NLRs are within the NRC-superclade, whereas NLRs outside of this superclade are NRC-independent (Fig. 4.2). A clear relationship between NLR phylogeny and activity emerged. Although it is impractical to test every single NLR from solanaceous species, I hypothesise that other sensor NLRs in the NRC-super-clade are dependent on NRC2/3/4 or other members of the NRC family.

To my knowledge, functional analyses of plant NLRs along with a phylogenetic framework have not been performed in a comprehensive

fashion. With an ever increasing number of NLR type resistance genes identified, it would be interesting to revisit studies about other components known to contribute to NLR activity. These include SGT1, HSP90, RAR1, EDS1, NDR1, NRG1, ADR1 and others. It is possible that different NLR clades show differential dependency for these components.

Convergence of signalling events induced by distantly related NLRs is unknown. One of the most common readouts of NLR-mediated responses is cell death, yet it is not clear whether the cell death responses induced by distantly related NLRs are activated through the same mechanism. It is also unclear to what degree signalling events from distantly related NLRs converge, and whether convergences correlate with the evolutionary history of the immune receptors. Leveraging phylogenetic information to perform comprehensive studies of NLR signalling may clarify these issues. In particular, it will be important to identify shared downstream elements of NLR signalling, the degree to which signalling converges, and which mechanisms are specific to certain NLR lineages.

6.4 Functionally redundant helper NLRs display high sequence polymorphism and copy number variation

Although the NRC2/3/4 display functional redundancy in NLR-triggered immunity, these three helper NLRs share only 49% to 66% protein sequence identity. Similarly, despite sharing only 66-68% sequence identity, members of the ADR1 family (ADR1, ADR1-L1, ADR1-L2) are also functionally redundant. It is possible that some critical residues involved in intra- or inter-molecular interaction are highly conserved among functionally redundant helper NLRs, whereas most other parts of the proteins have higher tolerance to mutations, and thus functionally redundant helper NLRs may display high degree of sequence polymorphism.

I initially identified *NRC2/3* and *NRC4* using distinct NLR immune receptors and, only later discovered that they play redundant roles in the immunity mediated by additional NLR immune receptors. The data presented

in this thesis about *NRC4* focused on one copy from the *N. benthamiana* genome. In fact, there are two highly similar *NRC4* copies in *N. benthamiana* and the VIGS silencing fragment used here targets both genes simultaneously. In contrast, there are three clustered *NRC4* orthologs in tomato, suggesting that identifying *NRC4* by gene silencing or mutation screens in tomato would be unlikely. This complexity and copy number variation was also observed with solanaceous *NRC2* homologs. For example, *N. benthamiana* has three NRC2 genes whereas tomato has only one *NRC2* gene (Fig. A2.1). This genetic redundancy with multiple functional copies may also explain why *NRC2/3/4* have not been identified in previous genetic screens for Pto/Prf-mediated immunity and Mi autoactivity (Lu et al., 2003; Mantelin et al., 2011). In summary, it would have been unlikely to identify the NRC-signalling network if the study was performed with Rx, Bs2 or other NLRs that are dependent on several NRC members.

6.5 Do NRC homologs function immediately downstream of NRC-dependent sensor NLRs?

My findings suggest that NRC family members serve as a point of signalling convergence for one-third to one-half of the NLRs of solanaceous species. However, it is still unclear whether NRCs are immediately downstream of the sensor NLRs, or whether there are other components in between. Several studies of NLR pairs found that the two NLR proteins physically associate with each other, and that one of them is responsible for pathogen perception whereas the other is responsible for signalling activation (Cesari et al., 2014a; Cesari et al., 2014b; Williams et al., 2014). It is also possible that NRC family members associate with corresponding sensor NLRs but these experiments have not been completed yet. Indeed, preliminary results from co-immunoprecipitation experiments I performed suggest that NRCs associate with sensor NLRs, supporting the hypothesis that NRCs are immediate downstream of sensor NLRs. However, more protein-protein interaction experiments are required to validate the biological relevance of this helper-sensor NLR association.

ADR1 and NRG1 in the RNL (CC_R-NB-LRR) clade are considered helper NLRs but this clade is distantly related to the NRC clade (Andolfo et al., 2014; Bonardi et al., 2011; Collier et al., 2011). ADR1 family members are genetically required by several TNLs in *A. thaliana*, whereas NRG1 has been tested only in *N*-mediated response to TMV in *N. benthamiana* (Bonardi et al., 2011; Peart et al., 2005). It is unclear whether ADR1/NRG1 function in a similar way to NRCs, and there is also no evidence of physical association between ADR1 or NRG1 with their upstream TNLs. ADR1/NRG1 are ancient NLR genes that originated from whole genome duplication (Shao et al., 2016), whereas NRC family evolved more recently, suggesting that the mechanism by which ADR1/NRG1 function in NLR-mediated immunity may be different from the NRC family.

It is possible that other helper NLR proteins occur in the genomes of angiosperms, but redundancy may have prevented their discovery. Moreover, in line with what was observed in the NRC and ADR1 families, redundant helper NLRs may not have high sequence identity. Thus, classical mutagenesis and silencing screens may not yield any phenotypes when only one or few of the homologs are targeted. As the NRC family forms a sister clade to NRC-dependent clade, it would be interesting to check other NLR phylogenetic clades for a similar branching structure. Further screens with multiple gene knockouts or simultaneous silencing may help identify novel helper NLRs in the plant genomes.

6.6 The LRR domain determines network specificity

The LRR domain in NLRs is thought to function in ligand binding, recognition specificity, and inter-domain interactions (Krasileva et al., 2010; Moffett et al., 2002; Ravensdale et al., 2012; Slootweg et al., 2013). Here, I describe a new activity to the LRR domain (Chapter 5). I mapped the sensor specificity determinants of NRC3 and NRC4 to the LRR region, suggesting that the LRR domains in NLRs can play a role in helper-sensor specificity. In another study about helper-sensor specificity, the RPS4/RRS1 NLR pair was

compared to RPS4B/RRS1B, and the TIR domain was found to be interchangeable between the two pairs (Saucet et al., 2015). This suggests that the TIR domains are not involved in determining the specificity in the RPS4/RRS1 pairs (Saucet et al., 2015). In line with the findings presented here, it is possible that the LRR domains in the RPS4/RRS1 pairs determine pairing specificity but this hypothesis remains to be tested.

Surprisingly, I found that some NRC3/4 chimeras that combined LRR1-7 from NRC4 and LRR8-13 from NRC3 have an expanded activity being able to function with both Prf and Rpi-blb2. This indicates that two independent protein regions contribute to sensor specificity in NRC3 and NRC4. I have mapped one of the protein regions to the amino acids between the 8th and 9th LRR units. However, the second protein region was more difficult to identify because several chimeras were either autoactive or non-functional. It is possible that the first half of the LRR domain with the ARC2 subdomain (Moffett et al., 2002; Slootweg et al., 2013), and thus any disturbance in this region would affect the overall integrity of the NLR protein. As the exposed residues between LRR units are likely to determine pairing specificity, further experiments could further explore the effects of polymorphisms between NRC3 and NRC4 in the regions between LRR units.

Although I narrowed down specificity determinants of the NRCs, the specificity determinants of the sensor NLRs have not yet been identified. I hypothesise that, similar to NRCs, exposed residues between the LRR units of sensor NLRs may drive helper-sensor paring specificity. This can be tested with chimeras between sensor NLRs, such as R1 and Prf, or with other combinations. Although there is no clear evidence that NRCs associate with corresponding sensor NLRs, it is possible that these helper and sensor NLRs form complexes and that the LRR domains of both NLRs play important roles in determining pairing specificity. Further experiments including protein-protein interaction assays may help to understand how helper NLR proteins combine with sensor NLRs, and how downstream immune signalling is activated upon pathogen recognition.

6.7 A gene silencing complementation assay using synthetic genes

The gene silencing complementation assay using synthetic genes is an important technical development to the work presented in this thesis. VIGS and other RNAi assays suffer from off target-effects, which may lead to misidentification of the gene of interest. Thus, the interpretation of results from silencing experiment needs to be done with caution (Senthil-Kumar and Mysore, 2011). Several solutions have been proposed, such as confirming the reduction of the target mRNA and related genes, performing gene expression profiling, checking the phenotype caused by different region of the target gene, and rescuing the silencing effect by siRNA-resistance gene copy (Senthil-Kumar and Mysore, 2011). Computational tools, such as VIGS-tool on SGN (http://vigs.solgenomics.net), have also been developed to improve the design of RNA silencing constructs (Fernandez-Pozo et al., 2015; Xu et al., 2006). These tools can help the prediction of the target gene as well as selecting the best region to achieve specific silencing or multiple silencing effects (Fernandez-Pozo et al., 2015; Xu et al., 2006).

Some studies use heterologous expression of functional homologs from different species to rescue the phenotype caused by RNAi (Liebrand et al., 2013; Peng et al., 2016). However, this approach is not ideal, particularly when the heterologous gene has high homology with the endogenous gene, or the polymorphisms of the protein sequences affect their activity in a heterologous system. In this study, I initially used tomato *NRC2* and *NRC3* to perform the complementation assay in *N. benthamiana*. I observed lower accumulation of tomato NRC2 and NRC3 in *NRC2/3*-silenced *N. benthamiana* as well as moderate to low activity in rescuing the cell death induced by Pto/AvrPto. These results suggest that the tomato *NRC2* and *NRC3* nucleotide sequences may not be divergent enough to fully evade the silencing effects caused by *N. benthamiana NRC2/3* fragments. To circumvent the issues mentioned above, I developed a method using synthetic genes that are resilient to gene silencing. I successfully validated the finding that the *N. benthamiana NRC2*, *NRC3,* and *NRC4* are redundantly or specifically contributing to the cell death mediated by different NLR proteins. This strategy

has been used successfully in only few other studies (Kumar et al., 2006; Pliego et al., 2013). For example, Kumar *et al.* (2006) used synthetic genes to validate the function of *SABP2* (salicylic acid-binding protein 2) in transgenic tobacco. Compared to the design by Kumar *et al*. (2006), in which synonymous substitutions were introduced into all codons in the open reading frame, I only changed the 450 bp region directly targeted by the VIGS fragment. One concern with the design was the effect of secondary small RNAs, which are generated during the process of silencing the endogenous gene. These secondary small RNAs may still target the complementing gene. However, protein accumulation levels of transiently expressed synthetic NRCs in the *NRC*-silenced background were similar to the control. According to the literature, initiation of secondary small RNA production requires asymmetrical mismatch in the structure of the dsRNA intermediate (Manavella et al., 2012). Since the VIGS fragments used here match the target gene perfectly, the generation of secondary small RNA may not have significant contribution to the gene silencing effect here.

In addition to validating the phenotype and identity of the causal gene, complementation with synthetic genes can also be used for functional analysis of the gene-of-interest (Kumar et al., 2006). For example, in this study, I used mutated synthetic *NRC4* to demonstrate that the p-loop is required for the activity of NRC4. Additionally, chimeric NRC3 and NRC4 were expressed as synthetic genes that evade the effects of silencing. Thus, the combinations of virus-induced gene silencing and complementation with synthetic genes provided an efficient and rapid assay for functional analyses of genes in *N. benthamiana*.

6.8 Concluding remarks and future challenges

In conclusion, I discovered that a large NLR immune signalling network with a complex architecture mediates immunity to oomycetes, bacteria, viruses, nematodes, and insects in solanaceous species. The network has emerged over 100 million years ago from an NLR pair that has since

diversified into up to one-half of the NLRs of asterids plants. I speculate that this NLR network increases the evolvability and robustness of immune signalling to counteract rapidly evolving plant pathogens.

There are still many unanswered questions about the NRC signalling network. For example, how do NRC helper and sensor NLRs operate together? Do they form protein complexes? Are these similar to NLR inflamasommes in animals? What plant components are immediately downstream of NRCs? From a broader perspective, how does this NRC signalling network correlate with the signalling mediated by NRC-independent NLRs? Do these signalling channels converge at some point in the downstream pathway? Lastly, do other helper NLRs also form networks with multiple sensor NLRs? Answering these fundamental questions about plant immunity would help advance our understanding of plant immunity and open up new opportunities for translational applications.

Appendix I

Supplemental figures for Chapter 3: The helper NLR proteins NRC2 and NRC3 but not NRC1 are required for *Pto*-mediated cell death and resistance in *Nicotiana benthamiana*

Table A1. 1 Pairwise comparison of tomato and *N. benthamiana* NRC homologs

Percentage of protein sequence identity was calculated using BLASTP. Results of comparisons of sequences from the same subclade (Fig. 3.1) are marked in grey.

	*Sl*NRC1	*Sl*NRC2	*Nb*NRC2a	*NbNRC2b*	*Nb*NRC2c	*Sl*NRC3
*Sl*NRC2	69					
*Nb*NRC2a	69	86				
*Nb*NRC2b	69	85	98			
*Nb*NRC2c	66	78	79	78		
*Sl*NRC3	64	69	68	68	65	
*Nb*NRC3	63	70	69	69	65	86

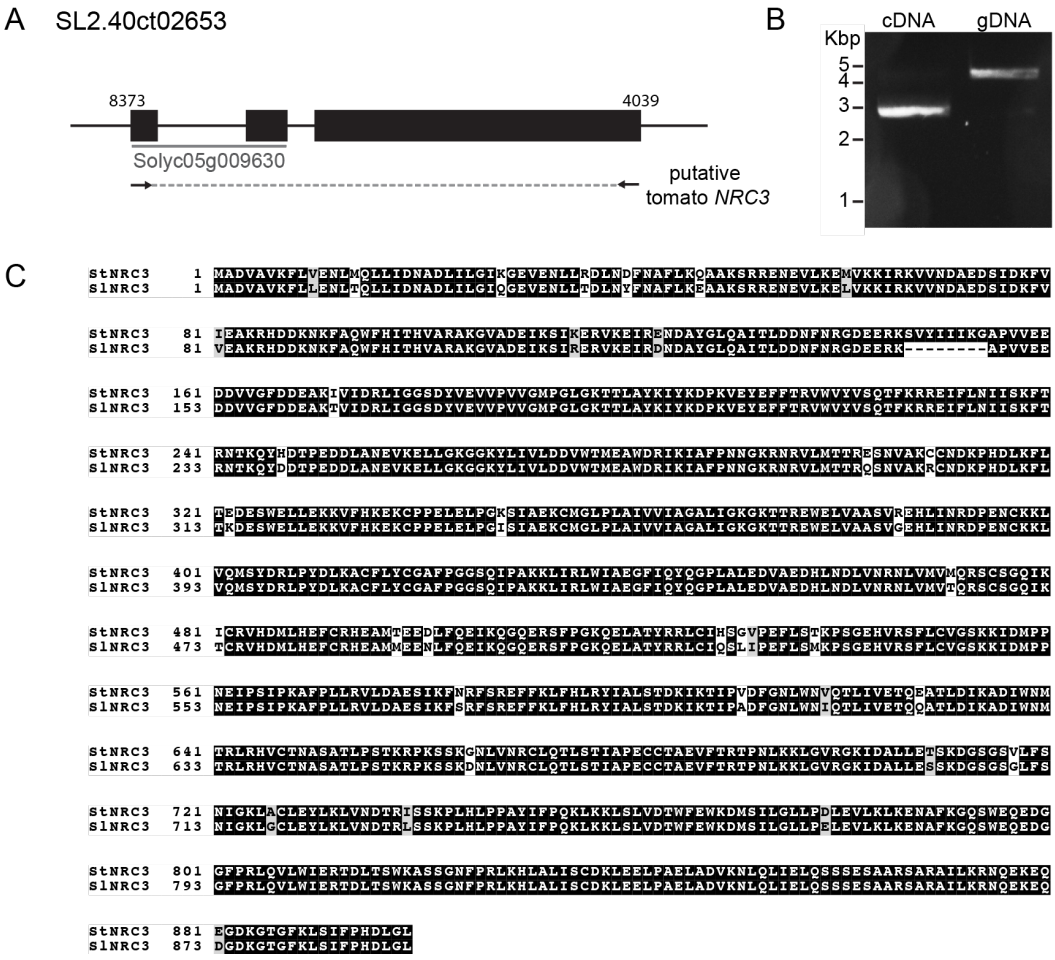

Figure A1. 1 Cloning of tomato *NRC3*

(A) Schematic representation of predicted gene model of tomato *NRC3* (*SlNRC3*). Black boxes represent the three exons of *SlNRC3*. Numbers on the top indicate positions of the start and stop codons in the contig. The first two exons were annotated as Solyco05g009630 in the database in SGN. (B) PCR amplification of *SlNRC3* with tomato cDNA and genomic DNA. (c) Sequence alignment of tomato NRC3 with potato NRC3 (Sotub05g007690). Sequences were aligned with ClustalW2 and analysed by BoxShade. Identical amino acids are highlighted in black and conserved amino acids are marked in grey.

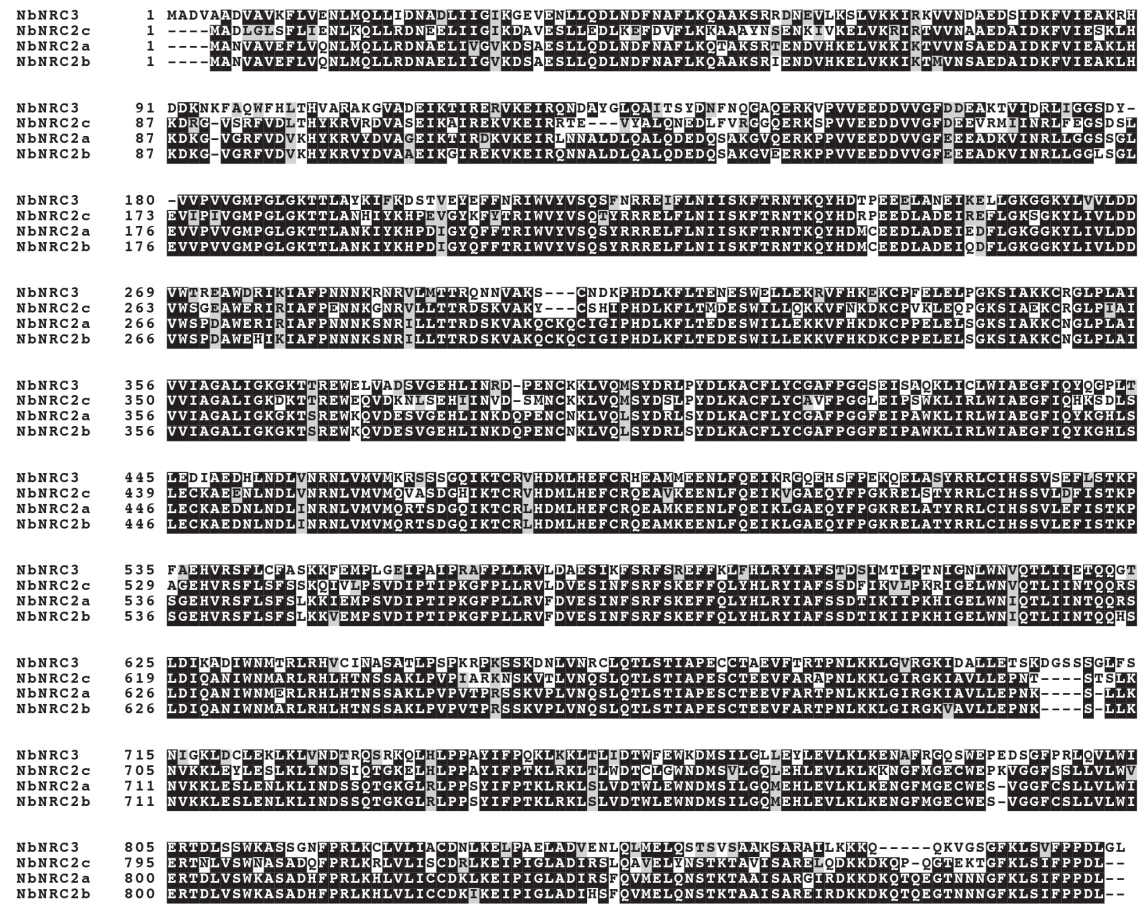

Figure A1. 2 Protein sequence alignment of NRC homologs in *N. benthamiana*

Sequences of NRC homologs in *N. benthamiana* were aligned with Clustal Omega and analysed by BoxShade. Identical amino acids are highlighted in black and conserved amino acids are marked in grey. The sequences of NRC2a, NRC2b and NRC3 were confirmed with evidence from cDNA.

A

```
NbNRC2a         ATCAAGATCATTCCTAAACACATTGGAGAACTGTGGAACATCCAAACACTCATAATTAAC 1860
SlNRC1_LRR      -TTAAAGTCATTCCGAAACATGTTGGGGAACTTTGGAACGTACAAACCCTCATTGTCAAC 59
                 * **..******* ***** .****.***** ******.*.*****.*****:.* ***

NbNRC2a         ACGCAACAACGCTCTCTTGATATCCAAGCAAACATATGGAATATGGAACGACTAAGGCAT 1920
SlNRC1_LRR      ACACAACAGATCAACCTTGATATTCAAGCAGACATATTGAACATGCCCCGGCTGAGGCAT 119
                **.*****.. *:. ******** ******.****** *** *** ..**.**.******

NbNRC2a         CTGCACACTAACTCTTCTGCTAAATTGCCTGTTCCTGTGACCCCAAGAAGTAGTAAAGTT 1980
SlNRC1_LRR      CTGCTCACCAACACGTCTGCTAAATTGCCTGCGCTTGCTAACCCCAAAACAAGTAAGACT 179
                ****:*** ***:* ****************  * **  *.***.*.** :*****.. *

NbNRC2a         CCTTTGGTAAATCAAAGCCTGCAAACTCTCTCCACCATTGCTCCCGAAAGCTGCACAGAA 2040
SlNRC1_LRR      ACCTTGGTAAATCAAAGCCTGCAAACCCTCTCCACAATTGCACCAGAAAGCTGCACTGAG 239
                .* ********************** ********.*****:**.***********:**.

NbNRC2a         GAAGTGTTTGCAAGGACTCCAAACCTGAAAAAACTGGGTATTCGTGGGAAAATAGCTGTG 2100
SlNRC1_LRR      TATGT----------TCTCTCGA----------------------------------- 252
                 *:**          :*** ..*
```

B

```
NbNRC3          TTATGACCATTCCTACAAACATTGGGAATCTTTGGAACGTACAAACACTTATAATTGAGA 1860
SlNRC1_LRR      TTAAAGTCATTCCGAAACATGTTGGGGAACTTTGGAACGTACAAACCCTCATTGTCAACA 60
                ***:.. ****** *.*.* .*****.*:****************.** **:.* .* *

NbNRC3          CACAACAGGGTACTCTTGACATTAAAGCAGACATTTGGAATATGACAAGATTAAGGCATG 1920
SlNRC1_LRR      CACAACAGATCAACCTTGATATTCAAGCAGACATATTGAACATGCCCCGGCTGAGGCATC 120
                ********.  *. ***** ***.**********:* *** ***.*..*. *.******

NbNRC3          TGTGCATAAACGCCTCTGCTACATTGCCTTCCCCTAAGCGCCCCAAGAGTAGCAAGGACA 1980
SlNRC1_LRR      TGCTCACCAACACGTCTGCTAAATTGCCTGCGCTTGCTAACCCCAAAACAAGTAAGACTA 180
                **  ** .***.* *******.******* * * *.. ..******.* :** ***.. *

NbNRC3          ACTTGGTGAATCGTTGCCTACAAACACTTTCTACCATAGCACCTGAATGTTGCACGGCAG 2040
SlNRC1_LRR      CCTTGGTAAATCAAAGCCTGCAAACCCTCTCCACAATTGCACCAGAAAGCTGCACTG--- 237
                .******.****.::****.*****.** ** **.**:*****:***:* ***** *
```

Figure A1. 3 Pairwise alignment of *SlNRC1* silencing fragment with *NbNRC2a* and *NbNRC3*

The fragment used in Gabriels et al. (2007) for silencing *NRC1* in *N. benthamiana* was aligned with *NbNRC2a* and *NbNRC3* sequences by using ClustalW2.

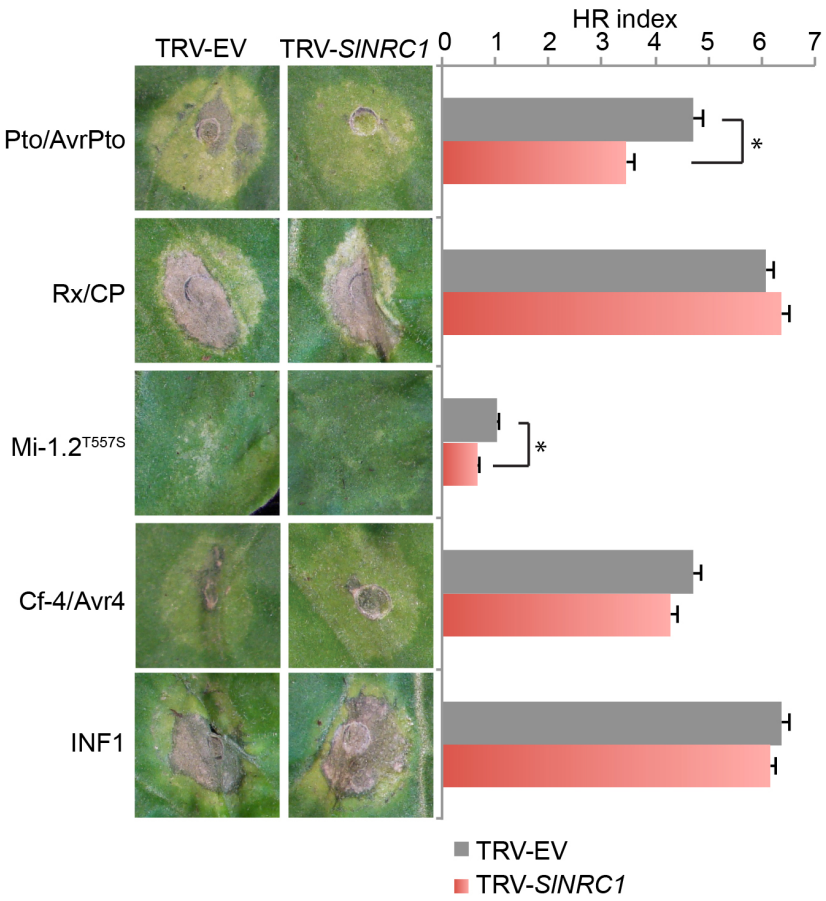

Figure A1. 4 VIGS in *N. benthamiana* with *SlNRC1* silencing fragment partially compromised Pto and Mi-1.2 mediated cell death

VIGS assay was performed with *SlNRC1* fragment described in Gabriels et al. (2007). Immune receptors and corresponding AVR proteins, autoactive immune receptor (Mi-1.2^{T557S}), or elicitin (INF1) were transiently expressed in *N. benthamiana* leaves. The HR results are presented with representative images. HR index was established at 7 days post infiltration (dpi). Bars represent mean ± SE of 24 infiltrations from one biological replicate. Statistical differences among the samples were analysed with Student's t-test (p-value < 0.001).

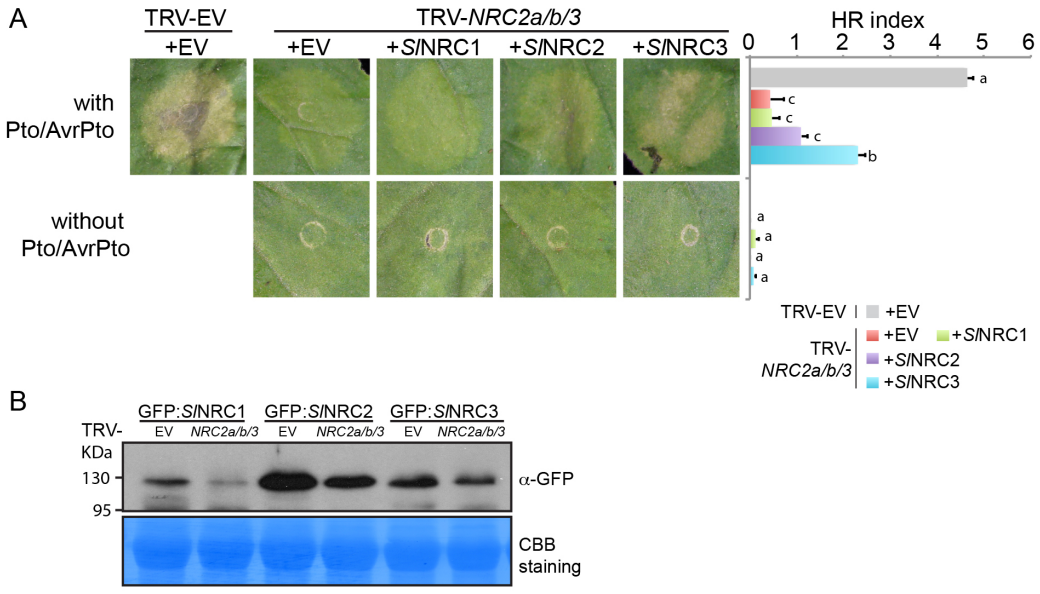

Figure A1. 5 Tomato NRC3 mediates Pto-induced cell death in *N. benthamiana*

(A) Complementation assay with tomato NRC homologs. Tomato NRC homologs (*Sl*NRC1, *Sl*NRC2 and *Sl*NRC3) were co-expressed with Pto/AvrPto in *NRC*-silenced (*NRC2a/b* and *NRC3*) *N. benthamiana*. Expression of Pto/AvrPto in VIGS control (EV) and expression of *Sl*NRC variants without Pto/AvrPto were used as controls. HR index was established at 7 days post infiltration (dpi). Bars represent mean + SE of 16 infiltrations from one biological replicate. Statistical differences among the samples were analysed with ANOVA and Tukey's HSD test (p-value < 0.001). Experiments were performed at least three times with similar results. (B) Protein accumulation of *Sl*NRC variants in VIGS control and *NRC2a/b/3*-silenced leaves. GFP is fused to *Sl*NRC variants at N-terminal and transiently expressed in VIGS control and *NRC2a/b/3*-silenced *N. benthamiana*. Samples were collected at 3dpi for western blot analysis.

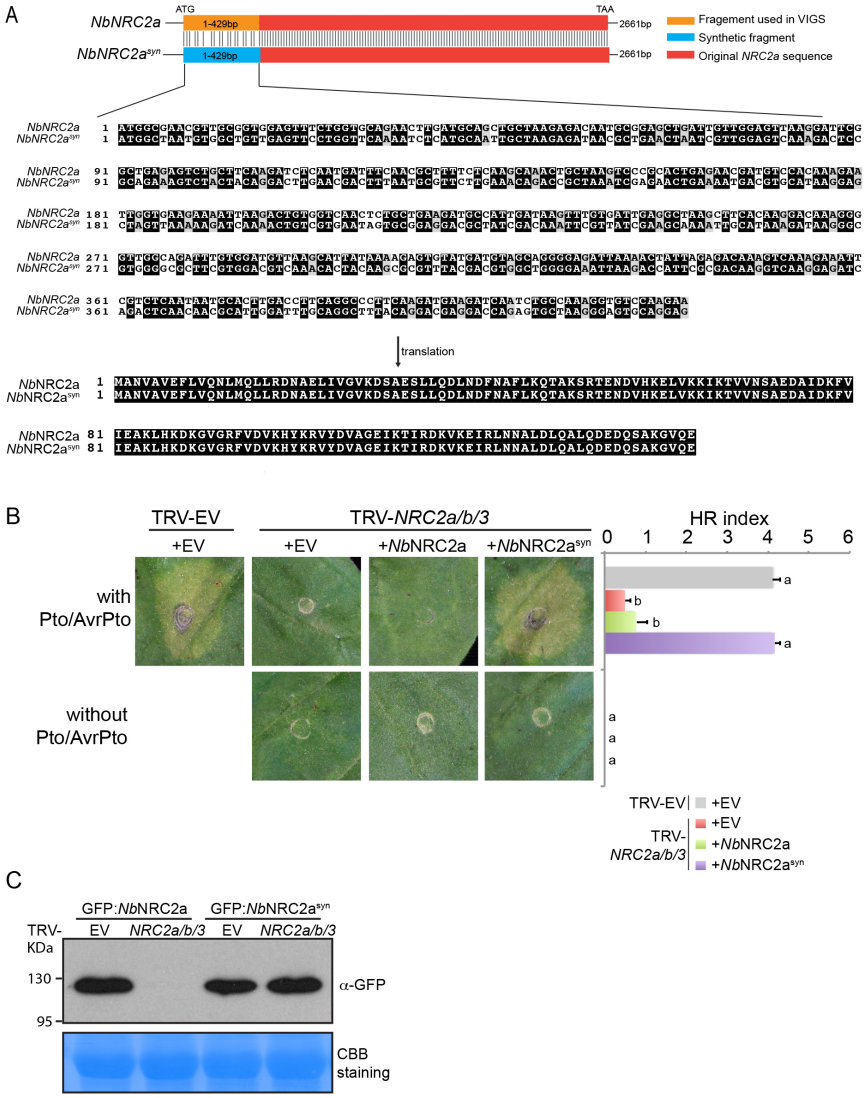

Figure A1. 6 Expression of synthetic *Nb*NRC2a rescues Pto-mediated cell death in *NRC*-silenced *N. benthamiana*

(A) Schematic representation of experimental design, DNA and protein sequences of the synthetic region. Shuffled synonymous codons were introduced in the synthetic sequence (*NbNRC2a*^{syn}) without changing the identity in protein sequence. (B) Expression of *NbRC2a*^{syn} rescues the cell death of Pto/AvrPto. *NbNRC2a* and *NbNRC2a*^{syn} were co-expressed with Pto/AvrPto in *NRC2a/b/3*-silenced *N. benthamiana* leaves. Expression of Pto/AvrPto in VIGS control (EV) and expression of *NbNRC2a* and *NbNRC2a*^{syn} without Pto/AvrPto were used as controls. HR was scored at 7 days post infiltration (dpi). Bars represent mean + SE of 14 infiltrations from one biological replicate. Statistical differences among the samples were analysed with ANOVA and Tukey's HSD test (p-value < 0.001). Experiments were performed at least three times with similar results. (C) Protein accumulation of NRC2a variants in VIGS control and *NRC2a/b/3*-silenced leaves. GFP is fused to NRC2a variants at N-terminal and transiently expressed in VIGS control and *NRC2a/b/3*-silenced *N. benthamiana*. Samples were collected at 3dpi for western blot analysis.

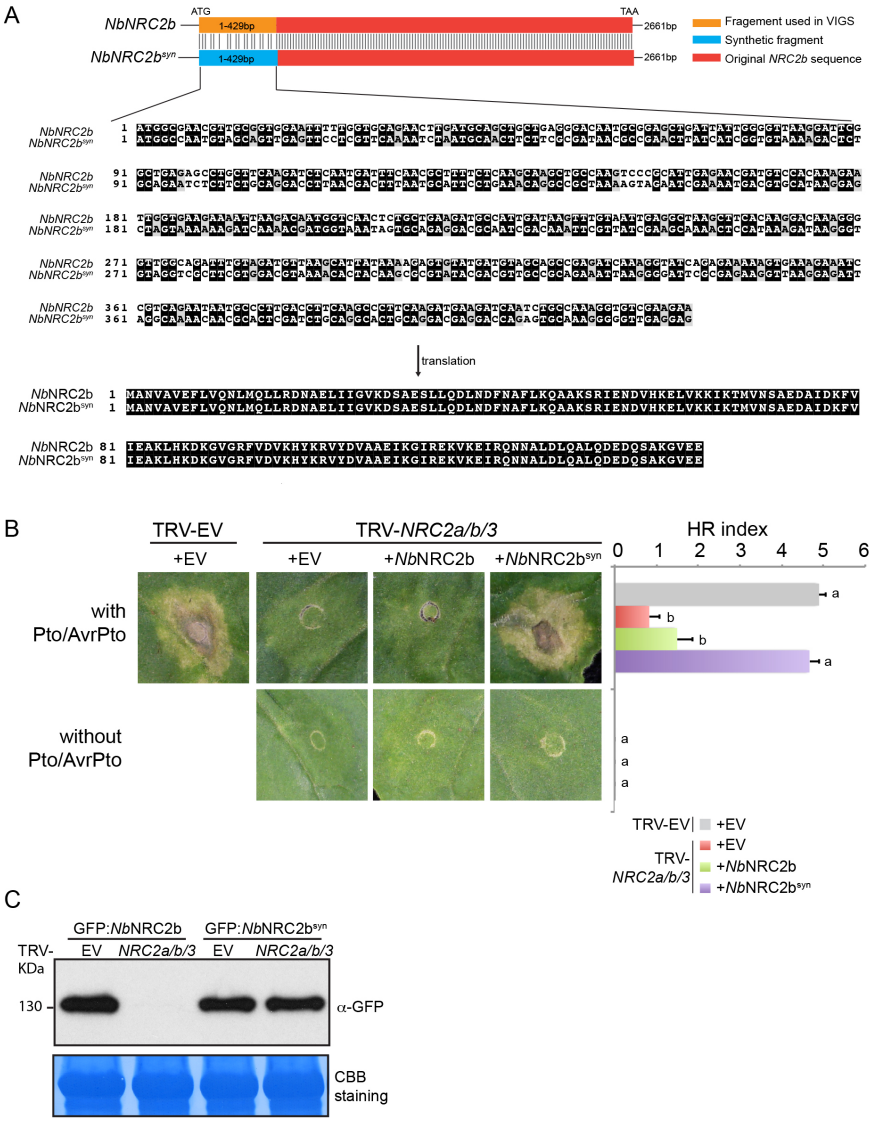

Figure A1. 7 Expression synthetic *Nb*NRC2b rescues Pto-mediated cell death in *NRC*-silenced *N. benthamiana*

(A) Schematic representation of experimental design, DNA and protein sequences of the synthetic region. Shuffled synonymous codons were introduced in the synthetic sequence (*NbNRC2b*^{syn}) without changing the identity in protein sequence. (B) Expression of *NbRC2b*^{syn} rescues the cell death of Pto/AvrPto. *NbNRC2b* and *NbNRC2b*^{syn} were co-expressed with Pto/AvrPto in *NRC2a/b/3*-silenced *N. benthamiana* leaves. HR was scored at 7 days post infiltration (dpi). Bars represent mean + SE of 18 infiltrations from one biological replicate. Statistical differences among the samples were analysed with ANOVA and Tukey's HSD test (p-value < 0.001). Experiments were performed at least three times with similar results. (C) Protein accumulation of NRC2b variants in VIGS control and *NRC2a/b/3*-silenced leaves. GFP is fused to NRC2b variants at N-terminal and transiently expressed in VIGS control and *NRC2a/b/3*-silenced *N. benthamiana*. Samples were collected at 3dpi for western blot analysis.

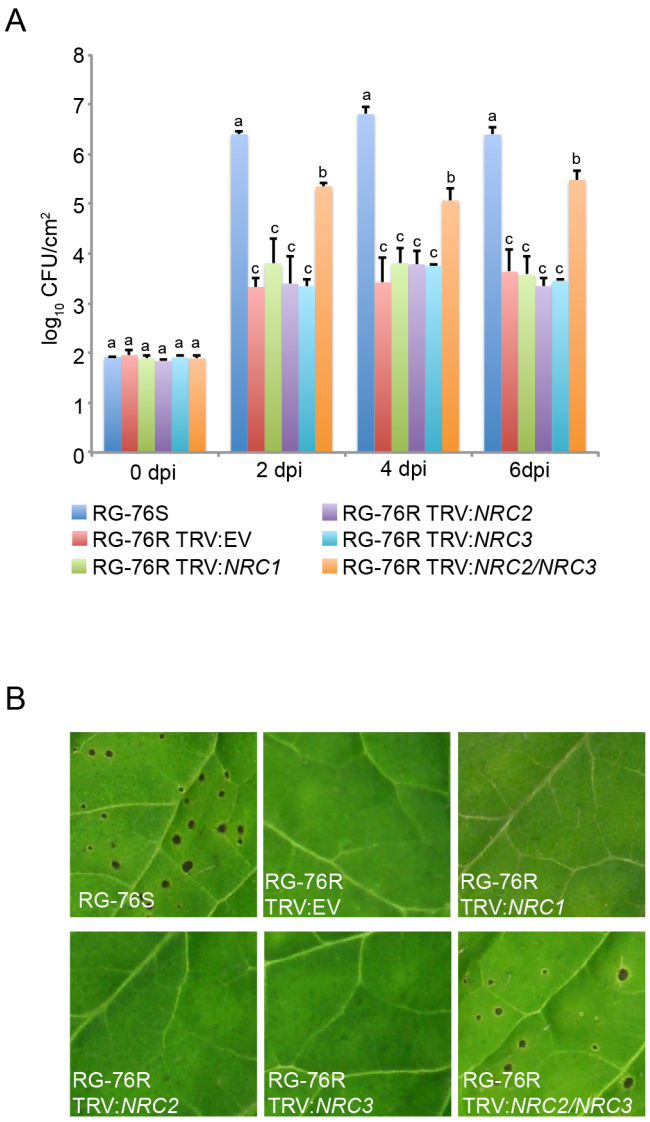

Figure A1. 8 *NRC2* and *NRC3* are required for *Pto/Prf*-mediated resistance in tomato

(A) Bacterial growth assay of *P. syringae* DC3000 in *NRC*-silenced tomato. Population of *P. syringae* DC3000 were measured at *P. syringae* DC3000 at 0, 2, 4, 6 days after inoculation. Error bars indicate the standard deviation of population from one representative biological replicate. Statistical differences among the samples were analysed with ANOVA and Tukey's HSD test (p-value < 0.05). Experiments were performed twice with similar results. (B) Bacterial speck symptom caused by *P. syringae* on tomato leaves. Pictures were taken 5 days after pathogen inoculation.

Appendix II

Supplemental figures for Chapter 4: A complex NLR signalling network mediates immunity to diverse plant pathogen

Table A2. 1 List of characterized CNL from solanaceous plants

Gene name	Origin species	Pathogen and protein recognised	In NRC-superclade	NRC-dependent
Rpi-blb2	*Solanum bulbocastanum*	*P. infestans*, AVRblb2	Y	Y
Mi-1.2	*Solanum peruvianum*	*Meloidogyne spp.* *Macrosiphum euphorbiae* *Bemisia tabaci*	Y	Y
Hero	*Solanum pimpinellifolium*	*Globodera rostochiensis* *Globodera pallida*	Y	n.d.[1]
Sw-5b	*Solanum peruvianum*	*Tomato spotted wilt virus*, NSm[2]	Y	Y
R8	*Solanum demissum*	*P. infestans*, AVR8	Y	Y
R1	*Solanum demissum*	*P. infestans*, AVR1	Y	Y
Prf	*Solanum pimpinellifolium*	*Ps. syringae*, AvrPto/AvrPtoB	Y	Y
Rx1	*Solanum andigena*	*Potato virus X*, CP[3]	Y	Y
Rx2	*Solanum acaule*	*Potato virus X*, CP[3]	Y	n.d.
Gpa2	*Solanum pimpinellifolium*	*Globodera pallida*, RBP-1	Y	n.d.
Bs2	*Capsicum chacoense*	*Xanthomonas campestris*, AvrBs2	Y	Y
Rpi-amr3	*Solanum americanum*	*P. infestans*	Y	n.d.
Rpi-vnt1	*Solanum venturii*	*P. infestans*, Avrvnt1	N	N
Tm2	*Solanum peruvianum*	*Tomato mosaic virus,* MP[4] *Tobacco mosaic virus,* MP[4]	N	n.d.
Rpi-mcq1	*Solanum mochiquense*	*P. infestans*	N	n.d.
R9	*Solanum demissum*	*P. infestans*	N	n.d.
Ph3	*Solanum pimpinellifolium*	*P. infestans*	N	n.d.
R2	*Solanum demissum*	*P. infestans*, AVR2	N	N
Rpi-blb3	*Solanum bulbocastanum*	*P. infestans*	N	n.d.
Rpi-chc1	*Solanum chacoense*	*P. infestans*	N	n.d.
Rpi-blb1	*Solanum bulbocastanum*	*P. infestans*, AVRblb1	N	N
I2	*Solanum pimpinellifolium*	*Fusarium oxysporum*, AVR2	N	n.d.
R3a	*Solanum demissum*	*P. infestans*, AVR3a	N	N
R3b	*Solanum demissum*	*P. infestans*, AVR3b	N	n.d.

[1] n.d., not determined experimentally.

[2] NSm, non-structural movement protein.

[3] CP, coat protein.

[4] MP, movement protein.

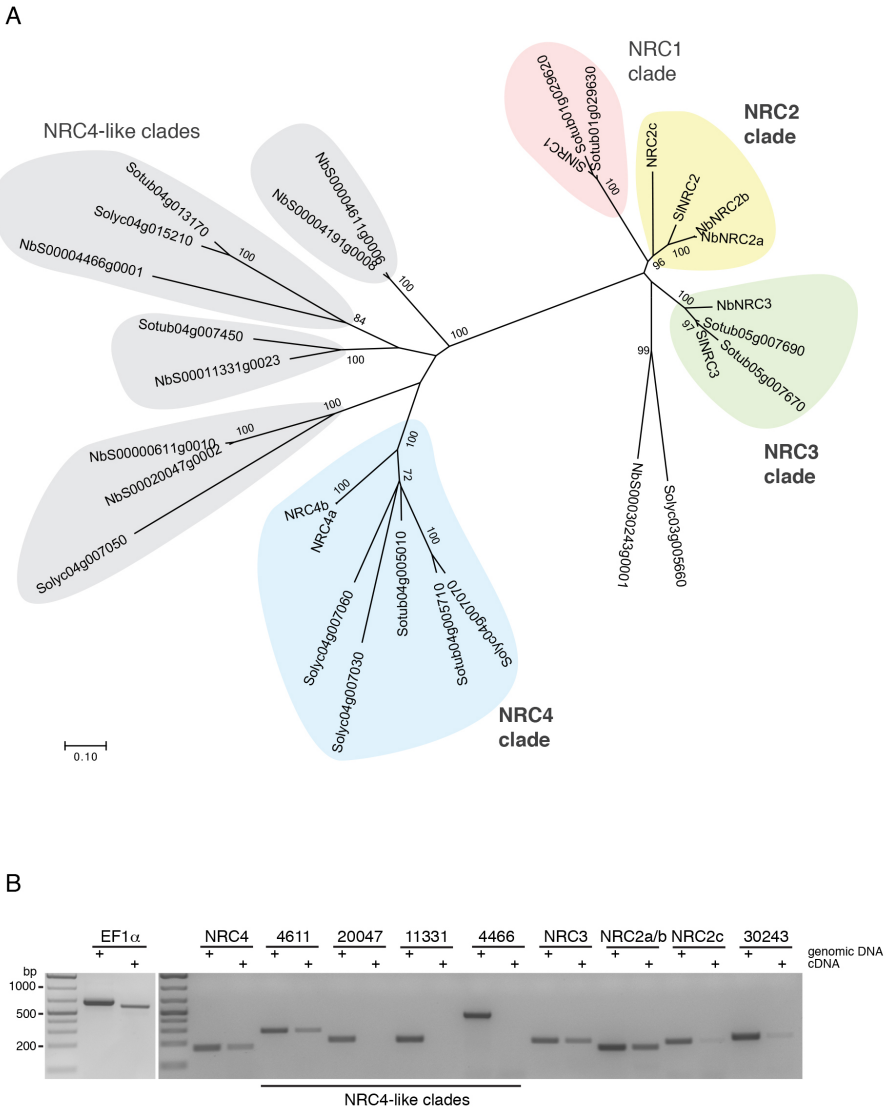

Figure A2. 1 Phylogeny and PCR analysis of NRC family members

(A) Maximum-likelihood phylogenetic tree of NRC family members. Protein sequences of NRC family members identified from *N. benthamiana* (NbS-), tomato (Solyc-), and potato (Sotub-) were aligned by using Clustal Omega, and then the NB-ARC domains were used for the further analysis. Phylogenetic tree was constructed in MEGA7 with Jones-Taylor-Thornton (JTT) substitution model and 1000 bootstrap iterations. Branches with bootstrap support higher than 70 are indicated. NRC1, NRC2, NRC3, NRC4 and NRC4-like clades were marked with red, green, yellow, blue and grey colour, respectively. (B) PCR and RT-PCR analysis of NRC family members. Primer pairs were designed based on cDNA sequences identified from *N. benthamiana* genome database. PCR with *N. benthamiana* genomic DNA (gDNA) was used to confirm the amplification with the primers. RT-PCR was used for checking the expression of the corresponding genes. Genes in the NRC4-like clades are labelled with the digital numbers from the accession numbers in (A).

A

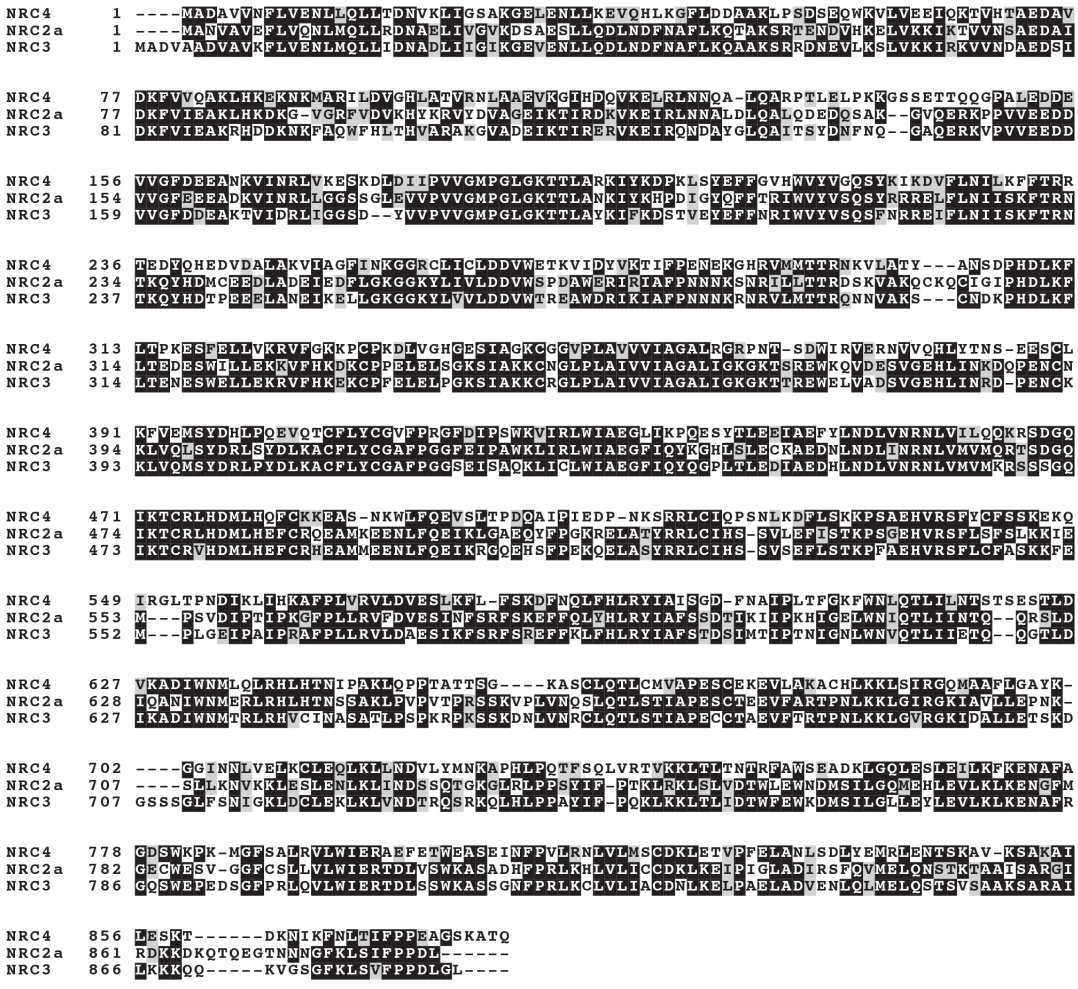

B

Sequence identity/similarity

	NRC2a	NRC3
NRC3	69/80	
NRC4	48/66	49/66

Figure A2. 2 Sequence alignment and pairwise comparison of NRC2/3/4

(A) Protein sequences of NRC2/3/4 were aligned with Clustal Omega and analysed by BoxShade. Identical amino acids are highlighted in black and conserved amino acids are highlighted in grey. (B) Pairwise comparison of identity/similarity of NRC2/3/4 protein sequences. Pairwise sequence comparisons were performed by aligning two sequences on BLASTP of NCBI.

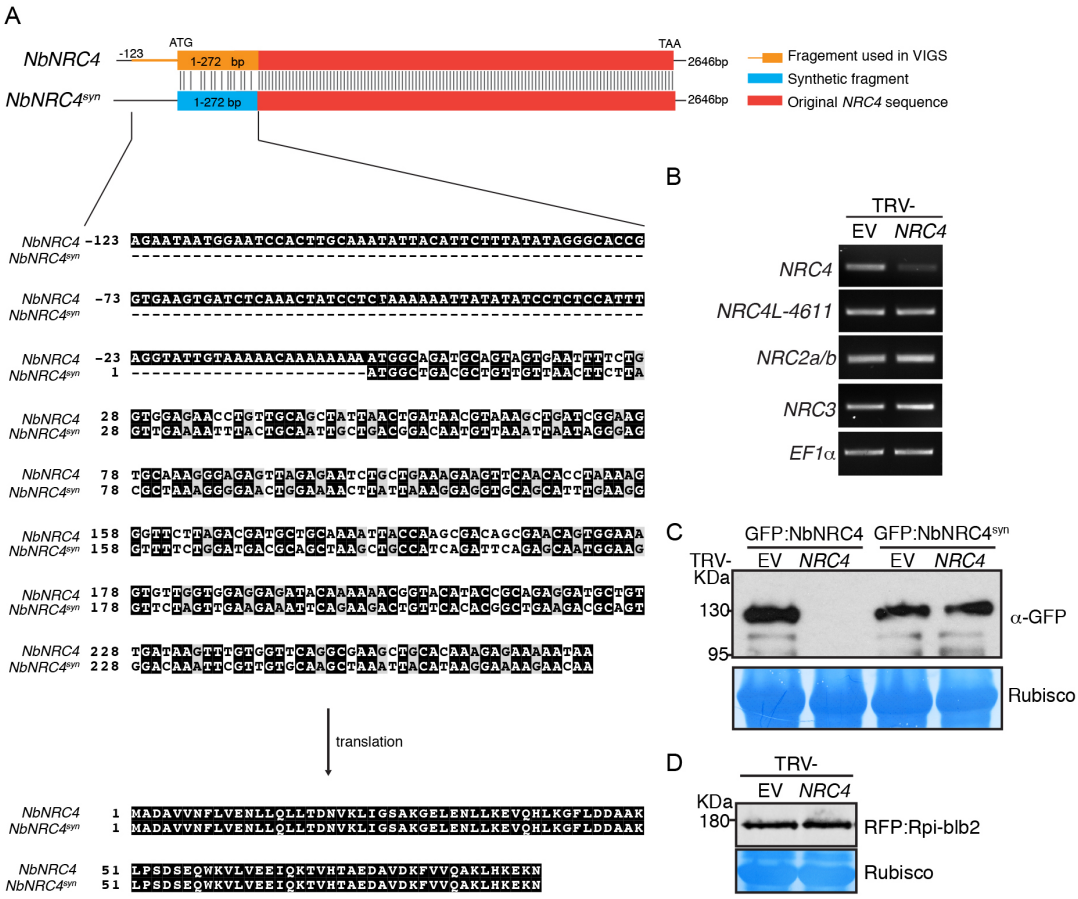

Figure A2. 3 Design of virus-induced gene silencing (VIGS) and complementation of NRC4

(A) Schematic representation of VIGS and complementation design. The region from -123bp to +272bp of *NRC4* was cloned into VIGS vector for silencing. Synonymous substitutions were introduced into synthetic *NRC4* (*NRC4*^{syn}) without changing the protein sequence. The nucleotide and protein sequence alignments indicate the synonymous changes in the synthetic variant. (B) Semi-quantitative RT-PCR of members in the NRC family. Leaves were collected three weeks after virus inoculation. The expression of *NRC2*, *NRC3*, *NRC4* and *NRC4L-4611* (NbS00004611g0006, see Fig. A2.1) were analysed. Elongation factor -1α (*EF1α*) was used as an internal control. (C) Protein accumulation of NRC4 variants in VIGS control and *NRC4*-silenced plants. N-terminal GFP-tagged NRC4 variants were transiently expressed in VIGS control and *NRC4*-silenced *N. benthamiana*. Samples were collected at 3dpi for immunoblot analysis. (D) Accumulation of Rpi-blb2 in *NRC4*-silenced *N. benthamiana*. RFP:Rpi-blb2 was transiently expressed in VIGS control and *NRC4*-silenced *N. benthamiana.* Samples were collected at 3 dpi for immunoblot analysis.

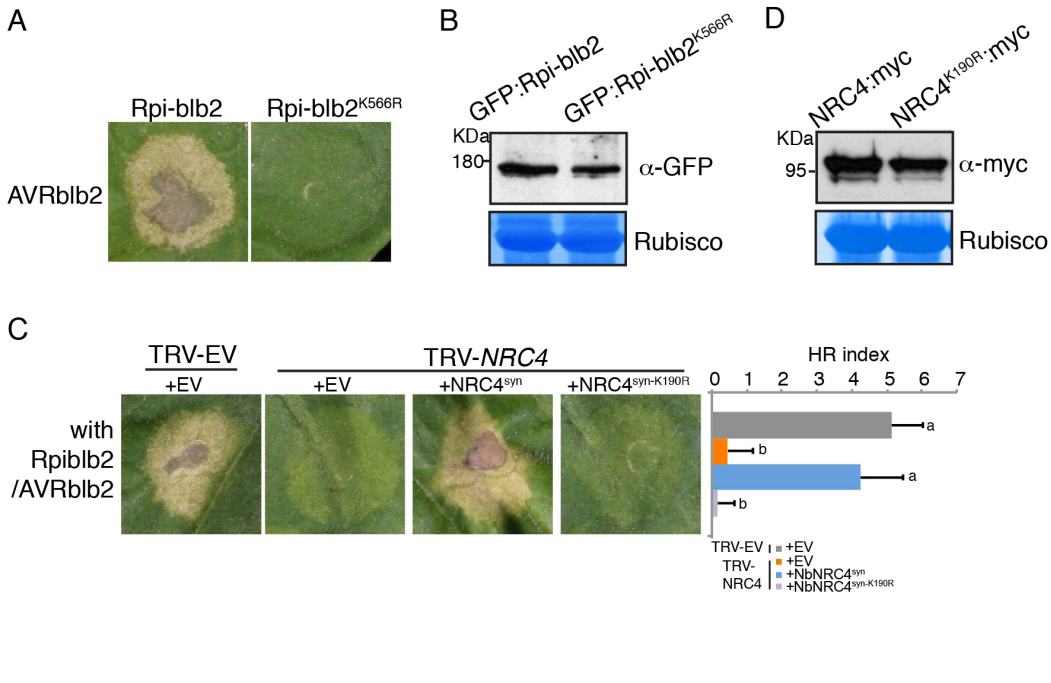

Figure A2. 4 Activity of both Rpi-blb2 and NRC4 are p-loop dependent

(A) P-loop is essential for the activity of Rpi-blb2. Wild type Rpi-blb2 and the p-loop mutant (K566R) were co-expressed with AVRblb2 in *N. benthamiana*. Images were taken 7 days after agroinfiltration. (B) Accumulation of Rpi-blb2 and Rpi-blb2 p-loop mutant. GFP:Rpi-blb2 variants were expressed in *N. benthamiana* by agroinfiltration. Samples were collected at 3 dpi for immunoblot analysis. (C) P-loop is essential for activity of NRC4. A lysine to arginine mutation was introduced into the p-loop of synthetic *NRC4*, and then the activity was examined by co-expression with Rpi-blb2 and AVRblb2 in *NRC4*-silenced plants. Hypersensitive response (HR) was scored at 7 days after agroinfiltration. Bars represent mean + SD of 24 infiltrations sites. Statistical differences among the samples were analysed with ANOVA and Tukey's HSD test (p-value < 0.001). (D) Accumulation of NRC4 and NRC4 p-loop mutant. NRC4:myc variants were expressed in *N. benthamiana* by agroinfiltration. Samples were collected at 3 dpi for immunoblot analysis.

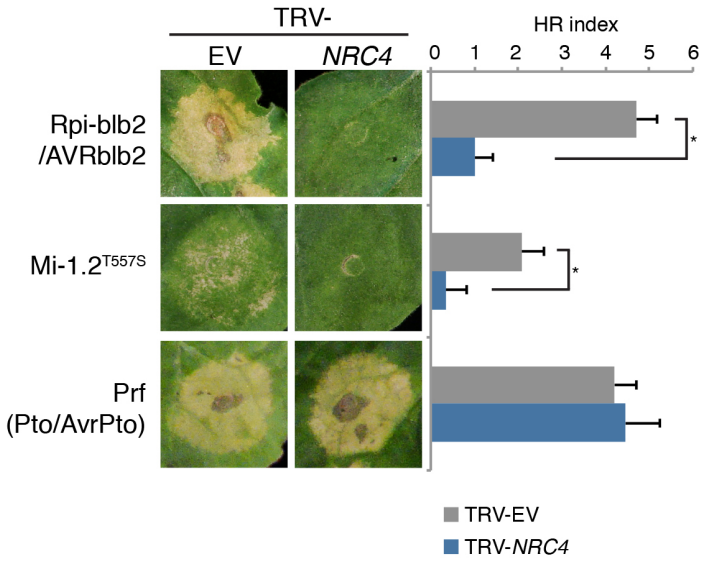

Figure A2. 5 *NRC4* is required for Mi-1.2-mediated cell death

Rpi-blb2/AVRblb2, autoactive Mi-1.2 (Mi-1.2^{T557S}), or Pto/AvrPto were transiently expressed in *N. benthamiana* by agroinfiltration. Hypersensitive response (HR) was scored at 7 days after agroinfiltration. Bars represent mean + SD from 24 infiltrations sites. Statistical differences among the samples were analysed with Student's t-test (p-value < 0.001).

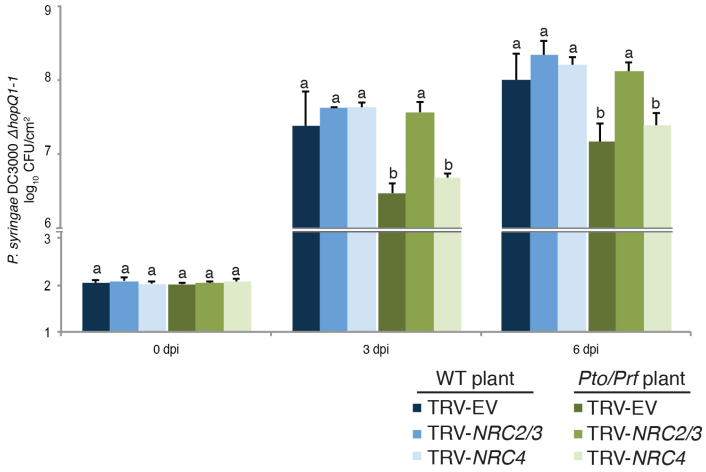

Figure A2. 6 *NRC4* is not required for Prf-mediated resistance

Bacterial growth assay of *Pseudomonas syringae* pv. *tomato* DC3000 *ΔhopQ1-1* in *NRC*-silenced *Pto/Prf* transgenic *N. benthamiana*. *NRC2/3* or *NRC4* were silenced in wild type or *Pto/Prf* transgenic *N. benthamiana* by VIGS. *Ps. syringae* pv. *tomato* DC3000 *ΔhopQ1-1* was infiltrated into *N. benthamiana* by using needless syringe and samples were collected at 0, 3, and 6 says post inoculation (dpi). The bars represent mean + standard deviation (SD) of population from four technical replicates in one representitive biological replicate. The different letters at the top of the columns indicate statistical significant differences based on ANOVA and Tukey's HSD test (p-value < 0.05). Experiments were performed three times with similar results.

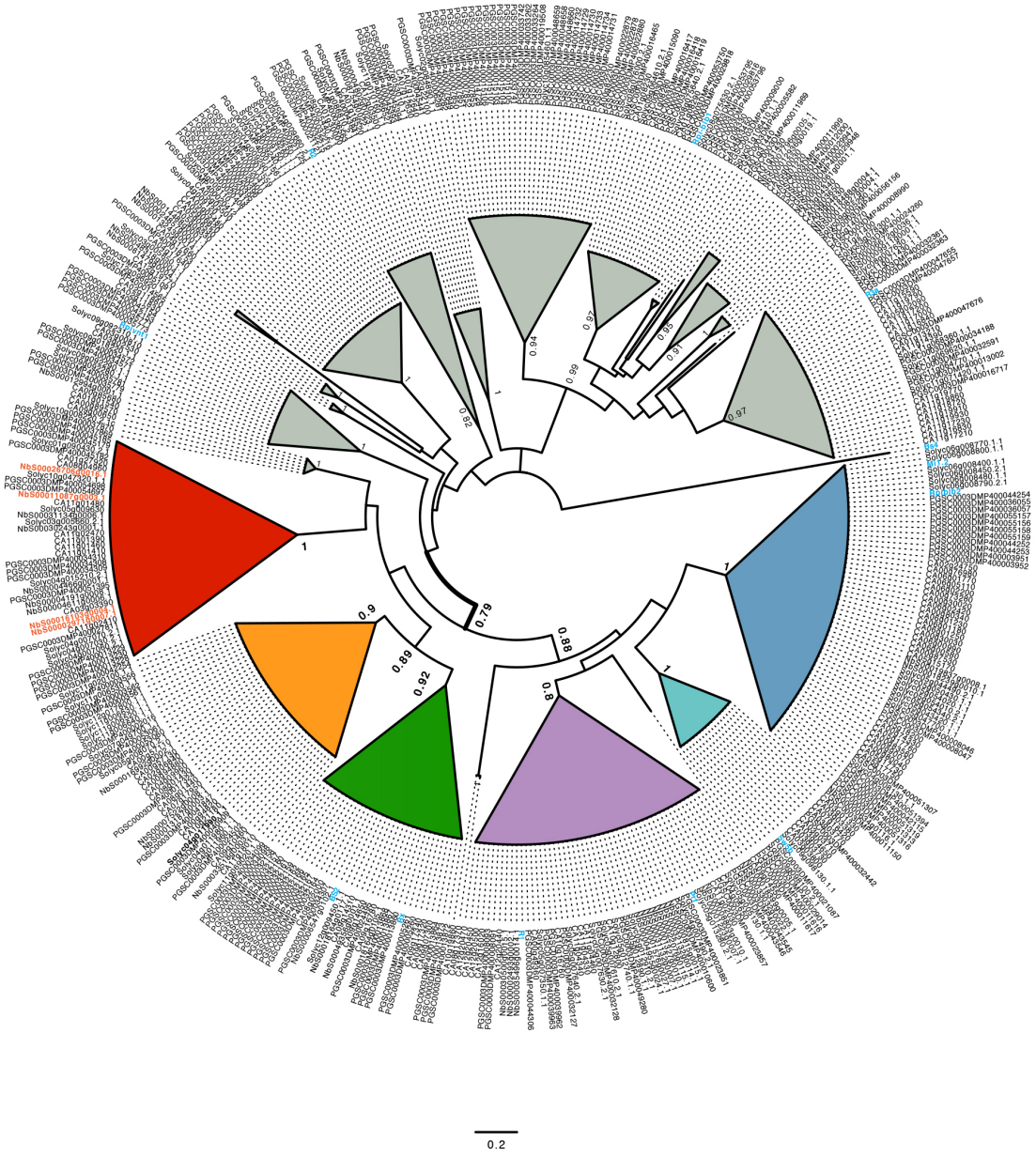

Figure A2. 7 Phylogenetic analysis of solanaceous NLR proteins

CNL proteins identified by NLR-parser from *N. benthamiana* (NbS-), tomato (Solyc-), potato (PGSC-) and pepper (CA-) were analysed by MEGA7 to generate maximum-likelihood phylogenetic tree. Only the NB-ARC domains of the sequences were used in the analysis. Sequences of several solanaceous CNL-type resistance proteins (marked in blue) were included as reference for different clades. Accession numbers of *N. benthamiana* NRC homologs are marked in orange. Branches with bootstrap support higher than 0.7 are indicated.

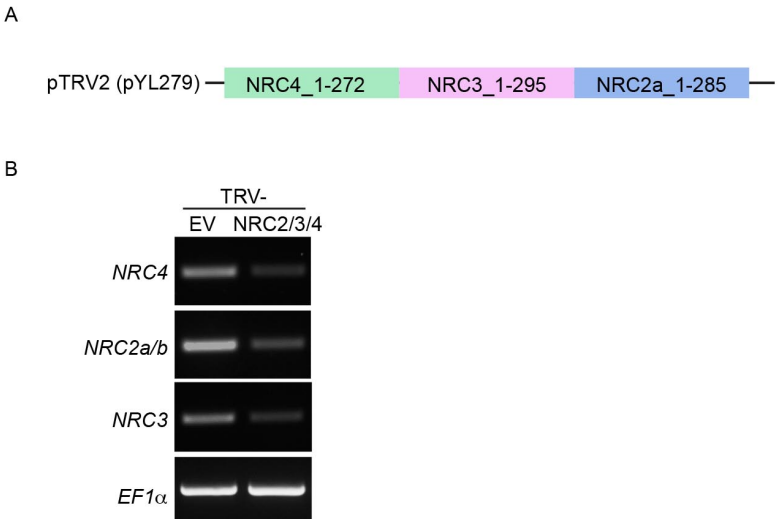

Figure A2. 8 *NRC2/3/4* triple silencing in *N. benthamiana*

(A) Schematic representation of design for *NRC2/3/4* triple silencing. Fragments from *NRC2/3/4* as indicated were combined together as one fragment and then cloned into TRV2 vector for silencing. (B) Semi-quantitative RT-PCR of *NRC2/3/4* triple silencing. Leaf samples were collected three weeks after virus inoculation. The expression of *NRC2*, *NRC3*, and *NRC4* were analysed. Elongation factor 1α (EF1α) was used as an internal control.

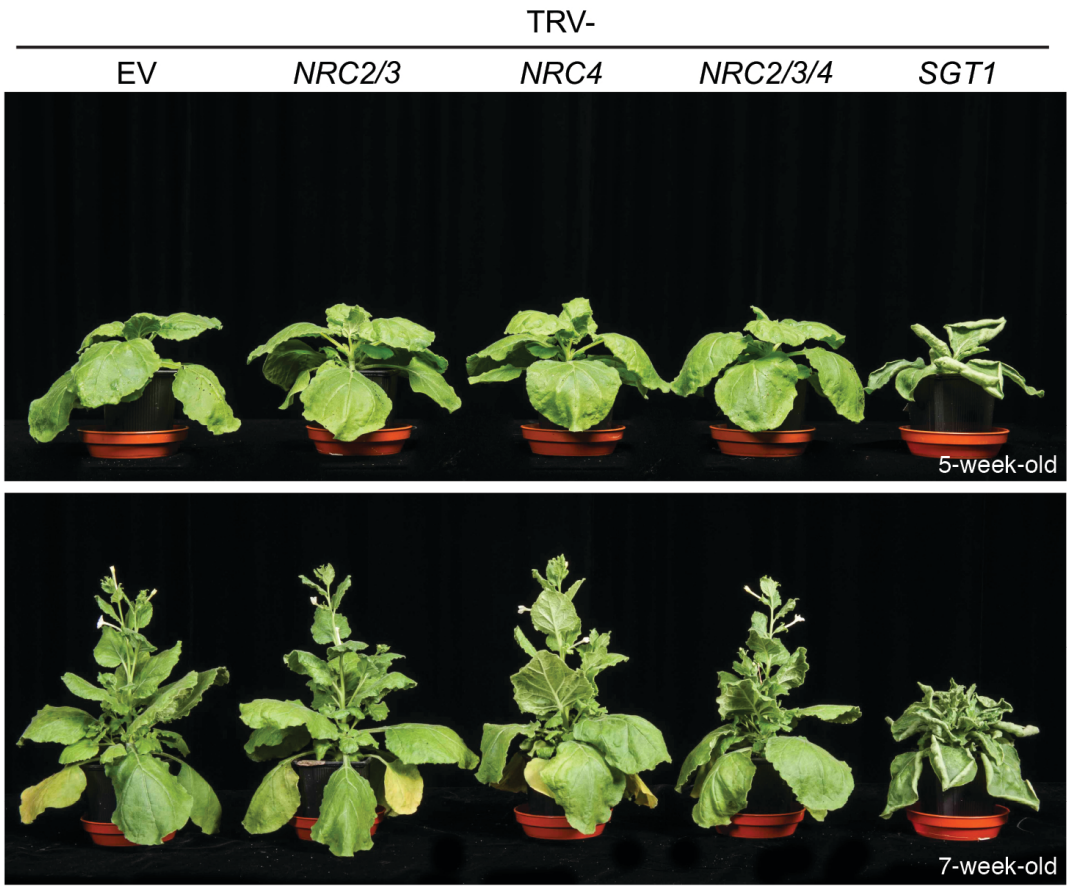

Figure A2. 9 Silencing of *NRC* homologs does not affect growth of *N. benthamiana*

NRC homologs or *SGT1* were silenced in *N. benthamiana*, and the plants were left in the greenhouse without any further treatment. Photos were taken at 3 weeks and 5 weeks after TRV inoculation, corresponding to 5 weeks and 7 weeks after sowing.

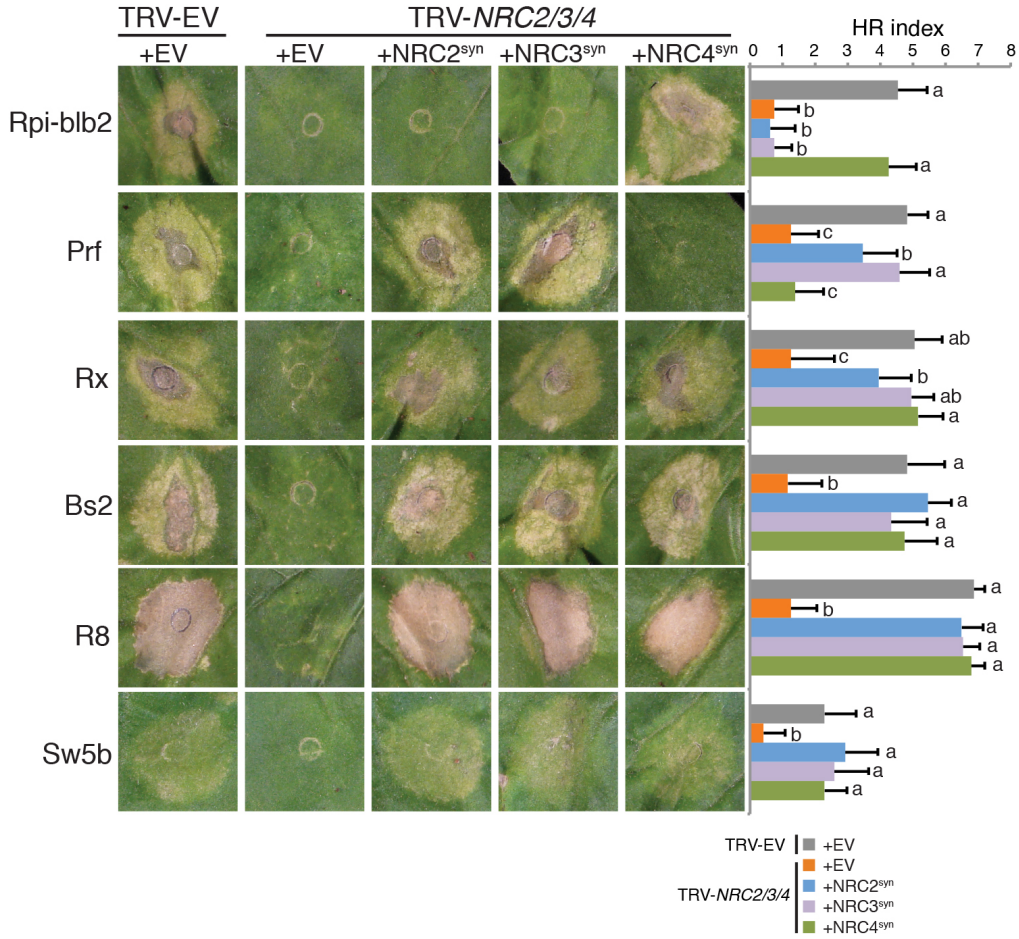

Figure A2. 10 *NRC2/3/4* display specificity and redundancy to different sensor NLRs from the NRC-superclade

Rpi-blb2, Pto (Prf), Rx, Bs2, R8, Sw5b were co-expressed with the corresponding AVR proteins and synthetic *NRC2*, *NRC3* or *NRC4* in *NRC2/3/4*-silenced *N. benthamiana*. Hypersensitive response (HR) was scored at 7 days after agroinfiltration. Bars represent mean + SD of 24 infiltrations sites. Statistical differences among the samples were analysed with ANOVA and Tukey's HSD test (p-value < 0.001).

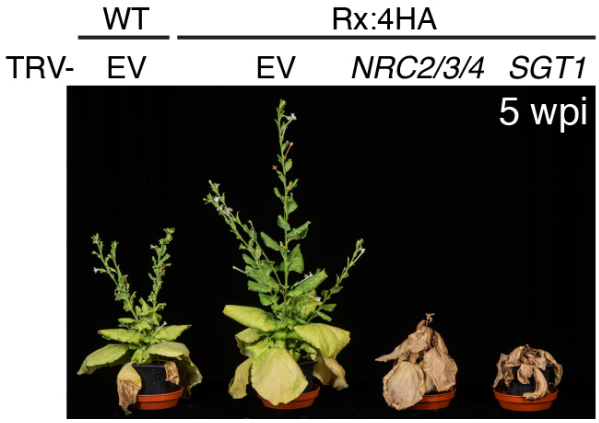

Figure A2. 11 Systemic spread of trailing necrosis induced by PVX in *NRC2/3/4*-silenced *Rx* plant

Control and *NRC2/3/4*-silenced *Rx* plants in Fig. 4.4 were left until 5 weeks post PVX inoculation (wpi). The susceptible wild type (WT) plant and resistant Rx plant showed normal senescence and viral symptoms, whereas the *NRC2/3/4*- and *SGT1*- silenced plants displayed trailing necrotic lesions throughout the whole plant.

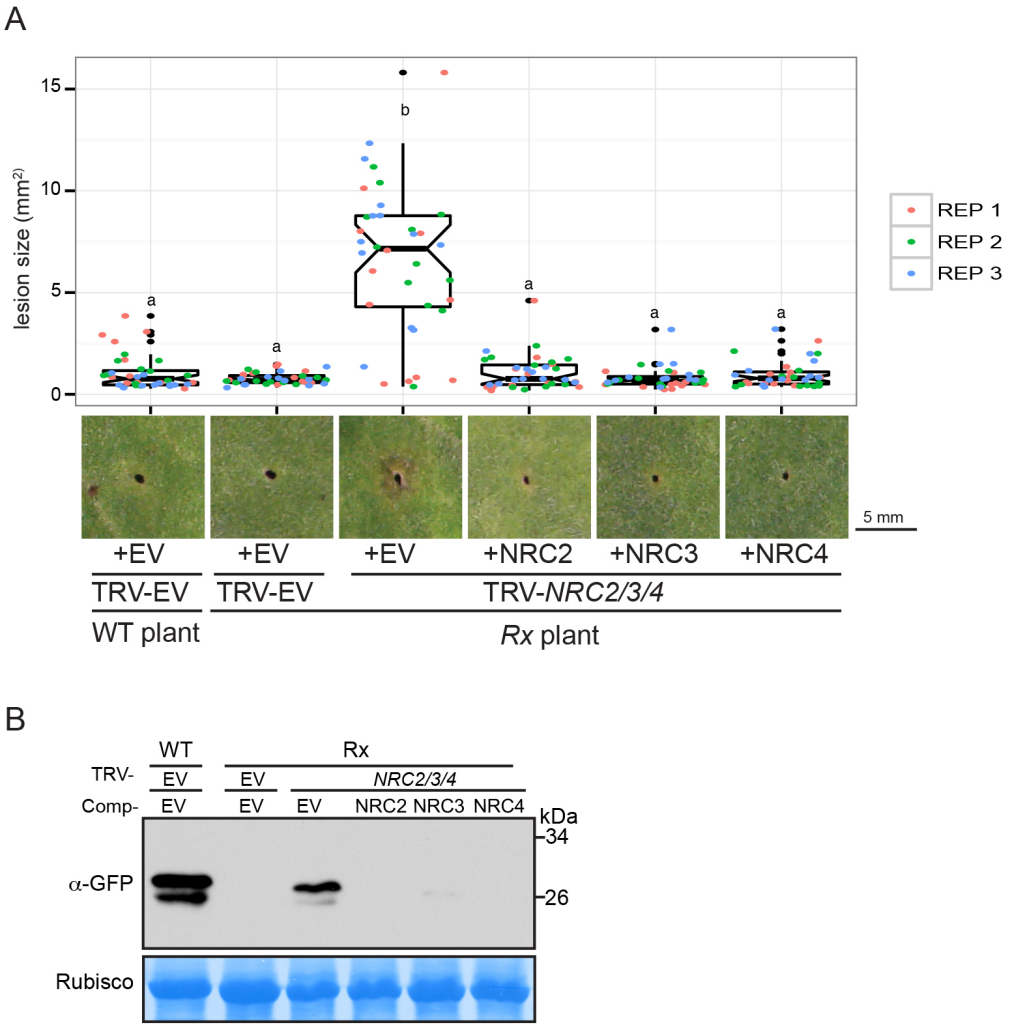

Figure A2. 12 Validation of *NRC2/3/4* redundancy in Rx-mediated resistance

(A) Expression of synthetic *NRC2*, *NRC3* or *NRC4* rescued Rx-mediated resistance in *NRC2/3/4*-silenced plants. *NRC2/3/4* were silenced together in *Rx* transgenic *N. benthamiana* and then synthetic *NRC2*, *NRC3*, or *NRC4* were expressed on the leaves one day before PVX inoculation. PVX-GFP was inoculated on the leaves by using toothpick inoculation method. Pictures were taken at 10 days after PVX inoculation and the size of necrotic lesions were measured by using Image J. Data acquired from different biological replicates (REP) were presented with different colours. Statistical differences among the samples were analysed with ANOVA and Tukey's HSD test (*p*-value < 0.01). (B) Immunoblot analysis of GFP accumulation of leaf discs collected in (A).

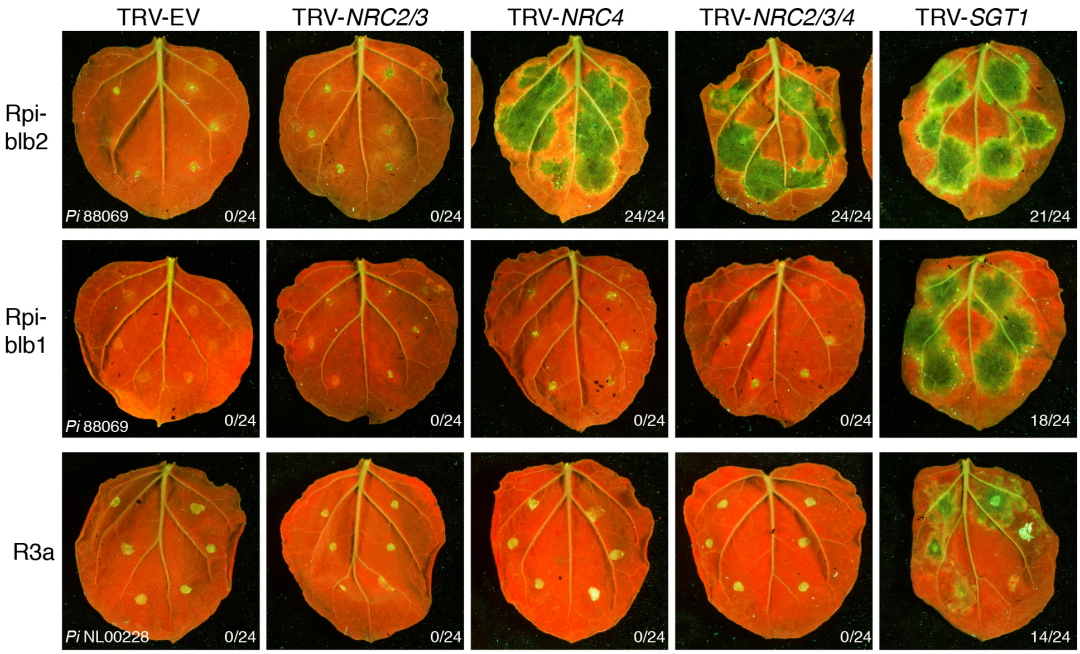

Figure A2. 13 Silencing of *NRC2/3/4* does not affect resistance mediated by R3a and Rpi-blb1

NRC2/3/4 were silenced individually or in combination in *Rpi-blb2*, *R3a*, and *Rpi-blb1* transgenic plants. *SGT1* silencing was used as a control. *P. infestans* 88069 or 00228 were inoculated on the leaves, and photos were taken under UV light at 4 days post inoculation (*Pi* 88069) or 5 days post inoculation (*Pi* NL00228). The numbers on the right bottom are the sum of spreading lesion/ total inoculation sites from one representative biological replicate.

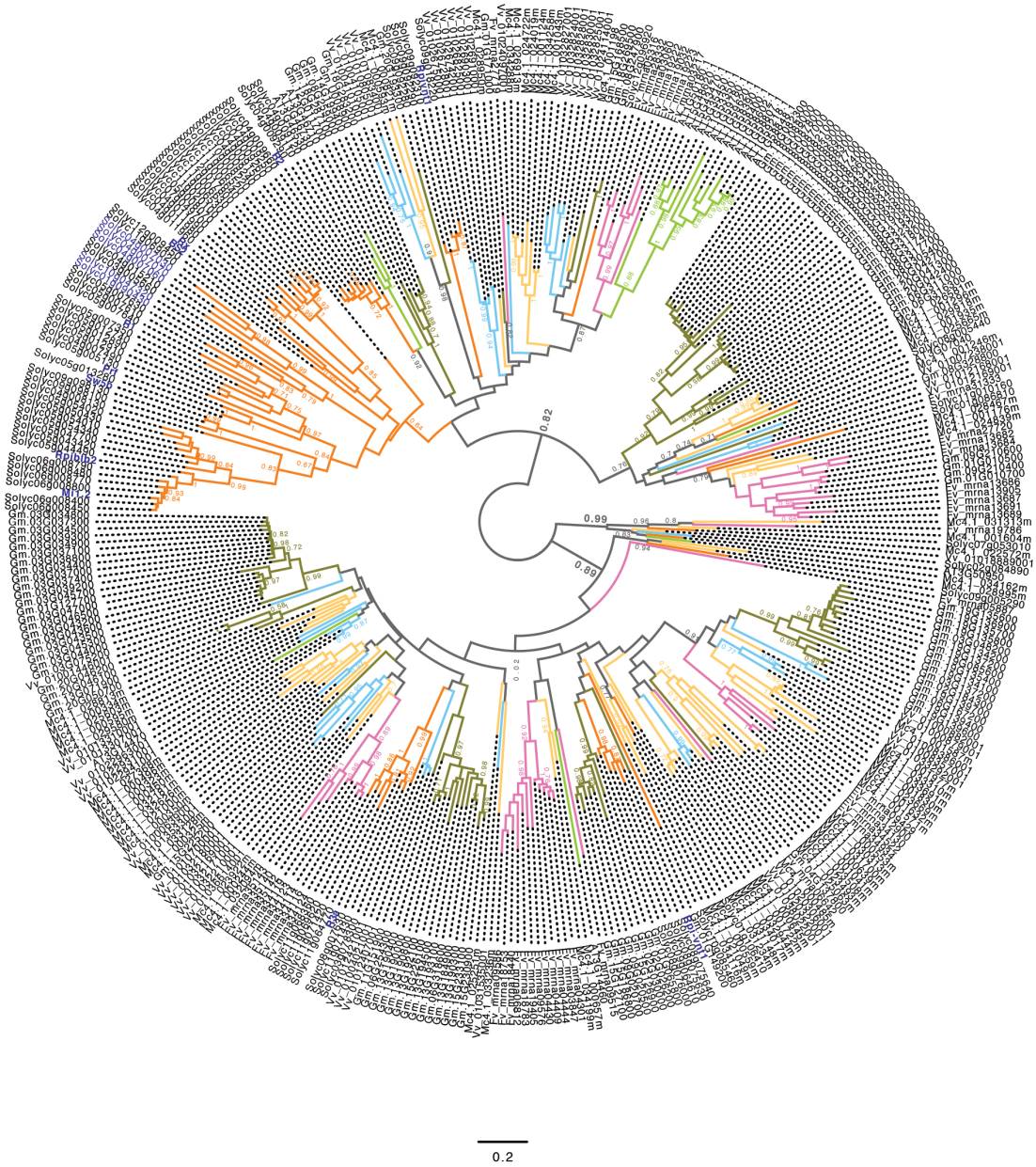

Figure A2. 14 Phylogenetic tree of CNL identified from rosids and asterids I

Polar tree layout of phylogeny presented in the left panel of Fig. 4.6A. Branches with bootstrap support higher than 0.7 are indicated.

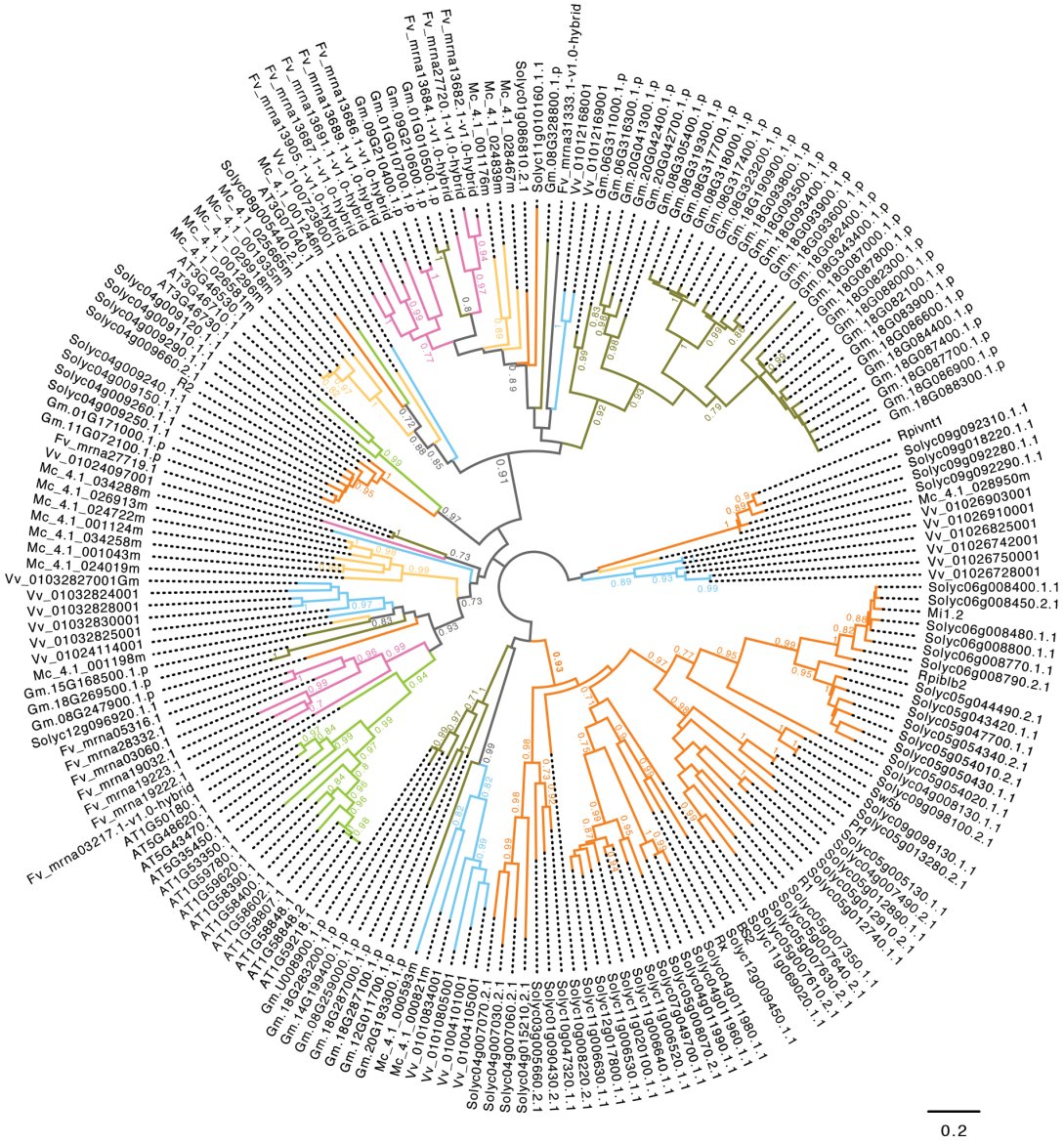

Figure A2. 15 Phylogenetic tree of CNL identified from rosids and asterids II

Polar tree layout of phylogeny presented in the right panel of Fig. 4.6A. Branches with bootstrap support higher than 0.7 are indicated.

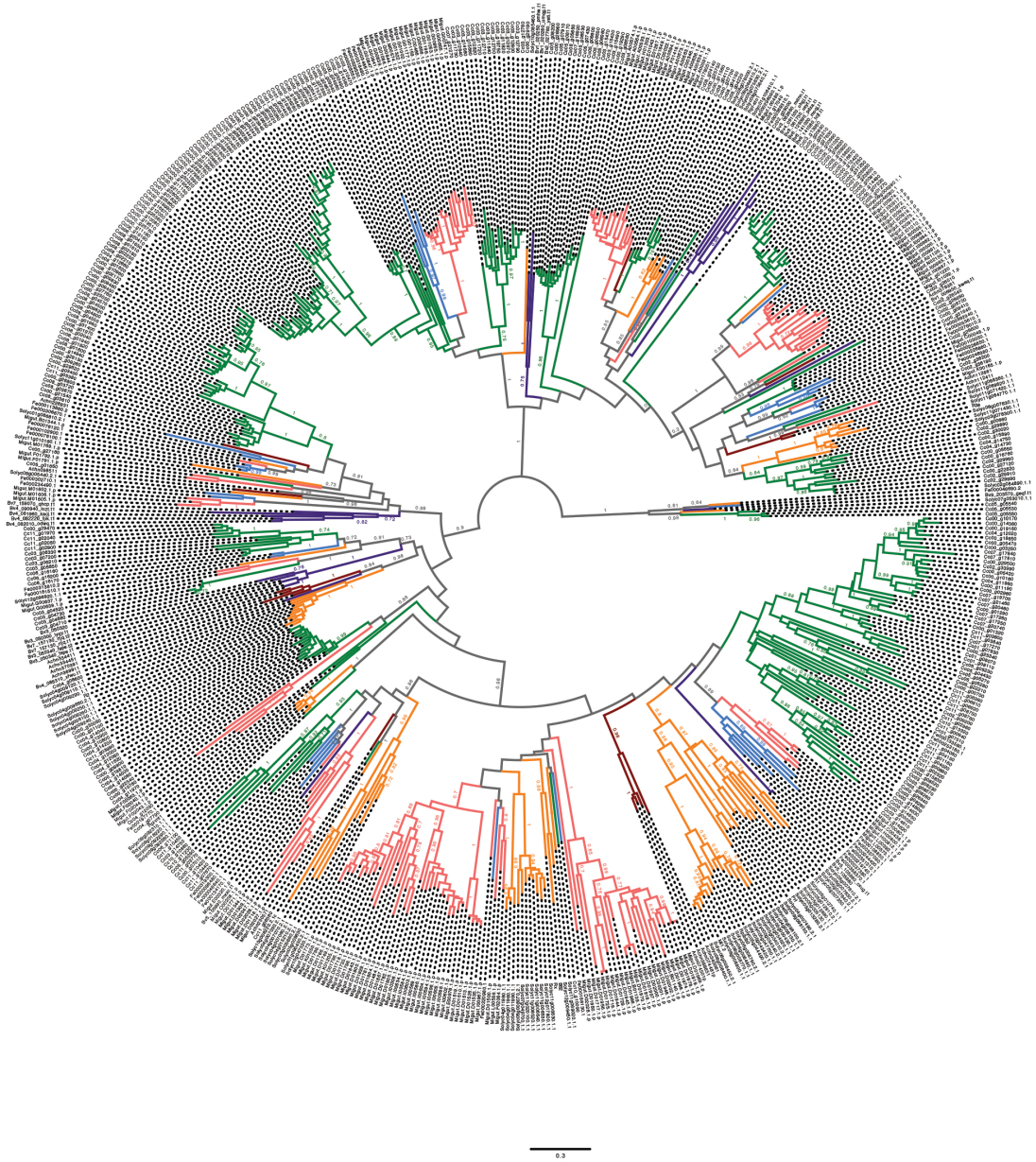

Figure A2. 16 Phylogenetic tree of CNL identified from asterids and caryophyllales I

Polar tree layout of phylogeny presented in the left panel of Fig. 4.6B. Branches with bootstrap support higher than 0.7 are indicated.

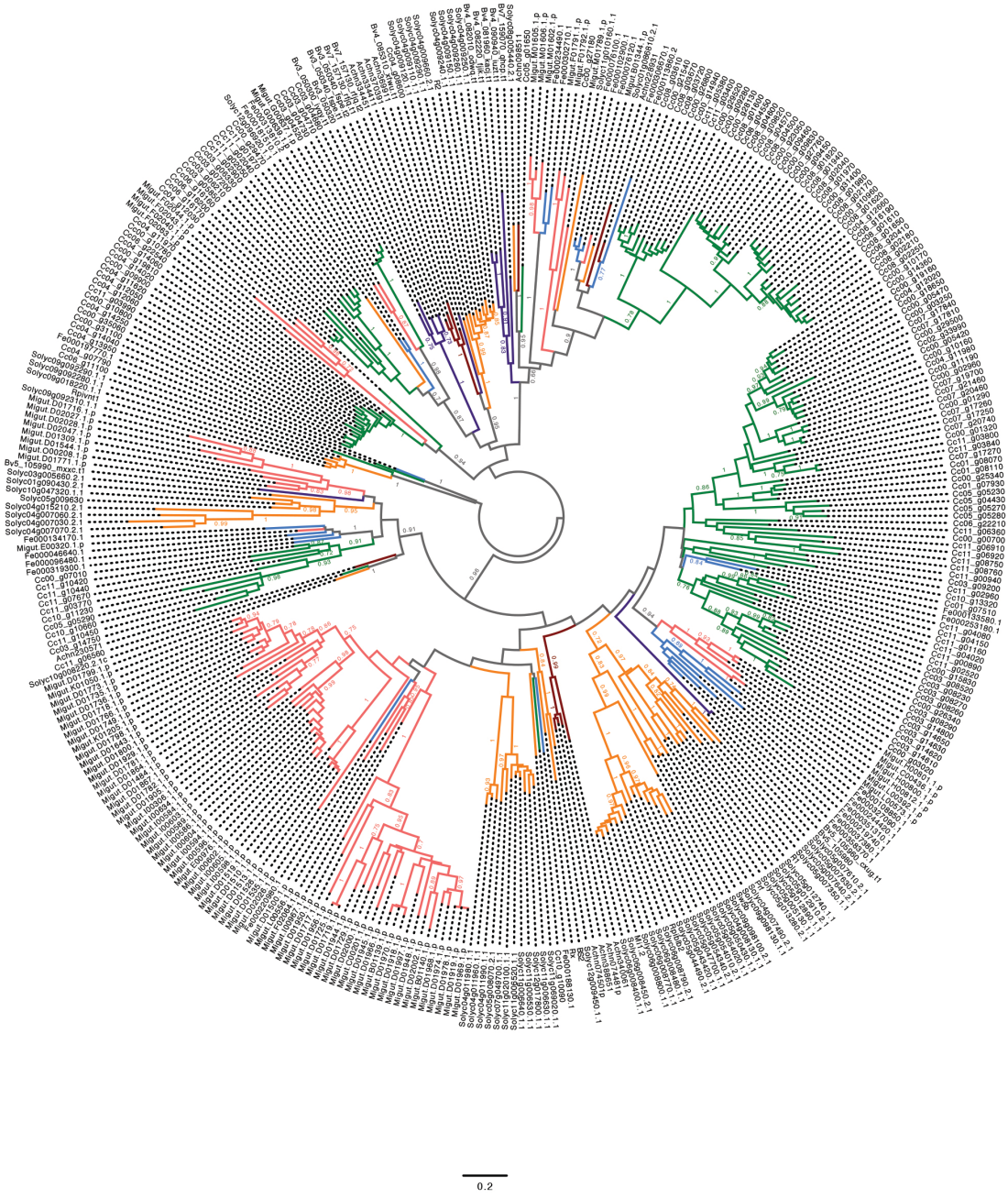

Figure A2. 17 Phylogenetic tree of CNL identified from asterids and caryophyllales II

Polar tree layout of phylogeny presented in the right panel of Fig. 4.6B. Branches with bootstrap support higher than 0.7 are indicated.

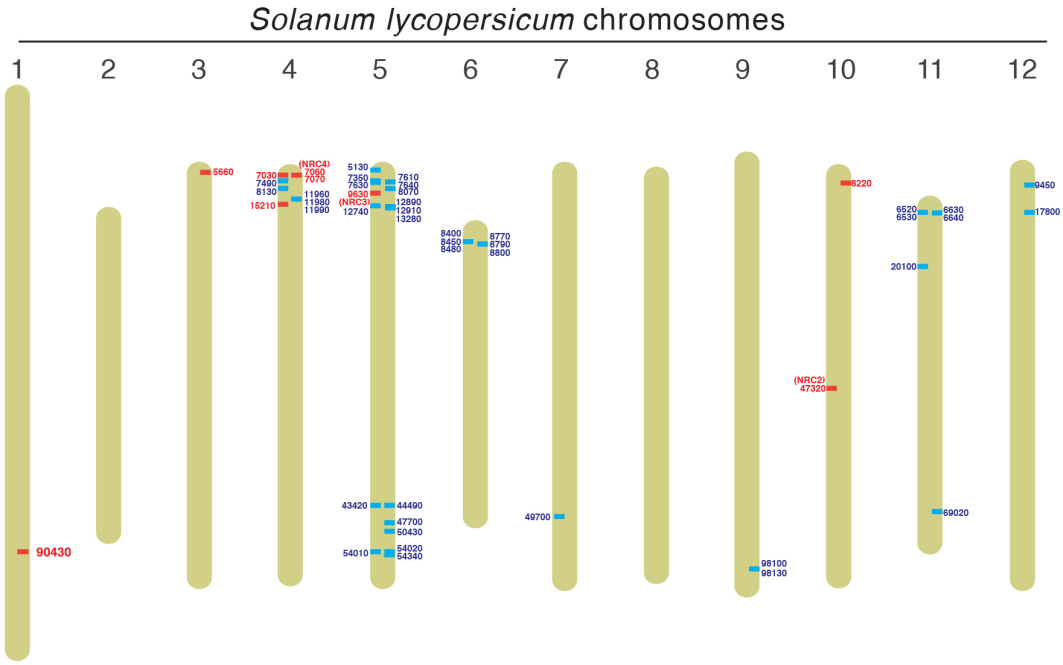

Figure A2. 18 Chromosomal distribution of NRC-helper/sensor homologs in tomato

Location of tomato NRC-helper/sensor homologs on the chromosomal map modified from Andolfo et al. (2014). NRC-helper NLR homologs are marked in red and NRC-dependent sensor NLR homologs (NRC-S) are marked in blue.

Appendix III

Supplemental figures for Chapter 5: Leucine-rich repeats determine NLR helper-sensor specificity in the NRC immune signalling network

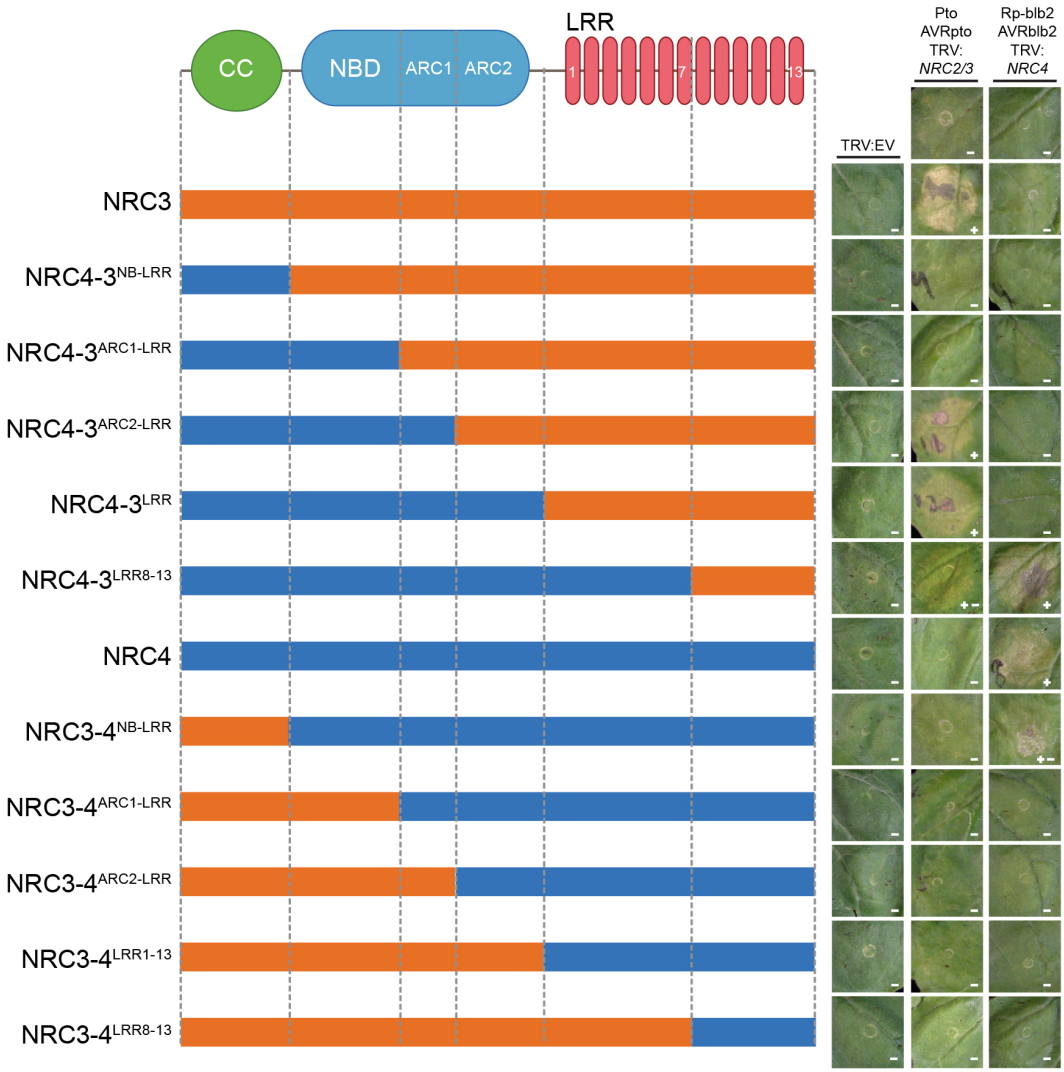

Figure A3. 1 Preliminary test of specificity of NRC3/NRC4 chimeric proteins – swapping of different domains

The chimeric proteins generated were tested for their ability to rescue Pto- and Rpi-blb2-mediated cell death in *NRC2/3*- or *NRC4*-silenced background. The LRR breakpoints were indicated in the schematics of corresponding constructs. These chimeric proteins are not autoactive when expressing along without any R/AVRs. The chimeric proteins were co-expressed with Pto/AvrPto or Rpi-blb2/AVRblb2 in *NRC2/3*- or *NRC4*-silenced background. Photos were taken at 7 days post infiltration (dpi). "+" indicates cell death were clearly observed. "-" indicates cell death was not observed. "+-" indicates weak cell death was observed. Experiments with some of the chimeric proteins were repeated and results were presented in Fig. 5.2.

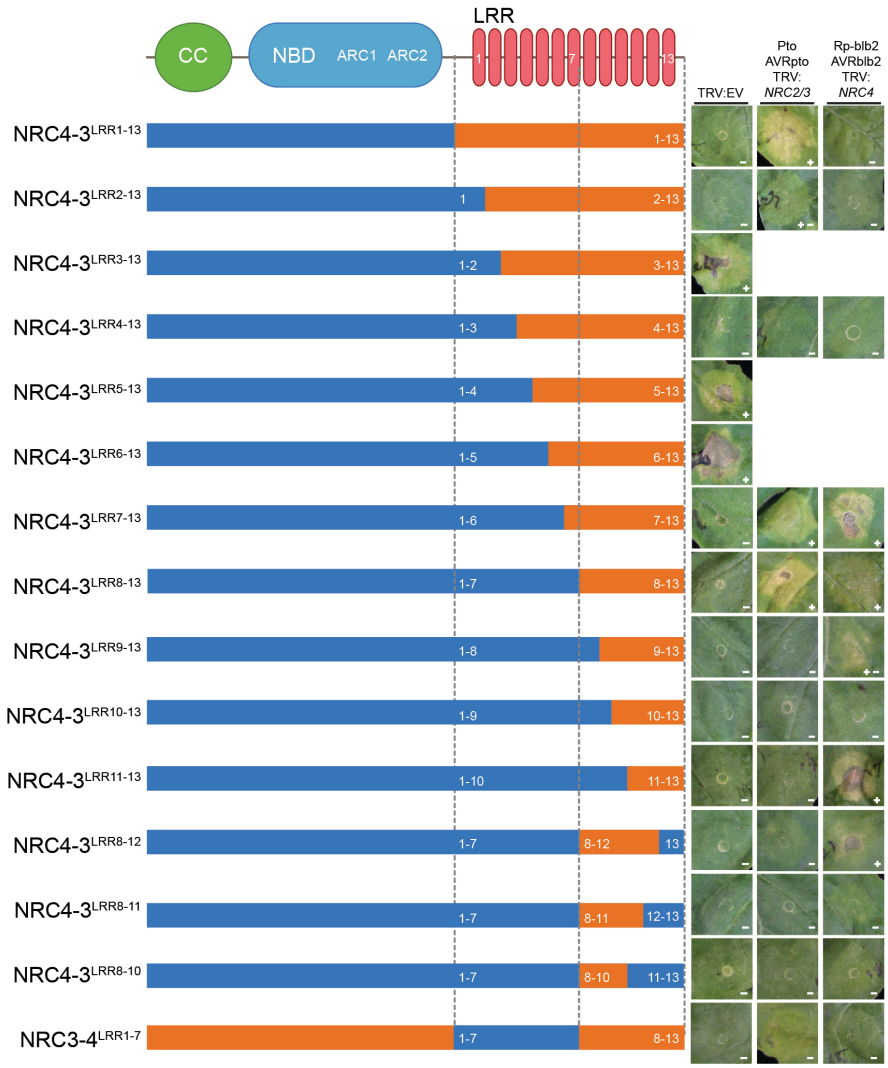

Figure A3. 2 Preliminary test of specificity of NRC3/NRC4 chimeric proteins – swapping of LRR repeats

The chimeric proteins generated were tested for their ability to rescue Pto- and Rpi-blb2-mediated cell death in *NRC2/3*- or *NRC4*-silenced background. The LRR breakpoints were indicated in the schematics of corresponding constructs. Three of these proteins are autoactive when expressing along, and these three proteins were excluded from further analyses. The chimeric proteins were co-expressed with Pto/AvrPto or Rpi-blb2/AVRblb2 in *NRC2/3*- or *NRC4*- silenced background. Photos were taken at 7 days post infiltration (dpi). "+" indicates cell death were clearly observed. "-" indicates cell death was not observed. "+-" indicates weak cell death was observed. Experiments with some of the chimeric proteins were repeated and results were presented in Fig. 5.2.

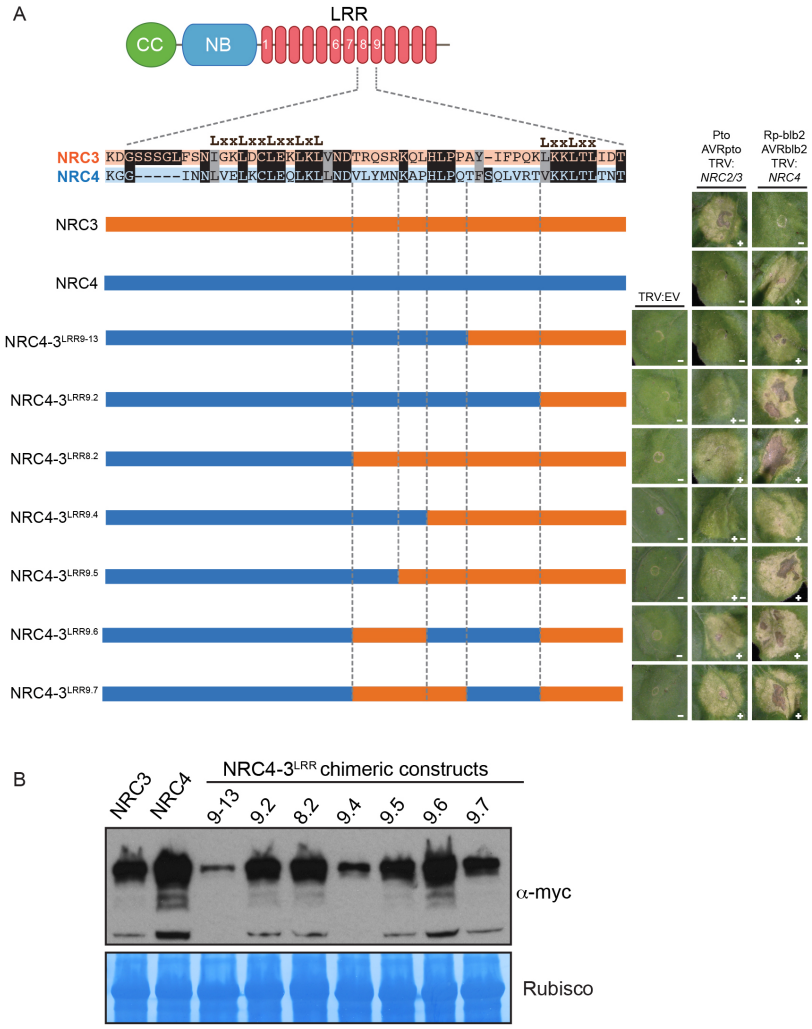

Figure A3. 3 Loop region of the 8th LRR is critical in determine specificity of NRCs

(A) The chimeric proteins generated were tested for their ability to rescue Pto- and Rpi-blb2-mediated cell death in *NRC2/3*- or *NRC4*-silenced background. The conserved lecuine-rich motifs (LxxLxxLxxLxL) of the 8th and 9th LRR were indicated in the alignment. The breakpoints were indicated in the sequence alignment. These chimeric proteins are not autoactive when expressed along without R/AVR. The chimeric proteins were co-expressed with Pto/AvrPto or Rpi-blb2/AVRblb2 in *NRC2/3*- or *NRC4*-silenced background. Photos were taken at 7 days post infiltration (dpi). "+" indicates cell death were clearly observed. "-" indicates cell death was not observed. "+-" indicates weak cell death was observed. (B) Immunoblot analysis of NRC3/NRC4 chimeric proteins used in (A).

References

Aarts, N., M. Metz, E. Holub, B.J. Staskawicz, M.J. Daniels, and J.E. Parker. 1998. Different requirements for *EDS1* and *NDR1* by disease resistance genes define at least two *R* gene-mediated signaling pathways in *Arabidopsis*. *Proc Natl Acad Sci U S A*. 95:10306-10311.

Abramovitch, R.B., Y.J. Kim, S. Chen, M.B. Dickman, and G.B. Martin. 2003. *Pseudomonas* type III effector AvrPtoB induces plant disease susceptibility by inhibition of host programmed cell death. *EMBO J*. 22:60-69.

Ade, J., B.J. DeYoung, C. Golstein, and R.W. Innes. 2007. Indirect activation of a plant nucleotide binding site-leucine-rich repeat protein by a bacterial protease. *Proc Natl Acad Sci U S A*. 104:2531-2536.

Ali, S., M. Magne, S. Chen, N. Obradovic, L. Jamshaid, X. Wang, G. Belair, and P. Moffett. 2015. Analysis of *Globodera rostochiensis* effectors reveals conserved functions of SPRYSEC proteins in suppressing and eliciting plant immune responses. *Front Plant Sci*. 6:623.

Altschul, S.F., W. Gish, W. Miller, E.W. Myers, and D.J. Lipman. 1990. Basic local alignment search tool. *J Mol Biol*. 215:403-410.

Andolfo, G., F. Jupe, K. Witek, G.J. Etherington, M.R. Ercolano, and J.D. Jones. 2014. Defining the full tomato NB-LRR resistance gene repertoire using genomic and cDNA RenSeq. *BMC Plant Biol*. 14:120.

Andolfo, G., W. Sanseverino, S. Rombauts, Y. Van de Peer, J.M. Bradeen, D. Carputo, L. Frusciante, and M.R. Ercolano. 2013. Overview of tomato (*Solanum lycopersicum*) candidate pathogen recognition genes reveals important *Solanum R* locus dynamics. *New Phytol*. 197:223-237.

Armstrong, M.R., S.C. Whisson, L. Pritchard, J.I. Bos, E. Venter, A.O. Avrova, A.P. Rehmany, U. Bohme, K. Brooks, I. Cherevach, N. Hamlin, B. White, A. Fraser, A. Lord, M.A. Quail, C. Churcher, N. Hall, M. Berriman, S. Huang, S. Kamoun, J.L. Beynon, and P.R. Birch. 2005. An ancestral oomycete locus contains late blight avirulence gene *Avr3a*, encoding a protein that is recognised in the host cytoplasm. *Proc Natl Acad Sci U S A*. 102:7766-7771.

Arya, P., G. Kumar, V. Acharya, and A.K. Singh. 2014. Genome-wide identification and expression analysis of NBS-encoding genes in *Malus x domestica* and expansion of NBS genes family in Rosaceae. *PLoS One*. 9:e107987.

Azevedo, C., S. Betsuyaku, J. Peart, A. Takahashi, L. Noel, A. Sadanandom, C. Casais, J. Parker, and K. Shirasu. 2006. Role of SGT1 in resistance protein accumulation in plant immunity. *EMBO J*. 25:2007-2016.

Ballvora, A., M.R. Ercolano, J. Weiss, K. Meksem, C.A. Bormann, P. Oberhagemann, F. Salamini, and C. Gebhardt. 2002. The *R1* gene for potato resistance to late blight (*Phytophthora infestans*) belongs to the leucine zipper/NBS/LRR class of plant resistance genes. *Plant J*. 30:361-371.

Balmuth, A., and J.P. Rathjen. 2007. Genetic and molecular requirements for function of the Pto/Prf effector recognition complex in tomato and *Nicotiana benthamiana*. *Plant J*. 51:978-990.

Barone, A., E. Ritter, U. Schachtschabel, T. Debener, F. Salamini, and C. Gebhardt. 1990. Localization by restriction fragment length polymorphism mapping in potato of a major dominant gene conferring resistance to the potato cyst nematode *Globodera rostochiensis*. *Mol Gen Genet*. 224:177-182.

Baumgarten, A., S. Cannon, R. Spangler, and G. May. 2003. Genome-level evolution of resistance genes in *Arabidopsis thaliana*. *Genetics*. 165:309-319.

Bendahmane, A., G. Farnham, P. Moffett, and D.C. Baulcombe. 2002. Constitutive gain-of-function mutants in a nucleotide binding site-leucine rich repeat protein encoded at the *Rx* locus of potato. *Plant J*. 32:195-204.

Bendahmane, A., B.A. Köhn, C. Dedi, and D.C. Baulcombe. 1995. The coat protein of potato virus X is a strain-specific elicitor of *Rx1*-mediated virus resistance in potato. *Plant J*. 8:933-941.

Bendahmane, A., M. Querci, K. Kanyuka, and D.C. Baulcombe. 2000. *Agrobacterium* transient expression system as a tool for the isolation of disease resistance genes: application to the *Rx2* locus in potato. *Plant J*. 21:73-81.

Bernoux, M., H. Burdett, S.J. Williams, X. Zhang, C. Chen, K. Newell, G.J. Lawrence, B. Kobe, J.G. Ellis, P.A. Anderson, and P.N. Dodds. 2016. Comparative analysis of the flax immune receptors L6 and L7 suggests an equilibrium-based switch activation model. *Plant Cell*. 28:146-159.

Bernoux, M., T. Ve, S. Williams, C. Warren, D. Hatters, E. Valkov, X. Zhang, J.G. Ellis, B. Kobe, and P.N. Dodds. 2011. Structural and functional analysis of a plant resistance protein TIR domain reveals interfaces for self-association, signaling, and autoregulation. *Cell Host Microbe*. 9:200-211.

Bhattacharjee, S., M.K. Halane, S.H. Kim, and W. Gassmann. 2011. Pathogen effectors target *Arabidopsis* EDS1 and alter its interactions with immune regulators. *Science*. 334:1405-1408.

Bhattarai, K.K., Q. Li, Y. Liu, S.P. Dinesh-Kumar, and I. Kaloshian. 2007. The *Mi-1*-mediated pest resistance requires *Hsp90* and *Sgt1*. *Plant Physiol*. 144:312-323.

Bieri, S., S. Mauch, Q.H. Shen, J. Peart, A. Devoto, C. Casais, F. Ceron, S. Schulze, H.H. Steinbiss, K. Shirasu, and P. Schulze-Lefert. 2004. RAR1 positively controls steady state levels of barley MLA resistance proteins and enables sufficient MLA6 accumulation for effective resistance. *Plant Cell*. 16:3480-3495.

Blanca, J., J. Montero-Pau, C. Sauvage, G. Bauchet, E. Illa, M.J. Diez, D. Francis, M. Causse, E. van der Knaap, and J. Canizares. 2015. Genomic variation in tomato, from wild ancestors to contemporary breeding accessions. *BMC Genomics*. 16:257.

Boller, T., and G. Felix. 2009. A renaissance of elicitors: perception of microbe-associated molecular patterns and danger signals by pattern-recognition receptors. *Annu Rev Plant Biol*. 60:379-406.

Bombarely, A., H.G. Rosli, J. Vrebalov, P. Moffett, L.A. Mueller, and G.B. Martin. 2012. A draft genome sequence of *Nicotiana benthamiana* to enhance molecular plant-microbe biology research. *Mol Plant Microbe Interact*. 25:1523-1530.

Bonardi, V., K. Cherkis, M.T. Nishimura, and J.L. Dangl. 2012. A new eye on NLR proteins: focused on clarity or diffused by complexity? *Curr Opin Immunol*. 24:41-50.

Bonardi, V., S. Tang, A. Stallmann, M. Roberts, K. Cherkis, and J.L. Dangl. 2011. Expanded functions for a family of plant intracellular immune receptors beyond specific recognition of pathogen effectors. *Proc Natl Acad Sci U S A*. 108:16463-16468.

Bos, J.I., T.D. Kanneganti, C. Young, C. Cakir, E. Huitema, J. Win, M.R. Armstrong, P.R. Birch, and S. Kamoun. 2006. The C-terminal half of *Phytophthora infestans* RXLR effector AVR3a is sufficient to trigger R3a-mediated hypersensitivity and suppress INF1-induced cell death in *Nicotiana benthamiana*. *Plant J*. 48:165-176.

Botër, M., B. Amigues, J. Peart, C. Breuer, Y. Kadota, C. Casais, G. Moore, C. Kleanthous, F. Ochsenbein, K. Shirasu, and R. Guerois. 2007. Structural and functional analysis of SGT1 reveals that its interaction with HSP90 is required for the accumulation of Rx, an R protein involved in plant immunity. *Plant Cell*. 19:3791-3804.

Bozkurt, T.O., S. Schornack, J. Win, T. Shindo, M. Ilyas, R. Oliva, L.M. Cano, A.M. Jones, E. Huitema, R.A. van der Hoorn, and S. Kamoun. 2011. *Phytophthora infestans* effector AVRblb2 prevents secretion of a plant immune protease at the haustorial interface. *Proc Natl Acad Sci U S A*. 108:20832-20837.

Brommonschenkel, S.H., A. Frary, A. Frary, and S.D. Tanksley. 2000. The broad-spectrum tospovirus resistance gene *Sw-5* of tomato is a homolog of the root-knot nematode resistance gene *Mi*. *Mol Plant Microbe Interact*. 13:1130-1138.

Burch-Smith, T.M., J.C. Anderson, G.B. Martin, and S.P. Dinesh-Kumar. 2004. Applications and advantages of virus-induced gene silencing for gene function studies in plants. *Plant J*. 39:734-746.

Burton, R.A., D.M. Gibeaut, A. Bacic, K. Findlay, K. Roberts, A. Hamilton, D.C. Baulcombe, and G.B. Fincher. 2000. Virus-induced silencing of a plant cellulose synthase gene. *The Plant Cell*. 12:691-706.

Cao, D., J.E. Froehlich, H. Zhang, and C.L. Cheng. 2003. The chlorate-resistant and photomorphogenesis-defective mutant *cr88* encodes a chloroplast-targeted HSP90. *Plant J*. 33:107-118.

Caplan, J.L., P. Mamillapalli, T.M. Burch-Smith, K. Czymmek, and S.P. Dinesh-Kumar. 2008. Chloroplastic protein NRIP1 mediates innate immune receptor recognition of a viral effector. *Cell*. 132:449-462.

Cesari, S., M. Bernoux, P. Moncuquet, T. Kroj, and P.N. Dodds. 2014a. A novel conserved mechanism for plant NLR protein pairs: the "integrated decoy" hypothesis. *Front Plant Sci*. 5:606.

Cesari, S., H. Kanzaki, T. Fujiwara, M. Bernoux, V. Chalvon, Y. Kawano, K. Shimamoto, P. Dodds, R. Terauchi, and T. Kroj. 2014b. The NB-LRR proteins RGA4 and RGA5 interact functionally and physically to confer disease resistance. *EMBO J*. 33:1941-1959.

Cesari, S., G. Thilliez, C. Ribot, V. Chalvon, C. Michel, A. Jauneau, S. Rivas, L. Alaux, H. Kanzaki, Y. Okuyama, J.B. Morel, E. Fournier, D. Tharreau, R. Terauchi, and T. Kroj. 2013. The rice resistance protein pair RGA4/RGA5 recognizes the *Magnaporthe oryzae* effectors AVR-Pia and AVR1-CO39 by direct binding. *Plant Cell*. 25:1463-81.

Chang, C., D. Yu, J. Jiao, S. Jing, P. Schulze-Lefert, and Q.H. Shen. 2013. Barley MLA immune receptors directly interfere with antagonistically acting transcription factors to initiate disease resistance signaling. *Plant Cell*. 25:1158-1173.

Chen, R., H. Li, L. Zhang, J. Zhang, J. Xiao, and Z. Ye. 2007. *CaMi*, a root-knot nematode resistance gene from hot pepper (*Capsium annuum* L.) confers nematode resistance in tomato. *Plant Cell Rep*. 26:895-905.

Chen, X., M. Zhu, L. Jiang, W. Zhao, J. Li, J. Wu, C. Li, B. Bai, G. Lu, H. Chen, P. Moffett, and X. Tao. 2016. A multilayered regulatory mechanism for the autoinhibition and activation of a plant CC-NB-LRR resistance protein with an extra N-terminal domain. *New Phytol*. 12: 161–175.

Christopoulou, M., S.R. Wo, A. Kozik, L.K. McHale, M.J. Truco, T. Wroblewski, and R.W. Michelmore. 2015. Genome-wide architecture of disease resistance genes in Lettuce. *G3 (Bethesda)*. 5:2655-2669.

Collier, S.M., L.P. Hamel, and P. Moffett. 2011. Cell death mediated by the N-terminal domains of a unique and highly conserved class of NB-LRR protein. *Mol Plant Microbe Interact*. 24:918-931.

de Vries, J.S., V.M. Andriotis, A.J. Wu, and J.P. Rathjen. 2006. Tomato *Pto* encodes a functional N-myristoylation motif that is required for signal transduction in *Nicotiana benthamiana*. *Plant J*. 45:31-45.

Denoeud, F., L. Carretero-Paulet, A. Dereeper, G. Droc, R. Guyot, M. Pietrella, C. Zheng, A. Alberti, F. Anthony, G. Aprea, J.M. Aury, P. Bento, M. Bernard, S. Bocs, C. Campa, A. Cenci, M.C. Combes, D. Crouzillat, C. Da Silva, L. Daddiego, F. De Bellis, S. Dussert, O. Garsmeur, T. Gayraud, V. Guignon, K. Jahn, V. Jamilloux, T. Joet, K. Labadie, T. Lan, J. Leclercq, M. Lepelley, T. Leroy, L.T. Li, P. Librado, L. Lopez, A. Munoz, B. Noel, A. Pallavicini, G. Perrotta, V. Poncet, D. Pot, Priyono, M. Rigoreau, M. Rouard, J. Rozas, C. Tranchant-Dubreuil, R. VanBuren, Q. Zhang, A.C. Andrade, X. Argout, B. Bertrand, A. de Kochko, G. Graziosi, R.J. Henry, Jayarama, R. Ming, C. Nagai,

S. Rounsley, D. Sankoff, G. Giuliano, V.A. Albert, P. Wincker, and P. Lashermes. 2014. The coffee genome provides insight into the convergent evolution of caffeine biosynthesis. *Science*. 345:1181-1184.

Dodds, P.N., and J.P. Rathjen. 2010. Plant immunity: towards an integrated view of plant-pathogen interactions. *Nat Rev Genet*. 11:539-548.

Dohm, J.C., A.E. Minoche, D. Holtgrawe, S. Capella-Gutierrez, F. Zakrzewski, H. Tafer, O. Rupp, T.R. Sorensen, R. Stracke, R. Reinhardt, A. Goesmann, T. Kraft, B. Schulz, P.F. Stadler, T. Schmidt, T. Gabaldon, H. Lehrach, B. Weisshaar, and H. Himmelbauer. 2014. The genome of the recently domesticated crop plant sugar beet (*Beta vulgaris*). *Nature*. 505:546-549.

Dong, O.X., M. Tong, V. Bonardi, F. El Kasmi, V. Woloshen, L.K. Wunsch, J.L. Dangl, and X. Li. 2016. TNL-mediated immunity in *Arabidopsis* requires complex regulation of the redundant *ADR1* gene family. *New Phytol*. 210:960-973.

Du, J., H. Rietman, and V.G. Vleeshouwers. 2014. Agroinfiltration and PVX agroinfection in potato and *Nicotiana benthamiana*. *J Vis Exp*:e50971.

Du, J., E. Verzaux, A. Chaparro-Garcia, G. Bijsterbosch, L. Keizer, J. Zhou, T. Liebrand, C. Xie, F. Govers, S. Robatzek, E. van der Vossen, E. Jacobsen, R. Visser, S. Kamoun, and V. Vleeshouwers. 2015a. Elicitin recognition confers enhanced resistance to *Phytophthora infestans* in potato. *Nat Plants*. 1:15034.

Du, Y., J. Berg, F. Govers, and K. Bouwmeester. 2015b. Immune activation mediated by the late blight resistance protein R1 requires nuclear localization of R1 and the effector AVR1. *New Phytol*. 207:735-747.

Du, Y., J. Zhao, T. Chen, Q. Liu, H. Zhang, Y. Wang, Y. Hong, F. Xiao, L. Zhang, Q. Shen, and Y. Liu. 2013. Type I J-domain NbMIP1 proteins are required for both Tobacco mosaic virus infection and plant innate immunity. *PLoS Pathog*. 9:e1003659.

Dubacq, C., R. Guerois, R. Courbeyrette, K. Kitagawa, and C. Mann. 2002. Sgt1p contributes to cyclic AMP pathway activity and physically interacts with the adenylyl cyclase Cyr1p/Cdc35p in budding yeast. *Eukaryot Cell*. 1:568-582.

Duxbury, Z., Y. Ma, O.J. Furzer, S.U. Huh, V. Cevik, J.D. Jones, and P.F. Sarris. 2016. Pathogen perception by NLRs in plants and animals: Parallel worlds. *Bioessays*. 38:769-781.

Eitas, T.K., and J.L. Dangl. 2010. NB-LRR proteins: pairs, pieces, perception, partners, and pathways. *Curr Opin Plant Biol*. 13:472-477.

Engler, C., M. Youles, R. Gruetzner, T.M. Ehnert, S. Werner, J.D. Jones, N.J. Patron, and S. Marillonnet. 2014. A golden gate modular cloning toolbox for plants. *ACS Synth Biol*. 3:839-843.

Enkhbayar, P., M. Kamiya, M. Osaki, T. Matsumoto, and N. Matsushima. 2004. Structural principles of leucine-rich repeat (LRR) proteins. *Proteins*. 54:394-403.

Erickson, F.L., S. Holzberg, A. Calderon-Urrea, V. Handley, M. Axtell, C. Corr, and B. Baker. 1999. The helicase domain of the TMV replicase proteins induces the *N*-mediated defence response in tobacco. *Plant J*. 18:67-75.

Ernst, K., A. Kumar, D. Kriseleit, D.U. Kloos, M.S. Phillips, and M.W. Ganal. 2002. The broad-spectrum potato cyst nematode resistance gene (*Hero*) from tomato is the only member of a large gene family of NBS-LRR genes with an unusual amino acid repeat in the LRR region. *Plant J*. 31:127-136.

Fares, M.A. 2015. The origins of mutational robustness. *Trends Genet*. 31:373-381.

Fenyk, S., C.H. Dixon, W.H. Gittens, P.D. Townsend, G.J. Sharples, L.O. Palsson, F.L. Takken, and M.J. Cann. 2016. The tomato nucleotide-binding leucine-rich repeat immune receptor I-2 couples DNA-binding to nucleotide-binding domain nucleotide exchange. *J Biol Chem*. 291:1137-1147.

Fenyk, S., P.D. Townsend, C.H. Dixon, G.B. Spies, A. de San Eustaquio Campillo, E.J. Slootweg, L.B. Westerhof, F.K. Gawehns, M.R. Knight, G.J. Sharples, A. Goverse, L.O. Palsson, F.L. Takken, and M.J. Cann. 2015. The potato nucleotide-binding leucine-rich repeat (NLR) immune receptor Rx1 is a pathogen-dependent DNA-deforming protein. *J Biol Chem*. 290:24945-24960.

Fernandez-Pozo, N., H.G. Rosli, G.B. Martin, and L.A. Mueller. 2015. The SGN VIGS tool: user-friendly software to design virus-induced gene silencing (VIGS) constructs for functional genomics. *Mol Plant*. 8:486-488.

Feys, B.J., M. Wiermer, R.A. Bhat, L.J. Moisan, N. Medina-Escobar, C. Neu, A. Cabral, and J.E. Parker. 2005. *Arabidopsis* SENESCENCE-ASSOCIATED GENE101 stabilizes and signals within an ENHANCED DISEASE SUSCEPTIBILITY1 complex in plant innate immunity. *Plant Cell*. 17:2601-2613.

Foster, S.J., T.H. Park, M. Pel, G. Brigneti, J. Sliwka, L. Jagger, E. van der Vossen, and J.D. Jones. 2009. *Rpi-vnt1.1*, a *Tm-2²* homolog from *Solanum venturii*, confers resistance to potato late blight. *Mol Plant Microbe Interact*. 22:589-600.

Fradin, E.F., Z. Zhang, J.C. Juarez Ayala, C.D. Castroverde, R.N. Nazar, J. Robb, C.M. Liu, and B.P. Thomma. 2009. Genetic dissection of *Verticillium* wilt resistance mediated by tomato Ve1. *Plant Physiol*. 150:320-332.

Fry, W. 2008. *Phytophthora infestans*: the plant (and *R* gene) destroyer. *Mol Plant Pathol*. 9:385-402.

Fukuoka, S., N. Saka, H. Koga, K. Ono, T. Shimizu, K. Ebana, N. Hayashi, A. Takahashi, H. Hirochika, K. Okuno, and M. Yano. 2009. Loss of function of a proline-containing protein confers durable disease resistance in rice. *Science*. 325:998-1001.

Gabriels, S.H., F.L. Takken, J.H. Vossen, C.F. de Jong, Q. Liu, S.C. Turk, L.K. Wachowski, J. Peters, H.M. Witsenboer, P.J. de Wit, and M.H. Joosten. 2006. cDNA-AFLP combined with functional analysis reveals novel genes

involved in the hypersensitive response. *Mol Plant Microbe Interact*. 19:567-576.

Gabriels, S.H., J.H. Vossen, S.K. Ekengren, G. van Ooijen, A.M. Abd-El-Haliem, G.C. van den Berg, D.Y. Rainey, G.B. Martin, F.L. Takken, P.J. de Wit, and M.H. Joosten. 2007. An NB-LRR protein required for HR signalling mediated by both extra- and intracellular resistance proteins. *Plant J*. 50:14-28.

Giannakopoulou, A., J.F. Steele, M.E. Segretin, T.O. Bozkurt, J. Zhou, S. Robatzek, M.J. Banfield, M. Pais, and S. Kamoun. 2015. Tomato I2 immune receptor can be engineered to confer partial resistance to the oomycete *Phytophthora infestans* in addition to the fungus *Fusarium oxysporum*. *Mol Plant Microbe Interact*. 28:1316-1329.

Goggin, F.L., L. Jia, G. Shah, S. Hebert, V.M. Williamson, and D.E. Ullman. 2006. Heterologous expression of the *Mi-1.2* gene from tomato confers resistance against nematodes but not aphids in eggplant. *Mol Plant Microbe Interact*. 19:383-388.

Goodin, M.M., D. Zaitlin, R.A. Naidu, and S.A. Lommel. 2008. *Nicotiana benthamiana*: its history and future as a model for plant-pathogen interactions. *Mol Plant Microbe Interact*. 21:1015-1026.

Guo, H., J.B. Callaway, and J.P. Ting. 2015. Inflammasomes: mechanism of action, role in disease, and therapeutics. *Nat Med*. 21:677-687.

Guo, Y.L., J. Fitz, K. Schneeberger, S. Ossowski, J. Cao, and D. Weigel. 2011. Genome-wide comparison of nucleotide-binding site-leucine-rich repeat-encoding genes in *Arabidopsis*. *Plant Physiol*. 157:757-769.

Hallwass, M., A.S. de Oliveira, E. de Campos Dianese, D. Lohuis, L.S. Boiteux, A.K. Inoue-Nagata, R.O. Resende, and R. Kormelink. 2014. The *Tomato spotted wilt virus* cell-to-cell movement protein (NS_M) triggers a hypersensitive response in *Sw-5*-containing resistant tomato lines and in *Nicotiana benthamiana* transformed with the functional *Sw-5b* resistance gene copy. *Mol Plant Pathol*. 15:871-880.

Hao, W., S.M. Collier, P. Moffett, and J. Chai. 2013. Structural basis for the interaction between the potato virus X resistance protein (Rx) and its cofactor Ran GTPase-activating protein 2 (RanGAP2). *J Biol Chem*. 288:35868-35876.

Harper, A.L., L.V. McKinney, L.R. Nielsen, L. Havlickova, Y. Li, M. Trick, F. Fraser, L. Wang, A. Fellgett, E.S. Sollars, S.H. Janacek, J.A. Downie, R.J. Buggs, E.D. Kjaer, and I. Bancroft. 2016. Molecular markers for tolerance of European ash (*Fraxinus excelsior*) to dieback disease identified using associative transcriptomics. *Sci Rep*. 6:19335.

Heese, A., D.R. Hann, S. Gimenez-Ibanez, A.M. Jones, K. He, J. Li, J.I. Schroeder, S.C. Peck, and J.P. Rathjen. 2007. The receptor-like kinase SERK3/BAK1 is a central regulator of innate immunity in plants. *Proc Natl Acad Sci U S A*. 104:12217-12222.

Holub, E.B. 2001. The arms race is ancient history in *Arabidopsis*, the wildflower. *Nat Rev Genet*. 2:516-527.

Huang, S., J. Ding, D. Deng, W. Tang, H. Sun, D. Liu, L. Zhang, X. Niu, X. Zhang, M. Meng, J. Yu, J. Liu, Y. Han, W. Shi, D. Zhang, S. Cao, Z. Wei, Y. Cui, Y. Xia, H. Zeng, K. Bao, L. Lin, Y. Min, H. Zhang, M. Miao, X. Tang, Y. Zhu, Y. Sui, G. Li, H. Sun, J. Yue, J. Sun, F. Liu, L. Zhou, L. Lei, X. Zheng, M. Liu, L. Huang, J. Song, C. Xu, J. Li, K. Ye, S. Zhong, B.R. Lu, G. He, F. Xiao, H.L. Wang, H. Zheng, Z. Fei, and Y. Liu. 2013. Draft genome of the kiwifruit *Actinidia chinensis*. *Nat Commun*. 4:2640.

Huang, S., E.A. van der Vossen, H. Kuang, V.G. Vleeshouwers, N. Zhang, T.J. Borm, H.J. van Eck, B. Baker, E. Jacobsen, and R.G. Visser. 2005. Comparative genomics enabled the isolation of the *R3a* late blight resistance gene in potato. *Plant J*. 42:251-261.

Huang, S., V.G. Vleeshouwers, J.S. Werij, R.C. Hutten, H.J. van Eck, R.G. Visser, and E. Jacobsen. 2004. The *R3* resistance to *Phytophthora infestans* in potato is conferred by two closely linked *R* genes with distinct specificities. *Mol Plant Microbe Interact*. 17:428-435.

Hubert, D.A., P. Tornero, Y. Belkhadir, P. Krishna, A. Takahashi, K. Shirasu, and J.L. Dangl. 2003. Cytosolic HSP90 associates with and modulates the *Arabidopsis* RPM1 disease resistance protein. *EMBO J*. 22:5679-5689.

Inoue, H., N. Hayashi, A. Matsushita, L. Xinqiong, A. Nakayama, S. Sugano, C.J. Jiang, and H. Takatsuji. 2013. Blast resistance of CC-NB-LRR protein Pb1 is mediated by WRKY45 through protein-protein interaction. *Proc Natl Acad Sci U S A*. 110:9577-9582.

Ishiguro, S., Y. Watanabe, N. Ito, H. Nonaka, N. Takeda, T. Sakai, H. Kanaya, and K. Okada. 2002. SHEPHERD is the *Arabidopsis* GRP94 responsible for the formation of functional CLAVATA proteins. *EMBO J*. 21:898-908.

Jo, K.R. 2013. Unveiling and deploying durability of late blight resistance in potato; from natural stacking to cisgenic stacking. *Ph.D. Thesis Wageningen University, Wageningen*.

Jo, K.R., M. Arens, T.Y. Kim, M.A. Jongsma, R.G. Visser, E. Jacobsen, and J.H. Vossen. 2011. Mapping of the *S. demissum* late blight resistance gene *R8* to a new locus on chromosome IX. *Theor Appl Genet*. 123:1331-1340.

Jo, K.R., R.G. Visser, E. Jacobsen, and J.H. Vossen. 2015. Characterisation of the late blight resistance in potato differential *MaR9* reveals a qualitative resistance gene, *R9a*, residing in a cluster of *Tm-2²* homologs on chromosome IX. *Theor Appl Genet*. 128:931-941.

Jonchere, V., and D. Bennett. 2013. Validating RNAi phenotypes in *Drosophila* using a synthetic RNAi-resistant transgene. *PLoS One*. 8:e70489.

Jones, J.D., and J.L. Dangl. 2006. The plant immune system. *Nature*. 444:323-329.

Jupe, F., L. Pritchard, G.J. Etherington, K. Mackenzie, P.J. Cock, F. Wright, S.K. Sharma, D. Bolser, G.J. Bryan, J.D. Jones, and I. Hein. 2012. Identification

and localisation of the NB-LRR gene family within the potato genome. *BMC Genomics*. 13:75.

Jupe, F., K. Witek, W. Verweij, J. Sliwka, L. Pritchard, G.J. Etherington, D. Maclean, P.J. Cock, R.M. Leggett, G.J. Bryan, L. Cardle, I. Hein, and J.D. Jones. 2013. Resistance gene enrichment sequencing (RenSeq) enables reannotation of the NB-LRR gene family from sequenced plant genomes and rapid mapping of resistance loci in segregating populations. *Plant J*. 76:530-544.

Kadota, Y., and K. Shirasu. 2012. The HSP90 complex of plants. *Biochim Biophys Acta*. 1823:689-697.

Kanzaki, H., K. Yoshida, H. Saitoh, K. Fujisaki, A. Hirabuchi, L. Alaux, E. Fournier, D. Tharreau, and R. Terauchi. 2012. Arms race co-evolution of *Magnaporthe oryzae AVR-Pik* and rice *Pik* genes driven by their physical interactions. *Plant J*. 72:894-907.

Karimi, M., D. Inze, and A. Depicker. 2002. GATEWAY vectors for *Agrobacterium*-mediated plant transformation. *Trends Plant Sci.* 7:193-195.

Katoh, K., and D.M. Standley. 2013. MAFFT multiple sequence alignment software version 7: improvements in performance and usability. *Mol Biol Evol*. 30:772-780.

Kay, S., J. Boch, and U. Bonas. 2005. Characterization of AvrBs3-like effectors from a Brassicaceae pathogen reveals virulence and avirulence activities and a protein with a novel repeat architecture. *Mol Plant Microbe Interact*. 18:838-848.

Kitagawa, K., D. Skowyra, S.J. Elledge, J.W. Harper, and P. Hieter. 1999. *SGT1* encodes an essential component of the yeast kinetochore assembly pathway and a novel subunit of the SCF ubiquitin ligase complex. *Mol Cell*. 4:21-33.

Kitano, H. 2007. Towards a theory of biological robustness. *Mol Syst Biol*. 3:137.

Kitano, H., and K. Oda. 2006. Robustness trade-offs and host-microbial symbiosis in the immune system. *Mol Syst Biol*. 2:2006 0022.

Kobe, B., and A.V. Kajava. 2001. The leucine-rich repeat as a protein recognition motif. *Curr Opin Struct Biol*. 11:725-732.

Kofoed, E.M., and R.E. Vance. 2011. Innate immune recognition of bacterial ligands by NAIPs determines inflammasome specificity. *Nature*. 477:592-595.

Krasileva, K.V., D. Dahlbeck, and B.J. Staskawicz. 2010. Activation of an *Arabidopsis* resistance protein is specified by the in planta association of its leucine-rich repeat domain with the cognate oomycete effector. *Plant Cell*. 22:2444-2458.

Kroj, T., E. Chanclud, C. Michel-Romiti, X. Grand, and J.B. Morel. 2016. Integration of decoy domains derived from protein targets of pathogen effectors into plant immune receptors is widespread. *New Phytol*. 210:618-626.

Kumar, D., C. Gustafsson, and D.F. Klessig. 2006. Validation of RNAi silencing specificity using synthetic genes: salicylic acid-binding protein 2 is required for innate immunity in plants. *Plant J.* 45:863-868.

Kumar, S., G. Stecher, and K. Tamura. 2016. MEGA7: Molecular Evolutionary Genetics Analysis version 7.0 for bigger datasets. *Mol Biol Evol*. 33:1870-1874.

Lanfermeijer, F.C., J. Dijkhuis, M.J. Sturre, P. de Haan, and J. Hille. 2003. Cloning and characterization of the durable tomato mosaic virus resistance gene *Tm-2²* from *Lycopersicon esculentum*. *Plant Mol Biol*. 52:1037-1049.

Le Roux, C., G. Huet, A. Jauneau, L. Camborde, D. Tremousaygue, A. Kraut, B. Zhou, M. Levaillant, H. Adachi, H. Yoshioka, S. Raffaele, R. Berthome, Y. Coute, J.E. Parker, and L. Deslandes. 2015. A receptor pair with an integrated decoy converts pathogen disabling of transcription factors to immunity. *Cell*. 161:1074-1088.

Lee, S.K., M.Y. Song, Y.S. Seo, H.K. Kim, S. Ko, P.J. Cao, J.P. Suh, G. Yi, J.H. Roh, S. Lee, G. An, T.R. Hahn, G.L. Wang, P. Ronald, and J.S. Jeon. 2009. Rice *Pi5*-mediated resistance to *Magnaporthe oryzae* requires the presence of two coiled-coil-nucleotide-binding-leucine-rich repeat genes. *Genetics*. 181:1627-1638.

Lee, S.S., H.S. Cho, G.M. Yoon, J.W. Ahn, H.H. Kim, and H.S. Pai. 2003. Interaction of NtCDPK1 calcium-dependent protein kinase with NtRpn3 regulatory subunit of the 26S proteasome in *Nicotiana tabacum*. *Plant J*. 33:825-840.

Leister, D. 2004. Tandem and segmental gene duplication and recombination in the evolution of plant disease resistance gene. *Trends Genet*. 20:116-122.

Li, G., S. Huang, X. Guo, Y. Li, Y. Yang, Z. Guo, H. Kuang, H. Rietman, M. Bergervoet, V.G. Vleeshouwers, E.A. van der Vossen, D. Qu, R.G. Visser, E. Jacobsen, and J.H. Vossen. 2011. Cloning and characterization of *R3b*; members of the *R3* superfamily of late blight resistance genes show sequence and functional divergence. *Mol Plant Microbe Interact*. 24:1132-1142.

Liebrand, T.W., P. Smit, A. Abd-El-Haliem, R. de Jonge, J.H. Cordewener, A.H. America, J. Sklenar, A.M. Jones, S. Robatzek, B.P. Thomma, W.I. Tameling, and M.H. Joosten. 2012. Endoplasmic reticulum-quality control chaperones facilitate the biogenesis of Cf receptor-like proteins involved in pathogen resistance of tomato. *Plant Physiol*. 159:1819-1833.

Liebrand, T.W., G.C. van den Berg, Z. Zhang, P. Smit, J.H. Cordewener, A.H. America, J. Sklenar, A.M. Jones, W.I. Tameling, S. Robatzek, B.P. Thomma, and M.H. Joosten. 2013. Receptor-like kinase SOBIR1/EVR interacts with receptor-like proteins in plant immunity against fungal infection. *Proc Natl Acad Sci U S A*. 110:10010-10015.

Liu, Y., M. Schiff, and S.P. Dinesh-Kumar. 2002a. Virus-induced gene silencing in tomato. *Plant J*. 31:777-786.

Liu, Y., M. Schiff, R. Marathe, and S.P. Dinesh-Kumar. 2002b. Tobacco *Rar1*, *EDS1* and *NPR1/NIM1* like genes are required for *N*-mediated resistance to tobacco mosaic virus. *Plant J*. 30:415-429.

Lokossou, A.A., T.H. Park, G. van Arkel, M. Arens, C. Ruyter-Spira, J. Morales, S.C. Whisson, P.R. Birch, R.G. Visser, E. Jacobsen, and E.A. van der Vossen. 2009. Exploiting knowledge of *R/Avr* genes to rapidly clone a new LZ-NBS-LRR family of late blight resistance genes from potato linkage group IV. *Mol Plant Microbe Interact*. 22:630-641.

Loutre, C., T. Wicker, S. Travella, P. Galli, S. Scofield, T. Fahima, C. Feuillet, and B. Keller. 2009. Two different CC-NBS-LRR genes are required for *Lr10*-mediated leaf rust resistance in tetraploid and hexaploid wheat. *Plant J*. 60:1043-1054.

Lozano, R., O. Ponce, M. Ramirez, N. Mostajo, and G. Orjeda. 2012. Genome-wide identification and mapping of NBS-encoding resistance genes in *Solanum tuberosum* group *phureja*. *PLoS One*. 7:e34775.

Lozano-Duran, R., G. Bourdais, S.Y. He, and S. Robatzek. 2014. The bacterial effector HopM1 suppresses PAMP-triggered oxidative burst and stomatal immunity. *New Phytol*. 202:259-269.

Lu, R., I. Malcuit, P. Moffett, M.T. Ruiz, J. Peart, A.J. Wu, J.P. Rathjen, A. Bendahmane, L. Day, and D.C. Baulcombe. 2003. High throughput virus-induced gene silencing implicates heat shock protein 90 in plant disease resistance. *EMBO J*. 22:5690-5699.

Lukasik-Shreepaathy, E., E. Slootweg, H. Richter, A. Goverse, B.J. Cornelissen, and F.L. Takken. 2012. Dual regulatory roles of the extended N terminus for activation of the tomato Mi-1.2 resistance protein. *Mol Plant Microbe Interact*. 25:1045-1057.

Ma, L., B.J. Cornelissen, and F.L. Takken. 2013. A nuclear localization for Avr2 from *Fusarium oxysporum* is required to activate the tomato resistance protein I-2. *Front Plant Sci*. 4:94.

Maekawa, T., W. Cheng, L.N. Spiridon, A. Toller, E. Lukasik, Y. Saijo, P. Liu, Q.H. Shen, M.A. Micluta, I.E. Somssich, F.L. Takken, A.J. Petrescu, J. Chai, and P. Schulze-Lefert. 2011. Coiled-coil domain-dependent homodimerization of intracellular barley immune receptors defines a minimal functional module for triggering cell death. *Cell Host Microbe*. 9:187-199.

Manavella, P.A., D. Koenig, and D. Weigel. 2012. Plant secondary siRNA production determined by microRNA-duplex structure. *Proc Natl Acad Sci U S A*. 109:2461-2466.

Mantelin, S., H.C. Peng, B. Li, H.S. Atamian, F.L. Takken, and I. Kaloshian. 2011. The receptor-like kinase *SlSERK1* is required for *Mi-1*-mediated resistance to potato aphids in tomato. *Plant J*. 67:459-471.

Maqbool, A., H. Saitoh, M. Franceschetti, C.E. Stevenson, A. Uemura, H. Kanzaki, S. Kamoun, R. Terauchi, and M.J. Banfield. 2015. Structural basis of pathogen

recognition by an integrated HMA domain in a plant NLR immune receptor. *Elife*. 4:e08709

Mathieu, J., S. Schwizer, and G.B. Martin. 2014. Pto kinase binds two domains of AvrPtoB and its proximity to the effector E3 ligase determines if it evades degradation and activates plant immunity. *PLoS Pathog*. 10:e1004227.

McHale, L., X. Tan, P. Koehl, and R.W. Michelmore. 2006. Plant NBS-LRR proteins: adaptable guards. *Genome Biol*. 7:212.

Meyers, B.C., A. Kozik, A. Griego, H. Kuang, and R.W. Michelmore. 2003. Genome-wide analysis of NBS-LRR-encoding genes in *Arabidopsis*. *Plant Cell*. 15:809-834.

Michael Weaver, L., M.R. Swiderski, Y. Li, and J.D. Jones. 2006. The Arabidopsis thaliana TIR-NB-LRR R-protein, RPP1A; protein localization and constitutive activation of defence by truncated alleles in tobacco and *Arabidopsis*. *Plant J*. 47:829-840.

Michelmore, R.W., and B.C. Meyers. 1998. Clusters of resistance genes in plants evolve by divergent selection and a birth-and-death process. *Genome Res*. 8:1113-1130.

Milligan, S.B., J. Bodeau, J. Yaghoobi, I. Kaloshian, P. Zabel, and V.M. Williamson. 1998. The root knot nematode resistance gene *Mi* from tomato is a member of the leucine zipper, nucleotide binding, leucine-rich repeat family of plant genes. *Plant Cell*. 10:1307-1319.

Moffett, P., G. Farnham, J. Peart, and D.C. Baulcombe. 2002. Interaction between domains of a plant NBS-LRR protein in disease resistance-related cell death. *EMBO J*. 21:4511-4519.

Mucyn, T.S., A. Clemente, V.M. Andriotis, A.L. Balmuth, G.E. Oldroyd, B.J. Staskawicz, and J.P. Rathjen. 2006. The tomato NBARC-LRR protein Prf interacts with Pto kinase in vivo to regulate specific plant immunity. *Plant Cell*. 18:2792-2806.

Naim, F., K. Nakasugi, R.N. Crowhurst, E. Hilario, A.B. Zwart, R.P. Hellens, J.M. Taylor, P.M. Waterhouse, and C.C. Wood. 2012. Advanced engineering of lipid metabolism in *Nicotiana benthamiana* using a draft genome and the V2 viral silencing-suppressor protein. *PLoS One*. 7:e52717.

Nakasugi, K., R. Crowhurst, J. Bally, and P. Waterhouse. 2014. Combining transcriptome assemblies from multiple de novo assemblers in the allo-tetraploid plant *Nicotiana benthamiana*. *PLoS One*. 9:e91776.

Narusaka, M., K. Shirasu, Y. Noutoshi, Y. Kubo, T. Shiraishi, M. Iwabuchi, and Y. Narusaka. 2009. *RRS1* and *RPS4* provide a dual resistance-gene system against fungal and bacterial pathogens. *Plant J*. 60:218-226.

National Research Council (U.S.). Advisory Committee on Technology Innovation. 1989. Lost crops of the Incas : little-known plants of the Andes with promise for worldwide cultivation. National Academy Press, Washington, D.C.

Nombela, G., V.M. Williamson, and M. Muniz. 2003. The root-knot nematode resistance gene *Mi-1.2* of tomato is responsible for resistance against the whitefly *Bemisia tabaci*. *Mol Plant Microbe Interact*. 16:645-649.

Ntoukakis, V., A.L. Balmuth, T.S. Mucyn, J.R. Gutierrez, A.M. Jones, and J.P. Rathjen. 2013. The tomato Prf complex is a molecular trap for bacterial effectors based on Pto transphosphorylation. *PLoS Pathog*. 9:e1003123.

Oh, C.S., K.F. Pedley, and G.B. Martin. 2010. Tomato 14-3-3 protein 7 positively regulates immunity-associated programmed cell death by enhancing protein abundance and signaling ability of MAPKKKα. *Plant Cell*. 22:260-272.

Oh, S.K., H. Kim, and D. Choi. 2014a. *Rpi-blb2*-mediated late blight resistance in *Nicotiana benthamiana* requires *SGT1* and salicylic acid-mediated signaling but not *RAR1* or *HSP90*. *FEBS Lett*. 588:1109-1115.

Oh, S.K., S.Y. Kwon, and D. Choi. 2014b. *Rpi-blb2*-mediated hypersensitive cell death caused by *Phytophthora infestans* AVRblb2 requires *SGT1*, but not *EDS1*, *NDR1*, salicylic acid-, jasmonic acid-, or ethylene-mediated signaling. *Plant Pathol J*. 30:254-260.

Oh, S.K., C. Young, M. Lee, R. Oliva, T.O. Bozkurt, L.M. Cano, J. Win, J.I. Bos, H.Y. Liu, M. van Damme, W. Morgan, D. Choi, E.A. Van der Vossen, V.G. Vleeshouwers, and S. Kamoun. 2009. In planta expression screens of *Phytophthora infestans* RXLR effectors reveal diverse phenotypes, including activation of the *Solanum bulbocastanum* disease resistance protein Rpi-blb2. *Plant Cell*. 21:2928-2947.

Okuyama, Y., H. Kanzaki, A. Abe, K. Yoshida, M. Tamiru, H. Saitoh, T. Fujibe, H. Matsumura, M. Shenton, D.C. Galam, J. Undan, A. Ito, T. Sone, and R. Terauchi. 2011. A multifaceted genomics approach allows the isolation of the rice *Pia*-blast resistance gene consisting of two adjacent NBS-LRR protein genes. *Plant J*. 66:467-479.

Oosumi, T., D.R. Rockhold, M.M. Maccree, K.L. Deahl, K.F. McCue, and W.R. Belknap. 2009. Gene *Rpi-bt1* from *Solanum bulbocastanum* confers resistance to late blight in transgenic potatoes. *Am J Pot Res.* 86:456.

Ori, N., Y. Eshed, I. Paran, G. Presting, D. Aviv, S. Tanksley, D. Zamir, and R. Fluhr. 1997. The *I2C* family from the wilt disease resistance locus *I2* belongs to the nucleotide binding, leucine-rich repeat superfamily of plant resistance genes. *Plant Cell*. 9:521-532.

Paal, J., H. Henselewski, J. Muth, K. Meksem, C.M. Menendez, F. Salamini, A. Ballvora, and C. Gebhardt. 2004. Molecular cloning of the potato *Gro1-4* gene conferring resistance to pathotype Ro1 of the root cyst nematode *Globodera rostochiensis*, based on a candidate gene approach. *Plant J*. 38:285-297.

Padmanabhan, M., P. Cournoyer, and S.P. Dinesh-Kumar. 2009. The leucine-rich repeat domain in plant innate immunity: a wealth of possibilities. *Cell Microbiol*. 11:191-198.

Padmanabhan, M.S., S. Ma, T.M. Burch-Smith, K. Czymmek, P. Huijser, and S.P. Dinesh-Kumar. 2013. Novel positive regulatory role for the SPL6 transcription factor in the N TIR-NB-LRR receptor-mediated plant innate immunity. *PLoS Pathog*. 9:e1003235.

Pearl, L.H., and C. Prodromou. 2006. Structure and mechanism of the Hsp90 molecular chaperone machinery. *Annu Rev Biochem*. 75:271-294.

Peart, J.R., R. Lu, A. Sadanandom, I. Malcuit, P. Moffett, D.C. Brice, L. Schauser, D.A. Jaggard, S. Xiao, M.J. Coleman, M. Dow, J.D. Jones, K. Shirasu, and D.C. Baulcombe. 2002. Ubiquitin ligase-associated protein SGT1 is required for host and nonhost disease resistance in plants. *Proc Natl Acad Sci U S A*. 99:10865-10869.

Peart, J.R., P. Mestre, R. Lu, I. Malcuit, and D.C. Baulcombe. 2005. NRG1, a CC-NB-LRR protein, together with N, a TIR-NB-LRR protein, mediates resistance against tobacco mosaic virus. *Curr Biol*. 15:968-973.

Peiro, A., M.C. Canizares, L. Rubio, C. Lopez, E. Moriones, J. Aramburu, and J. Sanchez-Navarro. 2014. The movement protein (NSm) of *Tomato spotted wilt virus* is the avirulence determinant in the tomato *Sw-5* gene-based resistance. *Mol Plant Pathol*. 15:802-813.

Pel, M.A. 2010. Mapping, isolation and characterization of genes responsible for late blight resistance in potato. *Ph.D. Thesis. Wageningen University, the Netherlands*.

Pel, M.A., S.J. Foster, T.H. Park, H. Rietman, G. van Arkel, J.D. Jones, H.J. Van Eck, E. Jacobsen, R.G. Visser, and E.A. Van der Vossen. 2009. Mapping and cloning of late blight resistance genes from *Solanum venturii* using an interspecific candidate gene approach. *Mol Plant Microbe Interact*. 22:601-615.

Peng, H.C., S. Mantelin, G.R. Hicks, F.L. Takken, and I. Kaloshian. 2016. The conformation of a plasma membrane-localized somatic embryogenesis receptor kinase complex is altered by a potato aphid-derived effector. *Plant Physiol*. 171:2211-2222.

Petre, B., D.G. Saunders, J. Sklenar, C. Lorrain, K.V. Krasileva, J. Win, S. Duplessis, and S. Kamoun. 2016. Heterologous expression screens in *Nicotiana benthamiana* identify a candidate effector of the wheat yellow rust pathogen that associates with processing bodies. *PLoS One*. 11:e0149035.

Pliego, C., D. Nowara, G. Bonciani, D.M. Gheorghe, R. Xu, P. Surana, E. Whigham, D. Nettleton, A.J. Bogdanove, R.P. Wise, P. Schweizer, L.V. Bindschedler, and P.D. Spanu. 2013. Host-induced gene silencing in barley powdery mildew reveals a class of ribonuclease-like effectors. *Mol Plant Microbe Interact*. 26:633-642.

Porter, B.W., M. Paidi, R. Ming, M. Alam, W.T. Nishijima, and Y.J. Zhu. 2009. Genome-wide analysis of *Carica papaya* reveals a small NBS resistance gene family. *Mol Genet Genomics*. 281:609-626.

Postma, W.J., E.J. Slootweg, S. Rehman, A. Finkers-Tomczak, T.O. Tytgat, K. van Gelderen, J.L. Lozano-Torres, J. Roosien, R. Pomp, C. van Schaik, J. Bakker,

A. Goverse, and G. Smant. 2012. The effector SPRYSEC-19 of *Globodera rostochiensis* suppresses CC-NB-LRR-mediated disease resistance in plants. *Plant Physiol*. 160:944-954.

Qi, D., U. Dubiella, S.H. Kim, D.I. Sloss, R.H. Dowen, J.E. Dixon, and R.W. Innes. 2014. Recognition of the protein kinase AVRPPHB SUSCEPTIBLE1 by the disease resistance protein RESISTANCE TO PSEUDOMONAS SYRINGAE5 is dependent on *s*-acylation and an exposed loop in AVRPPHB SUSCEPTIBLE1. *Plant Physiol*. 164:340-351.

Rairdan, G.J., and P. Moffett. 2006. Distinct domains in the ARC region of the potato resistance protein Rx mediate LRR binding and inhibition of activation. *Plant Cell*. 18:2082-2093.

Rathjen, J.P., J.H. Chang, B.J. Staskawicz, and R.W. Michelmore. 1999. Constitutively active *Pto* induces a *Prf*-dependent hypersensitive response in the absence of *avrPto*. *EMBO J*. 18:3232-3240.

Ravensdale, M., M. Bernoux, T. Ve, B. Kobe, P.H. Thrall, J.G. Ellis, and P.N. Dodds. 2012. Intramolecular interaction influences binding of the Flax L5 and L6 resistance proteins to their AvrL567 ligands. *PLoS Pathog*. 8:e1003004.

Rietman, H., G. Bijsterbosch, L.M. Cano, H.R. Lee, J.H. Vossen, E. Jacobsen, R.G. Visser, S. Kamoun, and V.G. Vleeshouwers. 2012. Qualitative and quantitative late blight resistance in the potato cultivar Sarpo Mira is determined by the perception of five distinct RXLR effectors. *Mol Plant Microbe Interact*. 25:910-919.

Rivas, S., and C.M. Thomas. 2005. Molecular interactions between tomato and the leaf mold pathogen *Cladosporium fulvum*. *Annu Rev Phytopathol.* 43:395-436.

Roberts, M., S. Tang, A. Stallmann, J.L. Dangl, and V. Bonardi. 2013. Genetic requirements for signaling from an autoactive plant NB-LRR intracellular innate immune receptor. *PLoS Genet*. 9:e1003465.

Ronald, P.C., J.M. Salmeron, F.M. Carland, and B.J. Staskawicz. 1992. The cloned avirulence gene *avrPto* induces disease resistance in tomato cultivars containing the *Pto* resistance gene. *J Bacteriol*. 174:1604-1611.

Rossi, M., F.L. Goggin, S.B. Milligan, I. Kaloshian, D.E. Ullman, and V.M. Williamson. 1998. The nematode resistance gene *Mi* of tomato confers resistance against the potato aphid. *Proc Natl Acad Sci U S A*. 95:9750-9754.

Sacco, M.A., K. Koropacka, E. Grenier, M.J. Jaubert, A. Blanchard, A. Goverse, G. Smant, and P. Moffett. 2009. The cyst nematode SPRYSEC protein RBP-1 elicits Gpa2- and RanGAP2-dependent plant cell death. *PLoS Pathog*. 5:e1000564.

Sacco, M.A., S. Mansoor, and P. Moffett. 2007. A RanGAP protein physically interacts with the NB-LRR protein Rx, and is required for Rx-mediated viral resistance. *Plant J*. 52:82-93.

Salmeron, J.M., S.J. Barker, F.M. Carland, A.Y. Mehta, and B.J. Staskawicz. 1994. Tomato mutants altered in bacterial disease resistance provide evidence for a new locus controlling pathogen recognition. *Plant Cell*. 6:511-520.

Sarkinen, T., L. Bohs, R.G. Olmstead, and S. Knapp. 2013. A phylogenetic framework for evolutionary study of the nightshades (Solanaceae): a dated 1000-tip tree. *BMC Evol Biol*. 13:214.

Sarris, P.F., V. Cevik, G. Dagdas, J.D. Jones, and K.V. Krasileva. 2016. Comparative analysis of plant immune receptor architectures uncovers host proteins likely targeted by pathogens. *BMC Biol*. 14:8.

Sarris, P.F., Z. Duxbury, S.U. Huh, Y. Ma, C. Segonzac, J. Sklenar, P. Derbyshire, V. Cevik, G. Rallapalli, S.B. Saucet, L. Wirthmueller, F.L. Menke, K.H. Sohn, and J.D. Jones. 2015. A plant immune receptor detects pathogen effectors that target WRKY transcription factors. *Cell*. 161:1089-1100.

Sarris, P.F., and J.D. Jones. 2015. Plant immune receptors mimic pathogen virulence targets. *Oncotarget*. 6:16824-16825.

Saucet, S.B., Y. Ma, P.F. Sarris, O.J. Furzer, K.H. Sohn, and J.D. Jones. 2015. Two linked pairs of *Arabidopsis* TNL resistance genes independently confer recognition of bacterial effector AvrRps4. *Nat Commun*. 6:6338.

Saunders, D.G., S. Breen, J. Win, S. Schornack, I. Hein, T.O. Bozkurt, N. Champouret, V.G. Vleeshouwers, P.R. Birch, E.M. Gilroy, and S. Kamoun. 2012. Host protein BSL1 associates with *Phytophthora infestans* RXLR effector AVR2 and the *Solanum demissum* immune receptor R2 to mediate disease resistance. *Plant Cell*. 24:3420-3434.

Schornack, S., A. Ballvora, D. Gurlebeck, J. Peart, D. Baulcombe, M. Ganal, B. Baker, U. Bonas, and T. Lahaye. 2004. The tomato resistance protein Bs4 is a predicted non-nuclear TIR-NB-LRR protein that mediates defense responses to severely truncated derivatives of AvrBs4 and overexpressed AvrBs3. *Plant J*. 37:46-60.

Schornack, S., M. van Damme, T.O. Bozkurt, L.M. Cano, M. Smoker, M. Thines, E. Gaulin, S. Kamoun, and E. Huitema. 2010. Ancient class of translocated oomycete effectors targets the host nucleus. *Proc Natl Acad Sci U S A*. 107:17421-17426.

Schreiber, K.J., A. Bentham, S.J. Williams, B. Kobe, and B.J. Staskawicz. 2016. Multiple domain associations within the *Arabidopsis* immune receptor RPP1 regulate the activation of programmed cell death. *PLoS Pathog*. 12:e1005769.

Segonzac, C., D. Feike, S. Gimenez-Ibanez, D.R. Hann, C. Zipfel, and J.P. Rathjen. 2011. Hierarchy and roles of pathogen-associated molecular pattern-induced responses in *Nicotiana benthamiana*. *Plant Physiol*. 156:687-699.

Segretin, M.E., M. Pais, M. Franceschetti, A. Chaparro-Garcia, J.I. Bos, M.J. Banfield, and S. Kamoun. 2014. Single amino acid mutations in the potato immune receptor R3a expand response to *Phytophthora* effectors. *Mol Plant Microbe Interact*. 27:624-637.

Senthil-Kumar, M., R. Hema, A. Anand, L. Kang, M. Udayakumar, and K.S. Mysore. 2007. A systematic study to determine the extent of gene silencing in *Nicotiana benthamiana* and other Solanaceae species when heterologous gene sequences are used for virus-induced gene silencing. *New Phytol*. 176:782-791.

Senthil-Kumar, M., and K.S. Mysore. 2011. Caveat of RNAi in plants: the off-target effect. *Methods Mol Biol*. 744:13-25.

Seo, E., S. Kim, S.I. Yeom, and D. Choi. 2016. Genome-Wide Comparative analyses reveal the dynamic evolution of nucleotide-binding leucine-rich repeat gene family among Solanaceae plants. *Front Plant Sci*. 7:1205.

Shao, Z.Q., J.Y. Xue, P. Wu, Y.M. Zhang, Y. Wu, Y.Y. Hang, B. Wang, and J.Q. Chen. 2016. Large-scale analyses of angiosperm nucleotide-binding site-leucine-rich repeat genes reveal three anciently diverged classes with distinct evolutionary patterns. *Plant Physiol*. 170:2095-2109.

Shao, Z.Q., Y.M. Zhang, Y.Y. Hang, J.Y. Xue, G.C. Zhou, P. Wu, X.Y. Wu, X.Z. Wu, Q. Wang, B. Wang, and J.Q. Chen. 2014. Long-term evolution of nucleotide-binding site-leucine-rich repeat genes: understanding gained from and beyond the legume family. *Plant Physiol*. 166:217-234.

Shirasu, K., T. Lahaye, M.W. Tan, F. Zhou, C. Azevedo, and P. Schulze-Lefert. 1999. A novel class of eukaryotic zinc-binding proteins is required for disease resistance signaling in barley and development in *C. elegans*. *Cell*. 99:355-366.

Simons, G., J. Groenendijk, J. Wijbrandi, M. Reijans, J. Groenen, P. Diergaarde, T. Van der Lee, M. Bleeker, J. Onstenk, M. de Both, M. Haring, J. Mes, B. Cornelissen, M. Zabeau, and P. Vos. 1998. Dissection of the fusarium *I2* gene cluster in tomato reveals six homologs and one active gene copy. *Plant Cell*. 10:1055-1068.

Sinapidou, E., K. Williams, L. Nott, S. Bahkt, M. Tor, I. Crute, P. Bittner-Eddy, and J. Beynon. 2004. Two TIR:NB:LRR genes are required to specify resistance to *Peronospora parasitica* isolate Cala2 in *Arabidopsis*. *Plant J*. 38:898-909.

Slootweg, E.J., L.N. Spiridon, J. Roosien, P. Butterbach, R. Pomp, L. Westerhof, R. Wilbers, E. Bakker, J. Bakker, A.J. Petrescu, G. Smant, and A. Goverse. 2013. Structural determinants at the interface of the ARC2 and leucine-rich repeat domains control the activation of the plant immune receptors Rx1 and Gpa2. *Plant Physiol*. 162:1510-1528.

Smilde, W.D., G. Brigneti, L. Jagger, S. Perkins, and J.D. Jones. 2005. *Solanum mochiquense* chromosome IX carries a novel late blight resistance gene *Rpi-moc1*. *Theor Appl Genet*. 110:252-258.

Sohn, K.H., C. Segonzac, G. Rallapalli, P.F. Sarris, J.Y. Woo, S.J. Williams, T.E. Newman, K.H. Paek, B. Kobe, and J.D. Jones. 2014. The nuclear immune receptor *RPS4* is required for *RRS1*^{SLH1}-dependent constitutive defense activation in *Arabidopsis thaliana*. *PLoS Genet*. 10:e1004655.

Song, J., J. Win, M. Tian, S. Schornack, F. Kaschani, M. Ilyas, R.A. van der Hoorn, and S. Kamoun. 2009. Apoplastic effectors secreted by two unrelated eukaryotic plant pathogens target the tomato defense protease Rcr3. *Proc Natl Acad Sci U S A*. 106:1654-1659.

Spassova, M.I., T.W. Prins, R.T. Folkertsma, R.M. Klein-Lankhorst, J. Hille, R.W. Goldbach, and M. Prins. 2001. The tomato gene *Sw5* is a member of the coiled coil, nucleotide binding, leucine-rich repeat class of plant resistance genes and confers resistance to *TSWV* in tobacco. *Mol Breed*. 7:151-161.

Stam, R., D. Scheikl, and A. Tellier. 2016. Pooled enrichment sequencing Identifies diversity and evolutionary pressures at NLR resistance genes within a wild tomato population. *Genome Biol Evol*. 8:1501-1515.

Steinbrenner, A.D., S. Goritschnig, and B.J. Staskawicz. 2015. Recognition and activation domains contribute to allele-specific responses of an *Arabidopsis* NLR receptor to an oomycete effector protein. *PLoS Pathog*. 11:e1004665.

Stelling, J., U. Sauer, Z. Szallasi, F.J. Doyle, 3rd, and J. Doyle. 2004. Robustness of cellular functions. *Cell*. 118:675-685.

Steuernagel, B., F. Jupe, K. Witek, J.D. Jones, and B.B. Wulff. 2015. NLR-parser: rapid annotation of plant NLR complements. *Bioinformatics*. 31:1665-1667.

Strange, R.N., and P.R. Scott. 2005. Plant disease: a threat to global food security. *Annu Rev Phytopathol*. 43:83-116.

Sueldo, D.J. 2014. Towards generating broad-spectrum resistance to pathogens in plants: Studies on a down-stream signalling NB-LRR of tomato. *Ph.D. Thesis. Wageningen University, the Netherlands*.

Sueldo, D.J., M. Shimels, L.N. Spiridon, O. Caldararu, A.J. Petrescu, M.H. Joosten, and W.I. Tameling. 2015. Random mutagenesis of the nucleotide-binding domain of NRC1 (NB-LRR Required for Hypersensitive Response-Associated Cell Death-1), a downstream signalling nucleotide-binding, leucine-rich repeat (NB-LRR) protein, identifies gain-of-function mutations in the nucleotide-binding pocket. *New Phytol*. 208:210-223.

Swiderski, M.R., D. Birker, and J.D. Jones. 2009. The TIR domain of TIR-NB-LRR resistance proteins is a signaling domain involved in cell death induction. *Mol Plant Microbe Interact*. 22:157-165.

Tai, T.H., D. Dahlbeck, E.T. Clark, P. Gajiwala, R. Pasion, M.C. Whalen, R.E. Stall, and B.J. Staskawicz. 1999. Expression of the *Bs2* pepper gene confers resistance to bacterial spot disease in tomato. *Proc Natl Acad Sci U S A*. 96:14153-14158.

Takahashi, A., C. Casais, K. Ichimura, and K. Shirasu. 2003. HSP90 interacts with RAR1 and SGT1 and is essential for RPS2-mediated disease resistance in *Arabidopsis*. *Proc Natl Acad Sci U S A*. 100:11777-11782.

Takken, F.L., M. Albrecht, and W.I. Tameling. 2006. Resistance proteins: molecular switches of plant defence. *Curr Opin Plant Biol*. 9:383-390.

Takken, F.L., and A. Goverse. 2012. How to build a pathogen detector: structural basis of NB-LRR function. *Curr Opin Plant Biol*. 15:375-384.

Tameling, W.I., and D.C. Baulcombe. 2007. Physical association of the NB-LRR resistance protein Rx with a Ran GTPase-activating protein is required for extreme resistance to *Potato virus X*. *Plant Cell*. 19:1682-1694.

Tameling, W.I., S.D. Elzinga, P.S. Darmin, J.H. Vossen, F.L. Takken, M.A. Haring, and B.J. Cornelissen. 2002. The tomato *R* gene products I-2 and Mi-1 are functional ATP binding proteins with ATPase activity. *Plant Cell*. 14:2929-2939.

Tameling, W.I., C. Nooijen, N. Ludwig, M. Boter, E. Slootweg, A. Goverse, K. Shirasu, and M.H. Joosten. 2010. RanGAP2 mediates nucleocytoplasmic partitioning of the NB-LRR immune receptor Rx in the Solanaceae, thereby dictating Rx function. *Plant Cell*. 22:4176-4194.

Tamura, K., G. Stecher, D. Peterson, A. Filipski, and S. Kumar. 2013. MEGA6: Molecular Evolutionary Genetics Analysis version 6.0. *Mol Biol Evol*. 30:2725-2729.

Tarr, D.E., and H.M. Alexander. 2009. TIR-NBS-LRR genes are rare in monocots: evidence from diverse monocot orders. *BMC Res Notes*. 2:197.

Tenthorey, J.L., E.M. Kofoed, M.D. Daugherty, H.S. Malik, and R.E. Vance. 2014. Molecular basis for specific recognition of bacterial ligands by NAIP/NLRC4 inflammasomes. *Mol Cell*. 54:17-29.

Thomma, B.P., T. Nurnberger, and M.H. Joosten. 2011. Of PAMPs and effectors: the blurred PTI-ETI dichotomy. *The Plant cell*. 23:4-15.

Ting, J.P., R.C. Lovering, E.S. Alnemri, J. Bertin, J.M. Boss, B.K. Davis, R.A. Flavell, S.E. Girardin, A. Godzik, J.A. Harton, H.M. Hoffman, J.P. Hugot, N. Inohara, A. Mackenzie, L.J. Maltais, G. Nunez, Y. Ogura, L.A. Otten, D. Philpott, J.C. Reed, W. Reith, S. Schreiber, V. Steimle, and P.A. Ward. 2008. The NLR gene family: a standard nomenclature. *Immunity*. 28:285-287.

Tornero, P., R.A. Chao, W.N. Luthin, S.A. Goff, and J.L. Dangl. 2002. Large-scale structure-function analysis of the *Arabidopsis* RPM1 disease resistance protein. *Plant Cell*. 14:435-450.

Trognitz, B.R., and F.C. Trognitz. 2007. Occurrence of the *R1* allele conferring resistance to late blight in potato *R*-gene differentials and commercial cultivars. *Plant Pathology*. 56:150-155.

Tsuda, K., M. Sato, T. Stoddard, J. Glazebrook, and F. Katagiri. 2009. Network properties of robust immunity in plants. *PLoS Genet*. 5:e1000772.

Ueda, H., Y. Yamaguchi, and H. Sano. 2006. Direct interaction between the tobacco mosaic virus helicase domain and the ATP-bound resistance protein, N factor during the hypersensitive response in tobacco plants. *Plant Mol Biol*. 61:31-45.

van der Biezen, E.A., and J.D. Jones. 1998. The NB-ARC domain: a novel signalling motif shared by plant resistance gene products and regulators of cell death in animals. *Curr Biol*. 8:R226-227.

van der Hoorn, R.A., and S. Kamoun. 2008. From Guard to Decoy: a new model for perception of plant pathogen effectors. *Plant Cell*. 20:2009-2017.

Van der Hoorn, R.A., F. Laurent, R. Roth, and P.J. De Wit. 2000. Agroinfiltration is a versatile tool that facilitates comparative analyses of *Avr9/Cf-9*-induced and *Avr4/Cf-4*-induced necrosis. *Mol Plant Microbe Interact*. 13:439-446.

van der Vossen, E., A. Sikkema, B. Hekkert, J. Gros, P. Stevens, M. Muskens, D. Wouters, A. Pereira, W. Stiekema, and S. Allefs. 2003. An ancient *R* gene from the wild potato species *Solanum bulbocastanum* confers broad-spectrum resistance to *Phytophthora infestans* in cultivated potato and tomato. *Plant J*. 36:867-882.

van der Vossen, E.A., J. Gros, A. Sikkema, M. Muskens, D. Wouters, P. Wolters, A. Pereira, and S. Allefs. 2005. The *Rpi-blb2* gene from *Solanum bulbocastanum* is an *Mi-1* gene homolog conferring broad-spectrum late blight resistance in potato. *Plant J*. 44:208-222.

van der Vossen, E.A., J.N. van der Voort, K. Kanyuka, A. Bendahmane, H. Sandbrink, D.C. Baulcombe, J. Bakker, W.J. Stiekema, and R.M. Klein-Lankhorst. 2000. Homologues of a single resistance-gene cluster in potato confer resistance to distinct pathogens: a virus and a nematode. *Plant J*. 23:567-576.

van Ooijen, G., G. Mayr, M.M. Kasiem, M. Albrecht, B.J. Cornelissen, and F.L. Takken. 2008. Structure-function analysis of the NB-ARC domain of plant disease resistance proteins. *J Exp Bot*. 59:1383-1397.

van Ooijen, G., H.A. van den Burg, B.J. Cornelissen, and F.L. Takken. 2007. Structure and function of resistance proteins in solanaceous plants. *Annu Rev Phytopathol*. 45:43-72.

Vleeshouwers, V.G., S. Raffaele, J.H. Vossen, N. Champouret, R. Oliva, M.E. Segretin, H. Rietman, L.M. Cano, A. Lokossou, G. Kessel, M.A. Pel, and S. Kamoun. 2011. Understanding and exploiting late blight resistance in the age of effectors. *Annu Rev Phytopathol*. 49:507-531.

Vleeshouwers, V.G., H. Rietman, P. Krenek, N. Champouret, C. Young, S.K. Oh, M. Wang, K. Bouwmeester, B. Vosman, R.G. Visser, E. Jacobsen, F. Govers, S. Kamoun, and E.A. Van der Vossen. 2008. Effector genomics accelerates discovery and functional profiling of potato disease resistance and *Phytophthora infestans* avirulence genes. *PLoS One*. 3:e2875.

Vossen, J.H., G. van Arkel, M. Bergervoet, K.R. Jo, E. Jacobsen, and R.G. Visser. 2016. The *Solanum demissum R8* late blight resistance gene is an *Sw-5* homologue that has been deployed worldwide in late blight resistant varieties. *Theor Appl Genet*. 129:1785-1796.

Wagner, A. 2014. Mutational robustness accelerates the origin of novel RNA phenotypes through phenotypic plasticity. *Biophys J*. 106:955-965.

Wagner, S., J. Stuttmann, S. Rietz, R. Guerois, E. Brunstein, J. Bautor, K. Niefind, and J.E. Parker. 2013. Structural basis for signaling by exclusive EDS1 heteromeric complexes with SAG101 or PAD4 in plant innate immunity. *Cell Host Microbe*. 14:619-630.

Weber, E., C. Engler, R. Gruetzner, S. Werner, and S. Marillonnet. 2011. A modular cloning system for standardized assembly of multigene constructs. *PLoS One*. 6:e16765.

Wei, C.F., B.H. Kvitko, R. Shimizu, E. Crabill, J.R. Alfano, N.C. Lin, G.B. Martin, H.C. Huang, and A. Collmer. 2007. A *Pseudomonas syringae* pv. *tomato* DC3000 mutant lacking the type III effector HopQ1-1 is able to cause disease in the model plant *Nicotiana benthamiana*. *Plant J*. 51:32-46.

Whitham, S., S.P. Dinesh-Kumar, D. Choi, R. Hehl, C. Corr, and B. Baker. 1994. The product of the tobacco mosaic virus resistance gene *N*: similarity to toll and the interleukin-1 receptor. *Cell*. 78:1101-1115.

Williams, S.J., K.H. Sohn, L. Wan, M. Bernoux, P.F. Sarris, C. Segonzac, T. Ve, Y. Ma, S.B. Saucet, D.J. Ericsson, L.W. Casey, T. Lonhienne, D.J. Winzor, X. Zhang, A. Coerdt, J.E. Parker, P.N. Dodds, B. Kobe, and J.D. Jones. 2014. Structural basis for assembly and function of a heterodimeric plant immune receptor. *Science*. 344:299-303.

Williams, S.J., P. Sornaraj, E. deCourcy-Ireland, R.I. Menz, B. Kobe, J.G. Ellis, P.N. Dodds, and P.A. Anderson. 2011. An autoactive mutant of the M flax rust resistance protein has a preference for binding ATP, whereas wild-type M protein binds ADP. *Mol Plant Microbe Interact*. 24:897-906.

Win, J., A. Chaparro-Garcia, K. Belhaj, D.G. Saunders, K. Yoshida, S. Dong, S. Schornack, C. Zipfel, S. Robatzek, S.A. Hogenhout, and S. Kamoun. 2012. Effector biology of plant-associated organisms: concepts and perspectives. *Cold Spring Harb Symp Quant Biol*. 77:235-247.

Win, J., S. Kamoun, and A.M. Jones. 2011. Purification of effector-target protein complexes via transient expression in *Nicotiana benthamiana*. *Methods Mol Biol*. 712:181-194.

Witek, K., F. Jupe, A.I. Witek, D. Baker, M.D. Clark, and J.D. Jones. 2016. Accelerated cloning of a potato late blight-resistance gene using RenSeq and SMRT sequencing. *Nat Biotechnol*. 34:656-660.

Wu, C.H., K.V. Krasileva, M.J. Banfield, R. Terauchi, and S. Kamoun. 2015. The "sensor domains" of plant NLR proteins: more than decoys? *Front Plant Sci*. 6:134.

Xiang, T., N. Zong, Y. Zou, Y. Wu, J. Zhang, W. Xing, Y. Li, X. Tang, L. Zhu, J. Chai, and J.M. Zhou. 2008. *Pseudomonas syringae* effector AvrPto blocks innate immunity by targeting receptor kinases. *Curr Biol*. 18:74-80.

Xing, W., Y. Zou, Q. Liu, J. Liu, X. Luo, Q. Huang, S. Chen, L. Zhu, R. Bi, Q. Hao, J.W. Wu, J.M. Zhou, and J. Chai. 2007. The structural basis for activation of plant immunity by bacterial effector protein AvrPto. *Nature*. 449:243-247.

Xu, F., P. Kapos, Y.T. Cheng, M. Li, Y. Zhang, and X. Li. 2014. NLR-associating transcription factor bHLH84 and its paralogs function redundantly in plant immunity. *PLoS Pathog*. 10:e1004312.

Xu, P., Y. Zhang, L. Kang, M.J. Roossinck, and K.S. Mysore. 2006. Computational estimation and experimental verification of off-target silencing during posttranscriptional gene silencing in plants. *Plant Physiol*. 142:429-440.

Zhai, C., F. Lin, Z. Dong, X. He, B. Yuan, X. Zeng, L. Wang, and Q. Pan. 2011. The isolation and characterization of *Pik*, a rice blast resistance gene which emerged after rice domestication. *New Phytol*. 189:321-334.

Zhang, C., L. Liu, Z. Zheng, Y. Sun, L. Zhou, Y. Yang, F. Cheng, Z. Zhang, X. Wang, S. Huang, B. Xie, Y. Du, Y. Bai, and J. Li. 2013a. Fine mapping of the *Ph-3* gene conferring resistance to late blight (*Phytophthora infestans*) in tomato. *Theor Appl Genet*. 126:2643-2653.

Zhang, H., J. Zhao, S. Liu, D.P. Zhang, and Y. Liu. 2013b. *Tm-2²* confers different resistance responses against *Tobacco mosaic virus* dependent on its expression level. *Mol Plant*. 6:971-974.

Zhang, M., Y. Kadota, C. Prodromou, K. Shirasu, and L.H. Pearl. 2010. Structural basis for assembly of Hsp90-Sgt1-CHORD protein complexes: implications for chaperoning of NLR innate immunity receptors. *Mol Cell*. 39:269-281.

Zhang, R., F. Murat, C. Pont, T. Langin, and J. Salse. 2014. Paleo-evolutionary plasticity of plant disease resistance genes. *BMC Genomics*. 15:187.

Zhang, Y.M., Z.Q. Shao, Q. Wang, Y.Y. Hang, J.Y. Xue, B. Wang, and J.Q. Chen. 2016. Uncovering the dynamic evolution of nucleotide-binding site-leucine-rich repeat (NBS-LRR) genes in Brassicaceae. *J Integr Plant Biol*. 58:165-177.

Zhao, J., Q. Liu, H. Zhang, Q. Jia, Y. Hong, and Y. Liu. 2013. The rubisco small subunit is involved in tobamovirus movement and *Tm-2²*-mediated extreme resistance. *Plant Physiol*. 161:374-383.

Zhao, Y., J. Yang, J. Shi, Y.N. Gong, Q. Lu, H. Xu, L. Liu, and F. Shao. 2011. The NLRC4 inflammasome receptors for bacterial flagellin and type III secretion apparatus. *Nature*. 477:596-600.

Zhou, T., Y. Wang, J.Q. Chen, H. Araki, Z. Jing, K. Jiang, J. Shen, and D. Tian. 2004. Genome-wide identification of NBS genes in japonica rice reveals significant expansion of divergent non-TIR NBS-LRR genes. *Mol Genet Genomics*. 271:402-415.

Zhu, S., Y. Li, J.H. Vossen, R.G. Visser, and E. Jacobsen. 2012. Functional stacking of three resistance genes against *Phytophthora infestans* in potato. *Transgenic Res*. 21:89-99.